Universidad Autónoma de Madrid

Treatment and valorisation of wastewater through aqueous phase reforming

Tratamiento y valorización de aguas residuales a través de reformado en fase acuosa

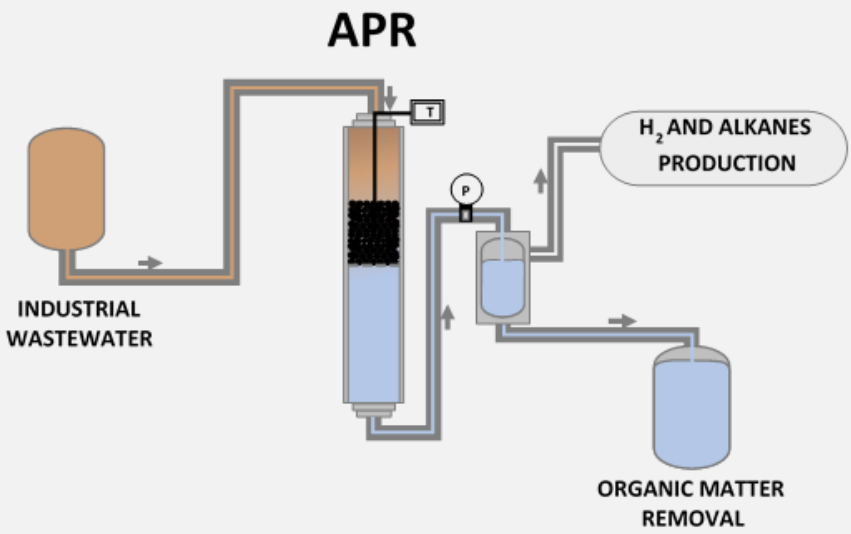

Adriana Souza de Oliveira

2020

UNIVERSIDAD AUTÓNOMA DE MADRID
FACULTAD DE CIENCIAS
Departamento de Ingeniería Química

Treatment and valorisation of wastewater through aqueous phase reforming

Tratamiento y valorización de aguas residuales a través de reformado en fase acuosa

Tesis Doctoral

Adriana Souza de Oliveira

Madrid, 2020

UNIVERSIDAD AUTÓNOMA DE MADRID

FACULTAD DE CIENCIAS

Departamento de Ingeniería Química

Treatment and valorisation of wastewater through aqueous phase reforming

Tratamiento y valorización de aguas residuales a través de reformado en fase acuosa

MEMORIA

que para optar al grado de

Doctor con Mención Internacional

presenta

Adriana Souza de Oliveira

Directores: Dr. Miguel Ángel Gilarranz Redondo

Dra. Luisa Calvo Hernández

Madrid, 2020

Dr. Miguel Ángel Gilarranz Redondo y Dra. Luisa Calvo Hernández, Profesores Titulares del Departamento de Ingeniería Química de la Universidad Autónoma de Madrid.

HACEN CONSTAR: que el presente trabajo, titulado "*Tratamiento y valorización de aguas residuales a través de reformado en fase acuosa*", presentado por Dña. Adriana Souza de Oliveira, ha sido realizado bajo su dirección, en los laboratorios del Departamento de Ingeniería Química, en la Universidad Autónoma de Madrid y que, a su juicio, reúne los requisitos de originalidad y rigor científico necesarios para ser presentados como Tesis Doctoral.

Y, para que conste a efectos oportunos, firmamos el presente informe en Madrid a 05 de febrero de 2020.

Miguel Ángel Gilarranz Redondo Luisa Calvo Hernández

La realización de este trabajo ha sido posible gracias al apoyo económico del Ministerio de Economía y Competitividad (MINECO) a través del proyecto CTQ2015-65491-R, y gracias a la concesión de un contrato de Formación de Personal Investigador (FPI) del MINECO (Referencia BES-2016-077244).

Para todos los que amo.

“A beleza de ser um eterno aprendiz”

(Gonzaguinha, O que É, o que É?)

Agradecimientos

Muchas veces me han preguntado porque sonreía y no es que siempre tenga una motivación especial para sonreír, simplemente soy feliz. Siempre llevo una sonrisa con la intención de que la vida me depare cosas buenas y hoy os puedo decir que sonrío porque me siento muy afortunada y grata con todo que la vida me ha regalado.

Tuve la suerte de ser elegida para hacer este trabajo por los mejores directores que alguien puede tener, Luisa Calvo y Miguel Ángel Gilarranz. Me gustaría daros las gracias por la confianza y por todo el apoyo y enseñanzas durante los últimos 3 años. También quería agradecer José, un compañero increíble que me ayudó con todo desde el primer día. Sin él este trabajo no hubiera sido posible.

Me gustaría agradecer también a todas personas del departamento de ingeniería química de esta universidad que de una manera directa o indirecta también han contribuido para la realización de esta tesis y sobre todo para mi formación personal y profesional. Especialmente quería dar la gracias a" las chicas" (Estefanía, Blanca, Alicia, Inés y Julia) por la amistad, por las risas, por los viajes y principalmente por los encuentros para comer cosas ricas. Mis días han sido más agradables y más alegres debido a vuestra presencia en el laboratorio. También quería agradecer de manera especial al "grupo de las barbacoas" por los maravillosos momentos que pasamos juntos cada vez que nos reunimos.

Agora escreverei em português, porque não poderia agradecer a minha família em outro idioma que não fosse o nosso. Agradeço as minhas avós por me ensinarem o valor da generosidade e aos meus pais e ao meu irmão por todo o amor e carinho. Também quero agradecer a todos meus tios,

tias e primos por toda torcida e amor e especialmente as minhas tias por me tratarem como filha e me darem um lar quando precisei de um.

Now I will change the language again to say thanks to Prof. Dmitry for hosting me in his lab during my predoctoral stay and teach me. To Prof. Atte to help me with the reactions and results and to all my friends in Abo Akademi. Thanks to you my stay was very pleasant and I have no words to thank you for your friendship. I just look forward to your visit to Madrid.

Por último, quería agradecer a Álvaro. Agradezco a Dios, a la vida y la suerte por haberme puesto en tu camino mi amor. Gracias por los ánimos, por decir venga hazlo, tu puedes, te va venir bien. Eres el coraje que me falta para iniciar los desafíos y el ánimo que necesito para terminarlos. Aprovecho también para agradecer a tu familia por tanto amor y cuidado desde que estamos juntos.

Por fin, vestida con mi mejor sonrisa doy las gracias a todos los que amo.

Summary

Aqueous phase reforming (APR) is an attractive alternative for H_2 and alkanes production from biomass-derived compounds. Good results have been reported in the literature for a variety of model compounds, although some studies have shown that the cost of the feedstock may be an important burden for the application of APR. In this sense, the use of APR could be extended to biomass-derived wastewater treatment, thus integrating wastewater treatment and valorisation of effluents. This new potential application could be of special interest in the case of wastewater that are difficult to treat by conventional technologies and for industries producing large volumes of wastewater with high loads of biomass-derived organic compounds. Accordingly, the main aim of this thesis is to evaluate the application of APR process to the simultaneous treatment and valorisation of wastewaters.

In order to evaluate the flexibility of the process, different types of industrial wastewater were treated by APR, mainly for H_2 production. Pt and Pt based bimetallic catalysts (PtRe and PtPd) supported on different carbons materials were used in the APR experiments and the influence of different variables that could affect the catalytic performance was investigated. Likewise, the catalysts stability was evaluated and two processes were coupled to APR (hydrogenation and catalytic wet air oxidation (CWAO)) in order to improve valorisation and/or reduce catalyst deactivation.

In the APR of tuna-cooking wastewater at 200 ºC using Pt catalysts supported on different carbon materials, high TOC and COD removal values (45 – 60 %) were achieved due to a combination of adsorption on the supports, hydrothermal carbonization (HTC) and APR. The gas production was low and CO_2 was the main gas component (82 – 99 %), due to the presence of components, such as chloride, that lead to catalyst deactivation. The use of a basic support significantly increased the gas production and the

H_2 percentage in the gas fraction. In addition, gas production increased in semi-continuous compared to batch operation.

In the APR of brewery wastewater, HTC was observed as a main contribution in the experiments without catalyst. In batch APR experiments with catalysts, the best catalytic performance was observed at higher temperature (225 ºC) and using highly mesoporous carbon black support with virtually no microporosity and high pH slurry (≈ 50 % of H_2 and 12.2 mmol H_2 / g COD_i). The removal of organic matter increased up to ca. 99 % decreasing organic load of the wastewater. The addition of KOH or NaOH to wastewater also resulted in a slightly lower TOC and COD removal, however higher H_2 yield was obtained in those cases where KOH was added. Increasing the KOH concentration led to CO_2-free H_2 without significant changes in H_2 yield and the results with real and synthetic brewery wastewater were relatively similar. In continuous APR experiments at 225 ºC, PtRe/C catalyst exhibited higher catalytic activity and H_2 production than Pt/C, which was attributed to an increase in the water-gas shift (WGS) activity. A longer residence time and a higher carrier gas flow also increased the H_2 production. At low time-on-stream (TOS) values, Pt catalysts supported on different modified carbons, whose microporosity was gradually decreased by impregnation and carbonization of resol resin, showed higher H_2 production than the reference Pt catalyst and an indirectly effect of the Pt nanoparticles (NPs) size was observed. All the catalysts tested showed an important deactivation with TOS and the characterization of used catalysts revealed that the main cause of the pronounced catalysts deactivation in the first hours of reaction was the coke deposition on the catalyst surface. Finally, a higher H_2 selectivity and yield were achieved after pretreatment of the feedstock by hydrogenation, and the coupled hydrogenation-APR was considered efficient since H_2 production compensated for the need for

hydrogenation. The durability of the catalyst was also increased, due to the reducing of the formation of carbonaceous deposits.

In the APR of fruit juice wastewater using Pt/C catalyst at 220 ºC, H_2 production was little affected by pH, yielding around 6.6 mmol H_2 / g COD_i, in the pH range tested. The organic carbon removal declined slightly at the highest loads tested and the highest H_2 yield value was observed with low-medium organic load. Finally, a decreased of H_2 yield from 7.8 to 4.2 mmol H_2 / g COD_i was observed at high salinity, due to catalyst deactivation.

In the APR of wastewater with phenolic compounds, a high range of TOC and COD removal (74 – 90 %) was observed for feedstocks with compounds representative of phenol oxidation pathway, with higher values for long chain acids. H_2 production was low in all cases, due to competing direct conversion of long and short chain acids into CH_4. In the APR of mixtures of feedstocks, the highest yield to CH_4 (11.0 mmol CH_4 / g TOC_i) was achieved for mixtures rich in acids. CWAO-APR resulted in a similar TOC and COD removal and higher gas production and CH_4 yield than direct APR, indicating that coupled CWAO-APR can overcome the low conversion and gas production observed in direct APR of phenol.

Resumen

El reformado en fase acuosa (APR) es una alternativa atractiva para la producción de H_2 y alcanos a partir de compuestos derivados de la biomasa. En la bibliografía se pueden encontrar buenos resultados para una variedad de compuestos modelo, aunque algunos estudios han demostrado que el coste de la materia prima puede ser una carga importante para la aplicación del APR. En este sentido, el uso de APR podría extenderse al tratamiento de aguas residuales derivadas de biomasa, integrando así el tratamiento de aguas residuales y la valorización de los efluentes. Esta nueva aplicación potencial podría ser de especial interés en el caso de aguas residuales que son difíciles de tratar con tecnologías convencionales y para industrias que producen grandes volúmenes de aguas residuales con altas cargas de compuestos orgánicos derivados de la biomasa. En consecuencia, el objetivo principal de esta tesis es evaluar la aplicación del proceso de APR para el tratamiento y valorización simultáneos de las aguas residuales.

Para evaluar la flexibilidad del proceso, se trataron diferentes tipos de aguas residuales industriales por APR, principalmente para la producción de H_2. Se utilizaron catalizadores de Pt y catalizadores bimetálicos basados en Pt (PtRe y PtPd) soportados en diferentes materiales de carbono, con los que se investigó la influencia de diferentes variables que podrían afectar el rendimiento catalítico. Asimismo, se evaluó la estabilidad de los catalizadores y se acoplaron dos procesos al APR (hidrogenación y oxidación húmeda catalítica con aire (CWAO)).

En el APR de aguas residuales de cocción de atún a 200 ºC utilizando catalizadores de Pt soportados en diferentes materiales de carbono, se lograron altos valores de eliminación de TOC y COD (45 – 60 %) debido a una combinación de adsorción en los soportes, carbonización hidrotermal (HTC) y APR. La producción de gases fue baja y el CO_2 fue el principal componente del gas (82 – 99 %), debido a la presencia de impurezas que condujeron a la desactivación del catalizador, como por ejemplo cloruros. El

uso de un soporte básico aumentó significativamente la producción de gases y el porcentaje de H_2 en la fracción gaseosa. Además, la producción de gases aumentó en la operación semi-continua en comparación con la discontinua.

En la APR de las aguas residuales de cerveceras, se observó que la HTC es la principal contribución en los experimentos sin catalizador. En los experimentos en discontinuo de APR con catalizadores, se observó el mejor rendimiento catalítico a temperaturas más altas (225 ºC) y utilizando un soporte de negro de humo altamente mesoporoso, prácticamente sin microporosidad y con elevado pH slurry (≈ 50 % de H_2 y 12,2 mmol H_2 / g COD_i). La eliminación de materia orgánica aumentó hasta el 99 % al disminuir la carga orgánica de las aguas residuales. La adición de KOH o NaOH al agua residual también dio lugar a una eliminación ligeramente menor de TOC y COD, sin embargo, se obtuvo un mayor rendimiento de H_2 en aquellos casos en los que se agregó KOH. El aumento de la concentración de KOH condujo a la producción de H_2 sin CO_2 y sin cambios significativos en el rendimiento de H_2 y los resultados con las aguas residuales reales y sintéticas de la cervecería fueron relativamente similares. En experimentos en continuo de APR a 225 ºC, los catalizadores PtRe/C exhibieron una mayor actividad catalítica y producción de H_2 que los de Pt/C, atribuible a un aumento en la actividad en la reacción del gas de agua (WGS). Un mayor tiempo de residencia y un mayor caudal de gas portador también aumentaron la producción de H_2. A bajos valores de *time-on-stream* (TOS), los catalizadores de Pt soportados en diferentes carbonos modificados, cuya microporosidad se redujo gradualmente por la impregnación y carbonización de una resina resol, mostraron una mayor producción de H_2 que el catalizador de Pt de referencia y se observó un efecto indirecto de tamaño de las nanopartículas (NPs) de Pt. Todos los catalizadores probados mostraron una desactivación importante con el TOS y la caracterización de los catalizadores usados reveló que la principal causa de la desactivación de los catalizadores

en las primeras horas de reacción fue la deposición de coque en la superficie de los mismos. Finalmente, se logró una mayor selectividad y rendimiento de H_2 después del pretratamiento de la alimentación por hidrogenación, y el acoplamiento hidrogenación-APR se consideró eficiente ya que la producción de H_2 compensó la necesidad de la hidrogenación y la durabilidad del catalizador también se incrementó, debido a la reducción de la formación de depósitos carbonosos.

En el APR de aguas residuales de la producción de zumos de frutas con catalizador de Pt/C a 220 ºC, la producción de H_2 se vio poco afectada por el pH, produciendo alrededor de 6,6 mmol H_2 / g COD_i, en el intervalo de pH probado. La eliminación de carbono orgánico disminuyó ligeramente con las cargas orgánicas más altas y se observó el mayor valor de rendimiento de H_2 con la carga orgánica baja-media. Finalmente, se observó una disminución del rendimiento de H_2 de 7,8 a 4,2 mmol de H_2 / g de COD_i a una alta salinidad, debido a la desactivación del catalizador.

En el APR de aguas residuales con compuestos fenólicos, se observó una elevada eliminación de TOC y COD (74 – 90 %) para alimentaciones con compuestos representativos de la ruta de oxidación del fenol, con valores más altos para ácidos de cadena larga. La producción de H_2 fue baja en todos los casos, debido a la conversión competitiva directa a CH_4 de los ácidos de cadena larga y corta. En el APR de mezclas de alimentaciones, se logró el mayor rendimiento de CH_4 (11,0 mmol de CH_4 / g TOC_i) para mezclas ricas en ácidos. EL acoplamiento CWAO-APR resultó en una eliminación similar de TOC y COD y una mayor producción de gases y rendimiento de CH_4 que la APR directa, lo que indica que dicho acoplamiento puede superar la baja conversión y producción de gases observada en la APR directa de fenol.

List of publications

1. Oliveira, A.S., Baeza, J.A., Calvo, L., Alonso-Morales, N., Heras, F., Lemus, J., Rodriguez, J.J., Gilarranz, M.A., **Exploration of the treatment of fish-canning industry effluents by aqueous-phase reforming using Pt/C catalysts**, Environ. Sci. Water Res. Technol. 4 (2018) 1979–1987.

2. Oliveira, A.S., Baeza, J.A., Calvo, L., Alonso-Morales, N., Heras, F., Rodriguez, J.J., Gilarranz, M.A., **Production of hydrogen from brewery wastewater by aqueous phase reforming with Pt/C catalysts**, Appl. Catal. B Environ. 245 (2019) 367–375.

3. Oliveira, A.S., Baeza, J.A., Garcia, D., Saenz de Miera, B., Calvo, L., Rodriguez, J.J., Gilarranz, M.A., **Effect of basicity in the aqueous phase reforming of brewery wastewater for H_2 production**, Renew. Energy. 148 (2020) 889–896.

4. Saenz de Miera, B., Oliveira, A.S., Baeza, J.A., Calvo, L., Rodriguez, J.J., Gilarranz, M.A., **Treatment and valorisation of fruit juice wastewater by aqueous phase reforming: Effect of pH, organic load and salinity**, J. Clean. Prod. 252 (2020) 119849.

5. Oliveira, A.S., Cordero-Lanzac, T., Baeza, J.A., Calvo, L., Rodriguez, J.J., Gilarranz, M.A., **Catalytic performance and deactivation of Pt/C and PtRe/C catalysts in continuous aqueous phase reforming of brewery wastewater**, (submitted).

6. Oliveira, A.S., Baeza, J.A., Saenz de Miera, B., Calvo, L., Rodriguez, J.J., Gilarranz, M.A., **Catalytic wet air oxidation coupled to aqueous phase reforming for the removal and valorisation of phenolic compounds**, (submitted)

7. Oliveira, A.S., Baeza, J.A., Calvo, L., Rodriguez, J.J., Gilarranz, M.A., **Optimised H_2 production in continuous aqueous phase reforming of brewery wastewater**, (not published).

8. Oliveira, A.S., Aho, A., Baeza, J.A., Calvo, L., Rodriguez, J.J., Gilarranz, M.A., Murzin, D., **H_2 production via aqueous phase reforming of maltose**, (not published).

List of publications

This thesis is based on eight original articles, four of them already published and the others in the process of publication. The author of the thesis is the main author of almost all articles, where the contribution includes experimental procedures, analysis of the results and article writing and editing.

List of related publications

1. Baeza, J.A., Oliveira, A.S., Calvo, L., Alonso-Morales, N., Heras, F., Rodriguez, J.J., Gilarranz, M.A.: "Reformado en fase acuosa de efluentes de cocción de atún empelando catalizadores soportados en materiales carbonosos", XIV Reunión del Grupo Español de Carbón, Malaga, Spain, 22-25 October, 2017 – *poster presentation*.

2. Oliveira, A.S., Baeza, J.A., Calvo, L., Alonso-Morales, N., Heras, F., Rodriguez, J.J., Gilarranz, M.A.: "Treatment of brewery wastewater through aqueous phase reforming", Workshop on Technologies for Monitoring and Treatment of Contaminants of Emerging Concern, Madrid, Spain, 23-24 November, 2017 – *poster presentation*.

3. Oliveira, A.S., Baeza, J.A., Calvo, L., Alonso-Morales, N., Heras, F., Rodriguez, J.J., Gilarranz, M.A.: "Aqueous phase reforming of brewery wastewater using carbon supported Pt catalysts", Carbon 2018, Madrid, Spain, 1-6 July, 2018 – *poster presentation*.

4. Baeza, J.A., Oliveira, A.S., Calvo, L., Alonso-Morales, N., Heras, F., Rodriguez, J.J., Gilarranz, M.A.: "Stability of carbon-supported Pt catalysts on the aqueous phase reforming of tuna-cooking wastewater", Carbon 2018, Madrid, Spain, 1-6 July, 2018 – *poster presentation*.

5. Oliveira, A.S., Baeza, J.A., Calvo, L., Alonso-Morales, N., Heras, F., Rodriguez, J.J., Gilarranz, M.A.: "Reformado en fase acuosa de aguas residuales de la industria cervecera usando catalizadores de Pt/C: Efecto del soporte, temperatura de reacción y carga orgánica inicial", XXVI Congresso Ibero-Americano de Catálise (CICAT 2018), Coimbra, Portugal, 9-14 September, 2018 – *oral presentation*.

6. Oliveira, A.S., Saenz de Miera, B., Baeza, J.A., Calvo, L., Rodriguez, J.J., Gilarranz, M.A.: "Efecto de la salinidad en el reformado en fase acuosa de aguas residuales de la industria de producción de zumos de frutas", Reunión de la SECAT (SECAT'19), Córdoba, Spain, 24-26 June, 2019 – *oral presentation*.

7. Gilarranz, M.A., Oliveira, A.S., Baeza, J.A., Garcia, D., Heras, F., Alonso-Morales, N., Saenz de Miera, B., Calvo, L., Rodriguez, J.J.: "Carbon-supported Pt catalysts for the treatment and valorisation of brewery

wastewater through aqueous phase reforming in alkaline medium", Carbon 2019, Lexington, KY, EUA, 14-19 July, 2019 – *oral presentation*.

8. Gilarranz, M.A., Oliveira, A.S., Cordero-Lanzac, T., Baeza, J.A., Heras, F., Calvo, L., Rodriguez, J.J.: "Study of the deactivation of carbon-supported mono- and bimetallic catalysts used in the aqueous phase reforming of brewery wastewater", Carbon 2019, Lexington, KY, EUA, 14-19 July, 2019 – *poster presentation*.

9. Oliveira, A.S., Saenz de Miera, B., Baeza, J.A., Calvo, L., Rodriguez, J.J., Gilarranz, M.A.: "Aqueous phase reforming of fruit juice wastewater: Effect of pH and salinity", International Congress on Catalysis for Biorefineries (CatBior 2019), Turku, Finland, 23-27 September, 2019 – *oral presentation*.

10. Gilarranz, M.A., Oliveira, A.S., Baeza, J.A., Saenz de Miera, B., Calvo, L., Heras, F., Rodriguez, J.J.: "Treatment of real brewery wastewater by aqueous phase reforming with carbon supported Pt catalysts", 8th International Conference on Carbon for Energy Storage and Environment Protection (CESEP'19), Alicante, Spain, 20-24 October, 2019 – *poster presentation*.

List of acronyms

A_{EXT} – External surface area

APR – Aqueous Phase Reforming

BOD – Biological Oxygen Demand

CIP – Cleaning-In-Place

COD – Chemical Oxygen Demand

CWAO – Catalytic Wet Air Oxidation

FJW – Fruit Juice Wastewater

FJW-HSC – Fruit Juice Wastewater – High Salt Concentration

FJW-LSC – Fruit Juice Wastewater – Low Salt Concentration

GC – Gas Chromatography

HMF – Hydroxymethylfurfural

HPLC – High Performance Liquid Chromatography

HTC – Hydrothermal Carbonization

IC – Ionic Chromatography

NPs – Nanoparticles

RBW – Real Brewery Wastewater

S_{BET} – Specific surface area

SBW – Synthetic Brewery Wastewater

STEM – Scanning Transmission Electron Microscopy

TCW – Tuna Cooking Wastewater

TG – Thermogravimetry

TGA – Thermogravimetric Analysis

TOC – Total Organic Carbon

TOF – Turnover Frequency

TOS – Time-on-stream

TPD – Temperature Programmed Desorption

TPO – Temperature Programmed Oxidation

WGS – Water-Gas Shift

WHSV – Weight hour space velocity

XPS – X-ray Photoelectron Spectroscopy

List of figures

List of tables

Table of contents

Chapter I. General introduction

1. Motivation

The circular economy approach has attracted much interest in the last few years, given the current scenario of high dependence on fossil fuels and human-borne climate change. This approach involves, among others aspects, transitioning from fossil-based to renewable energy sources and a more efficient use of raw materials and products, aimed to minimize waste and pollution. In this sense, waste valorisation is an essential approach to close the loop and meet the circular economy aims [1]. On the other hand, H_2 is a powerful fuel considered as an alternative to replace fossil fuels in the future as energy carrier for transportation and power generation [2–4]. In addition, according to technical and environmental comparison studies between H_2 energy and fossils fuels, such as oil, natural gas and coal, H_2 could be a solution for some environmental challenges [5], since this energy carrier is more sustainable and cleaner than current fossil fuels. However, most of the H_2 currently produced is obtained from non-renewable sources, mainly through gasification and thermocatalytic process of natural gas [6,7]. Therefore, to generalize H_2 as an environmentally friendly energy carrier, its production should be made from clean and renewable sources.

In this context, H_2 production from biomass derived compounds through aqueous phase reforming (APR) has received great attention since it was reported by Cortright *et al.* in 2002 [8], as this process shows potential advantages over conventional catalytic steam reforming of hydrocarbons. For instance, APR is carried out in liquid phase, under mild reaction conditions (200 – 250 ºC, 15 – 50 bar) and without previous vaporization of both water and oxygenated hydrocarbons, which leads to a significant reduction of energy consumption and minimizes undesirable parallel decomposition reactions of the compounds, typically favoured at high temperatures [9]. In addition, this process is generally performed under conditions that favour

water-gas shift (WGS) reaction, generating H_2 with negligible CO concentration, and the reaction pressure could facilitate the gas purification processes [8,9].

H_2 production through APR has also been reported as more energy efficient than autoreforming and steam reforming process [10]. Figure I-1 shows the energy (thermal and electrical) and cooling needs for H_2 production from glycerol and the operating conditions of the processes using three reforming technologies. The higher requirements of autoreforming and steam reforming are due to vaporization of the feedstock, while APR generates energy in the form of low pressure steam [10]. Therefore, APR offers an efficient route for H_2 production from renewable sources.

	autoreforming	steam reforming	aqueous phase
oxygen added (mol/mol)	0.187		
steam added (mol/mol)	3.038	2.738	
temperature (°C)	746	587	265

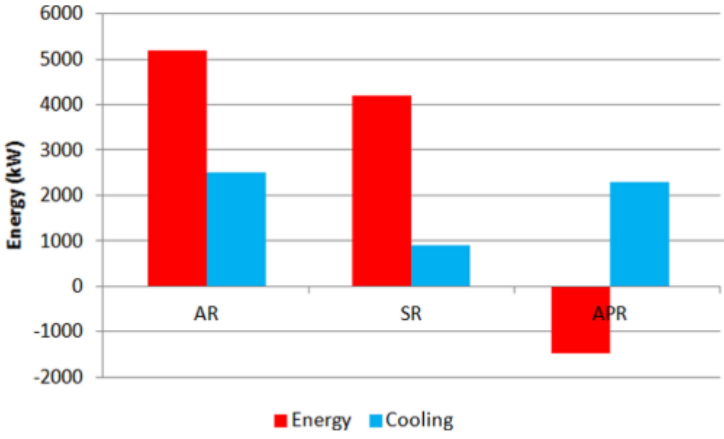

Figure I-1. Net energy balance and operations conditions for H_2 production by reforming of glycerol [10]

Main substrates traditionally studied in APR are oxygenated hydrocarbons model compounds including sorbitol, xylitol, glycerol, ethylene glycol, etc. [11–14], for which promising results have been reported in terms of conversion, H_2 selectivity and yields of valuable gases (H_2 and alkanes) produced. However, concerning the feasibility of the process, techno-economic studies on APR have shown that the feedstock is the major contributor to H_2 production cost, having a significant impact on the economy of the process [15]. Therefore, feeding APR processes with waste materials is worthwhile to investigate. With this perspective, the use of APR could be extended to biomass-derived wastewater treatment, thus integrating wastewater treatment and valorisation of effluents. Industries producing large volumes of wastewater with high loads of biomass-derived organic compounds or with effluents that are difficult to treat by conventional technologies are interesting candidates for the implementation of wastewater treatment by APR. Consequently, in this work, different types of wastewaters have been selected to evaluate the application of this process to simultaneous treatment and valorisation of residues. Likewise, different variables that could affect the performance of the process and catalysts deactivation have been evaluated. Finally, the combination of hydrogenation and APR reactions has been performed to increase H_2 production and reduce catalyst deactivation by coke deposition. Likewise, the coupling of catalytic wet air oxidation to the APR process has been carried out as an approach to improve the removal and valorisation of compounds to valuable gases.

2. Aqueous phase reforming reaction

The main reactions in APR of oxygenated hydrocarbons with a C:O stoichiometry ratio of 1:1 can be described by Equations (1-3), where WGS reaction is presented in Equation (2).

$$C_nH_{2n}O_n \rightleftarrows n\,CO + n\,H_2 \quad (1)$$

$$CO + H_2O \rightleftarrows CO_2 + H_2 \quad (2)$$

$$C_nH_{2n}O_n + n\,H_2O \rightleftarrows n\,CO_2 + 2n\,H_2 \quad (3)$$

In addition to the reforming and WGS reactions, other reactions such as methanation, Fischer-Tropsch, decarboxylation, dehydrogenation or dehydration/hydrogenation also occur in different extent [8]. Figure I-2 shows simplified reaction pathways for H_2 and alkanes production from oxygenated hydrocarbons over a metal catalyst. The first step is the dehydrogenation of the compound on the metal surface generating adsorbed intermediates followed by C-C or C-O bonds cleavage. The following step, C-C bond cleavage, leads to the formation of CO and H_2, and CO can react through WGS reaction generating more H_2 and CO_2. On the other hand, C-O bond cleavage followed by hydrogenation leads to alcohols and alkanes formation. Alcohols can also be formed by dehydration reactions followed by hydrogenation on the metal surface and alkanes can be produced by methanation, Fisher-Tropsch reaction, dehydration/hydrogenation of alcohols or by parallel pathways from organic acids and alcohols. Finally, acids can be formed by dehydrogenation reactions catalysed by the metal, followed by rearrangement reactions in parallel pathways [8,9].

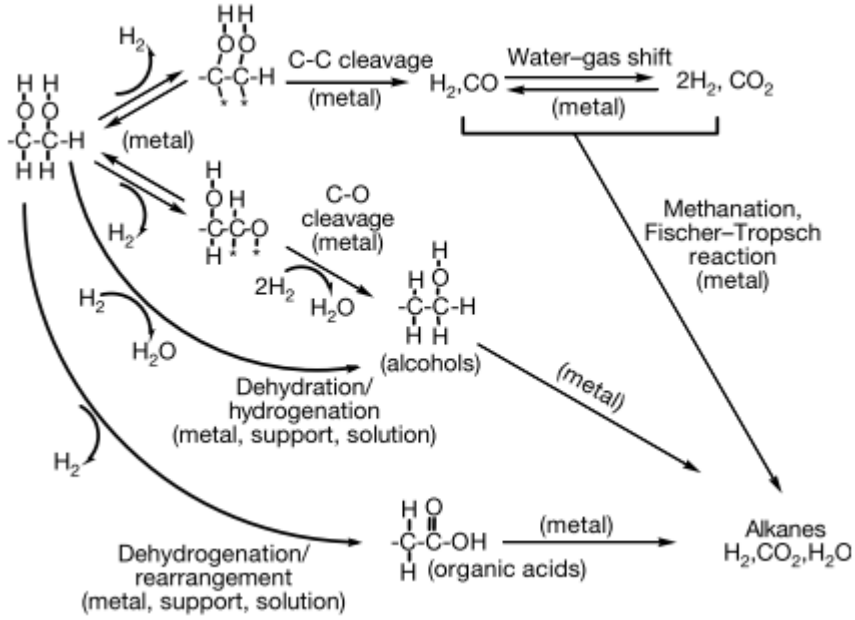

Figure I-2. Reaction pathways for H_2 and alkanes production from reactions of oxygenated hydrocarbons over a metal catalyst (*represents a surface metal site) [8]

Due to the various reactions involved, the APR process can be adjusted to the production of H_2, alkanes as well as other chemicals. Activity and selectivity in APR are strongly dependent on the catalytic system and the reaction conditions, including pressure, temperature, active metal, support, additives, type of reactor, etc. [16,17]. The effect of some of these parameters is described below.

2.1. Effect of active metal

High selectivity for H_2 production through APR of oxygenated hydrocarbons require an efficient catalyst that promote C-C bond cleavage and WGS reaction and minimize C-O bond cleavage [9]. Accordingly, a diversity of catalytic systems, mainly based on VIII group metals, has been

described in the literature [11,17]. Pt and Pd monometallic catalysts exhibited higher selectivity for H_2 production and lower selectivity for alkane production, while Rh, Ru and Ni catalysts showed low selectivity for production of H_2 and favoured alkane production [11]. Ni catalysts exhibited a similar catalytic activity than Pt catalyst [11], however low stability has been observed for this type of catalyst [18]. Regarding Re catalysts, they showed significantly lower activity than Pt catalyst [19]. Therefore, Pt-based catalysts have showed to be the most effective among monometallic catalysts in terms of activity and selectivity toward H_2-rich gas [9].

On the other hand, different bimetallic Pt based catalysts (PtNi, PtCo, PtRu, PtFe and PtRe) have also been used in APR reaction, showing in general a higher catalytic activity than monometallic ones [19–21]. In this sense, He *et al.* [22] compared the H_2 and CH_4 selectivities of different bimetallic catalysts (atomic ratio 1:1) with Pt catalyst in the APR of glycerol. All second metals added facilitated the formation of CH_4 in different extension and the addition of Ni and Co also decreased the H_2 selectivity. H_2 selectivity followed a descending order of PtPd > PtRu > PtCu > Pt > PtCo > PtNi, while the order for CH_4 selectivity was PtPd > PtCu > PtRu > PtNi > PtCo > Pt. PtRe catalysts have shown a superior performance compared to other bimetallic catalysts (PtNi, PtCo and PtRu) in the APR of xylitol, although the H_2 selectivity was lower due to reaction shifting to alkanes formation [19]. Ciftci *et al.* [23] attributed the increase in the catalytic activity in the APR of glycerol with PtRe/C catalyst to an increase in the WGS activity, although they pointed out that the main effect of Re addition was the increase of dehydration reactions. In addition, the catalytic activity of Pd catalysts in the APR of ethylene glycol has also been improved by addition of Fe as a WGS promoter [20].

The interaction between the metal and the catalyst support also influences the APR performance of the catalysts. In this sense, the dispersion

of Pt nanoparticles (NPs) is closely connected to the catalytic performance. A high metal dispersion results in higher APR activity and H_2 production [24,25]. On the other hand, the catalytic activity has also been shown to be affected by the mean Pt NPs size, although the influence of nanoparticle size has not been totally elucidated. For instance, Lehnert and Claus [26] studied the influence of Pt NPs size and reported that H_2 selectivity in the APR of glycerol increased from 78 to 95 % with increasing the mean NPs size from 1.6 to 3.2 nm, while glycerol conversion remained almost constant. They suggested that the adsorption of the oxygenated hydrocarbon for subsequent C-C bond cleavage is more favoured at terraces than at edges and corner atoms, and as the metal NPs size increases the surface contains more atoms in terraces at the expense of edge and corner atoms. In contrast, Chen *et al.* [27] reported that the gas volume produced and the H_2 selectivity increased when the Pt NPs size decreased from 5.7 nm to 1.6 nm in the APR of low-boiling fraction of bio-oil. They suggested that smaller NPs size could provide more stable Pt-C bond than Pt-O bond and facilitate the C-C bond cleavage for H_2 production. Similarly, Ciftci *et al.* [28] have investigated the influence of Pt NPs size in the APR of glycerol in the 1.2 to 4.2 nm range. They found that the catalyst with an intermediate NPs size of 2 nm exhibited optimum C-C bond cleavage rates as well as optimum activity towards H_2 production, due to higher WGS activity of NPs with this intermediate size. Likewise, Callison *et al.* [29] have also found a higher H_2 yield for smaller Pt NPs size (2.2 nm) in the APR of glycerol. In addition, these authors have also reported that an increase in Pt NPs size from 2.2 to 3.6 nm led to a higher glycerol conversion and changed the reaction pathway showing a different product distribution.

2.2. Effect of support

The catalytic support used may also have an impact on the APR process. Different supports have been tested in APR, including oxides, such as SiO_2, Al_2O_3, ZrO_2, CeO_2, MgO and TiO_2 [11,30–32], and carbon materials [21,33]. Basic supports resulted in higher activity and H_2 yield, whereas acidic and neutral supports led to an increase in alkane formation [12]. Furthermore, the basic sites are important for WGS reaction, playing a key role in H_2 production, thus enhancing the performance of the APR process [32]. Pt catalysts supported on solid basic oxides exhibited excellent activity in APR reaction [32] and most of the publications on APR are focused on Pt supported on γ-Al_2O_3, due to the high selectivity to H_2 [34–36]. However, γ-Al_2O_3 has shown limited stability under APR conditions [35,36] since undergoes phase transformation to boehmite [37], which cause catalyst deactivation [38,39]. In addition, the activity of catalysts supported on γ-Al_2O_3 is generally poor when compared with those using other supports such as carbon materials [40]. Consequently, carbon supports have generated attention in recent years, due to superior activity, high hydrothermal stability, and tuneable textural surface and chemical properties of carbon supported catalysts.

Different types of carbon supports, such as, activated carbons, carbon nanotubes and mesoporous carbons have been used in APR reactions [21,24,25,40,41]. Additionally, some authors [24], have also reported that the textural surface properties of carbon materials are also important for catalytic performance, since mesoporous carbon materials have exhibited better catalytic activity compared to activated carbons, mainly microporous. These authors suggested that the irregular porous structure of activated carbon and its microporosity hinder the access of reactants to the catalytic active sites in the liquid phase and prevent the removal of products in the gas phase.

Moreover, textural characteristics such as irregular pore arrangements, broad distribution of pore size and high microporosity have been reported to diminish the activity and reduce H_2 selectivity [24].

2.3. Effect of type and organic load of feedstock

The type of substrate and the organic load of feedstock have a significant impact on the catalytic performance. Oxygenated hydrocarbons having a C:O stoichiometry ratio of 1:1 have been used as model compounds in many studies [8,9]. Chheda *et al.* [42] reported that a C:O ratio of 1:1 is needed to obtain high H_2 selectivity and some studies reported that APR reaction pathway may depend on the C:O ratio of substrate [8,13]. The related studies suggested that O atoms bounded to C atoms favour the production of H_2 and CO because of C-C bond weakening [43]. On the other hand, H_2 selectivity and yield have been found to increase as the length of the carbon chain decreases, while the selectivity for alkanes production increases, due at least partially to a lower contribution of side reactions [8,9,44]. Consequently, APR of more reduced compounds (e.g. sorbitol, glycerol, ethylene glycol and methanol) leads to higher H_2 selectivity and yield values than APR of glucose. Therefore H_2 selectivity and yield improve in the following order: glucose < sorbitol < glycerol < ethylene glycol < methanol [8,44].

APR of less concentrated feedstocks has been found to proceed with higher H_2 yield and higher carbon conversion to gas [35]. In the APR of glycerol, some authors [45,46] have reported that the increase of glycerol concentration significantly decreases conversion and H_2 yield. In the case of sugars, such as glucose, the rate of homogeneous side reactions that consume H_2 increases with the increase of organic load, thus decreasing the H_2 selectivity and yield [47]. In addition, these undesired reactions can produce carbonaceous deposits that promotes catalyst deactivation [9].

2.4. Effect of additives and impurities

Most of the literature on APR is focused on model compounds and is addressed mainly to learn on the effect of the catalytic system and the reaction conditions on the performance of the process [9,17,35], while studies based on more complex substrates are infrequent. There are only few studies that analyse the effect of impurities or mixtures of compounds on catalytic performance [26,48–51]. These studies deal mostly with the APR of crude glycerol in aqueous fractions from biorefineries. For instance, Lehnert and Claus [26] observed that the inorganic salts of crude glycerol strongly affect the catalytic activity, leading to lower H_2 production compared to pure glycerol. That loss of activity is probably due to catalyst poisoning by blockage of active sites. Boga *et al.* [48] also found similar results for APR of crude glycerol using 1 wt. % Pt on Al_2O_3 as catalyst. They reported that H_2 selectivity decreased dramatically from 64 to 1 % when pure glycerol was replaced by crude glycerol. The deactivation for this type of complex feedstocks was attributed to fatty acids, such as stearic and oleic and their salts, long chain alkanes and olefins, formed from the fatty acid derivatives in the feed, which can block partially the Pt active sites. The use of activated carbon, instead of Al_2O_3, as support has been observed to significantly improve glycerol conversion and H_2 selectivity, due to adsorption of stearic acid on the carbon support [48].

Regarding the effect of the basic or acidic nature of the reaction medium, acidic solutions promote alkane formation because favour acid-catalysed dehydration reactions followed by hydrogenation. In contrast, neutral and basic solutions favour high H_2 selectivity and low alkane selectivity [9]. In this sense, He *et al.* [22] and Liu *et al.* [52] reported that addition of CaO or KOH to the reaction medium can favour the WGS reaction by gas withdrawal through the *in-situ* removal of CO_2, displacing the

reactions towards H_2 production. Liu *et al.* [52] also suggested that KOH addition could favour WGS reaction by providing hydroxyl anions that could induce polarization and dissociation of water. Additionally, Huber *et al.* [53] reported that H_2 selectivity decreased from 43 to 6 % in the APR of sorbitol when the pH of the feedstock decreased from 7 to 2 by the addition of HCl, while the alkane selectivity increased from 27 to 47 %. Moreover, the alkanes distribution also shifted to heavier alkanes when the pH decreased. Similarly, Remón *et al.* [49] analysed the effect of biodiesel-derived impurities (CH_3OH, CH_3COOH and KOH) on the APR of glycerol. The presence of KOH increased gas production, whereas CH_3COOH and CH_3OH led to decreased gas production and glycerol conversion, respectively.

Remón *et al.* [50] also studied the effect of different acids (H_3PO_4, H_2SO_4, and CH_3COOH) and bases (KOH and NaOH) in the APR of glycerol using Ni-La/Al_2O_3 catalyst. They reported that these compounds significantly accelerated catalyst deactivation, especially in the case of H_2SO_4 and KOH. King *et al.* [54] studied the effect of KOH in the APR of glycerol with PtRe/C and Pt/C catalysts, and found that glycerol conversion and production of liquids increased, while H_2 production was barely affected. Likewise, they suggested that C-O bond cleavage is more favoured than C-C bond cleavage by the addition of KOH, due to the increase of base-catalysed dehydration followed by hydrogenation reactions that reduce H_2 production. Karim *et al.* [55] also found similar results in the APR of glycerol with Pt/C catalysts. The addition of KOH did not affect the gas phase products, while a higher glycerol conversion was observed. These authors have also attributed the results to a higher selectivity toward dehydration reactions, which has been reflected in a higher C-O/C-C ratio and lower H_2 and CO_2 selectivities in the presence of KOH.

According to these studies, some additives and impurities can significantly alter the catalyst performance and the role of some of them in the reaction medium is not well addressed.

2.5. Effect of temperature and pressure

The effect of reaction temperature and pressure on the APR process has been studied in various works. Lower reaction temperatures result in lower carbon conversion to gas, but also higher H_2 selectivity, in part due to lower conversion and lower consumption by H_2 reaction with liquid-phase products [8]. On the contrary, higher temperatures increase the H_2 yield, mainly due to the increase of conversion [56], favoured by the increase in the fragmentation of the initial compound through C-C and C-O bonds cleavage [57], and decrease the carbon conversion to liquid. The total pressure also has a significant effect on the catalytic performance. Higher pressures, above the bubble point of the feedstock, increase alkanes production and decrease H_2 production and selectivity [44]. Likewise, lower conversions have also been observed with the increase of total pressure [44,58]. The partial pressure of gaseous products increase with the total reaction pressure, consequently increasing H_2 partial pressure and the rate of hydrogenation reactions, thus decreasing H_2 production and selectivity, as C-C bond cleavage on the catalyst surface is not enhanced at high pressure [9].

Seretis and Tsiakaras [45] evaluated the effect of temperature (200 – 240 ºC) in the APR of glycerol (1 wt. %) under autogenous pressure (16 – 33.5 bar). The maximum H_2 yield (8.3 %) and H_2 production (0.64 mol H_2 / g Pt) was obtained at 240 ºC. Similarly, using a high concentration of glycerol (80 wt. %) Özgür and Uysal [59] have also studied the effect of reaction temperature (160 – 280 ºC), and reported that the optimum temperature for H_2 production is 230 ºC, since the extent of some undesired side reactions increased above this temperature.

Roy *et al.* [58] reported that in the APR of butanol at 215 ºC the H_2 and CO_2 selectivities presented a maximum at the bubble pressure value and then decreased with the increase of pressure. This has been attributed to a competitive adsorption of gases on the catalyst surface at higher pressures, leading to a lower availability of active sites. Additionally, Remón *et al.* [60] have studied the effect of temperature (200 – 240 ºC) and pressure (38 – 50 bar) in the APR of crude glycerol. Gas production was favoured at low pressure (39 bar) and high temperature (238 ºC), while high pressure (45 bar) and medium temperature (216 ºC) favoured the production of liquids. Thus, low pressure could make the active sites more available by increasing the rate of desorption of gaseous products, while higher temperatures favoured fragmentation of the organic matter increasing gas production.

2.6. Effect of other parameters

Many other parameters can affect the catalytic performance in APR, among them, the effect of carrier gas flow and liquid space velocity can be highlighted in continuous experiments. Higher reforming rates have been obtained when N_2 was fed as carrier gas to the reactor combined with the liquid feed [47]. Some authors [61] proposed N_2 co-feeding gas as stripping agent in a microchannel reactor to promote mass transfer and decrease H_2 concentration on catalyst surface. Thanks to this strategy, both sorbitol conversion and H_2 selectivity increased by a factor of 2.4 and 5.2, respectively, using N_2 co-feeding, due to lower extent of side reactions involving H_2.

On the other hand, Luo *et al.* [35] reported the effect of liquid hourly space velocity (1.56 – 3.12 h^{-1}) in the APR of glycerol using a flow reactor. Decreasing the hourly space velocity (i.e. increasing contact time) resulted in a higher H_2 yield, H_2 selectivity and carbon conversion to gas. On the contrary, Duarte *et al.* [62] related a decrease of H_2 selectivity and an increase

of H_2 yield and xylitol conversion with an decrease of weight hourly space velocity. This discrepancy could be due to different conversion values of substrate compounds in each study. At higher conversions levels, the H_2 selectivity decreases using lower space velocities due to a larger H_2 consumption in side reactions [14]. In contrast, when the conversion decrease at increasing space velocities, the H_2 selectivity also decrease [14]. Therefore, generally conversion and the rate of formation of gaseous products goes to a maximum increasing contact time [57].

3. Application of aqueous phase reforming to the treatment and valorisation of wastewater

Different types of substrate compounds, such as alcohols, polyols, sugar [13,14,16,34,47], bio-oil [27,63], cellulose [64,65] and different types of lignocellulosic biomass [21,66], have been used as feedstocks for the APR process, mainly for H_2 production. According to the promising results reported in terms of conversion and H_2 selectivity and yield, the process could be extended to new potential applications, such as the treatment and valorisation of wastewater. However, most of the reported studies have investigated the APR of model compounds, ranging from C1 to C6, while studies using more complex feedstocks, such as wastewater, are scarce.

On the other hand, valorisation of the biomass-derived pollutants contained in wastewater and the possible economic advantage of the use of wastewater as a feedstock are some of the strong points of this approach. In this sense, a recent study focused on process design and techno-economic analysis of H_2 production by APR of sorbitol reported that the main burden of the process derives from the feedstock, accounting close to 92 % of the total H_2 production cost [15]. Consequently, APR appears as a promising solution integrating wastewater treatment and a way of valorisation for those

industries producing large volumes of wastewater with high loads of biomass-derived organic compounds or with pollutants that are difficult to treat by conventional technologies.

4. Catalysts stability

The catalyst stability is a relevant issue in APR studies. In the literature, there are some studies on this matter, using mainly alumina as support and model compounds in the APR experiments, which does not reflect the magnitude of deactivation expected in practical applications. On the other hand, the deactivation of carbon supported catalysts under severe APR hydrothermal conditions is a common characteristic for all systems investigated. The studies about catalyst stability have reported that loss of the surface area, due to the collapse and blockage of the support structure [39], sintering [31,44] and leaching of metal phase [67] are the main causes of deactivation. In addition, some studies have also reported coke deposition on the catalyst surface [67,68]. However, there is a lack of information on the deactivation of catalysts using more complex feedstocks.

5. Improvement strategies

Some improvement strategies may be applied to the APR process to improve the catalytic performance. Some of these strategies are related to the improvement of the mass transfer of H_2, since studies reported that this parameter affect the selectivity and distribution of process products [69]. In this sense, Neira D'Angelo *et al.* [69] reported that H_2 selectivity was twice as high using a microchannel reactor than a fixed bed reactor, due to the fast mass transfer of H_2 in the microchannel reactor, which avoid H_2 consumption in side reactions. Membrane reactor could also be used to remove H_2 and

avoid its consumption in undesired reactions, achieving a H_2 yield 2.5 times higher than using a reactor without membrane [70].

Another improvement strategy is the use of hydrogenation as a pretreatment stage of the feedstock in the APR of sugars, especially for more concentrated solutions. The APR of very dilute solutions is not economically attractive, although high H_2 selectivity and yield are achieved. On the other hand, the use of concentrated solutions of sugars lead to a rate increase in homogeneous side reactions and carbonaceous deposits formation [9]. For this reason, the processing of more concentrated feedstocks with more reduced compounds, such as sorbitol, glycerol or ethylene glycol, could be an alternative to reduce the undesirable homogeneous reactions observed with glucose [8]. In this sense, Davda and Dumesic [47] performed a study that combined hydrogenation and APR of glucose for H_2 production. They reported that glucose was completely hydrogenated to sorbitol in the first step and then sorbitol was converted to H_2 and CO_2, also achieving a high H_2 selectivity (62.4 %). Additionally, the net production of H_2 per mol of glucose was improved a 290 %. Irmak *et al.* [71] also performed hydrogenation experiments of glucose and biomass hydrolysates before APR and reported that reduced solutions produced significantly higher H_2 yield and selectivity than non-reduced solutions.

Chapter II. Aim and scope of the thesis

Based on the background described in the general introduction, the main aim of this thesis is to evaluate the application of APR process to the simultaneous treatment and valorisation of wastewaters. In order to verify the sensitiveness of the process to the type and concentration of organic pollutants, organic load, pH, salinity and C:O ratio, wastewaters from different types of industries have been considered, with the focus mainly in H_2 production. The behaviour of these different feedstocks, varying from single compounds to mixtures usually found in industrial wastewater, has been analysed. In addition, the effect of some process parameters, such as reaction temperature, wastewater concentration, addition of bases and impurities on the catalytic performance has been investigated.

The current work has been conducted using mainly Pt catalysts, in accordance with the best performance presented for H_2 production. Likewise, Pt based bimetallic catalysts (PtRe and PtPd) have also been used in some experiments. Different carbon materials have been used as supports, and the effect of the chemical composition, structure and textural properties of the support and the active metal on the catalytic performance has been investigated.

Another aim of this work is the evaluation of catalysts stability. Catalyst deactivation is a relevant issue in APR studies, therefore the catalyst stability has been evaluated for most of the types of wastewaters treated, in order to understand the factors that affect deactivation and how to reduce it. With this purpose batch experiments have been complemented with long-term continuous experiments. The reduction of the deactivation of catalysts and the increase in the processability of feedstocks in APR has been addressed by coupling two different reactions to APR. Hydrogenation has been performed as a pre-treatment for APR of sugars with the objective to increase the H_2 production and reduce the formation of carbonaceous deposits. Likewise, catalytic wet air oxidation (CWAO) has been used to

degrade phenolic compounds into intermediates that could be more easily converted by APR process, avoiding some drawbacks of direct APR of phenolic compounds. In this last coupling scheme, the hypothesis that intermediates generated by oxidation with less carbon atoms and a C:O ratio closer or equal to 1:1 should be more selective to H_2 production has been also tested.

According to the proposed objectives, the work presented in this thesis has been structured in a series of independent, but interlinked chapters, as described below.

Chapter I presents the general state-of-the-art for the thesis. The motivation of this work is described and the APR process, together with the main parameters that could affect yield, catalytic performance and deactivation, is detailed. The new potential application of APR process to the treatment and valorisation of wastewater is introduced. Likewise, some improvement strategies to improve the catalytic performance are described. Chapter II presents the aim and scope of the thesis, according to the state-of-the-art.

Chapter III presents the experimental techniques used for preparation and characterization of supports, catalysts and feedstocks. This chapter also presents the procedures for the APR experiments and others reactions used in this work. Main aspects of the experimental procedure also included in the rest of chapters to ease reading. Chapter IV describes the results of the general characterization of supports and catalysts.

Chapter V is devoted to the results of the APR of fish-canning wastewater, using Pt catalysts supported on different carbon materials. APR experiments were carried out in batch and semi-continuous modes and the catalysts stability was also evaluated, with the focus in the effect of wastewater salinity.

Chapter VI shows the results of the APR of brewery wastewater. Different carbon supported Pt catalysts are used in a batch reactor to evaluate the effect of support, organic load and temperature on the process performance (Section 1). Likewise, the effect of the basicity of the feedstock is evaluated and the results of the APR of synthetic and real wastewaters are compared (Section 2). The H_2 production in continuous APR is optimised through the evaluation of the effect of active metal (carbon supported Pt and PtRe catalysts), residence time and carrier gas flow (Section 3). In addition, the catalytic performance and deactivation of the catalysts used in the continuous APR is analysed (Section 4). Finally, hydrogenation of the main compound present in the brewery wastewater (maltose) is evaluated as an approach to increase processability of brewery wastewater and H_2 production in continuous mode using a carbon supported PtPd catalyst (Section 5).

Chapter VII describes the results for the APR of fruit juice wastewater. In this chapter the effect of pH, organic load and salinity are studied in a batch reactor using a carbon supported Pt catalyst.

Chapter VIII shows the results of the CWPO coupled to APR to the treatment and valorisation of wastewater with phenolic compounds. The APR experiments were carried out in batch mode using a carbon supported Pt catalyst.

Finally, Chapter IX summarizes the conclusions from the results and discussions of the previous chapters.

Chapter III. General experimental

This chapter describes the preparation of the supports, catalysts and feedstocks, together with the techniques used to characterize them. The reaction setups are also described, together with the analytical tools for the determination of the composition of both produced gas and liquid effluent. All the equations necessary to obtain all the performance parameters used in the discussion are also listed. A short summary of the experimental procedure is also given at the beginning of each chapter.

1. Preparation and characterization of supports and catalysts

Pt/C catalysts (3 wt. % Pt, carbon basis) were prepared by incipient wetness impregnation using three commercial activated carbons: Norit© CAPSUPER, Norit© SXPLUS (Cabot Corporation) and Merck (Merck); four carbon blacks: ENSACO 250G and 350G (TIMCAL Canada Inc.), Ketjenblack EC-600JD (Akzonobel), Sibunit; and a mesoporous graphitized carbon black (Sigma-Aldrich) as supports. A modified Merck activated carbon was also used as support in some experiments. Modification of Merck was carried out by impregnation with 1, 10, 20 and 40 wt. % of phenolic resol resin (Merck basis) in order to progressively reduce microporosity. Modified activated carbons were denoted as MERxRES, where x corresponds to the mass percentage of resol inserted. Resol impregnation was carried out after dissolution in ethanol, using 0.65 mL of ethanol per g of Merck carbon. Resol in the impregnated materials was cured at 130 ºC in air for 2 h, and then the samples were pyrolyzed at 700 ºC under N_2 flow for 1 h. Metal impregnation was carried out using an aqueous solution of H_2PtCl_6 (8 wt. % in H_2O, Sigma-Aldrich). The impregnated samples were dried overnight in an oven at 60 ºC, calcined in air at 200 ºC during 2 h and then reduced under 25 N mL / min H_2 flow at 300 ºC during 2 h.

PtRe/C (3 wt. % PtRe, carbon basis) catalysts were prepared by sequential incipient wetness impregnation with metal molar ratios of 1:1, 1:2 and 2:1 using Merck as support. Metal impregnation was carried out using an aqueous solution of H_2PtCl_6 (8 wt. % in H_2O, Sigma-Aldrich) and an aqueous solution of $HReO_4$ (75 – 80 wt. % in H_2O, Sigma-Aldrich). These catalysts were calcined at 250 ºC for 2 h and reduced under the same conditions as Pt/C catalysts.

PtPd/C (2.5 wt. % Pt and 1.25 wt. % Pd, carbon basis) catalyst was prepared by incipient wetness impregnation using Sibunit as support. After co-impregnation of the metal precursors (H_2PtCl_6 (8 wt. % in H_2O, Sigma-Aldrich) and $PdCl_2$ (99 wt. %, Sigma-Aldrich)) the catalyst was dried overnight at 110 ºC, calcined at 200 ºC for 2 h and reduced at 250 ºC for 2 h under 40 N mL / min H_2 flow.

The stipulated nomenclature for all supports and catalysts used in this work is described in the Table III-1. Likewise, it also shows the chapter and section in which each catalyst was used.

Table III-1. An overview of the supports and catalyst used in this work

Carbon support	Nomenclature support	Metal active	Nominal Metal loading	Nomenclature catalyst	Chapter (Section)
CAPSUPER	CAP	Pt	3 wt. %	Pt/CAP	V (1), VI (1, 2)
SXPLUS	SXP	Pt	3 wt. %	Pt/SXP	V (1)
ENSACO 350G	E250	Pt	3 wt. %	Pt/E350	V (1), VI (1)
ENSACO 250G	E350	Pt	3 wt. %	Pt/E250	VI (1, 2), VII (1), VIII (1)
Mesoporous carbon black	C-MESO	Pt	3 wt. %	Pt/C-MESO	VI (1)
Merck	MER	Pt	3 wt. %	Pt/MER	VI (2, 3, 4)
		PtRe	3 wt. %	PtRe(1:1)*/MER	VI (4)
		PtRe	3 wt. %	PtRe(1:2)*/MER	VI (3, 4)
		PtRe	3 wt. %	PtRe(2:1)*/MER	VI (4)
Ketjenblack EC-600JD	KJB	Pt	3 wt. %	Pt/KJB	VI (2)
Modified Merck (1 wt. % resol)	MER1RES	Pt	3 wt. %	Pt/MER1RES	VI (4)
Modified Merck (10 wt. % resol)	MER10RES	Pt	3 wt. %	Pt/MER10RES	VI (4)
Modified Merck (20 wt. % resol)	MER20RES	Pt	3 wt. %	Pt/MER20RES	VI (4)
Modified Merck (40 wt. % resol)	MER40RES	Pt	3 wt. %	Pt/MER40RES	VI (4)
Sibunit	SIB	PtPd	3.75 wt.%	PtPd/SIB	VI (5)

*Metal molar ratio.

The porous texture of the supports and catalysts was characterized by nitrogen adsorption-desorption at 77 K (Micromeritics TriStar II). The pH slurry of the carbon support materials and catalysts was determined by measuring, until a constant value, the pH of an aqueous suspension of the material in distilled water (1 g of solid per 10 mL of water). The catalysts were characterized by scanning transmission electron microscopy (STEM, JEOL- 3000F at 300 kV), thermogravimetric analysis (TGA Q500, TA Instruments and TG/TPD-TPO), elemental analysis (LECO CHNS-932), X-ray photoelectron spectroscopy (XPS, K-Alpha – Thermo Scientific or PHI VersaProbe II instrument equipped with an X-ray excitation source, 1486.6 eV) and CO chemisorption (Micromeritics ASAP 2020C instrument). Software 'ImageJ 1.44i or 1.51k' was used for counting and measuring Pt NPs on digital STEM images (more than 200 NPs were measured per catalyst). The mean size of the Pt NPs and the size distribution were calculated. Software 'XPS peak v4.1' was used for the deconvolution of the spectrograms in order to obtain the relative occurrence of Pt^{2+} and Pt^{0} species. The C 1s peak (284.6 eV) was used as an internal standard for binding energy corrections due to sample charging. In the CO adsorption measurements, the metal dispersion on the support was evaluated from the amount of chemisorbed CO by assuming the stoichiometry of CO/Pt = 1.

2. Preparation and characterization of feedstocks

In this work, different types of wastewaters were used as feedstocks for treatment and valorisation by APR. These feedstocks varied from individual model compounds and mixtures, which are usually found in industrial wastewater, to real wastewater. The general procedure used for the preparation and characterization of synthetic wastewaters treated in this work is described below. Feedstocks composed of solutions of model compounds

or real wastewater, and their modifications for the purpose of a section are also described in the specific experimental part of each section.

2.1. Preparation of tuna-cooking wastewater

Tuna-cooking wastewater (TCW) was obtained by boiling tuna (*Thunnus alalunga*) in water (250 g tuna / L, 5 g NaCl / L) for 30 min, according to the procedure communicated by a local fish canning industry. The resulting liquor was filtered through 0.45 μm PTFE filters (Scharlab).

2.2. Preparation of synthetic brewery wastewater

Synthetic brewery wastewater (SBW) was prepared based on pH and typical concentrations of Biological Oxygen Demand (BOD), Chemical Oxygen Demand (COD) and nutrients found in real brewery wastewater [72]. The standard SBW feedstock contained 1 g / L malt extract, 0.5 g / L yeast extract, 0.15 g / L peptone, 0.86 g / L maltose, 1 g / L $(NH_4)_2SO_4$, 2.80 mL / L C_2H_5OH, 0.08 g / L NaH_2PO_4 and 0.14 g / L of Na_2HPO_4. All compounds were purchase from Sigma-Aldrich.

2.3. Preparation of synthetic fruit juice wastewater

Fruit juice wastewater (FJW) was prepared based on typical COD values [73] and concentrations of individual components found in these type of wastewaters [74–76]. The standard FJW feedstock contained 2.18 g / L glucose, 1.98 g / L fructose, 0.77 g / L citric acid, 0.32 g / L ascorbic acid and 0.35 g / L galacturonic acid. All compounds were purchase from Sigma-Aldrich.

2.4. Preparation of wastewater with phenolic compounds

Different feedstocks were prepared as mixtures of selected representative compounds identified in the phenol oxidation routes proposed by Zazo *et al.* [77] and Joglekar *et al.* [78]. An initial theoretical total organic carbon (TOC) of 76.5 mg / L was considered for all feedstocks. All compounds were purchase from Sigma-Aldrich.

2.5. Characterization of the wastewater

The analytical characterization included TOC, using a TOC-VCSH apparatus (Shimadzu); COD, determined according to the standard method ASTM D1252 and ionic chromatography (IC) (883 Basic IC Plus, Metrohm). Phenolic compounds were analysed by high performance liquid chromatography (HPLC, Varian Pro Star-UV/DAD, C_{18} column, 4 mM H_2SO_4).

3. APR experiments and analytic procedures

- **Batch and semi-continuous reactors**

Batch experiments were carried out in 50 mL stainless steel stoppered reactors (BR100, Berghoff). The reaction time was established in 4 h and the proportion of 50 mL of feedstock per g catalyst was used. The reactor was purged several times with Ar before heating up and stirring (500 rpm). The experiments were performed at 200, 220 and 225 ºC. The total reaction pressure (24 – 29 bar) was the result of contribution of the vapour pressure of water, the pressure of the gases produced and the initial Ar pressure set at 10 bar for the experiments performed at 200 ºC and 5 bar for those conducted at

220 and 225 ºC. All batch APR experiments were performed at least by duplicate.

Semi-continuous experiments were performed in the same reactor as for batch experiments by supplying an Ar flow into the reactor (1 N mL / min) using a high pressure flow meter (100L, Sierra) and a backpressure regulator (Swagelok). The experiments were performed at 200 ºC using the same conditions described for batch runs.

After the reaction time, the heating system was stopped and the reactor was cooled down to room temperature. The gases produced during both modes of the reaction were collected in multilayer foil sample bags (Supelco, USA). The volume was measured using a gas burette and it was expressed in normal conditions (NTP). The gases were analysed by gas chromatography (GC/FID-TCD 7820A, Agilent) using 2 packed columns and a molecular sieve. This system allowed analysing H_2, CO, CO_2, CH_4, C_2H_6 and C_3H_8. The final effluents were filtered and processed to measure TOC, COD and ionic species (IC).

- **Continuous reactors**

First setup: The continuous APR experiments were carried out at 225 ºC, 28 bar with 1 g of catalyst during 24 h time-on-stream (TOS), using a fix bed reactor equipped with temperature and pressure controllers. The reactor was heated externally and the reaction temperature was monitored using a thermocouple placed inside the stainless-steel reactor tube (300 x 10 mm i.d.) positioned above the catalyst. The feedstock was fed into the reactor with a HPLC pump using different flow rates (0.25 – 4 mL / min). Ar was used to purge the reaction system and as carrier gas throughout the reaction. The flow rate of Ar varied from 5 to 40 N mL / min. The gas produced was measured by a mass flow controller and it was analysed online by a gas

chromatography (as described above for batch reactions). The treated liquid effluent was characterized by TOC and COD measurement.

Second setup: The experiments in continuous mode were also carried out at 175, 200 and 225 ºC, 30 bar with 0.5 g of catalyst during at least 56 h TOS. The reactor, equipped with temperature and pressure controllers, was heated externally and the reaction temperature was monitored using a thermocouple placed outside the stainless-steel reactor tube (520 x 6.4 mm i.d.) next to the position of catalyst bed. The catalyst bed consisted of a mix of catalyst and sand placed in the middle of the reactor tube between two layers of sand. In addition to the reduction during the synthesis, the catalysts were reduced *in-situ* before the APR experiments using a temperature of 250 ºC and a H_2 flow rate of 40 N mL / min. The APR experiments were started at 175 ºC, which was raised to 200 ºC after 24 h TOS and to 225 ºC after 48 h TOS. Feedstocks were fed into the reactor with a HPLC pump using 0.035 and 0.1 mL / min of liquid flow rate. N_2 containing 1 % He was used to purge the reaction system, to maintain the pressure inside the reactor and as carrier gas throughout the reaction, using a constant flow rate 34 N mL / min. The gas produced was analysed online by a micro-gas chromatograph (Agilent Micro-GC 3000A) equipped with four columns (Plot U, OV-1, Alumina and Molsieve). H_2, CO, CO_2 and various alkanes (from C1 to C7) were detected in the gas produced. The initial liquid feedstock and liquid effluent were analysed by HPLC (Aminex HPX-87H, RI detector, 45 ºC, 5 mM H_2SO_4, isocratic conditions, 0.6 mL / min).

3.1. Coupled hydrogenation and APR

The hydrogenation was performed in a batch reactor (300 mL, Hasteloy) over 4.6 wt. % Ru/C catalyst at 120 ºC and 20 bar of H_2 [79]. The feedstock (100 mL) and the catalyst (0.2 g) were loaded and the reactor was purged several times with Ar before heating up, stirring (1000 rpm) and

pressurizing with H_2. The liquid samples were analysed by HPLC following the same procedure applied for the analysis of the initial feedstock and final effluents in continuous APR experiments (second setup). After hydrogenation, a solution was prepared with the main compound obtained and it was subjected to APR as indicated above (continuous APR experiments, second setup). All the compounds used in the aqueous solutions were purchased from Sigma-Aldrich.

3.2. Coupled of CWAO and APR

The partial oxidation of the feedstock was carried out to in stainless steel batch reactors (BR100, Berghoff) at 220 ºC during 4 h, using 0.5 g of a commercial catalyst (0.5 wt. % Pt/Al_2O_3) and 30 mL of feedstock. Before heating, a gas mixture (30 % air, 70 % Ar) was used to purge the reactor and increase pressure up to 20 bar. The conditions for oxidation were set after preliminary experiments based in former works [78,80]. After CWAO the resulting aqueous phase was subjected to APR as indicated above (batch experiments).

4. Calculations

The following equations were used to quantify the results of experiments and define performance parameters.

TOC and COD removal was calculated as (Equation. 4):

$$TOC\ or\ COD\ Removal\ (\%) = \frac{X_{initial} - X_{final}}{X_{initial}} x\ 100\ \% \qquad (4)$$

where X is the TOC or COD value in the initial feedstock ($X_{initial}$) and final effluent (X_{final}) in mg / L (or the corresponding mass flow in mg / min).

Conversion of single compounds was calculated as (Equation 5):

$$Conversion\ (\%) = \frac{FC_{initial} - FC_{final}}{FC_{initial}} x\ 100\ \% \quad (5)$$

where FC is the feed concentration in the initial feedstock ($FC_{initial}$) and final effluent (FC_{final}) in mol / L.

Carbon conversion to gas (*CC gas*) was defined in the following way (Equation 6):

$$CC\ gas\ \ (\%) = \frac{C_{gas}}{C_{initial}} x\ 100\ \% \quad (6)$$

where C_{gas} is the total amount of carbon detected in all gas phase products (CO, CO_2 and alkanes) or the corresponding molar carbon flow (mol C or mol C / min) and $C_{initial}$ is the amount of carbon in the initial feedstock or the corresponding molar carbon flow (mol C or mol C / min).

Carbon conversion to liquid (*CC liq*), including unreacted compounds, was calculated according to Equation (7).

$$CC\ liq\ \ (\%) = \frac{C_{liq}}{C_{initial}} x\ 100\ \% \quad (7)$$

where C_{liq} is the total amount of carbon detected in all liquid phase or the corresponding molar carbon flow (mol C or mol C / min).

Carbon conversion to solid (*CC sol*) was estimated according to Equation (8).

$$CC\ sol\ \ (\%) = 100\ \% - CC\ liq\ (\%) - CC\ gas\ (\%) \quad (8)$$

In the experiments carried out with model compounds present in the FJW the H_2 selectivity (S_{H2}) was calculated by Equation (9).

$$S_{H2}\ (\%) = \frac{H_{2\,gas}}{C_{gas}} x\ \frac{1}{R} x\ 100\ \% \quad (9)$$

where *R* is the H_2/CO_2 stoichiometric reforming ratio (R = 12/6 for glucose, 12/6 for fructose, 9/6 for citric acid, 10/6 for ascorbic acid and 10/6 for galacturonic acid).

In the experiments carried out with the model compounds present in the SBW or after hydrogenation, the H_2 selectivity were calculated by Equation (10). This equation was used because it allows the comparison of results of APR of model compound with the APR of SBW.

$$S_{H2}\ (\%) = \frac{H_{2\,gas}}{Total\ of\ H_2\ of\ gas\ molecules}\ x\ 100\ \% \tag{10}$$

In the experiments with model compounds the H_2 yield (Y_{H2}) was calculated according to Equation (11).

$$Y_{H2}\ (\%) = \frac{H_{2\,gas}}{H_{2\,stoichiometric}}\ x\ 100\ \% \tag{11}$$

For selectivity to CO, CO_2 and alkanes the Equation (12) was used.

$$Selectivity_j\ (\%) = \frac{C_{j\,gas}}{C_{gas}}\ x\ 100\ \% \tag{12}$$

where $C_{j\,gas}$ is the carbon content in a product j in the gas phase, in mol or mol C / min.

For APR experiments with complex wastewater as feedstock, H_2 yield (Y_{H2}) and CH_4 yield (Y_{CH4}) were calculated according to Equation (13) and Equation (14), respectively.

$$Y_{H_2}\ (\frac{mmol_{H_2}}{g_{TOC_i\ or\ COD_i}}) = \frac{H_{2\,gas}}{X_{initial\ x\ V}} \tag{13}$$

$$Y_{CH_4}\ (\frac{mmol_{H_2}}{g_{TOC_i\ or\ COD_i}}) = \frac{CH_{4\,gas}}{X_{initial\ x\ V}} \tag{14}$$

where V is the volume of initial feedstock used in the experiment.

The yield of liquid products was determined by Equation (15).

$$Yield_j\ (\%) = \frac{C_{j_{liq}}}{C_{initial}}\ x\ 100\ \% \quad (15)$$

where $C_{j_{liq}}$ is the carbon content in a product j in the liquid phase, in mol or mol C / min.

Turnover frequency for H_2 production (TOF H_2) was defined by Equation (16).

$$TOF\ H_2\ (min^{-1}) = \frac{H_{2gas}}{M_d\ x\ m_{cat}\ x\ M_l\ x\ M_{MM}}\ \% \quad (16)$$

where M_d is the metal dispersion, m_{cat} is the mass of catalyst, M_l is the metal loading and M_{MM} is the molar mass of metal.

Chapter IV. General characterization of supports and catalysts

This Chapter includes the results of the general characterization of supports and catalysts used in this work. In some chapters an additional characterization of the catalysts used was performed, this additional characterization was reported in the experimental or results and discussion section of each specific work.

Table IV-1 shows the porous texture parameters and pH slurry of supports considered in this work. The CAP support yielded the highest specific surface area (S_{BET}) (1750 m^2 / g), followed by KJB and SXP, also with fairly high values (1415 and 1210 m^2 / g, respectively). The highest external surface area (A_{EXT}) was exhibited by KJB (1415 m^2 / g). MER and E350 supports showed the same S_{BET} value (930 m^2 / g), however MER support presented significantly lower A_{EXT} than E350 (120 vs 655 m^2 / g), due to high micropore volume. E250 and C-MESO supports gave significantly lower S_{BET} values (65 and 100 m^2 / g, respectively). All the supports showed some contribution of mesoporosity, while E250, C-MESO and KJB did not have a significant microporosity. Regarding the MER modified supports (MERxRES), both S_{BET} and A_{EXT}, as well as micro and mesopore volume, were gradually reduced with phenolic resol resin infiltration and further carbonization. However, support microporosity was not completely eliminated, even when 40 wt. % of resol resin was infiltrated due to microporous nature of char formed by resol carbonization.

The pH slurry of the supports varied from frankly acidic (CAP: 2.6), to slightly acidic or basic (SXP: 6.5 and C-MESO: 7.5) and basic (MER: 8.3, E250: 8.9, E350: 10.3 and C-MESO: 10.6). In addition, the pH slurry of MERxRES was also basic and increased from 8.3 to 9.8 for those modified supports with higher percentages of resol. The acidic character of CAP can be attributed to the surface acids groups generated by chemical activation of the carbon.

Table IV-1. Characterization of carbon supports

Support	S_{BET} (m^2 / g)	A_{EXT} (m^2 / g)	Micropore volume (cm^3 / g)	Mesopore volume (cm^3 / g)	pH slurry
CAP	1750	705	0.48	0.75	2.6
SXP	1210	-	0.53	0.40	6.5
E250	65	65	< 0.001	0.09	8.9
E350	930	655	0.12	0.74	10.3
C-MESO	100	100	< 0.001	0.25	7.5
KJB	1415	1415	< 0.001	1.67	10.6
MER	930	120	0.38	0.15	8.3
MER1RES	870	110	0.37	0.13	8.3
MER10RES	770	100	0.32	0.12	9.8
MER20RES	600	80	0.25	0.10	9.8
MER40RES	490	65	0.20	0.08	9.8

The porous texture parameters and pH slurry of catalyst is showed in Table IV-2. The Pt catalysts presented slightly lower values of S_{BET}, A_{EXT} and pore volume than the corresponding supports due to partial pore blockage by the Pt NPs. Although pH slurry of some of MERxRES supports was higher than MER support, pH slurry of the Pt/MER and Pt/MERxRES catalysts was similar. For the rest of Pt catalysts the pH slurry value did not present any significant difference in comparison to the supports. PtRe catalysts showed lower S_{BET} and micropore volume than Pt/MER and more acidic pH slurry. Some authors have also reported an increase in surface acidity by Re loading in Pt/C catalysts, although this additional acidity was attributed to different species. King *et al.* [54] reported that acidity is provided by ReOx species, while Zhang *et al.* [81] indicated that acidity was introduced through a Pt-O-Re structure instead of ReOx.

Table IV-2. Characterization of catalysts

Catalyst	S_{BET} (m^2 / g)	A_{EXT} (m^2 / g)	Micropore volume (cm^3 / g)	Mesopore volume (cm^3 / g)	pH slurry
Pt/CAP	1360	675	0.31	0.75	2.9
Pt/SXP	1040	345	0.33	0.40	7.0
Pt/E250	65	65	< 0.001	0.09	8.6
Pt/E350	900	620	0.12	0.69	9.9
Pt/C-MESO	90	90	< 0.001	0.14	7.3
Pt/KJB	1350	1350	< 0.001	1.59	10.2
Pt/MER	910	120	0.38	0.14	8.5
Pt/MER1RES	820	105	0.34	0.12	8.0
Pt/MER10RES	695	90	0.29	0.11	8.6
Pt/MER20RES	570	70	0.24	0.09	8.2
Pt/MER40RES	445	60	0.19	0.06	7.9
PtRe(1:1)/MER	820	120	0.34	0.15	3.2
PtRe(1:2)/MER	800	110	0.35	0.13	5.8
PtRe(2:1)/MER	810	120	0.34	0.14	3.6

Elemental analysis of Pt/MERxRES catalysts was carried out in order to evaluate changes by impregnation and carbonization of resol resin. As it can be observed in Table IV-3, C percentage in Pt/MERxRES catalysts was only slightly modified by resol resin addition, not showing a clear trend. On the other hand, H percentage gradually increased with resol addition.

Table IV-3. Elemental composition of Pt/MER and Pt/MERxRES catalysts

Catalyst	% C	% H	% N	% S	% O*
Pt/MER	86.1 ± 0.1	0.4 ± 0.1	0.5 ± 0.1	0.7 ± 0.1	12.3 ± 0.1
Pt/MER1RES	87.0 ± 0.2	0.4 ± 0.1	0.5 ± 0.1	0.7 ± 0.1	11.4 ± 0.1
Pt/MER10RES	87.6 ± 0.2	0.5 ± 0.1	0.5 ± 0.1	0.6 ± 0.1	10.8 ± 0.2
Pt/MER20RES	88.0 ± 0.5	0.6 ± 0.1	0.6 ± 0.1	0.6 ± 0.1	10.2 ± 0.5
Pt/MER40RES	86.1 ± 0.5	0.8 ± 0.2	0.5 ± 0.1	0.6 ± 0.1	12.0 ± 0.4

*Calculated by difference.

Figure IV-1 shows STEM images and the corresponding Pt NPs size distribution for all monometallic Pt catalysts, except Pt/MER and Pt/MERxRES catalysts. Pt/SXP catalyst showed the largest mean NPs size (11.3 nm), while the Pt/KJB one gave a smallest value (2.3 nm). On the other hand, the mean NPs size and size distribution for the Pt/CAP, Pt/E250, Pt/E350 and Pt/C-MESO catalysts were quite similar, in the 4.0 – 4.7 nm range. As shown in the STEM images, the Pt NPs were quite homogeneously dispersed onto the carbon supports.

Pt/CAP

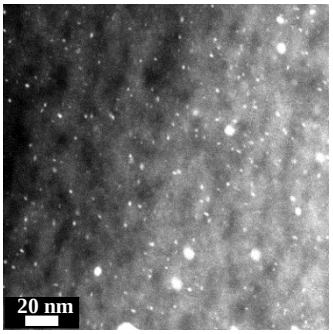

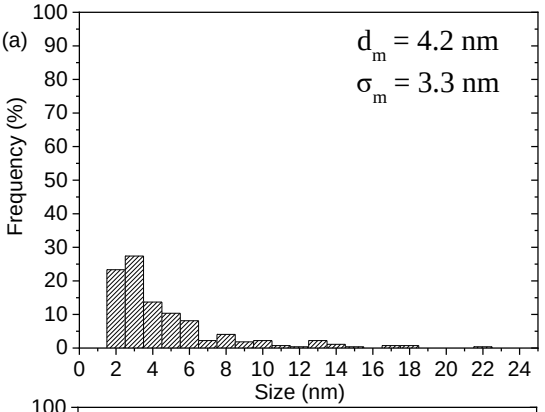

Pt/SXP

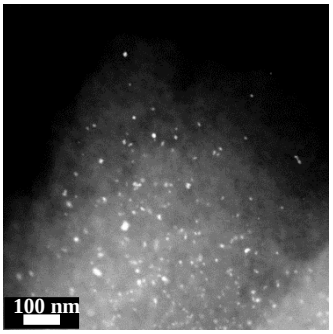

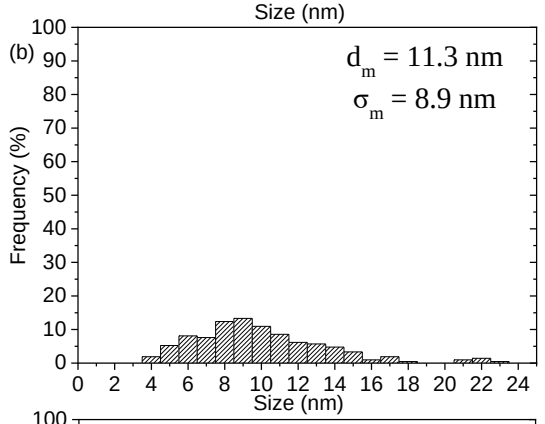

Pt/E250

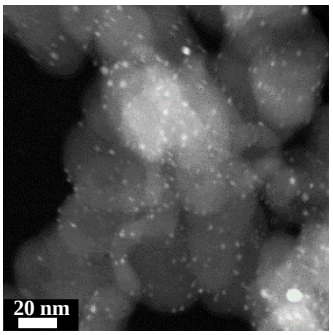

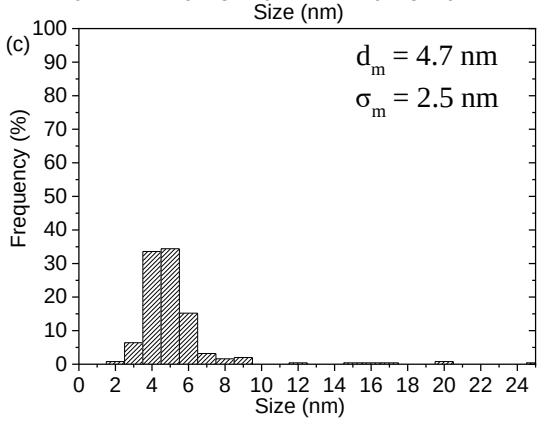

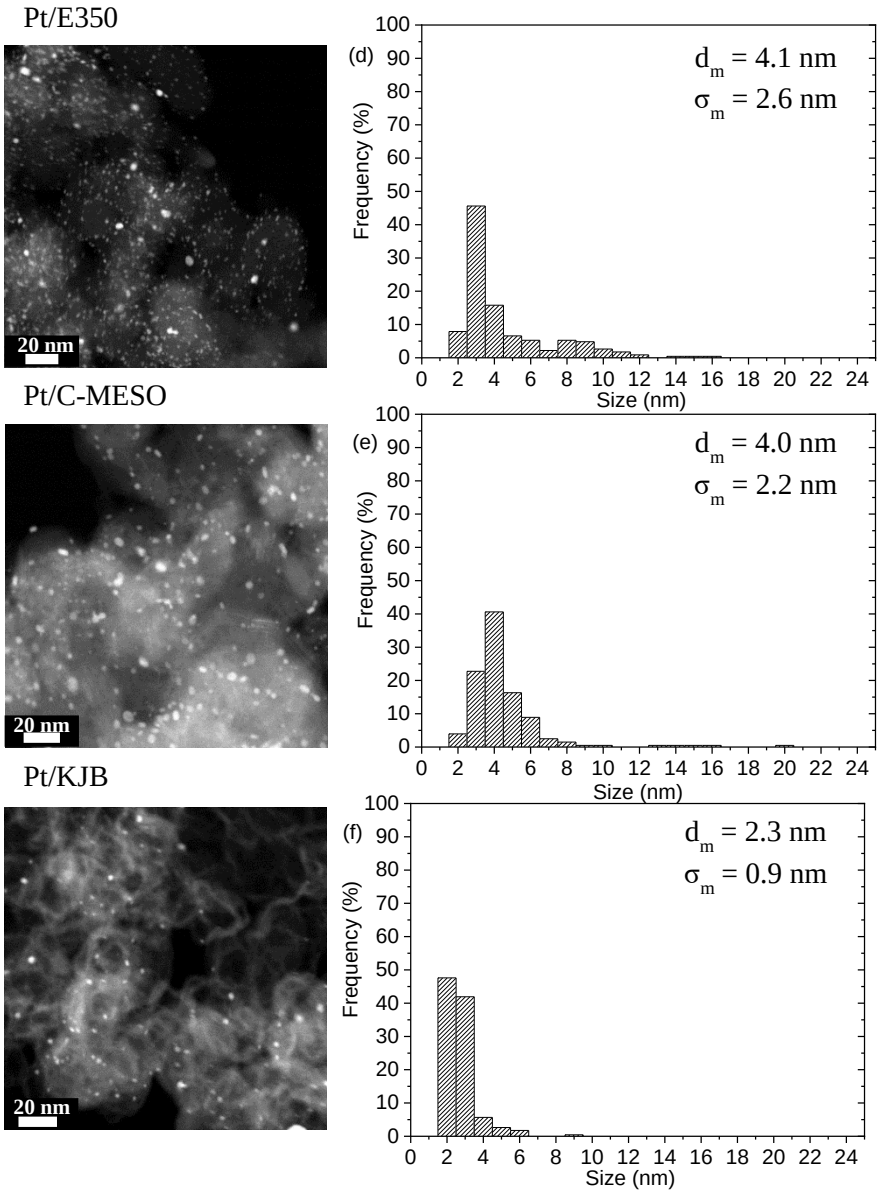

Figure IV-1. STEM images and NPs size distribution (a) Pt/CAP, (b) Pt/SXP, (c) Pt/E250, (d) Pt/E350, (e) Pt/C-MESO and (f) Pt/KJB catalysts

Figure IV-2 shows STEM images and the corresponding Pt NPs size distribution for Pt/MER and Pt/MERxRES catalysts. Catalysts with support modified by addition and carbonization of resol (Pt/MERxRES) exhibited smaller NPs mean size (1.8 – 3.5 nm) than Pt/MER (4.6 nm) and narrower size distribution. The dispersion of Pt was favoured by the modification of the support by deposition of char creating anchoring sites. Pt/MER catalyst showed in some STEM images higher agglomeration of NPs, which were not considered for histograms.

Pt/MER

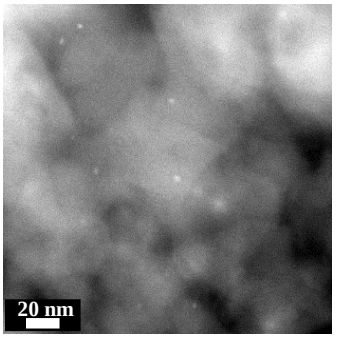

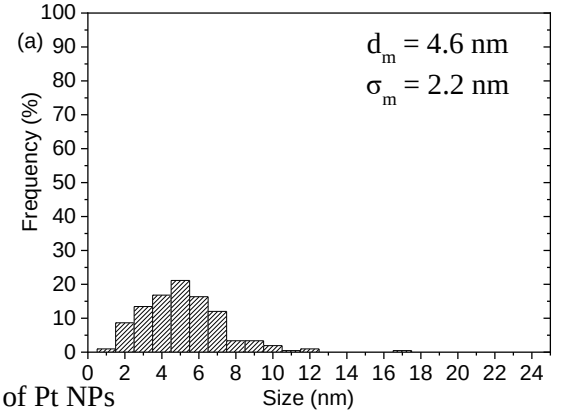

Pt/MER – Agglomeration of Pt NPs

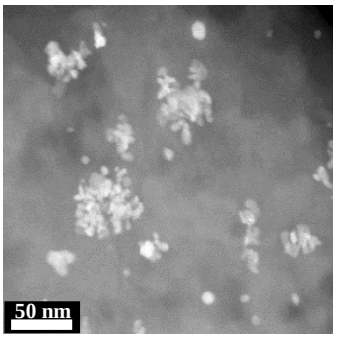

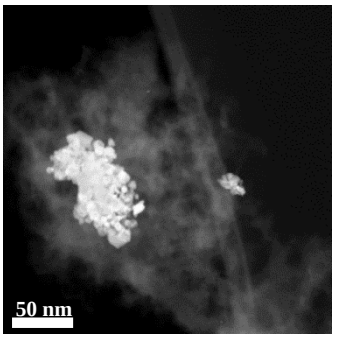

Pt/MER1RES

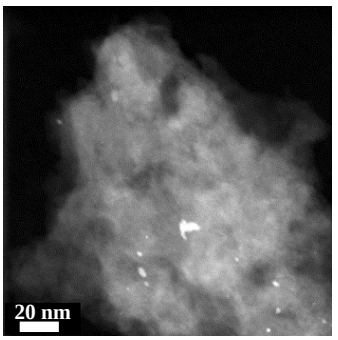

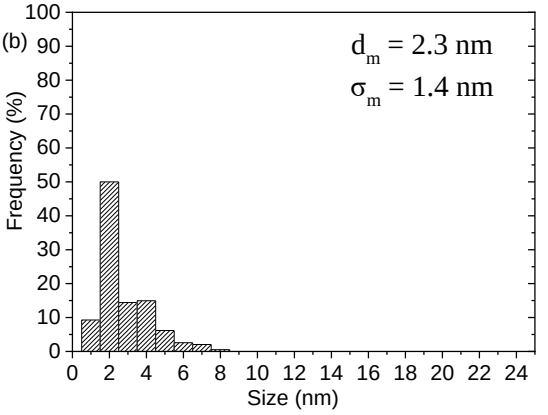

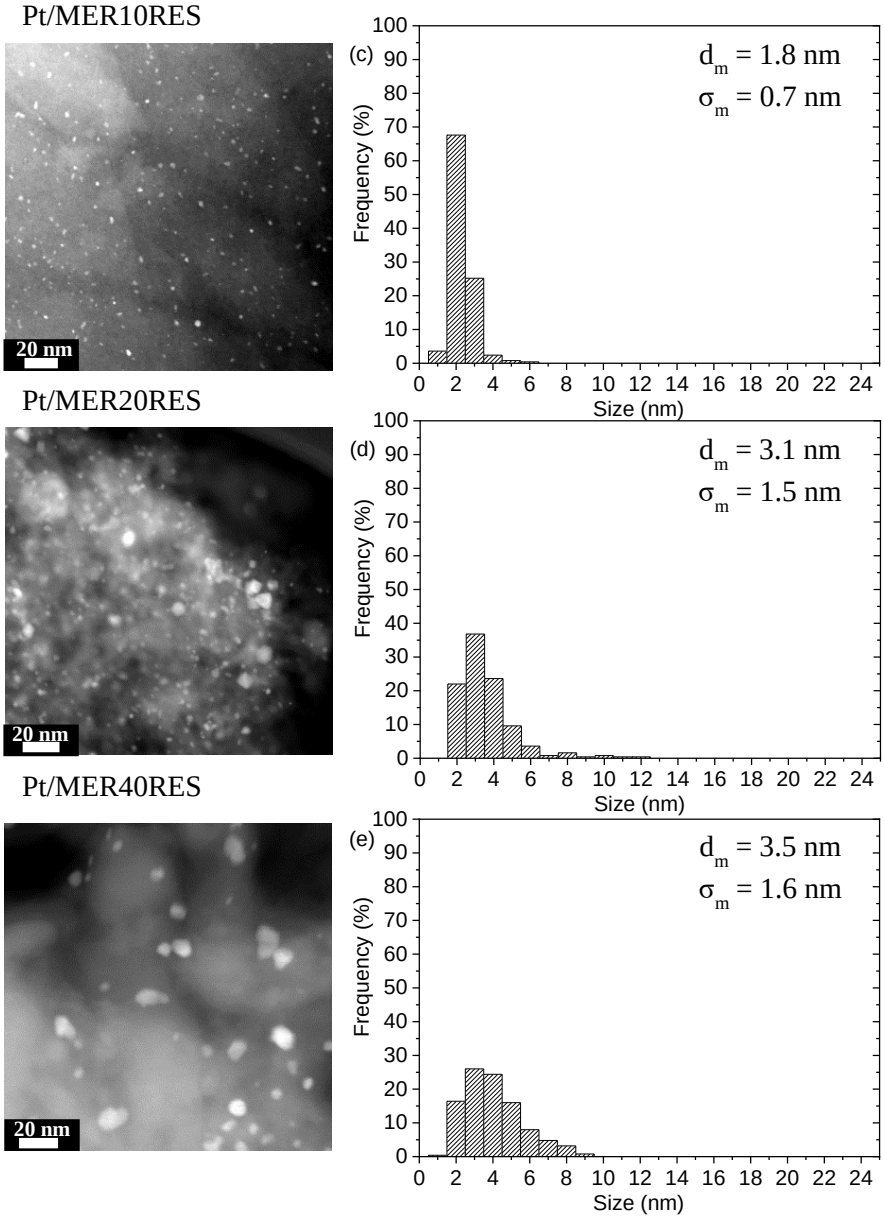

Figure IV-2. STEM images and NPs size distribution (a) Pt/MER, (b) Pt/MER1RES, (c) Pt/MER10RES, (d) Pt/MER20RES and (e) Pt/MER40RES catalysts

Figure IV-3 shows the STEM images and NPs size distributions for PtRe bimetallic catalysts. PtRe/MER catalysts showed a smaller NPs size than Pt/MER, especially PtRe(1:1)/MER catalyst, which showed a remarkable dispersion and the smallest NPs mean size (1.2 nm) among all the catalysts studied. In general, PtRe catalysts have smaller particle sizes and narrower particle size distribution compared with the monometallic Pt [82].

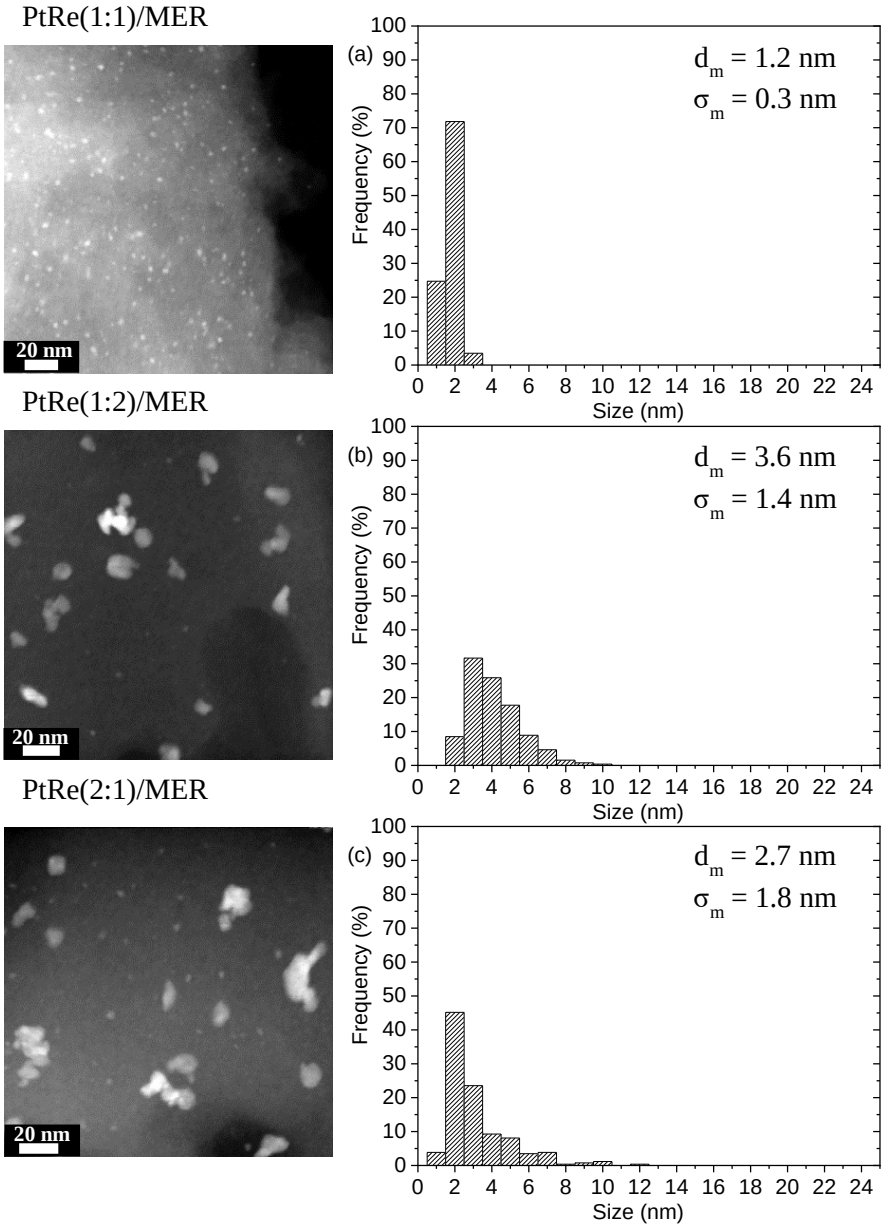

Figure IV-3. STEM images and NPs size distribution (a) PtRe(1:1)/MER, (b) PtRe(1:2)/MER and (c) PtRe(2:1)/MER catalysts

Chapter V. Treatment and valorisation of fish-canning wastewater

1. Treatment of fish-canning industry effluents by APR using Pt/C catalysts

This chapter was adapted from: Oliveira, A.S., Baeza, J.A., Calvo, L., Alonso-Morales, N., Heras, F., Lemus, J., Rodriguez, J.J., Gilarranz, M.A., **Exploration of the treatment of fish-canning industry effluents by aqueous-phase reforming using Pt/C catalysts**, Environ. Sci. Water Res. Technol. 4 (2018) 1979–1987. doi:10.1039/c8ew00414e.

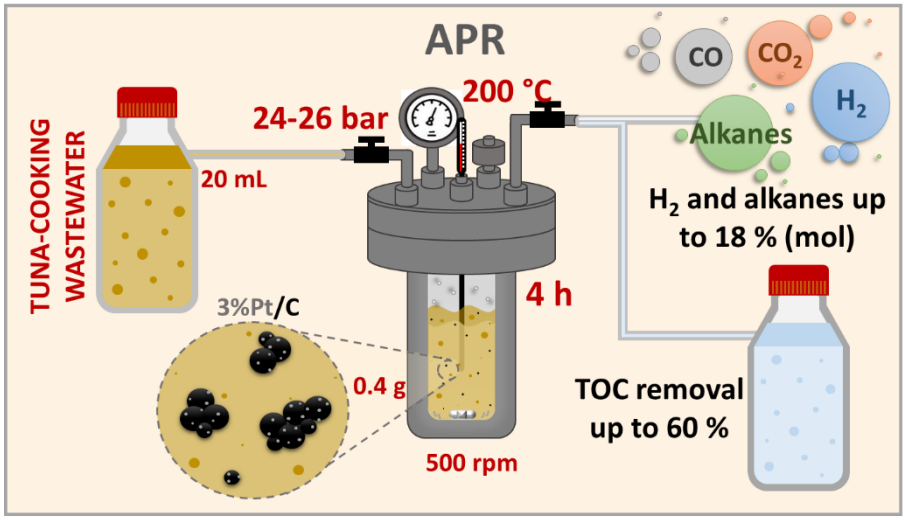

1.1. Introduction

Tuna-cooking effluents have been selected for this study due to their significance in the fish-canning industry. The fish-canning industry has been considered as good candidate to this new application of APR since the different production lines generate wastewater with high salinity and variable organic loads that hinder their treatment by biological methods [83,84]. In addition, the insight into the effect of mixtures of compounds and presence of impurities on APR is of special interest when complex matrices are proposed as substrates in the APR process. In particular, compounds such as acetic and phosphoric acids and sodium chloride are at high concentration in tuna-cooking effluents and they can affect the catalyst performance. Thus, the use of this type of wastewater could be interesting to evaluate the application of APR process to complex feedstocks with high content of inorganic salts.

Accordingly, the current chapter presents a first exploratory study on the application of APR to the treatment of tuna-cooking wastewater (TCW), using Pt catalysts supported on different carbon materials. Experiments in batch and semi-continuous mode were carried out in order to check the catalyst performance in both reaction systems. Likewise, the stability of the catalysts was evaluated upon three successive applications.

1.2. Experimental

Pt/C (3 wt. % Pt) catalysts and TCW were prepared and characterized according to the procedure reported in Chapter III. Two commercial activated carbons (CAP and SXP) and a carbon black (E350) were used as supports.

APR experiments were carried out in batch and semi-continuous reactors (described in Chapter III) at 200 ºC, during 4 h, using 0.4 g of

catalysts in 20 mL of reaction volume under Ar atmosphere. The total reaction pressure was 24 – 26 bar.

Catalyst stability was assessed in 3 cycles of use in batch mode. After each cycle of use, the catalyst was separated by filtration and simply dried in an oven at 60 ºC overnight. Then it was used for the next cycle.

1.3. Results and discussion

1.3.1. Characterization of catalysts

XPS characterization yielded Pt^{2+}/Pt^{0} ratios of 0.5 for the Pt/SXP and Pt/E350 catalysts, whereas in the case of Pt/CAP was as much as 1.5 in spite of the equivalent conditions used in the reduction step. According to the pH slurry and the TPD profiles of CAP [85], that difference could be related to the occurrence of acid groups on its surface, attracting electrons from Pt.

1.3.2. Characterization of the tuna-cooking wastewater

Table V-1 shows the TOC and COD values of the starting TCW, as well as its pH and the main ionic species. As can be seen, fairly high TOC and COD values were measured (≈ 1900 and 5000 mg / L, respectively). The COD/TOC ratio (≈ 2.6) suggests a relative abundance of oxygen-containing organic species, most probably with carboxylic acid groups, consistent with the measured pH value. The five main anions detected corresponded to chloride, acetate, formate, phosphate and sulphate. Chloride was added in the preparation of the tuna-cooking synthetic wastewater, emulating the high salinity medium used in the industrial cooking of tuna. Acetate and formate are short chain fatty acid groups which could come from larger fatty acids breakdown upon cooking. Blue fish, such as tuna, is a well-known source of P hence phosphate was found as one of the main anionic species. Sulphate

was detected at lower concentrations, mainly ascribed to sulphur-containing amino acids degradation.

Table V-1. TOC, COD, main anions detected and initial pH of the TCW

TOC (mg / L)	1895 ± 258
COD (mg / L)	4996 ± 501
Chloride (mg / L)	3815 ± 219
Acetate (mg / L)	1895 ± 321
Formate (mg / L)	10 ± 9
Phosphate (mg / L)	523 ± 22
Sulphate (mg / L)	16 ± 14
Initial pH	6.1 ± 0.2

1.3.3. APR experiments

1.3.3.1. TOC and COD removal

Figure V-1 shows the TOC and COD removal in the APR experiments carried out with the catalysts and the bare carbon supports in batch and semi-continuous mode. A blank experiment was carried out in absence of support, yielding ca. 20 % TOC and COD removal, which can be partly ascribed to hydrothermal carbonization (HTC), since a dark brown solid was recovered by filtration [86].

The experiments with the bare support yielded higher TOC and COD removal than the ones with catalysts (55 – 75 % vs 45 – 60 %). As already seen, the carbon supports tested have high surface area and a porous texture including both micro and mesoporosity (Table IV-1). Thus, adsorption of species from the tuna cooking wastewater can represent a main contribution to the disappearance of TOC and COD.

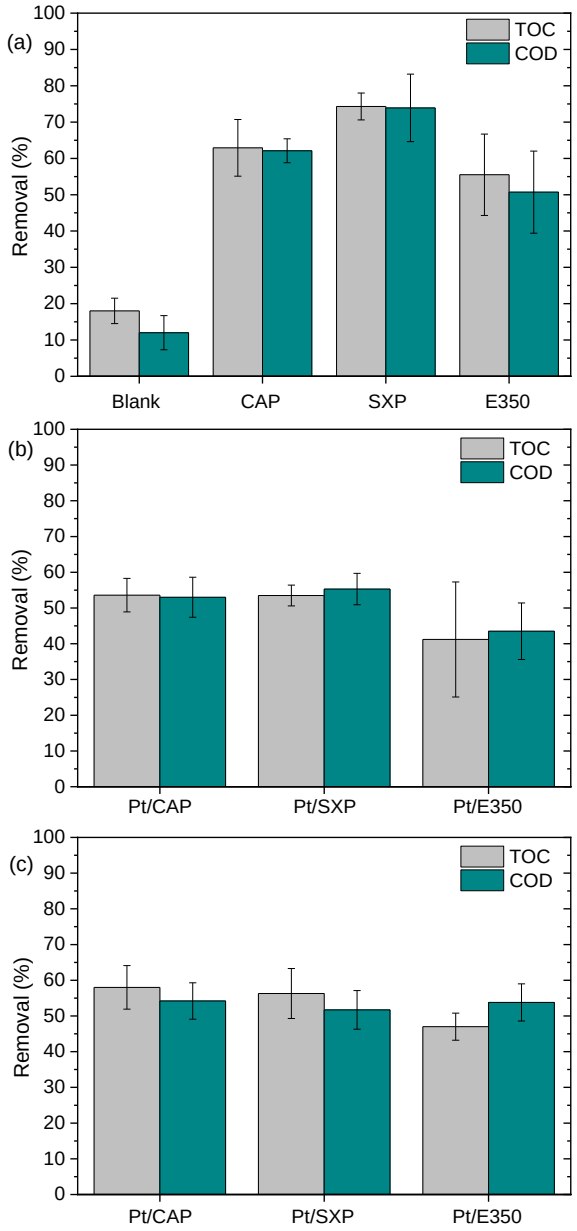

Figure V-1. TOC and COD removal upon APR of TCW with (a) the carbon supports in batch experiments; the Pt/C catalysts (b) in batch experiments and (c) in semi-continuous experiments*

*Reaction conditions: 200 ºC, total reaction pressure: 24 – 26 bar, 20 mL of TCW, 0.4 g of catalyst, 500 rpm, 4 h.

Figure V-2 shows the dTGA curves under N_2 flow of the supports before and after the APR experiments. Differences between the TGA (dTGA) curves for the fresh and used supports can be observed, mainly within the 200 – 400 ºC range, confirming the adsorption onto the carbon materials. However, the TGA curves do not allow determining the amount of organic species adsorbed. From the unmatched balance of C it was estimated that between 80 – 90 % of the TOC removal could be due to adsorption, this representing up to 4 – 6 % of the C weight of the supports.

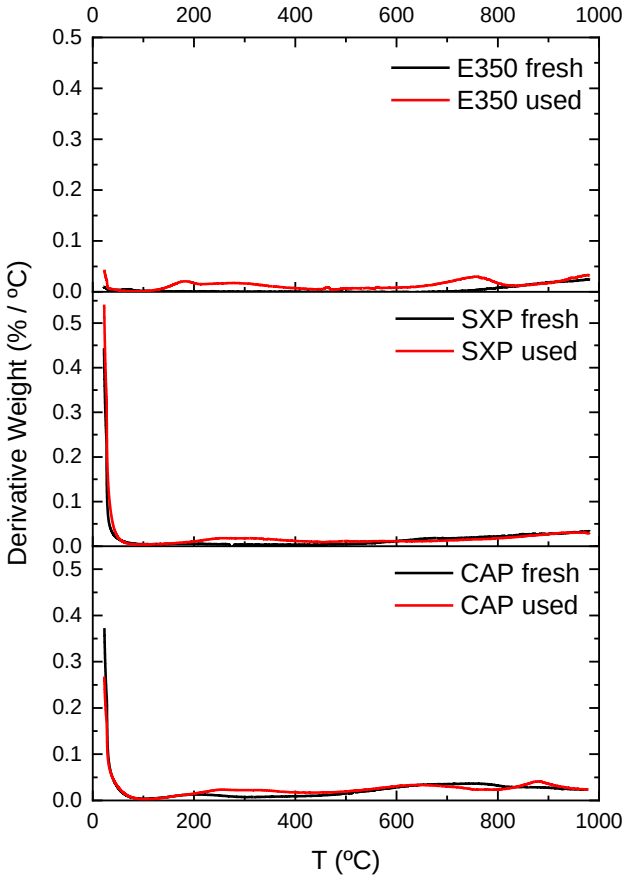

Figure V-2. TGA curves of the fresh and used supports

Table V-2 shows the elemental analysis of the fresh and used CAP carbon, which shows a lower relative amount C, and relative higher of both H and N for the used support, consistent with the adsorption of organic species.

Table V-2. Elemental composition of the fresh and used CAP support

Support	% C	% H	% N	% S	% O*
CAP fresh	81.7 ± 0.7	2.5 ± 0.1	0.2 ± < 0.1	< 0.1	15.6
CAP used	80.5 ± 0.2	2.7 ± 0.1	2.2 ± < 0.1	< 0.1	14.6

*Calculated by difference.

Therefore, the main differences in TOC and COD removal in the experiments with the bare supports and the catalysts can be ascribed mostly to adsorption on the carbon support. The lower removal of TOC and COD with the catalysts can be explained by the reduction of specific surface area accompanying Pt impregnation (Table IV-2).

1.3.3.2. Evolution of the anionic species upon APR

Figure V-3 depicts the main anionic species detected, excluding chloride, in the initial TCW and after the APR experiments. As analysed by IC, acetate was the major component (ca. 1900 mg / L) in the initial wastewater and its concentration was barely reduced upon the APR process, indicating its refractory character under the operating conditions tested [87]. Phosphate was found in much less concentration than acetate and was not affected by the APR treatment. In the reactions performed with CAP and Pt/CAP the phosphate concentration raised from ca. 550 – 600 up to close to 1200 mg / L, which can be ascribed to leaching from the support, which was obtained by activation with phosphoric acid. Formate was detected at 10 mg / L in the initial TCW and increased up to over 120 mg / L in the blank experiment. Its concentration reached between 50 and 100 mg / L in the

experiments with bare supports, whereas it remained between 5 – 10 mg / L when the Pt catalysts were used. Formic acid can be produced from glucose conversion upon HTC through several intermediates such as erythrose, 1,6-anhydro-glucose, hydroxymethylfurfural (HMF) or lactic acid [88]. This can explain the higher levels of formate in the blank experiment and in those performed with the carbon supports, where HTC must be the main process. With the Pt catalysts the final formate concentration was lower because formic acid is reformed to CO_2 and H_2 and/or CO and H_2O. Sulphate concentrations lower than 20 mg / L were found. No significant differences in formate and sulphate concentrations are observed between the batch and semi-continuous operation. Finally, chloride was not significantly affected by the APR treatment.

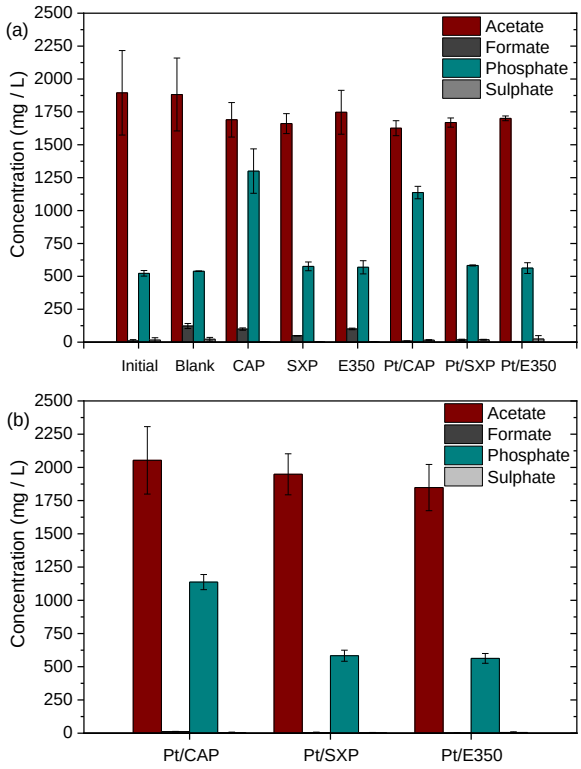

Figure V-3. Main anionic species detected by IC in the initial and after APR with (a) supports and catalysts in batch experiments and (b) catalysts in semi-continuous experiments*

*Reaction conditions: 200 ºC, total reaction pressure: 24 – 26 bar, 20 mL of TCW, 0.4 g of catalyst, 500 rpm, 4 h.

1.3.3.3. Gas phase composition

Table V-3 shows the measured amount of gas under batch and semi-continuous operation, as analysed by GC. The total amount ranged between 63 and 366 µmol. The lowest amount was obtained in the blank experiment, while with the bare carbon supports it increased to 123 – 257 µmol. The carbon black-supported catalyst (Pt/E350) gave the highest gas yield (twice the obtained with the bare support), while the two other catalysts allowed

increases only in the semi-continuous experiments. The improved gas yield in this operation mode could be related to gas withdrawal displacing the reaction towards products [17]. The valuable gases produced significantly increased when catalysts were used, with Pt/E350 showing a production higher than both Pt/CAP and Pt/SXP.

Table V-3. Amount of gas produced and C conversion to detected gases in the APR experiments of TCW

Operation mode	Experiments	Total detected gas (µmol)	Valuable gases (H_2 + alkanes, µmol)	*CC gas* (%)
Batch	Blank	63 ± 10	1.0 ± 1.0	2 ± 1
	CAP	257 ± 32	1.4 ± 1.0	8 ± 1
	SXP	174 ± 27	2.6 ± 1.0	5 ± 1
	E350	124 ± 8	1.4 ± 1.0	4 ± 1
	Pt/CAP	173 ± 25	5.4 ± 1.0	5 ± 1
	Pt/SXP	158 ± 18	6.3 ± 1.0	5 ± 1
	Pt/E350	268 ± 35	48.3 ± 5.0	8 ± 1
Semi-continuous	Pt/CAP	279 ± 35	6.6 ± 1.0	8 ± 1
	Pt/SXP	229 ± 37	6.1 ± 1.0	6 ± 1
	Pt/E350	366 ± 47	47.8 ± 6.0	10 ± 1

*Reaction conditions: 200 ºC, total reaction pressure: 24 – 26 bar, 20 mL of TCW, 0.4 g of catalyst, 500 rpm, 4 h.

H_2, CO_2, CH_4 and C_2H_6 were the components detected in the gas phase, whereas CO was never detected. Figure V-4 shows the composition of the gas fraction from the batch experiments. The blank run produced mainly CO_2 (98.4 % of the gas fraction) and in much less quantity H_2 (1.3 %) and alkanes (0.3 %), which can be ascribed to gas products from HTC. With the bare supports CO_2 was also by far the major component of the gas fraction (98 – 99 %), being H_2 (0.4 – 1.1 %) and alkanes (0.1 – 0.3 %) in much lower proportion. However, with the catalysts, the CO_2 percentage slightly decreased (96 – 97 % of the gas fraction) in the case of Pt/CAP and Pt/SXP. Likewise, the valuable gases (H_2 and alkanes) increased. The increase of H_2

percentage of the gas fraction was significant in the case of Pt/CAP and Pt/E350. With Pt/E350 the CO_2 percentage decreased (82 % of the gas fraction, while H_2 and alkanes represented 9 and 9 %, respectively). The higher activity, in terms of production of gases and H_2 of Pt/E350 could be partly ascribed to the effect of the basic properties of the support on the catalytic performance. In this sense, different authors [12,32,52,54] reported that the APR of glycerol was favoured in terms of conversion and selectivity to H_2 with catalysts using basic supports or after addition of KOH to the substrate. Liu *et al.* [52] suggested that basic medium provokes the polarization of H_2O and induces its dissociation and/or directly provides the OH groups to be adsorbed onto the catalysts, which is an important step in the WGS reaction [89]. Likewise, He *et al.* [22] and Liu *et al.* [52] reported that addition of CaO or KOH to the initial biomass solution could *in-situ* remove the CO_2 favouring the WGS reaction by displacing the reaction towards products and inhibiting methanation reactions. Thus, the basicity of the catalyst on the reaction medium improves the H_2 yield.

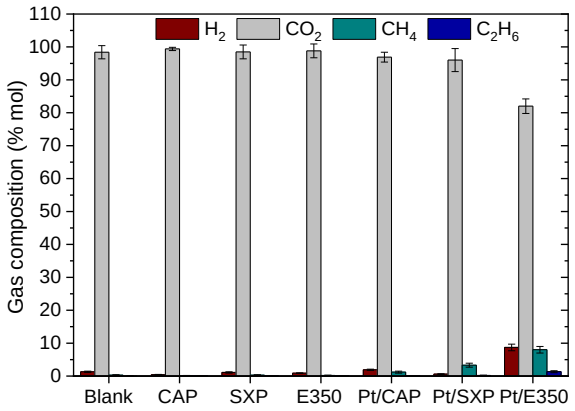

Figure V-4. Composition of the gas fraction from the batch APR experiments of TCW*

*Reaction conditions: 200 ºC, total reaction pressure: 24 – 26 bar, 20 mL of TCW, 0.4 g of catalyst, 500 rpm, 4 h.

Differences were found with the catalysts in semi-continuous runs (Figure V-5). In the cases of Pt/CAP and Pt/SXP, the alkanes percentage decreased compared to the batch experiments (from 1.3 % to 0.3 % and from 3.5 % to 2.0 % of the gas fraction, respectively). With Pt/E350 the resulting gas was also less rich in H_2 (from 9 % to 4.5 %) while the CO_2 percentage increased from 82 % to 87 % and that of alkanes remained almost similar (≈ 9 %). In the semi-continuous experiments, part of the gas phase is withdrawn during the reaction, displacing the reaction towards products. Nevertheless, the total amount of valuable gases did not vary significantly except for Pt/CAP, where the semi-continuous experiments yielded 6.6 µmol vs 5.4 µmol in batch mode. Likewise, since the amount of gas products in the reactor is lower, side reactions consuming H_2, such as the methanation, Fischer-Tropsch, dehydration and hydrogenation reactions are hindered. This could explain the lower alkanes percentage in the case of Pt/CAP and Pt/SXP.

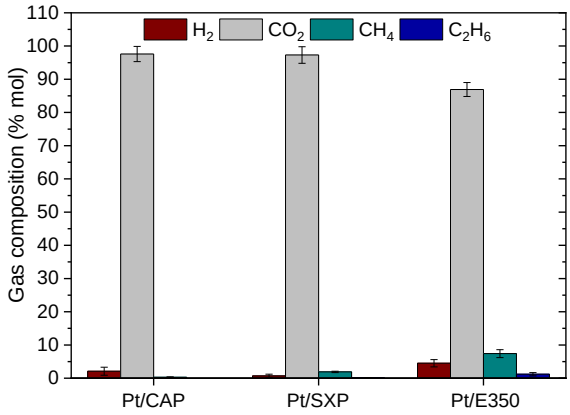

Figure V-5. Composition of the gas fraction from the semi-continuous APR experiments of TCW*

*Reaction conditions: 200 ºC, total reaction pressure: 24 – 26 bar, 20 mL of TCW, 0.4 g of catalyst, 500 rpm, 4 h.

1.3.3.4. Catalysts stability

The catalysts were used in three successive cycles in batch mode. TOC and COD removal ranged between 20 – 30 % after three successive uses, but no significant changes were found with regard to the anionic species. The results on the amount and composition of the gas fraction are summarized in Table V-4. The total amount of gases produced did not vary upon the successive cycles in the case of Pt/CAP and Pt/SXP, whereas in the case of Pt/E350 decreased from 268 to 190 μmol. This deactivation can be provoked by acetic and phosphoric acids or by chloride, which are in higher concentrations in the reaction medium and have been recognized as deactivating species in the APR of crude glycerol [26,50]. Their effects can be better observed with the more active catalysts, since Pt/CAP and Pt/SXP did not show significant differences in the amount of gases produced compared with the bare supports. The H_2 percentage remained unchanged in the case of Pt/CAP after the 3 successive cycles, whereas in the case of Pt/SXP and Pt/E350 significantly increased. Meanwhile, the alkanes percentage significantly decreased in all the cases.

Table V-4. Gas production with the catalysts tested upon 3 successive cycles

Catalyst cycle	Total gas (μmol)	Gas composition (% mol)			
		H_2	CO_2	CH_4	C_2H_6
Pt/CAP					
1st	173 ± 25	1.8 ± 0.2	96.9 ± 1.5	1.2 ± 0.2	0.1 ± 0.05
2nd	220 ± 54	1.2 ± 0.4	98.3 ± 1.3	0.5 ± 0.2	0
3rd	150 ± 20	1.5 ± 0.2	98.2 ± 1.6	0.3 ± 0.2	0
Pt/SXP					
1st	158 ± 18	0.5 ± 0.2	96.0 ± 3.5	3.3 ± 0.6	0.2 ± 0.1
2nd	200 ± 47	2.7 ± 0.3	96.2 ± 3.3	1.1 ± 0.2	0
3rd	120 ± 37	4.2 ± 0.3	95.4 ± 3.6	0.4 ± 0.1	0
Pt/E350					
1st	268 ± 35	8.7 ± 1.6	82.0 ± 2.0	8 ± 0.8	1.3 ± 0.3
2nd	230 ± 39	6.3 ± 1.5	86.7 ± 1.8	6.2 ± 0.7	0.8 ± 0.2
3rd	190 ± 25	12.9 ± 2.0	84.8 ± 2.2	2.2 ± 0.3	0.1 ± 0.05

Table V-5 shows the Pt NPs mean size, Pt^{2+}/Pt^0 ratio and specific surface area of the catalysts after the 3 successive cycles. The Pt NPs mean size increased with the number of cycles due to sintering. However, in the case of Pt/E350 there were no significant differences in NPs size after the first use, but after the 3rd cycle, Pt/E350 showed significantly lower mean size and standard deviation than Pt/CAP and Pt/SXP. Thus, Pt/E350 showed a higher resistance to NPs sintering. The increase in the H_2 and the decrease in the alkanes percentages can be explained by the lower number of low-coordinated Pt sites, promoting methanation reactions, as the Pt NPs size increases [90].

Small changes in the Pt^{2+}/Pt^0 ratio along the cycles were observed, except for Pt/CAP, where that ratio significantly decreased after the first use, showing the influence of the support. The S_{BET} of the catalysts decreased upon the 3 successive uses probably due to the adsorption of organic species, condensation and/or carbon formation.

Table V-5. Pt NPs mean size, Pt^{2+}/Pt^0 ratio and S_{BET} of the catalysts tested upon 3 successive cycles

Catalysts	Mean NPs size (nm)	Pt^{2+}/Pt^0 ratio	S_{BET} (m^2 / g)
Pt/CAP			
initial	4.2 ± 3.3	1.5	1360
after 1st cycle	8.8 ± 6.9	1.0	-
after 2nd cycle	13.4 ± 12.0	-	1160
after 3rd cycle	27.8 ± 56.9	1.2	-
Pt/SXP			
initial	11.3 ± 8.9	0.5	1040
after 1st cycle	-	-	-
after 2nd cycle	17.6 ± 24.9	0.7	454
after 3rd cycle	26.3 ± 45.2	0.7	-
Pt/E350			
initial	4.1 ± 2.6	0.5	900
after 1st cycle	3.8 ± 2.7	0.3	-
after 2nd cycle	-	-	401
after 3rd cycle	14.6 ± 18.9	0.5	-

Table V-6 shows the atomic percentage of some elements of interest in the catalysts surface as obtained by XPS after each cycle of use. The relative abundance of the major element (C) decreased while that of N increased with the number of cycles, probably due to the adsorption of N-containing compounds, such as aminoacids. In the case of Pt/CAP the relative amount of O did not vary after the 3 successive cycles, whereas in Pt/SXP and Pt/E350 increased. Interestingly, the surface concentration of Na increased in the three catalysts up to 0.3 %. Boga *et al* .[48] found that Na salts of fatty acids greatly inhibited the activity of Pt/Al_2O_3 (1 wt. %) catalysts in the APR of synthetic crude glycerol effluent, decreasing the selectivity to H_2. Thus, the presence of Na may have a role in the decreased performance of our catalysts upon use. Phosphorous was found mainly in Pt/CAP and in less extent in Pt/SXP, but not in the case of Pt/E350. On the contrary, Cl was in higher concentration in Pt/E350 and Pt/SXP. Mostany *et al.* [91] performed thermodynamic studies of phosphate adsorption on Pt surface in acid medium reporting a stronger interaction of adsorbed phosphate species with Pt, even higher than in the case of sulphate. Likewise, the adsorption of P species can prevent CO adsorption on Pt [92], hindering the WGS.

Table V-6. Atomic percentage of selected elements in the catalysts surface as obtained by XPS

Catalysts	% C	% O	% N	% Na	% P	% Cl
Pt/CAP						
initial	92.0	6.8	0	0.1	1.0	0
after 1st cycle	91.2	6.8	2.0	0.2	0.4	0
after 2nd cycle	88.8	6.8	2.8	0.3	0.5	0
after 3rd cycle	87.6	6.7	3.6	0.3	0.6	0
Pt/SXP						
initial	96.6	3.2	0	0	0	0
after 1st cycle	93.5	3.7	1.8	0.2	0	0.1
after 2nd cycle	90.8	4.6	2.5	0.2	0.2	0.1
after 3rd cycle	88.8	6.8	2.9	0.3	0.5	0.1
Pt/E350						
initial	98.5	1.1	0	0	0	0
after 1st cycle	96.1	1.8	1.2	0.3	0	0.5
after 2nd cycle	-	-	-	-	-	-
after 3rd cycle	94.8	2.3	2.1	0.3	0	0.5

Due to the complex matrix of the wastewater, from the results in this chapter it is not possible to ascribe to individual compounds contributions to catalysts deactivation. Besides, deactivation takes place also due to the contribution of HTC and aging of the metal phase due to hydrothermal treatment. However, tuning of catalysts properties according to the nature of the reaction medium is needed to prevent deactivation, which deserves future research work.

1.4. Conclusions

A first exploratory study on APR of TCW was performed at 200 ºC and 24 – 26 bar using Pt catalysts (3 wt. %) supported on different carbon materials (two activated carbons and a carbon black). HTC (20 % of TOC and COD removal) was observed when the reactions were carried out without support/catalysts in the reaction medium. The carbon supports adsorbed TCW components (up to 90 % of TOC removal and promoted the production

of gases, although CO_2 was the predominant gas component). With the catalysts, the percentage of valuable gases (H_2 and alkanes) increased significantly, reaching those components up to 18 % of the gas fraction. However, the total amount of gas produced was low (366 μmol from a starting 20 mL of wastewater volume with 100 mg of COD) probably due to the presence of large amounts of acetic and phosphoric acids as well as salt leading to catalysts deactivation. With the catalysts supported on carbon black, of frankly basic character, the total amount of gas increased significantly as well as the percentage of valuable components (H_2 and light alkanes). The type of reaction system affected the production of gases, yielding the semi-continuous experiments higher amount of gas, since withdrawn gas displaces the reaction towards products. As a general trend, the percentage of alkanes and H_2 decreased and increased, respectively, upon the 3 successive cycles. This could be ascribed to the decreasing number of the low-coordinated Pt sites (responsible of methanation) as the size of Pt NPs increased.

Chapter VI. Treatment and valorisation of brewery wastewater

1. Production of H_2 from brewery wastewater by APR with Pt/C catalysts

This chapter was adapted from: Oliveira, A.S., Baeza, J.A., Calvo, L., Alonso-Morales, N., Heras, F., Rodriguez, J.J., Gilarranz, M.A., **Production of hydrogen from brewery wastewater by aqueous phase reforming with Pt/C catalysts**, Appl. Catal. B Environ. 245 (2019) 367–375. doi:10.1016/j.apcatb.2018.12.061.

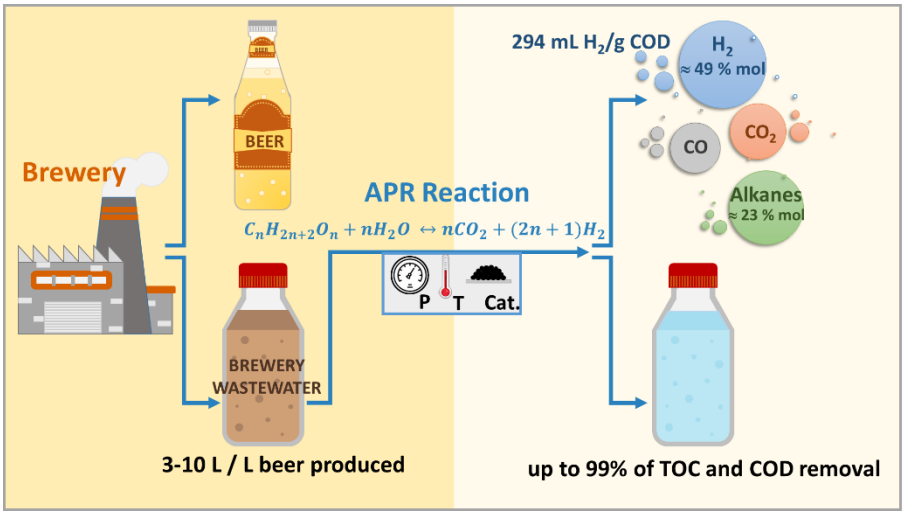

1.1. Introduction

Brewery wastewater has also been selected as a candidate for the treatment and valorisation through APR. Brewing industry generates large amounts of wastewater (3 – 10 L wastewater / L beer produced [93]), with highly variable composition, although characterized by containing high loads of organic matter and suspended solids, which cannot be discharged without convenient cleaning into the waterway or municipal sewer system. Additionally, the main compound present in this type of wastewater is maltose (a sugar containing two glucoses) which could be considered as biomass derived resource for APR reaction.

Therefore, the aim of this chapter is to evaluate the treatment and valorisation of brewery wastewater through APR with Pt catalysts using different carbon materials as supports. The effects of support type and the organic load of the wastewater on the process performance were investigated at two temperatures. Likewise, the stability of the catalyst showing the best performance was evaluated upon successive cycles.

1.2. Experimental

Pt/C (3 wt. % Pt) catalysts and standard SBW feedstock were prepared and characterized according to the procedure reported in Chapter III. One commercial activated carbon (CAP), two carbon blacks (E250 and E350) and mesoporous graphitized carbon black (C-MESO) were used as supports.

In order to analyse the influence of organic load, wastewater samples with COD values within the usual range in breweries [72] were prepared, diluting or concentrating the standard SBW feedstock described in Chapter III.

APR experiments were carried out in a batch reactor (described in Chapter III) during 4 h, using 0.3 g of catalyst in 15 mL of reaction volume under Ar atmosphere. The experiments were performed at 200 and 225 ºC in order to study the effect of the reaction temperature. The total reaction pressure was 24 – 29 bar.

Catalyst stability was assessed in 5 cycles of use. After each cycle of use, the catalyst was separated by filtration and simply dried in an oven at 60 ºC overnight. Then it was used for the next cycle. Pt leaching was below the TXRF detection limits after the APR experiments, therefore leaching can be considered negligible.

1.3. Results and discussion

1.3.1. Characterization of synthetic brewery wastewater

Table VI-1 shows the TOC and COD values of the standard SBW, as well as its pH and the main ionic species. The TOC of the standard SBW feedstock was close to 2000 mg / L and the COD was approximately 6200 mg / L, being the COD/TOC ratio about 3. This relatively high ratio suggests that there is a relative abundance of oxygen-containing organic species in the wastewater. The initial pH value was 6.9. The main anion species analysed by IC were chloride, glycolate, acetate, formate, phosphate and sulphate. Chloride was detected at low concentrations (4 mg / L), mainly ascribed to malt extract and peptone, which may contain chlorides. The glycolate concentration was 9 mg / L and acetate and formate were detected at much lower concentrations, not exceeding 1 mg / L, mainly ascribed to malt extract and maltose, which may contain different compounds including acetic, formic, fumaric, oxalic and glycolic acids [94]. Phosphate and sulphate were the main anions since they were directly introduced in the preparation of the SBW.

Table VI-1. TOC, COD, main anions detected and initial pH of the standard SBW

TOC (mg / L)	1968 ± 111
COD (mg / L)	6229 ± 341
Chloride (mg / L)	4 ± 1
Glycolate (mg / L)	9 ± 1
Acetate (mg / L)	1 ± < 1
Formate (mg / L)	1 ± < 1
Phosphate (mg / L)	215 ± 89
Sulphate (mg / L)	772 ± 124
Initial pH	6.9 ± 0.2

In order to analyse the influence of organic load, samples with different organic matter concentration were prepared. Table VI-2 shows the TOC and COD values for all of the wastewater concentrations studied in this chapter.

Table VI-2. TOC and COD of the SBW tested with different organic load

TOC_i (mg / L)	COD_i (mg / L)
474 ± 47	1531 ± 120
974 ± 24	3046 ± 62
1968 ± 111*	6229 ± 341*
4124 ± 222	11204 ± 486

*Standard SBW feedstock.

1.3.2. Performance of the Pt/C catalysts

1.3.2.1. Effect of the support

The effect of the support on the performance of the Pt catalysts in the APR of brewery wastewater (COD_i = 6229 mg / L) was investigated at 200 and 225 ºC. Figure VI-1 shows the TOC and COD removal after the 4 h APR experiments. The results of blank tests (without catalysts) are also included.

In general, the removal was higher at 225 than at 200 ºC, which indicates that C-C and C-O bond cleavage is favoured by increasing the temperature [57].

Blank experiments resulted in TOC and COD removal values between 48 – 54 %, which can be partly ascribed to HTC, since a dark brown solid was recovered by filtration after the treatment. Table VI-3 shows the elemental composition of the solid recovered after blank experiments, which is similar to those found in the literature for hydrochars [95]. The TOC and COD removal was improved from values ca. 50 % for blank runs to values ca. 80 % for catalyzed runs, particularly in the case of Pt/CAP, Pt/E250 and Pt/E350 catalysts. In spite of their significantly different surface area, these three catalysts showed quite similar efficiency for the conversion of the organic matter present in SBW upon APR. The porous texture neither seems to be a determining factor looking at the dramatically different pore size distribution of the microporous activated carbon (CAP) and the E250 carbon black and their similar results in terms of organic matter breakdown.

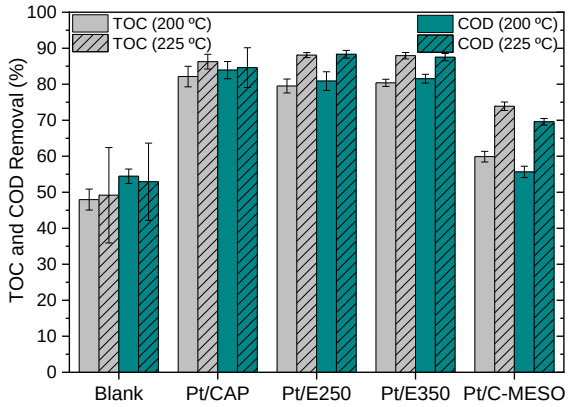

Figure VI-1. TOC and COD removal after APR experiments of SBW at 200 and 225 ºC*

*Reaction conditions: total reaction pressure: 24 – 29 bar, 15 mL of SBW (1968 mg / L TOC_i, 6229 mg / L COD_i), 0.3 g of catalyst, 500 rpm, 4 h.

Table VI-3. Elemental composition of the solid recovered after blank experiments

T (ºC)	% C	% H	% N	% S	% O*
200	60.2	4.3	6.1	0.3	29.1
225	60.5	4.4	5.5	0.4	29.2

*Calculated by difference.

Figure VI-2 depicts the concentrations of the main organic anions analysed in the initial and APR-treated wastewater. Other anionic species such as chloride, phosphate and sulphate were detected by IC, however, they were not significantly affected by the APR treatment. Only in the reactions carried out with Pt/CAP the phosphate concentration raised up to 1092 – 1263 mg / L, which can be ascribed to release from the support, which was manufactured by activation with phosphoric acid.

In the case of the blank experiments, the formate and glycolate concentrations decreased at higher temperature. Glycolic, acetic and formic acids are secondary/tertiary byproducts from glucose decay upon HTC. Glycolic acid can be produced through intermediates such as erythrose or glycolaldehyde, acetic acid through intermediates such as erythrose or 1,6-anhydro-glucose and formic acid through several intermediates such as erythrose, 1,6-anhydro-glucose, HMF or lactic acid [96]. This can explain the higher levels of glycolate, acetate and formate in these blank experiments, where HTC must be the main process. Glycolate, acetate and formate were detected in very low concentrations in the initial brewery wastewater and increased up to over 113 – 136 mg / L, 62 – 68 mg / L and 54 – 106 mg / L, respectively, in the blank experiments (equivalent to 7 – 9 % of TOC of the final liquid phase). Increasing the temperature, the glycolate concentration in the final effluent decreased (from 136 to 113 mg / L) as well as formate concentration (from 106 to 54 mg / L), while acetate concentration hardly varied. Higher temperatures generally increase gas production by HTC and it

is more likely that glycolic and formic acids are converted to gaseous products [96,97]. Similar results were found by Quitain *et al.* [98] who reported that formic acid was readily produced at lower temperature but it easily decomposed at increasing temperature. Knezevic *et al.* [96] also found that acetic acid did not contribute to gas production, while glycolic and formic acids produced significant amounts of gas upon glucose conversion.

Catalytic APR can produce a diversity of oxygenated compounds (aldehydes, alcohols, carboxylic acids) as a result of series/parallel reactions such as dehydration or isomerization [99]. In the current chapter the amount of glycolate, acetate and formate detected corresponded to 7 – 15 % of TOC of the final effluent at 200 ºC and this proportion increased to 10 – 17 % at 225 ºC. Similar results were found by Remón *et al.* [60] who observed that at high catalyst/glycerol ratio increasing the temperature increased in the proportion of carboxylic acids in the liquid phase. Acetate was not converted easily upon the APR process with the Pt catalysts tested, indicating its refractory character under the operating conditions. The anions glycolate and formate were found at much lower concentrations than in the blank experiments since they can be reformed to CO_2 and H_2 and/or CO and H_2O. Additionally, it was observed that, except with the Pt/C-MESO catalyst, the final concentration of glycolate was significantly higher at lower temperature, an effect that was not observed for acetate and formate. Finally, the Pt/CAP catalyst produced a treated wastewater with a higher acetate and lower formate concentration than the other catalysts.

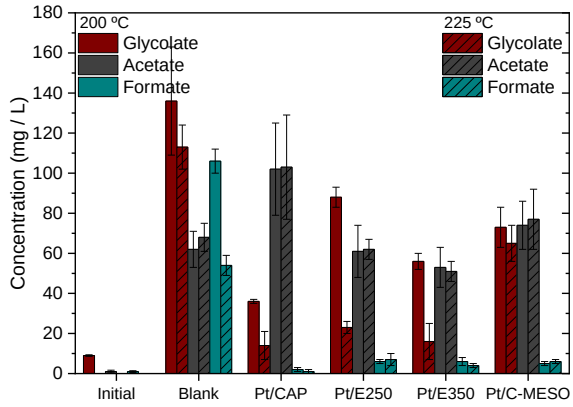

Figure VI-2. Main anions detected by IC in the initial SBW and after APR experiments*

*Reaction conditions: 200 and 225 ºC, total reaction pressure: 24 – 29 bar, 15 mL of SBW (1968 mg / L TOC_i, 6229 mg / L COD_i), 0.3 g of catalyst, 500 rpm, 4 h.

The main components identified in the gas fraction from APR were H_2, CO_2, CH_4 and C_2H_6 with all the catalysts tested. CO was only detected in the blank experiments, amounting between 5.3 – 5.5 % mol of the gas fraction. The virtual absence of CO in the catalysed experiments can be attributed to the activation of the WGS reaction by Pt. Table VI-4 shows the amount of gas produced and the composition of the gas fraction (except CO) obtained in the APR experiments together with the corresponding *CC gas* and Y_{H2} values. Blank experiments produced a very low gas volume (2.2 – 3.3 mL), consisting mainly of CO_2, essentially ascribed to HTC [97]. Catalysed APR increased substantially the volume of gas produced (15.3 – 56.1 mL) with high percentage of valuable gases, H_2 and alkanes (41.7 – 71.6 %). It can be seen that the production of gases strongly depends on the catalyst used, thus indicating some important effects of the support. The reaction temperature is also important. At the highest temperature (225 ºC) the gas volume, the percentage of H_2 and therefore Y_{H2}, were significantly higher with all the catalysts, while the percentage of alkanes (CH_4 and C_2H_6) and

CO_2 were smaller, due to a lower extent of methanation and alkanes formation reactions, which are thermodynamically favoured at lower temperatures. The value of *CC gas* also increased with temperature, consequently the remaining TOC of the liquid phase decreased, due to the favoured fragmentation of the organic matter through C-C and C-O bonds cleavage [57]. Although catalytic APR allowed always a significant increase of the *CC gas*, this varied within a fairly broad range (22.0 – 50.0 %) depending on the catalyst and temperature. Pt/E250 yielded the highest gas volume, *CC gas* and H_2 percentage in the gas fraction at the two temperatures tested. This catalyst was also the one for which the effect of temperature was more pronounced. Pt/C-MESO also allowed a high percentage of H_2 in the gas, although the gas volume obtained with this catalyst was lower. The percentage of CH_4 in the gas was higher with the Pt/CAP catalyst, representing more than 30 % of that component in the gas fraction. The performance of Pt/E350 and Pt/C-MESO catalysts, in terms of gas production, *CC gas* and Y_{H2}, was quite similar.

The best performance observed for Pt/E250 could be partially attributed to the effect of the basic character of the support. This has been found to be beneficial for carbon conversion into gas products and H_2 formation [19], while acid supports have been reported to favour alkane formation [12]. Moreover, catalysts with basic sites improve the APR process through the promotion of the WGS reaction [32]. However, the basicity of the support must not be the only responsible of the better catalytic performance, since Pt/E350 has the support with the highest pH slurry but showed lower gas production, *CC gas* and Y_{H2} than Pt/E250. The textural properties of the carbon support have also been claimed to strongly effect the results of APR [19]. Thus, some authors have associated the textural properties, such as irregular pore arrangement and high microporosity, to mass-transfer limitations [100,101]. Kim *et al.* [24] and Wang *et al.* [33] suggested that a high mesopore volume would facilitate the transport of

reactants and products, whereas microporosity limits mass transfer, thus affecting to yield and products distribution. Likewise, Kim *et al.* [102] reported that in APR of glycerol mesoporous carbon-supported Pt catalysts showed better performance in terms of *CC gas*, H_2 selectivity, yield and H_2 production rate than Pt catalysts supported on commercial activated carbon of essentially microporous texture. Therefore, the best performance shown by Pt/E250 can be most likely associated to both the moderate basic character of the support and its mesoporous texture. The similar performance showed by Pt/C-MESO and Pt/E350 catalysts could be also explained by the mesoporous structure of the support C-MESO.

The maximum Y_{H2} values in the APR of brewery wastewater were obtained with Pt/E250 at 225 ºC (293.9 mL H_2 / g COD_i). Some works in literature studied the production of H_2 from brewery wastewater by batch anaerobic digestion [103]. At the optimum H_2 production conditions Y_{H2} reached values of 149.6 mL H_2 / g COD from a wastewater of similar composition to the one used in this work (COD_i = 6000 mg / L) [104]. Therefore, in this context the APR process clearly outperforms the production of H_2 by anaerobic digestion and shows an interesting potential for the treatment of wastewater. Moreover, the gas heating values calculated from gas composition (Table VI-4) ranged within 2600 – 3200 kcal/kg, supporting the interest of the potential application of APR to this type of biomass derived wastewater.

Table VI-4. Gas volume, composition of the gas fraction, *CC gas* and Y_{H2} in the APR experiments of SBW*

Catalyst	T (ºC)	Gas volume (mL)	Gas composition (% mol)				*CC gas* (%)	Y_{H2} (mmol H_2 / g COD_i)
			H_2	CO_2	CH_4	C_2H_6		
Blank	200	2.2 ± 0.4	2.2 ± 0.4	87.5 ± 3.7	3.3 ± 3.5	1.6 ± 1.9	3.8 ± 0.8	< 0.1
	225	3.3 ± 0.7	4.2 ± 1.9	80.1 ± 5.6	8.2 ± 4.0	2.0 ± 0.2	5.7 ± 1.0	0.1 ± 0.1
Pt/CAP	200	17.7 ± 0.5	5.7 ± 2.7	58.3 ± 1.2	33.9 ± 1.7	2.2 ± 0.2	28.9 ± 0.1	0.4 ± 0.2
	225	23.1 ± 2.5	19.1 ± 1.0	48.6 ± 1.8	30.4 ± 0.9	2.0 ± 0.1	32.3 ± 3.0	2.0 ± 0.3
Pt/E250	200	29.8 ± 2.1	35.4 ± 1.7	37.8 ± 3.6	23.9 ± 1.7	2.9 ± 0.2	34.0 ± 3.1	4.7 ± 0.1
	225	56.1 ± 4.6	48.9 ± 0.9	28.4 ± 0.5	21.0 ± 0.3	1.7 ± 0.1	50.0 ± 3.3	12.2 ± 1.2
Pt/E350	200	15.3 ± 1.6	19.2 ± 0.9	54.0 ± 3.7	22.6 ± 2.3	4.2 ± 0.4	22.0 ± 2.4	1.3 ± 0.1
	225	28.6 ± 0.9	34.3 ± 0.7	41.7 ± 1.5	20.6 ± 0.6	3.3 ± 0.1	33.3 ± 1.3	4.4 ± 0.1
Pt/C-MESO	200	19.4 ± 1.4	33.2 ± 1.6	45.5 ± 3.2	18.5 ± 1.3	2.8 ± 0.2	22.9 ± 2.1	2.9 ± 0.1
	225	25.0 ± 1.0	41.1 ± 1.2	39.2 ± 2.0	17.1 ± 0.7	2.5 ± 0.1	26.0 ± 1.5	4.6 ± 0.1

*Reaction conditions: 200 and 225 ºC, total reaction pressure: 24 – 29 bar, 15 mL of SBW (1968 mg / L TOC_i, 6229 mg / L COD_i), 0.3 g of catalyst, 500 rpm, 4 h.

1.3.2.2. Effect of the organic load

The effect of the organic load of the wastewater was investigated at the two temperatures of 200 and 225 ºC with the Pt/E250 catalyst, the one showing the best performance so far. Figure VI-3 shows the values of TOC and COD removal at different starting organic loads. At the lowest organic load tested (COD_i = 1531 mg / L), removal values in the range of 80 – 99 % were obtained. Nearly identical removal rates were achieved when the COD_i was increased to 3046 mg / L, while at 11204 mg / L of COD_i, the TOC and

COD removal decreased to 51 – 77 %. The trend observed is in good agreement with Kirilin *et al.* [57], who reported that the reforming of more concentrated feedstocks resulted in a reduction of the transformation of organic matter to gaseous products.

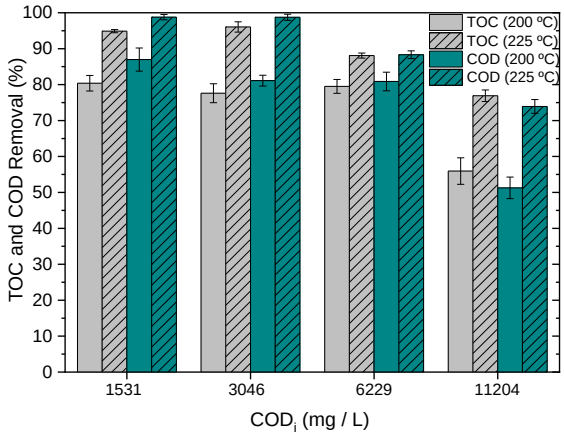

Figure VI-3. TOC and COD removal upon APR at 200 and 225 ºC at different organic load*

*Reaction conditions: total reaction pressure: 24 – 29 bar, 15 mL of wastewater, 0.3 g Pt/E250 catalyst, 500 rpm, 4 h.

Figure VI-4 depicts the concentration of the main organic anions detected after these APR experiments. Increasing the starting concentration from 1531 to 11204 mg / L COD_i caused a clear increase of the final concentration of anionic species in the liquid phase. The concentration of glycolate, acetate and formate reached maximum values of 180, 139 and 16 mg / L, respectively. No significant differences were observed in the individual anions species with temperature, except for glycolate in some cases. However, the relative amount of these species with respect to TOC increased with the temperature at all organic loads tested, varying within 4 – 51 % of TOC in the final effluent. Moreover, increasing the starting COD from 3046 to 11204 mg / L caused a decrease of the final proportion of these

species, respect to TOC, from 51 % to 12 % at 225 ºC. In this sense, Remón *et al.* [60] also observed that the proportion of carboxylic acids in the liquid phase decreased at increasing concentration of glycerol .

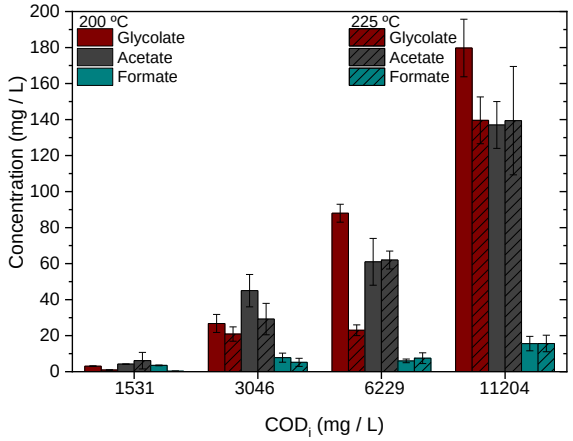

Figure VI-4. Main anions detected at 200 and 225 ºC at different organic load*

*Reaction conditions: total reaction pressure: 24 – 29 bar, 15 mL of wastewater, 0.3 g Pt/E250 catalyst, 500 rpm, 4 h.

Table VI-5 shows the gas volume produced, the *CC gas*, the composition of the gas fraction and the Y_{H2} obtained in the experiments of Figure VI-3. The gas volume produced increased gradually at increasing organic loads, up to a value of 59.7 mL at the highest concentration and temperature tested. No systematic trends could be observed respect to the composition of the gaseous products at 200 ºC. However, in the experiments carried out at 225 ºC, the percentage of H_2 increased monotonically with the starting organic load of the wastewater, reaching almost 50 % at the highest COD_i tested. An opposite trend was observed for alkanes (CH_4 and C_2H_6) although of relatively low significance. In a previous work on the APR of glycerol, Luo *et al.* [35] reported that increasing the feed concentration of glycerol from 5 to 10 wt. % increased by about 10 % the H_2 selectivity while

slightly decreasing the selectivity to CH_4. The *CC gas* and Y_{H2} decreased gradually at increasing the starting organic load, which is in good agreement with the reported by Luo *et al.* [35]. For the lowest wastewater concentration, *CC gas* values up to 73.4 % and 93.0 % were obtained at 200 and 255 ºC, respectively, while those values decreased dramatically (18.4 % and 25.4 %) at the highest organic load tested. Similar trend was observed for Y_{H2}, with also a pronounced decrease when increasing the COD of the starting wastewater.

Table VI-5. Gas volume, composition of the gas fraction, *CC gas* and Y_{H2} at different organic load*

COD_i (mg / L)	T (ºC)	Gas volume (mL)	Gas composition (% mol)				*CC gas* (%)	Y_{H2} (mmol H_2 / g COD_i)
			H_2	CO_2	CH_4	C_2H_6		
1531 ± 120	200	17.1 ± 1.1	40.7 ± 1.9	35.4 ± 3.5	22.0 ± 1.4	1.9 ± 0.1	73.4 ± 6.9	12.6 ± 0.2
	225	21.0 ± 0.8	40.5 ± 1.1	35.0 ± 2.0	20.8 ± 0.8	3.6 ± 0.1	93.0 ± 4.9	15.4 ± 0.2
3046 ± 62	200	24.0 ± 1.6	44.2 ± 2.2	32.0 ± 3.8	22.1 ± 1.5	1.8 ± 0.1	47.3 ± 4.8	9.7 ± 0.2
	225	33.0 ± 1.1	46.7 ± 1.2	30.0 ± 2.0	21.2 ± 0.7	2.1 ± 0.1	62.3 ± 3.3	14.0 ± 0.1
6229 ± 341	200	29.8 ± 2.1	35.4 ± 1.7	37.8 ± 3.6	23.9 ± 1.7	2.9 ± 0.2	34.0 ± 3.1	4.7 ± 0.1
	225	56.1 ± 4.6	48.9 ± 0.9	28.4 ± 0.5	21.0 ± 0.3	1.7 ± 0.1	50.0 ± 3.3	12.2 ± 1.2
11204 ± 1486	200	33.2 ± 1.8	34.1 ± 1.2	43.5 ± 2.4	19.7 ± 1.0	2.7 ± 0.1	18.4 ± 1.3	2.8 ± 0.1
	225	59.7 ± 1.3	49.4 ± 0.8	30.6 ± 1.3	17.8 ± 0.4	2.2 ± 0.1	25.4 ± 0.9	7.3 ± 0.1

*Reaction conditions: total reaction pressure: 24 – 29 bar, 15 mL of wastewater, 0.3 g Pt/E250 catalyst, 500 rpm, 4 h.

1.3.2.3. Catalyst stability

The stability of the Pt/E250 catalyst was investigated upon 5 successive APR cycles (4 h reaction each) at 225 ºC with the standard SBW (6229 mg / L of COD_i). Figure VI-5 shows the results obtained based on TOC and COD removal and referred to the main organic anions detected. The removal of TOC and COD decreased slowly along the 4 first cycles and then recovered although to values somewhat below those of the fresh catalyst. These results indicate a fairly stable performance of the catalyst, supported also by the evolution of the anionic species given in Figure VI-5 (b).

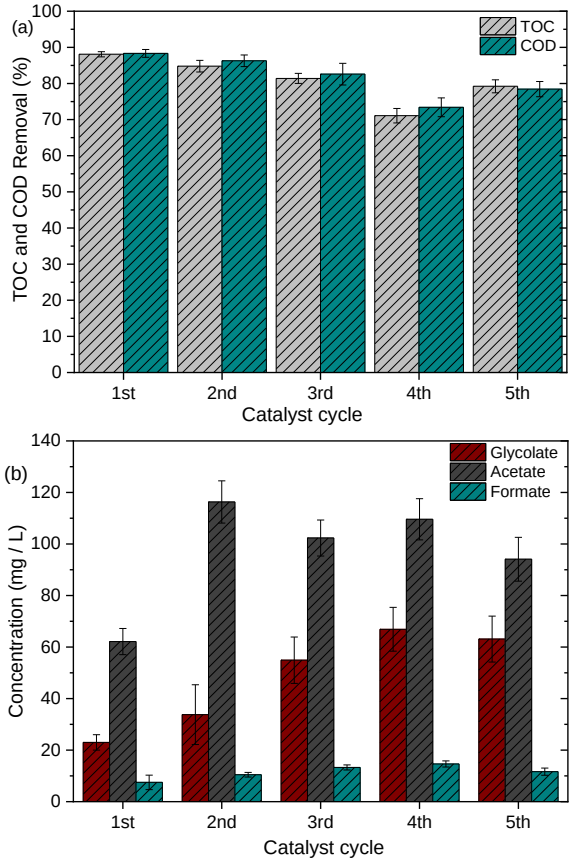

Figure VI-5. (a) TOC and COD removal and (b) anions detected upon 5 successive APR cycles*

*Reaction conditions: 225 ºC, total reaction pressure: 24 – 29 bar, 15 mL of wastewater (1968 mg / L TOC_i, 6229 mg / L COD_i), 0.3 g Pt/E250 catalyst, 500 rpm, 4 h.

The gas volume produced, the composition of the gas fraction, the Y_{H2} and the *CC gas* obtained in each cycle are summarized in Table VI-6. The production of gases and the *CC gas* decreased monotonically upon the cycles, showing these results a poorer stability of the catalyst than the suggested by the previous ones based on TOC and COD removal. As a result of the lower production of gases, Y_{H2} also decreased gradually up to about one half of the

obtained with the fresh catalysts after the 5th cycle. However, the results on the composition of the gas fraction were more stable, with a relatively small decrease of H_2 (≈ 10 %) and a moderate increase of CO_2 (≈ 25 %) in the gas composition.

Table VI-6. Gas volume, composition of the gas fraction, *CC gas* and Y_{H2} obtained upon 5 successive APR cycles*

Catalyst cycle	Gas volume (mL)	Gas composition (% mol)				*CC gas* (%)	Y_{H2} (mmol H_2 / g COD_i)
		H_2	CO_2	CH_4	C_2H_6		
1st	56.1 ± 4.6	48.9 ± 0.9	28.4 ± 0.5	21.0 ± 0.3	1.7 ± 0.1	50.0 ± 3.3	12.2 ± 1.2
2nd	48.6 ± 0.8	47.7 ± 0.6	30.9 ± 0.9	19.5 ± 0.3	1.9 ± 0.1	44.6 ± 1.2	10.3 ± 0.1
3rd	40.2 ± 1.0	46.9 ± 0.9	31.8 ± 1.5	19.3 ± 0.5	2.0 ± 0.1	37.4 ± 1.6	8.4 ± 0.1
4th	37.5 ± 0.7	46.3 ± 0.7	31.6 ± 1.1	20.0 ± 0.4	2.1 ± 0.1	35.3 ± 1.1	7.7 ± 0.1
5th	29.2 ± 1.1	43.6 ± 1.3	35.7 ± 2.1	18.5 ± 0.7	2.2 ± 0.1	34.7 ± 1.7	6.8 ± 0.1

*Reaction conditions: 225 ºC, total reaction pressure: 24 – 29 bar, 15 mL of wastewater (1968 mg / L TOC_i, 6229 mg / L COD_i), 0.3 g Pt/E250 catalyst, 500 rpm, 4 h.

To learn more on the performance of the catalyst upon successive cycles, the fresh and used Pt/E250 were characterized by adsorption-desorption of N_2, STEM, XPS and CO chemisorption. The results are collected in Table VI-7. The BET surface area remained almost constant upon use. The electrodeficient to zerovalent Pt ratio increased after the 1st cycle but then remained almost constant, so that it cannot be conclusively associated to the loss of catalytic activity. The mean size of Pt NPs, as obtained from STEM, suffered only a slow monotonical increase. However, major changes were evidenced by CO chemisorption. Pt dispersion decreased dramatically, which is not consistent with the particle size obtained by STEM. These

discrepancies can be explained through the formation of carbonaceous deposits covering Pt NPs, thus hindering CO chemisorption. That would explain the decreased activity with a lower effect on the selectivity [105]. Interestingly, deactivation of the catalyst by acetic acid has been also observed in reforming reactions with Pt-based catalysts, promoting the generation of coke precursors [106].

Table VI-7. Characterization of the fresh and used Pt/E250 catalyst upon 5 successive APR cycles*

Catalysts	Mean Pt NPs Size** (nm)	S_{BET} (m^2 / g)	Pt^{2+} / Pt^0 ratio	Pt dispersion*** (%)
initial	4.7 ± 2.5	65	0.2	21
after 1st cycle	5.2 ± 2.8	63	0.6	-
after 3rd cycle	5.5 ± 3.3	61	0.5	9
after 5th cycle	6.5 ± 3.9	61	0.6	3

*Reaction conditions: 225 ºC, total reaction pressure: 24 – 29 bar, 15 mL of wastewater (1968 mg / L TOC_i, 6229 mg / L COD_i), 0.3 g Pt/E250 catalyst, 500 rpm, 4 h.
**From STEM images.
***From CO chemisorption.

1.4. Conclusions

The APR of brewery wastewater was studied for the first time using Pt catalysts (3 wt. %) supported on different carbon materials. Two working temperatures 200 and 225 ºC were tested. In the absence of catalysts, HTC was the main process, leading to moderate TOC and COD removal (48 – 54 %) and fairly low production of gas consisting mainly of CO_2. With the Pt/C catalysts tested, APR led to substantially higher TOC and COD removal, with some significant differences between the catalysts depending on the carbon support used. The highest values of gas production were obtained with Pt/E250 at 225 ºC, possibly due to the effect of the basic character and the

mesoporous texture of the support (a non-microporous commercial carbon black).

The organic load (expressed as COD) of the starting wastewater exerts a significant influence on the catalytic performance and the results of APR. At the lowest wastewater concentration (1531 mg / L of COD_i), TOC and COD removal values up 99 % were obtained, while at the highest concentration (11204 mg / L of COD_i), these values were reduced dramatically to 51 %. However, the percentage of H_2 in the gas fraction increased with the concentration of the wastewater. The results indicate that APR can be a promising technology for biomass-derived wastewater through the production of H_2 and alkanes.

The activity of the catalysts decreased upon successive cycles of use, although no substantial changes were observed in the composition of the gas produced. Formation of carbonaceous deposits on the metal surface, appears a main cause of catalyst deactivation. The loss of activity affected mostly to the gas production and the H_2 yield and in a much lower extent to the removal of TOC and COD from the wastewater.

2. Effect of basicity in the aqueous phase reforming of brewery wastewater for H_2 production

This chapter was adapted from: Oliveira, A.S., Baeza, J.A., García, D., Saenz de Miera, B., Calvo, L., Rodriguez, J.J., Gilarranz, M.A., **Effect of basicity in the aqueous phase reforming of brewery wastewater for H_2 production**, Renew. Energy. 148 (2020) 889–896. doi:10.1016/j.renene.2019.10.173.

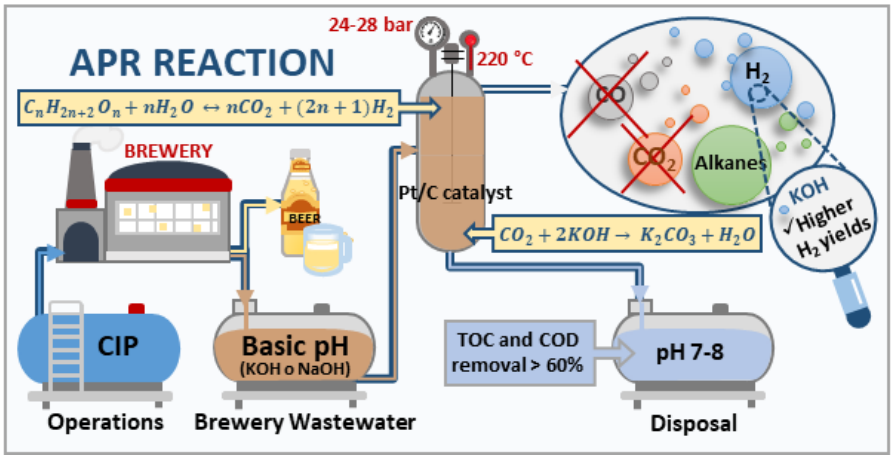

2.1. Introduction

In the previous chapter, the application of APR for the treatment of SBW with an initial pH of about 7 was analysed. Good results were obtained in terms of TOC and COD removal (up to 99 %) and valuable gases yield (up to 12.2 mmol H_2 / g COD_i), showing the potential of APR for the treatment of this sort of effluents. However, the effect of basicity of the feedstock on the catalytic performance was not evaluated. This parameter is considered relevant for the application of APR to wastewater treatment and valorisation, since bases are present in a number of industrial wastewaters due to the cleaning-in-place (CIP) operations commonly used in industries such as processing food, beverages, brewing or pharmaceuticals, among others. In addition, usually, the CIP cycle involves several water-consuming steps, above ambient temperatures and the use of caustic solutions, leading to basic wastewaters that cannot be treated by conventional biological methods without previous neutralization.

Although some APR studies evaluated the effect of the pH of the feedstock [9,53], the role of bases (i.e KOH, NaOH) in the reaction medium is not well addressed. Several authors have reported positive effects of a basic medium on the APR process due to favoured WGS reaction [22,52], *in-situ* removal of CO_2 [22,52,107], or increased gas production [49]. However, some authors indicated a negative effect on catalyst deactivation [50]. For instance, in the case of glycerol using Ni-La/Al_2O_3 catalysts, some authors [49] reported that the presence of acetic acid decreased gas production, while KOH increased it. In another related study [50] using similar catalysts, the effect of different acids (phosphoric, sulphuric and acetic) and bases (KOH and NaOH) on the APR of glycerol was investigated, concluding that these compounds affected to catalyst deactivation, particularly in the case of phosphoric acid and KOH.

Accordingly, in the current chapter, the effect of NaOH and KOH concentration on the catalysts performance in APR of SBW was analysed. NaOH and KOH are commonly found in the formulation of detergents for CIP systems used in breweries, therefore, they were the bases selected for this study. Likewise, a real brewery wastewater (RBW) has been tested to learn on the potential of application APR to these effluents.

2.2. Experimental

Pt/C (3 wt. % Pt) catalysts were prepared and characterized according to the procedure reported in Chapter III. Two commercial activated carbons (CAP and MER) and two carbon blacks (E250 and KJB) were used as supports.

In order to evaluate the effect of basicity on the catalytic performance, SBW feedstock (described in Chapter III) was prepared without addition of NaH_2PO_4 and Na_2HPO_4. Moreover, NaOH and KOH were added to adjust the pH of SBW. The pH of SBW was 7, and was adjusted to 11 for some experiments since this is the pH value for the RBW studied. This last was collected from the plant of an international brewing company based nearby Madrid (Spain). SBW and RBW were characterized by TOC and COD measurements.

APR experiments were carried out in a batch reactor (described in Chapter III) during 4 h, using 0.3 g of catalyst in 15 mL of reaction volume under Ar atmosphere. The experiments were performed at 200 ºC and the total reaction pressure was 24 – 28 bar.

2.3. Results and discussion

2.3.1. Synthetic and real brewery wastewater characterization

The comparison of characterization of the SBW and RBW, including TOC, COD, pH and main anions analysed, is summarized in Table VI-8. The RBW showed TOC and COD values of 1646 and 4674 mg / L, respectively. The pH of RBW was basic (pH 11) since it contains significant amounts of the NaOH commonly used in the CIP operations carried out in the food processing and beverages industry. The main organic anions detected correspond to short chain organic acids, which are commonly present in malt extract [94]. The SBW was prepared with a TOC and COD of 1968 and 6229 mg / L, respectively, which are close to above values for RBW and in good agreement with the range of TOC and COD reported for this type of wastewater [72]. The starting pH of SBW was neutral. The main differences found between SBW and RBW in terms of anions composition were relative to acetate and sulphate, which were in significantly higher and lower concentration, respectively, in the case of RBW.

Table VI-8. Comparison between characterization of the SBW and RBW

	SBW	RBW
TOC (mg / L)	1968 ± 111	1646 ± 230
COD (mg / L)	6229 ± 341	4764 ± 586
Glycolate (mg / L)	9 ± 1	39 ± 3
Acetate (mg / L)	1 ± < 1	172 ± 10
Formate (mg / L)	1 ± < 1	37 ± 3
Phosphate (mg / L)	18 ± 3	15 ± 1
Sulphate (mg / L)	772 ± 124	41 ± 4
Initial pH	7	11

2.3.2. APR of synthetic brewery wastewater

Figure VI-6 depicts the TOC and COD removal in the blank (without catalyst) and catalysed APR experiments with SBW. Likewise, the results of the experiments with SBW modified with NaOH (SBW+NaOH) or KOH (SBW+KOH) up to a pH value of 11 are included. The lowest TOC and COD removal (40 – 60 %) corresponded to the blank and can be ascribed mostly to HTC of the organic substrates, which is favoured under the operating conditions used [108]. In general, the TOC and COD removal were higher when catalysts were used, particularly in the case of Pt/KJB, Pt/MER and Pt/CAP, which reached removal values close to 70 %. The addition of KOH and NaOH to SBW provoked a slight decrease in TOC and COD removal in all experiments, except with Pt/E250 catalyst. Base addition increased the selectivity towards liquid phase products, probably through base-catalysed dehydration followed by hydrogenation reactions [54], thus reducing the TOC and COD removal. No significant differences in TOC and COD removal were found by using NaOH or KOH in the experiments with SBW.

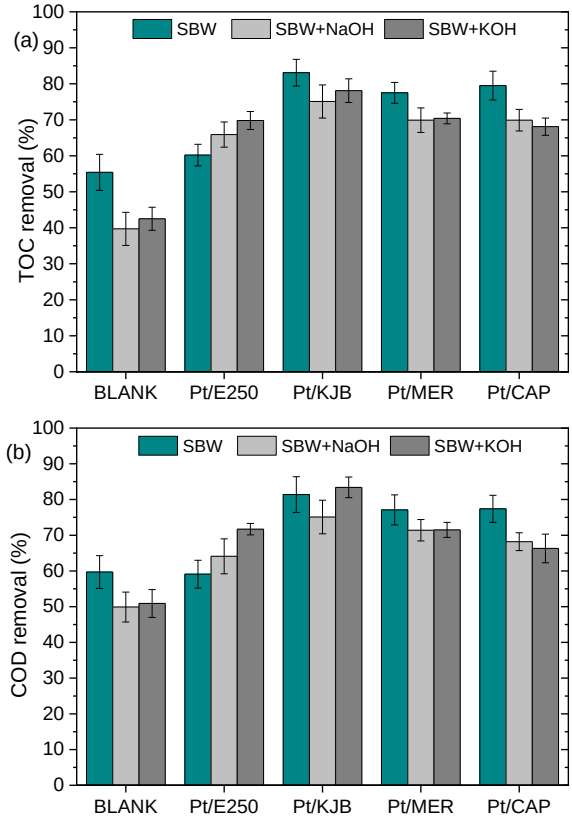

Figure VI-6. (a) TOC and (b) COD removal in the APR of SBW (pH_i = 7), and SBW+NaOH and SBW+KOH (pH_i = 11)[*]

[*]Reaction conditions: 220 ºC, total reaction pressure: 24 – 28 bar, 15 mL of wastewater, 0.3 g of catalyst, 500 rpm, 4 h.

Table VI-9 shows the concentration of short chain carboxylic anions and the pH values measured before and after APR experiments. Acetate, formate and glycolate were the most representative in the initial SBW. These three anions significantly increased their concentration in experiments without catalyst (blank), especially in the case of SBW+NaOH and SBW+KOH. During the HTC process organics acids such as formic, acetic and levulinic acids are produced from biomass-derived organic compounds. Some authors [109] have reported that basic conditions significantly affect

the decomposition pathway of HMF, which is converted to levulinic or formic acid, increasing the concentration of these acids. In the catalytic APR test, the concentration of these anions decreased in general, particularly in the case of formate, indicating that conversion of the initial substrates takes place upon APR reactions through mechanisms different from those of HTC. Acetate concentration was barely affected by the operating conditions, indicating its refractory character, whereas the glycolate concentration was very sensitive to the type of catalyst, being higher in the SBW+NaOH and SBW+KOH experiments. The carboxylic anions from the blank experiments amounted 9 – 19 % of the final TOC, this increasing to 13 – 24 % with bases addition. Moreover, the Pt/MER and Pt/CAP catalysts yielded in general effluents with higher glycolate concentration and percentage of short chain carboxylic anions in the final liquid phase of TOC (20 – 24 %). A similar observation was made by King *et al.* [54] in the APR of glycerol, who found a higher production of acids with the addition of a base to the reaction medium. They suggested that KOH could promote the Cannizzaro reaction, facilitating the production of acids. Another study using *in-situ* X-ray absorption spectroscopy reported a higher selectivity to acids (four-fold) upon addition of KOH (pH_i = 11.8) in the APR of glycerol [55]. This effect was explained through the interaction between KOH and adsorbed reaction intermediates, especially aldehydes, on the surface of Pt. The final pH of the effluents was 3 – 4 in the APR experiments with SBW (starting pH = 7), whereas it ranged between 6 and 8 in the SBW+NaOH and SBW+KOH experiments, when amounts of acids were produced, giving rise to base neutralization.

Table VI-9. Short chain carboxylic anions in the effluents from the SBW, SBW+NaOH and SBW+KOH APR experiments*

Sample	Wastewater	Short chain carboxylic anions (mg / L)			Initial pH	Final pH
		Acetate	Formate	Glycolate		
Initial	SBW	2 ± 1	1 ± 1	8 ± 2	7	-
BLANK	SBW	74 ± 9	66 ± 7	105 ± 9	7	3
	SBW+NaOH	123 ± 11	118 ± 14	221 ± 12	11	8
	SBW+KOH	126 ± 12	121 ± 13	209 ± 10	11	7
Pt/E250	SBW	98 ± 6	2 ± 1	64 ± 5	7	4
	SBW+NaOH	104 ± 9	10 ± 4	103 ± 8	11	8
	SBW+KOH	106 ±7	6 ± 3	82 ± 9	11	8
Pt/KJB	SBW	61 ± 5	1 ± 1	34 ± 2	7	3
	SBW+NaOH	80 ± 4	6 ± 1	111 ± 6	11	8
	SBW+KOH	89 ± 5	7 ± 1	91 ± 8	11	8
Pt/MER	SBW	79 ± 5	4 ± 1	102 ± 8	7	3
	SBW+NaOH	71 ± 3	12 ± 2	199 ± 10	11	8
	SBW+KOH	73 ± 6	14 ± 1	200 ± 12	11	7
Pt/CAP	SBW	117 ± 8	1 ± 1	67 ± 3	7	3
	SBW+NaOH	72 ± 4	19 ± 3	249 ± 11	11	6
	SBW+KOH	100 ± 6	11 ± 2	256 ± 12	11	6

*Reaction conditions: 220 ºC, total reaction pressure: 24 – 28 bar, 15 mL of wastewater, 0.3 g of catalyst, 500 rpm, 4 h.

Table VI-10 summarizes the gas volume produced, gas composition, *CC gas* and H_2 yield in the APR experiments. The volume of gas produced varied within a wide range (1.0 – 40.1 mL), with the blanks showing the lowest production (1.0 – 2.2 mL). The blanks gave *CC gas* between 1.7 – 3.8 %, consisting mainly of CO_2 (50 – 87 %) with low H_2 yields (< 0.03 mmol H_2 / COD_i). CO was only detected in the blank experiments, representing 9 % of the gas fraction from the APR of SBW and reaching more than 30 % from SBW+NaOH and SBW+KOH. The catalysts supported on carbon blacks showed a gas production between 12.2 and 40.1 mL, with *CC gas* in the 15.8 – 41.3 % range and H_2 yields between 1.4 and 8.9 mmol H_2 / g COD_i. These values were significantly higher than the obtained with the activated carbon supported catalysts (gas volume: 2.9 – 8.4 mL; *CC gas*: 3.7 – 15.1 %;

H_2 yield: 0.05 – 0.15 mmol H_2 / g COD_i). This frankly higher production of H_2 can be attributed to the fact that the E250 and KJB carbon blacks are basic supports that can enhance the WGS reaction. Some authors [52] have suggested that the basic medium can favours the polarization and dissociation of H_2O, providing hydroxyl anions that can be adsorbed on the catalysts surface, enhancing the WGS reaction [89]. However, the Pt/MER catalyst yielded basic pH slurry while giving low amounts of H_2 and other gases. This behaviour of the Pt/MER catalyst can be related to its porous texture, since the MER support has a high contribution of micropores opposite to E250 and KJB. That would determine severe mass transfer limitations of reactants and products, resulting in low gas production, H_2 selectivity and yield [24,33,102]. The Pt/CAP catalyst has an important contribution of mesopores, but both the presence of micropores and the low pH slurry of the support may causes the low H_2 production observed, similar to that of Pt/MER.

Regarding the effect of the addition of bases to the wastewater, it has been reported [22,52] that CaO or KOH can favour the WGS reaction by gas withdrawal through the *in-situ* removal of CO_2, displacing the reactions towards H_2 production. In the current chapter the addition of bases led to lower percentages of CO_2 in the gas fraction with all the catalysts tested, particularly in the experiments with SBW+KOH, indicating that the addition of a base was effective for the removal of CO_2. However, the Y_{H2} in the SBW+KOH and SBW+NaOH experiments was higher than in the SBW ones only with the Pt/KJB catalyst. King *et al.* [54] studied the effect of KOH addition in the APR of glycerol using 3 wt. % Pt/C and 3 wt. % Pt-Re/C catalysts and found a dramatic increase of glycerol conversion. However, they reported a higher production of liquids, being the gas product and H_2 yield barely affected. Likewise, they suggested that the addition of KOH favoured the C-O bond cleavage, compared to C-C bond cleavage, by base-

catalysed dehydration followed by hydrogenation that reduces the H_2 production. Karim *et al.* [55] also found similar results in the APR of glycerol with Pt/C catalysts. The addition of KOH did not affect the gas phase products, while a higher glycerol conversion was observed. These authors also attributed the results to a higher selectivity toward dehydration reactions, which was reflected in a higher C-O/C-C ratio and lower H_2 and CO_2 selectivities in the presence of that base.

Comparing the bases used, the highest percentage of H_2 was obtained with KOH. The experiments carried out with SBW+KOH also led to higher gas production, *CC gas*, Y_{H2}, and in some cases a lower percentage of alkanes in the gas fraction. This can be better appreciated for the catalysts that yielded higher amounts of gases (Pt/E250 and Pt/KJB). Similar results were obtained by Liu *et al.* [52] in the APR of ethylene glycol using Ni catalysts with different potassium salts and NaOH. The authors concluded that KOH leads to higher *CC gas* and Y_{H2} and lower alkanes yields, probably due to blockage of active sites enabling CO methanation. The addition of K to Pt/hydrotalcite catalysts was studied in the APR of glycerol [110] and the results showed that it enhanced the basicity of the catalysts and increased the glycerol conversion and H_2 selectivity, although an excess of K loading blocked the active sites of Pt NPs, having the opposite effect.

In the SBW+KOH experiments the Pt/E250 catalyst gave the highest percentage of valuable gases (H_2 and alkanes) in the gas fraction (≈ 75 %) and H_2 yield (8.9 mmol H_2 / g COD_i ≈ 213.6 mL H_2 / g COD_i). This production of gas is higher than the reported in the literature from the anaerobic biological treatment of an equivalent brewery wastewater (initial COD ca. 6000 mg / L, 149.6 mL H_2 / g COD_i) [104], thus showing the potential of APR as way of valorisation of brewery wastewater.

Table VI-10. Gas volume produced, composition of the gas fraction, *CC gas* and Y_{H2} in the APR of SBW (pH_i = 7), SBW+NaOH (pH_i = 11) and SBW+KOH (pH_i = 11)*

Sample	Wastewater	Gas Volume (mL)	Gas composition (% mol)			*CC gas* (%)	Y_{H2} (mmol H_2 / g COD_i)
			H_2	CO_2	Alkanes		
BLANK	SBW	2.2 ± 0.3	1.8 ± 0.3	86.8 ± 6.1	2.2 ± 0.3	3.8 ± 0.4	< 0.1
	SBW+NaOH	1.0 ± 0.4	6.6 ± 1.0	50.4 ± 6.4	7.5 ± 3.5	1.7 ± 0.7	< 0.1
	SBW+KOH	1.4 ± 0.4	4.2 ± 0.1	58.8 ± 7.0	6.7 ± 2.1	2.5 ± 0.7	< 0.1
Pt/E250	SBW	40.1 ± 0.5	46.7 ± 0.5	32.0 ± 0.8	21.3 ± 0.3	41.3 ± 0.9	8.9 ± 0.1
	SBW+NaOH	23.7 ± 7.1	51.4 ± 2.0	25.6 ± 1.7	23.0 ± 3.7	21.8 ± 7.5	5.8 ± 1.5
	SBW+KOH	35.5 ± 6.9	52.7 ± 0.4	25.1 ± 0.1	22.2 ± 0.4	1.8 ± 6.1	8.9 ± 1.7
Pt/KJB	SBW	12.2 ± 0.5	23.5 ± 0.6	56.9 ± 1.4	19.6 ± 0.9	17.5 ± 0.9	1.4 ± 0.1
	SBW+NaOH	12.5 ± 0.5	32.7 ± 1.0	44.5 ± 1.9	22.8 ± 1.0	15.8 ± 0.9	1.9 ± 0.1
	SBW+KOH	19.3 ± 3.5	38.6 ± 3.4	39.7 ± 2.3	21.7 ± 1.1	22.3 ± 3.1	3.5 ± 0.9
Pt/MER	SBW	4.3 ± 0.4	3.2 ± 0.8	87.4 ± 0.2	9.4 ± 0.9	7.5 ± 0.7	0.1 ± 0.1
	SBW+NaOH	2.2 ± 0.4	4.4 ± 1.3	89.6 ±0.1	6.0 ± 1.2	3.7 ± 0.7	0.1 ± 0.1
	SBW+KOH	2.8 ± 0.4	9.5 ± 0.2	76.4 ± 1.6	14.1 ± 1.8	4.7 ± 0.6	0.1 ± 0.1
Pt/CAP	SBW	8.4 ± 0.4	1.6 ± 0.4	72.1 ± 0.7	26.3 ± 1.1	15.1 ± 0.6	0.1 ± 0.1
	SBW+NaOH	2.9 ± 0.4	5.6 ± 0.6	86.2 ± 0.4	8.2 ± 1.0	4.9 ± 0.6	0.1 ± 0.1
	SBW+KOH	2.9 ± 0.4	10.6 ± 0.1	80.3 ± 1.2	9.1 ± 1.2	4.7 ± 0.6	0.1 ± 0.1

*Reaction conditions: 220 ºC, total reaction pressure: 24 – 28 bar, 15 mL of wastewater, 0.3 g of catalyst, 500 rpm, 4 h.

2.3.3. Effect of pH on the catalyst performance

Given the good results obtained with the Pt/E250 catalyst it was selected to assess the effect of the pH in the APR of SBW+KOH. The pH values tested were selected taking into account the previous results of CO_2 production in the corresponding experiments at an initial pH value of 11. An initial pH value of 13.0 was calculated as the one providing the stoichiometric amount of KOH needed to convert all the CO_2 produced, according to Equation (17). Initial pH values below and above that value (11 and 13.5, respectively) were selected.

$$CO_2 + 2\,KOH \rightarrow K_2CO_3 + H_2O \quad (17)$$

Figure VI-7 shows the TOC and COD removal achieved at these three initial pH values. Around 70 % of TOC and COD removal reached at pH_i = 11, while lower percentages were achieved at higher pH. Similar results were found in the APR of glycerol with 3 wt. %Pt/C upon the addition of KOH (pH_i = 12) [54]. Therefore, this base may change the reaction pathway, increasing the production of liquids without increasing significantly the H_2 yield, due to competitive reactions involving base-catalysed dehydration followed by subsequent hydrogenation.

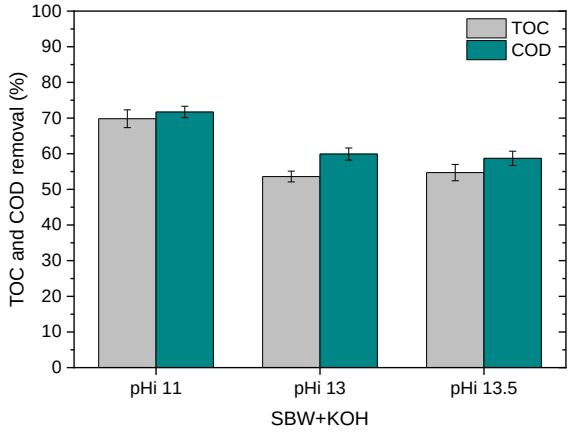

Figure VI-7. TOC and COD removal in the APR of SBW+KOH with Pt/E250 at different initial pH[*]

[*]Reaction conditions: 220 ºC, total reaction pressure: 24 – 28 bar, 15 mL of SBW+KOH, 0.3 g Pt/E250 catalyst, 500 rpm, 4 h.

Table VI-11 shows the concentration of representative anions from the APR experiments of SBW+KOH at different initial pH values. In all cases the pH decreased along the APR due to de the generation of organic acids. Acetate, formate and glycolate concentration was much lower at the lowest starting pH (pH_i = 11). The amount of these anions corresponded to 14 % of the final TOC, while increasing up to 30 and 36 % at 13 and 13.5 initial pH, respectively. Thus confirming that organic acids formation is favoured at increased pH [54,55].

Table VI-11. Short chain carboxylic anions the APR of SBW+KOH with Pt/E250 at different initial pH[*]

Sample	Initial pH	Short chain carboxylic anions (mg / L)			Final pH
		Acetate	Formate	Glycolate	
Pt/E250	11	106 ±7	6 ± 3	82 ± 9	8
	13	235 ± 11	33 ± 4	392 ± 12	10
	13.5	330 ± 16	30 ± 4	419 ± 14	12

[*]Reaction conditions: 220 ºC, total reaction pressure: 24 – 28 bar, 15 mL of SBW+KOH, 0.3 g Pt/E250 catalyst, 500 rpm, 4 h.

Table VI-12 shows the gas volume produced, the composition of the gas fraction, *CC gas* and Y_{H2} at the different values of initial pH tested. The *CC gas* significantly decreased from around 32 %, for an initial pH of 11, to around 15 % for 13 and 13.5 initial pH, due to the *in-situ* removal of the CO_2 giving rise to potassium carbonate. Table VI-12 also shows that for those initial pH values no CO_2 was found in the gas fraction. A *corrected-CC gas* (*Cor.-CC gas*) was estimated for the reactions performed under those conditions by adding the amount of CO_2 produced in the experiment at pH 11. No significant differences were found between the *CC gas* of the reaction carried out at initial pH 11 and the *Cor.-CC gas* at 13 and 13.5. Therefore, the *in-situ* removal of CO_2 did not affect to the total carbon conversion to gases. The volume of gas produced decreased from 35.5 mL, for an initial pH 11, to 25.8 – 27.1 mL at 13 and 13.5. The Y_{H2} did not change significantly with the initial pH of the wastewater (8.7 – 9.0 mmol H_2 / g COD_i) and the amount of alkanes was similar in all the experiments (0.31 – 0.34 mmol). However, looking at the results in more detail, it can be seen that the molar fraction of C_2H_6 and C_3H_8 of the total alkanes ((C_2H_6 + C_3H_8) / (CH_4 + C_2H_6 + C_3H_8) decreased from 10 % at initial pH 11, to 3 and 2 % at 13 and 13.5, respectively. This indicates that the addition of KOH reduce the formation of C_2^+, probably because the dehydration-hydrogenation of alcohols is hindered [54].

Table VI-12. Gas volume produced, composition of the gas fraction and Y_{H2} in the APR of SBW+KOH with Pt/E250 at different initial pH[*]

Initial pH	Gas produced (mL)	Gas composition (% mol)			*CC gas* (%)	*Cor.-CC gas* (%)	Y_{H2} (mmol H_2 / g COD_i)
		H_2	CO_2	Alkanes			
11	35.5 ± 6.9	52.7 ± 0.4	25.1 ± 0.1	22.2 ± 1.7	31.8 ± 6.1	-	8.9 ± 1.7
13	27.1 ± 1.9	70.2 ± 2.0	0	29.8 ± 2.0	15.0 ± 0.1	30.9	9.0 ± 0.9
13.5	25.8 ± 1.4	71.0 ± 1.5	0	29.0 ± 1.4	13.8 ± 0.1	29.6	8.7 ± 0.7

[*]Reaction conditions: 220 ºC, total reaction pressure: 24 – 28 bar, 15 mL of SBW+KOH, 0.3 g Pt/E250 catalyst, 500 rpm, 4 h.

2.3.4. APR of real brewery wastewater

The study of the treatment by APR of RBW was carried out with a sample of pH_i 11, from a brewing plant. However, as indicated above, RBW with pH values even higher can be generated depending on the dosage of alkali used in the CIP operations and could contribute to total or partial removal of CO_2 from the resulting gas without affecting significantly the production of valuable gases. The percentages of TOC and COD removal upon APR of that RBW are depicted in Figure VI-8. They ranged between 22 – 75 % and 30 – 78 %, respectively. The lowest values corresponded to the blank which undergoes basically HTC at a lower than the SBW previously tested. The results show that minor components of RBW are determining in the case of blank experiments, as observed in other works showing that complex carbohydrates contribute largely to the formation of hydrochar [111]. The removal of TOC and COD from SBW and RBW was equivalent with Pt/E250 and Pt/KJB and slightly lower with Pt/MER.

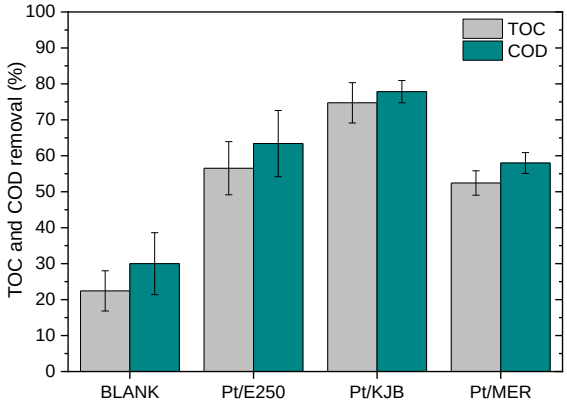

Figure VI-8. TOC and COD removal after APR experiments of RBW with different catalysts*

*Reaction conditions: 220 ºC, total reaction pressure: 24 – 28 bar, 15 mL of RBW, 0.3 g of catalyst, 500 rpm, 4 h.

Table VI-13 shows the concentration of short chain carboxylic anions and the pH values measured before and after APR of RBW. The concentrations of acetate, formate and glycolate significantly increased in the blank experiments. The amount of those species in the starting RBW corresponded to 6 % of the TOC and this proportion increased to 34 % in the blank experiment, being two-fold the percentage achieved in the blank experiments previously conducted with SBW. In the catalysed APR reactions the formate concentration hardly changed, while the concentration of acetate, glycolate and maleate increased significantly, leading to final pH values between 7 and 8. Moreover, the Pt/MER catalyst yielded higher glycolate concentration than the other catalysts, as observed in the APR of SBW as well. In the APR of RBW, in contrast to SBW, the proportion of carboxylic anions in the remaining TOC was higher with the Pt/KJB catalyst (60 % of final TOC) than with the Pt/MER one (44 %).

Table VI-13. Short chain carboxylic anions and final pH upon APR of RBW by APR with different catalysts (pH_i = 11)*

Sample	Short chain carboxylic anions (mg / L)				Final pH
	Acetate	Formate	Glycolate	Maleate	
Initial	172 ± 10	37 ± 3	39 ± 3	4 ± 1	-
BLANK	449 ± 13	260 ± 3	463 ± 3	0	7
Pt/E250	481 ± 13	44 ± 7	242 ± 7	25 ± 3	8
Pt/KJB	420 ± 8	30 ± 2	109 ± 2	12 ± 4	8
Pt/MER	386 ± 17	31 ± 2	504 ± 7	26 ± 1	8

*Reaction conditions: 220 ºC, total reaction pressure: 24 – 28 bar, 15 mL of RBW, 0.3 g of catalyst, 500 rpm, 4 h.

Table VI-14 shows the volume and composition of the gas fraction, *CC gas* and Y_{H2} from the APR of RBW. The lowest *CC gas* (3 %) was obtained in the blank experiments. The carbon-black catalyst (Pt/E250 and Pt/KJB), yielded *CC gas* between 27 and 40 %, significantly higher than the obtained with Pt/MER. Likewise, those catalysts gave the highest *CC gas* from both SBW and RBW, being similar with Pt/E250 and significantly higher from the real wastewater with the Pt/KJB catalyst. The H_2 yield in the last case reached 12.9 mmol H_2 / g COD_i (≈ 309.1 mL H_2 / g COD), which is equivalent to the highest H_2 yield found in the previous chapter with SBW but at higher temperature (225 ºC, 12.2 mmol H_2 / g COD_i). This H_2 yield achieved doubles the optimized value reported from anaerobic biological treatment (149.6 mL H_2 / g COD) [104].

Table VI-14. Gas volume produced, composition of the gas fraction, *CC gas* and Y_{H2} in the APR of RBW*

Sample	Gas produced (mL)	Gas composition (% mol)			*CC gas* (%)	Y_{H2} (mmol H_2 / g COD_i)
		H_2	CO_2	Alkanes		
BLANK	1.6 ± 0.1	0.9 ± 0.6	94.2 ± 2.1	3.6 ± 0.2	3.3 ± 0.1	< 0.1
Pt/E250	26.3 ± 4.1	51.1 ± 3.2	28.8 ± 2.1	20.1 ± 1.1	27.0 ± 4.0	7.8 ± 1.4
Pt/KJB	41.2 ± 2.4	53.6 ± 6.3	26.5 ± 5.6	19.9 ± 0.7	40.0 ± 2.9	12.9 ± 2.3
Pt/MER	4.7 ± 0.9	11.7 ± 6.9	78.9 ± 7.6	9.4 ± 0.7	8.5 ± 1.0	0.3 ± 0.3

*Reaction conditions: 220 ºC, total reaction pressure: 24 – 28 bar, 15 mL of RBW, 0.3 g of catalyst, 500 rpm, 4 h.

2.4. Conclusions

The APR of brewery wastewater was studied using different Pt/C catalysts (3 wt. %) and alkaline agents (NaOH, KOH) in order to assess the influence of the basicity conferred to wastewaters by CIP operations. TOC and COD removal in blank experiments was between 40 – 60 %, mainly ascribable to HTC of organic substrates, while removal values were higher when catalysts were used (up to 83 %). The addition of NaOH or KOH to SBW resulted in slightly lower TOC and COD removal, although an increase in the percentage of valuable gases (H_2 and alkanes) and H_2 yield was observed, mainly when KOH was added. Catalysts supported on carbon blacks showed better performance in the APR of SBW in terms of gas production, carbon conversion to gas and H_2 yields, respect to activated carbons due to higher basicity. Pt/E250 yielded the highest percentage of valuable gases in the gas fraction (≈ 75 %) and the highest H_2 yield (8.9 mmol H_2 / g COD_i) in the APR of SBW+KOH with an initial pH of 11. Increasing the initial pH of SBW+KOH up to pH 13 and 13.5, led to CO_2-free H_2 without

modifying the H_2 yield. Virtually CO free H_2 was also obtained, which relevant in applications such as fuel cells. The results obtained with SBW or RBW were relatively similar, indicating that SBW is a good representative of RBW for testing as a wastewater treatment and valorisation approach. However, the different H_2 yields obtained with Pt/KJB from SBW and RBW suggest that the composition of the wastewater needs to be considered for the sake of optimization.

3. Optimised H_2 production in continuous aqueous phase reforming of brewery wastewater

This chapter was adapted from: Oliveira, A.S., Baeza, J.A., Calvo, L., Rodriguez, J.J., Gilarranz, M.A., **Optimised H_2 production in continuous aqueous phase reforming of brewery wastewater**, (not published).

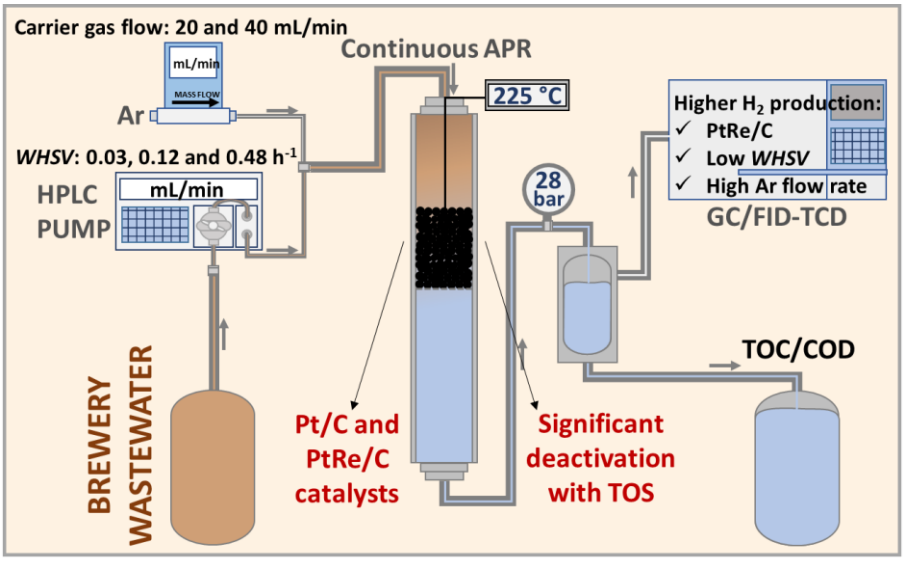

3.1. Introduction

In previous chapters, APR has been proposed as an alternative route for the treatment and valorisation of brewery wastewater. The study has been focussed mainly in the evaluation of the effect of different variables on the catalyst performance in a batch reactor. However, these reactors are not suitable for larger scales, especially using diluted feedstocks as those used in this work, and make studies of catalyst stability difficult. These aspects are approached in commonly by the use continuous instead of batch reactors. The differences in contact mode, concentration profiles, etc. between batch and continuous reactors affect the APR process and avoid direct comparison of the results.

Accordingly, the focus of the current chapter is to evaluate the effect of important parameters in brewery wastewater treatment by APR in continuous reactor, and to find the appropriate reaction conditions that favours H_2 production. The selected parameters have been the type of active metal, weight hour space velocity (*WHSV*) and carrier gas flow.

3.2. Experimental

Pt/C (3 wt. % Pt) and PtRe/C (3 wt. %, metal ratio 1:2) catalysts were prepared and characterized according to the procedure reported in Chapter III, both of them using a commercial activated carbon (MER) as support.

SBW feedstock (described in Chapter III) was prepared without addition of NaH_2PO_4 and Na_2HPO_4. Moreover, KOH was added to the SBW to adjust pH value to 10, since the real brewery wastewater is usually basic due to the use of CIP processes, which are common in food and beverages industries. SBW was characterized by TOC and COD measurements and

TOC and COD values of 1968 ± 111 mg / L and 6229 ± 341 mg / L of were obtained, respectively.

APR experiments were carried out in a continuous reactor (described in Chapter III, first setup) at 225 ºC and 28 bar during 24 h TOS using 1 g of catalyst. The effect of *WHSV* was evaluated providing a 0.25, 1 and 4 mL / min flow into the reactor, which corresponds to 0.03, 0.12 and 0.48 h^{-1} *WHSV*, respectively, based on C content in brewery wastewater (i.e. g of C per h and per g of catalyst). Ar was used to purge the reaction system and as carrier gas throughout the reaction. The effect of carrier gas flow was evaluated using different flow rates (20 and 40 N mL / min).

3.3. Results and discussion

3.3.1. Effect of active metal

The effect of active metal on the catalytic performance was investigated by comparing Pt/C and PtRe/C catalyst at a *WHSV* of 0.12 h^{-1}. The experiments were performed using 20 N mL / min of Ar flow rate. Figure VI-9 shows the TOC and COD removal with TOS for Pt/MER and PtRe(1:2)/MER catalysts. PtRe(1:2)/C catalyst showed higher TOC and COD removal values than Pt/MER, indicating that Re addition increased the catalytic activity of Pt/MER catalyst. This increase in activity is due to synergistic effects through the combination of both metals, since monometallic Re catalysts exhibit in general lower activity in APR that monometallic Pt catalysts [23].

TOC and COD removal peaked for values of TOS between 1-3 h for both Pt/MER and PtRe(1:2)/MER catalysts. A stabilization time is of ca. 1 h is needed before the removal peaks for Pt/MER catalyst, whereas a longer time of 2 h is required for catalyst PtRe(1:2)/MER. The difference between the two catalysts may indicate also induction time due to acclimation of the

catalysts. Some authors have interpreted this induction time as a stabilization stage where the metallic phase evolves to a more active structure [105].

After peaking, the TOC and COD removal values significantly decreased and then remained at relatively constant but much lower values for long TOS. This pattern suggests that the catalysts tested undergo significant deactivation in the first hours of reaction.

For both catalysts, TOC was removed in a larger extent than COD, showing that the remaining organic load in the effluent consumes more oxygen in the COD oxidation test than the original constituents of the wastewater. The higher ratio between COD and TOC removal for Pt/MER catalyst (e.g. 0.65 vs 0.42 for PtRe(1:2)/MER at peak activity) may indicate different degradation routes for different active phases. Deactivation also leads to a change in the degradation routes since COD removal to TOC removal ratio increases to 0.89 for Pt/MER and decreases to 0.40 for PtRe(1:2)/MER for longer TOS.

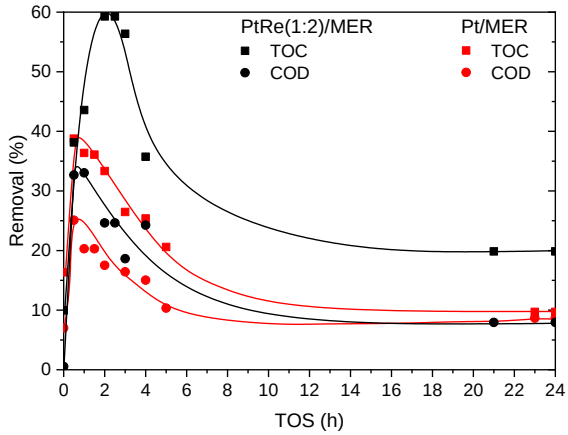

Figure VI-9. TOC and COD removal for Pt/MER and PtRe(1:2)/MER catalysts vs TOS*

*Reaction conditions: 225 ºC, 28 bar, 1 g of catalyst, *WHSV* = 0.12 h^{-1}, 20 N mL / min Ar.

Figure VI-10 shows the evolution of *CC gas* for Pt/MER and PtRe(1:2)/MER with TOS. PtRe(1:2)/MER catalyst showed higher *CC gas* than Pt/MER for the peak at low TOS values, in agreement with the TOC removal pattern commented above. *CC gas* decreased abruptly after 2 h TOS, exhibiting for both catalysts very low values, less than 2 %, thus showing that the deactivation of the catalysts for the APR of brewery wastewater occurred in the first hours on stream.

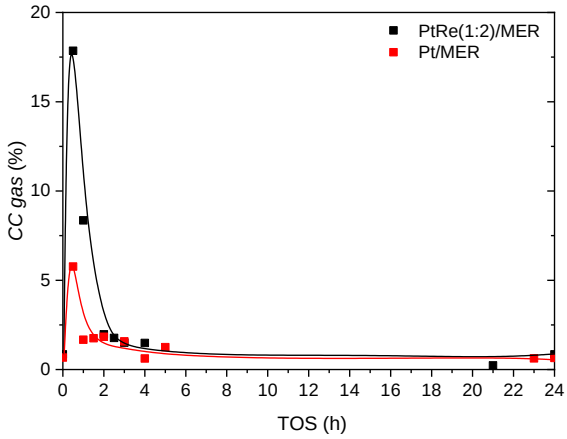

Figure VI-10. *CC gas* for Pt/MER and PtRe(1:2)/MER catalysts vs TOS*

*Reaction conditions: 225 ºC, 28 bar, 1 g of catalyst, *WHSV* = 0.12 h^{-1}, 20 N mL / min Ar.

Figure VI-11 shows the evolution of H_2, total alkanes and CO_2 production for Pt/MER and PtRe(1:2)/MER catalysts with TOS. CO was not detected in the experiments, indicating good conditions for WGS reaction. At low TOS values, PtRe(1:2)/MER catalyst showed a higher activity than Pt/MER in the production of H_2. A maximum H_2 production of 5.6 μmol / min and alkanes production of 4.4 μmol / min (89.3 % of CH_4) was observed during the first hour of reaction (Figure VI-11 (a) and (b)) using PtRe(1:2)/MER catalyst, whereas Pt/MER catalyst had a maximum H_2 production of 0.6 μmol / min. In the literature [23,54,112], some studies also

reported a higher catalytic activity and H_2 production with PtRe(1:2)/MER catalyst compared to Pt/MER ones, although it was also reported that for PtRe catalysts, H_2 selectivity can decrease due to the consumption in the hydrogenation of intermediates obtained in dehydration reactions due to the acidity of PtRe alloy. These works also attributed Re in the bimetallic catalysts a role in the increase of the WGS activity through the facilitation of water dissociation, producing OH species which are involved in the WGS reaction pathway.

The maximum production of CO_2 was also obtained at low TOS values. In spite of that, it is important to mention that, in the current chapter, the CO_2 production and consequently the *CC gas* are affected by addition of KOH to the brewery wastewater. The base addition abstract some of the CO_2 produced giving rise to the formation of carbonates in the liquid phase, thus decreasing the *CC gas*.

Both Pt/MER and PtRe(1:2)/MER catalysts showed similar pattern for the generation of gases, which may indicate that they undergo deactivation through a similar mechanism. For long TOS values both catalysts maintain a similar residual H_2 and CO_2 production. Nevertheless, the pattern in H_2 may indicate that deactivation in the case of Pt/MER takes place in earlier stages, as peak H_2 production is similar to that at long TOS and alkanes production is very low after 1 h TOS.

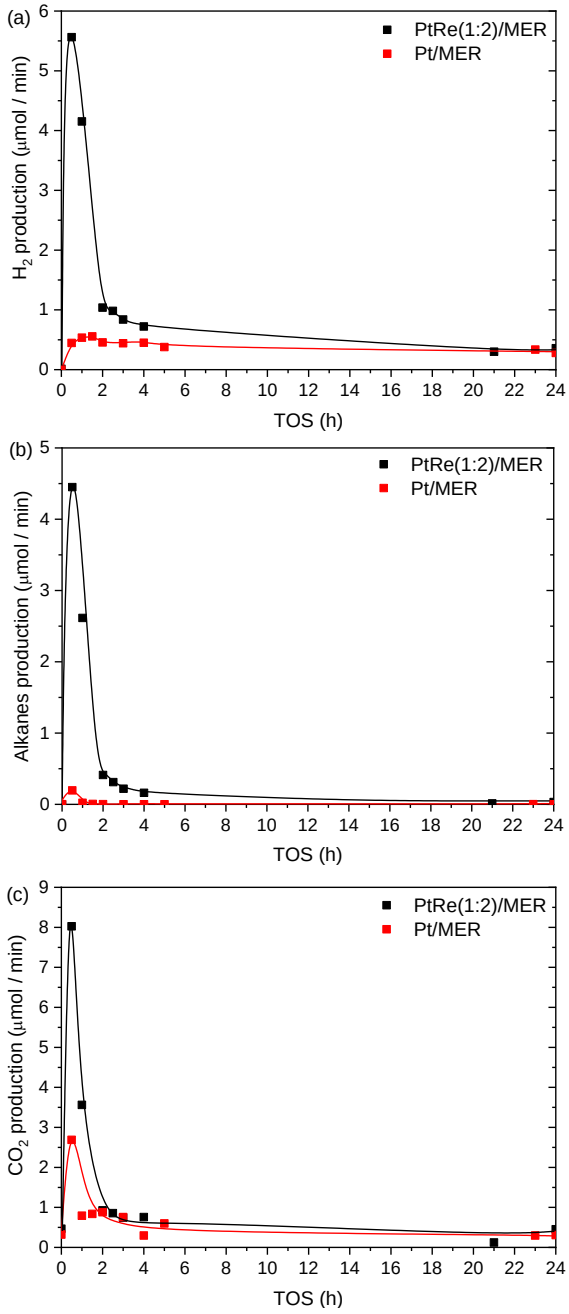

Figure VI-11. (a) H_2, (b) total alkanes and (c) CO_2 production for Pt/MER and PtRe(1:2)/MER catalysts vs TOS*

*Reaction conditions: 225 ºC, 28 bar, 1 g of catalyst, *WHSV* = 0.12 h^{-1}, 20 N mL / min Ar.

Regarding the alkanes production, the percentage of CH_4 in the total alkanes produced was high for both catalysts, between 65 and 95 %, and decreased with TOS, especially in the case of Pt/MER catalyst (Figure VI-12). The results indicate that the formation of CH_4 was also affect by catalyst deactivation, possible reducing the methanation and/or formation of intermediates related to CH_4 formation, such as methanol [34] or acetic acid [41].

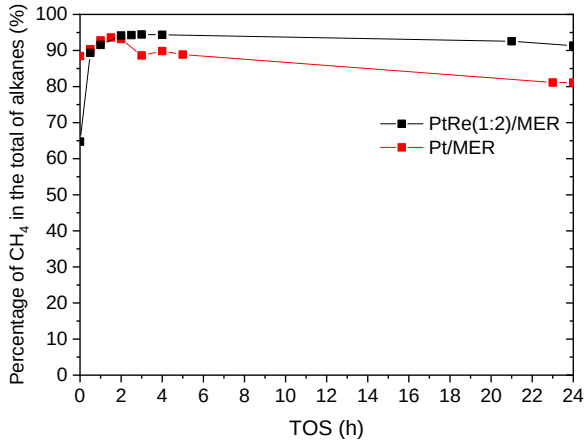

Figure VI-12. Percentage of CH_4 in the total of alkanes produced for Pt/MER and PtRe(1:2)/MER catalysts*

*Reaction conditions: 225 ºC, 28 bar, 1 g of catalyst, *WHSV* = 0.12 h^{-1}, 20 N mL / min Ar.

3.3.2. Effect of weight hourly space velocity

In order to investigate the effect of space velocity on catalytic performance, the brewery wastewater was fed into the reactor with different flow rates, from 0.25 to 4 mL / min, which correspond to *WHSV* values from 0.03 to 0.48 h^{-1}. The experiments were performed using PtRe(1:2)/MER catalyst, since it exhibited a higher catalytic activity and H_2 production than Pt/MER catalyst, and using 20 N mL / min of Ar flow rate. Figure VI-13 shows the evolution of TOC and COD removal with TOS at different *WHSV*.

A clear trend with *WHSV* was not observed, nevertheless, the removal of organic matter of wastewater, especially TOC removal, was significantly lower at 0.48 h^{-1} due to lower contact time and lower extent of the reactions leading to removal. The peak TOC and COD removal was obtained for TOS values between 1 and 5 h, and were followed by a gradual decrease in removal indicating deactivation of the catalysts. At a *WHSV* of 0.48 h^{-1}, this decline was less pronounced and the TOC and COD removal was more stable with the TOS.

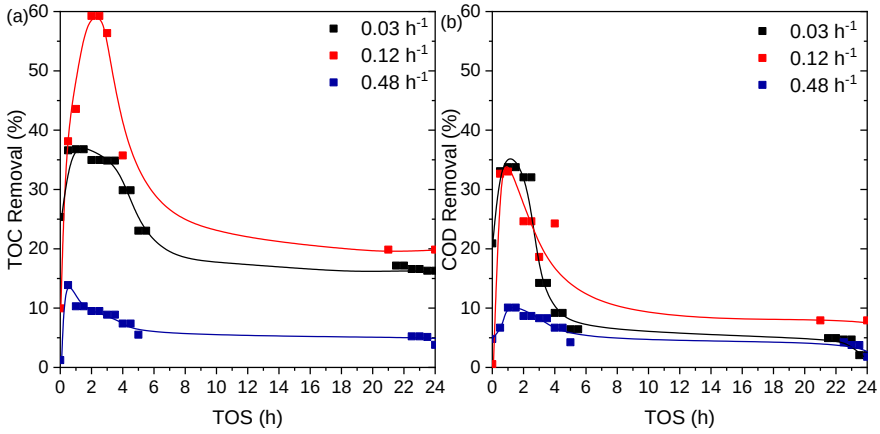

Figure VI-13. (a) TOC and (b) COD removal at different *WHSV* vs TOS*

*Reaction conditions: 225 ºC, 28 bar, 1 g of PtRe(1:2)/MER catalyst, 20 N mL / min Ar.

WHSV showed an important influence in the generation of gas products. The evolution of *CC gas* with TOS at different *WHSV* is displayed in Figure VI-14. It can be observed that *CC gas* decreased when *WHSV* increased due to shorter contact times. Kirilin *et al.* [113] and Kim *et al.* [114] also reported a similar behaviour in the APR of xylitol and ethylene glycol using PtRe catalysts. Similar to TOC and COD removal, a significantly decreased was observed with TOS, especially at lower *WHSV*. At low TOS of around 1 h a remarkable maximum of *CC gas* of 32.8 % was obtained at

0.03 h^{-1}, which matches with TOC and indicates that the degradation routes leading to gases are promoted by a higher contact between the organic species and the catalyst. It can also be observed that for a *WHSV* of 0.03 h^{-1} the removal of TOC and COD show nearly identical values. When *WHSV* increased to 0.12 h^{-1} the peak value of *CC gas* decreased to 6.2 %, and when *WHSV* increased to 0.48 h^{-1} a very low maximum conversion to gases of only 0.1 % was achieved. This trend is coherent with the lower TOC removal at 0.48 h^{-1}, but there is a large unbalance between the organic matter removed from the liquid phase and the gas produced. This lack of carbon balance closure could be due to solid phase production under these conditions, which could also be one of the causes of catalysts deactivation.

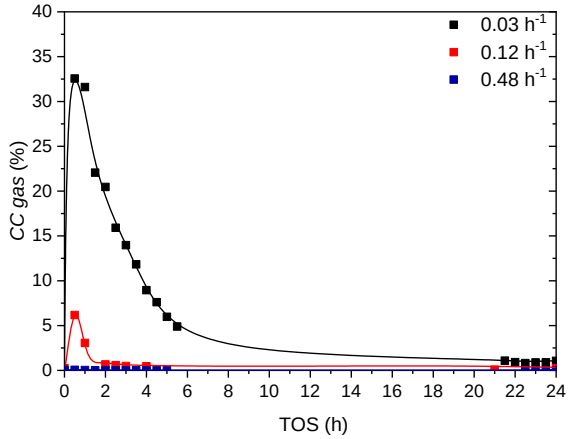

Figure VI-14. *CC gas* at different *WHSV* vs TOS*

*Reaction conditions: 225 ºC, 28 bar, 1 g of PtRe(1:2)/MER catalyst, 20 N mL / min Ar.

Figure VI-15 represents the production of H_2, alkanes and CO_2 with TOS at different *WHSV*. It can be observed the gas products follow similar trends, reaching a maximum at low TOS. The peak values for gas production can be observed for shorter TOS values than the peaks for TOC and COD removal. Likewise, the decline in gas products generation is faster than the

decline in TOC and COD removal. At lower *WHSV* (0.03 h^{-1}) the maximum of H_2 production was 17.6 μmol / min, while the production of alkanes (94.5 % of CH_4) and CO_2 was 4.2 and 7.1 μmol / min, respectively. The maximum of H_2 production decreased to 1.8 μmol / min, as well as the production of alkanes (87.4 % of CH_4) and CO_2 decreased to 0.3 and 0.1 μmol / min, respectively, when the *WHSV* increased to 0.48 h^{-1}. These results are similar to those reported by Kirilin *et al.* [14] in the APR of 10 % of xylitol solutions under similar conditions (225 ºC, 29 bar) using Pt catalyst. They reported that the rate of H_2 formation decreased from around $7x10^{-4}$ mol / min to $6x10^{-4}$ mol / min and the total alkanes formation decreased from $6x10^{-5}$ mol / min to $5x10^{-6}$ mol / min, while the conversion of xylitol decreased from around 65 to 40 %, when the *WHSV* increased from 1.8 to 3.9 h^{-1}. An increase in *WHSV* implies a higher mass of carbon substrate reacting per time and per mass of catalysts, which could lead to a higher H_2 production, however, the carbon removal decreased due to a shorter contact time. Therefore, in the range studied, the H_2 production was favoured by low *WHSV* values because of the longer contact time between the catalyst and the organic matter present in the wastewater. The H_2 produced also participates in the side reactions for alkanes formation, which justifies a higher alkanes production at lower values of *WHSV*.

The effect of *WHSV* in the deactivation of the catalysts is very significant, for values of 0.12 and 0.48 h^{-1} the decrease in the production of H_2 was very fast, whereas it became slower and gradual for 0.03 h^{-1}. Again the catalyst loosed almost totally the ability to produce alkanes but maintained a residual production of H_2, which was relatively high (1.8 μmol / min) at 0.03 h^{-1}.

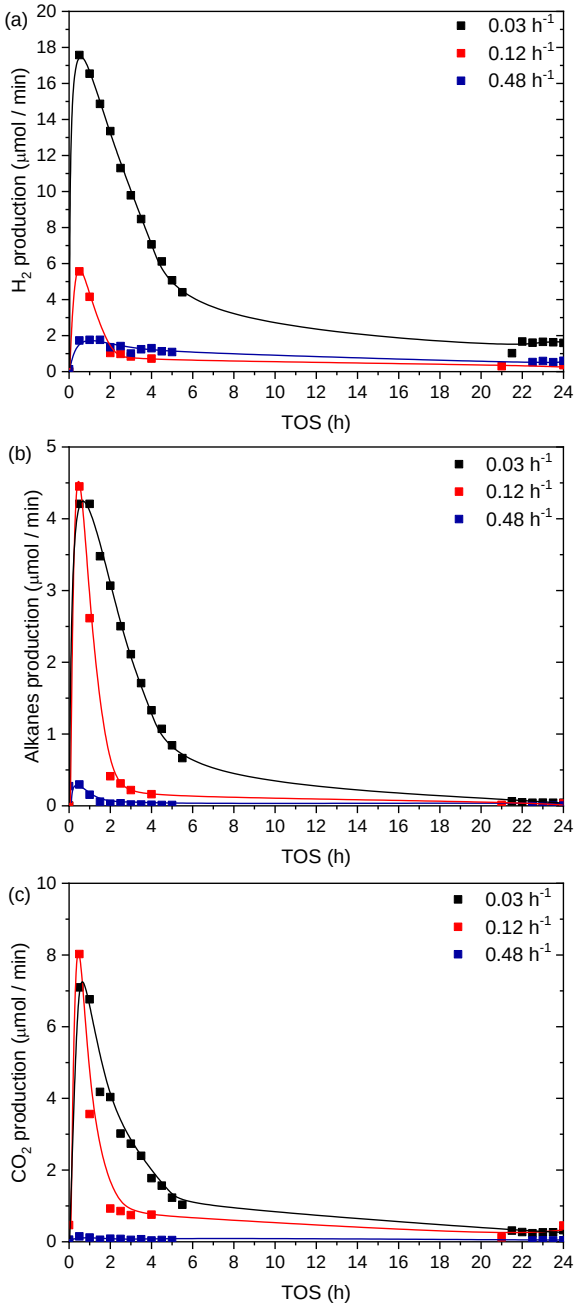

Figure VI-15. (a) H_2, (b) total alkanes and (c) CO_2 production at different *WHSV* vs TOS*

*Reaction conditions: 225 ºC, 28 bar, 1 g of PtRe(1:2)/MER catalyst, 20 N mL / min Ar.

3.3.3. Effect of carrier gas flow

The effect of carrier gas flow was evaluated increasing the Ar flow rate from 20 N mL / min to 40 N mL / min. The experiments were performed using PtRe(1:2)/MER catalyst and an intermediate space velocity value (*WHSV* of 0.12 h^{-1}). As it can be observed in Figure VI-16, TOC and COD removal decreased with the increase of the carrier gas flow and with TOS, although the decrease in the removal values with TOS was less pronounced. It is noteworthy than for a carrier gas flow of 40 N mL / min the values of TOC and COD removal are very similar.

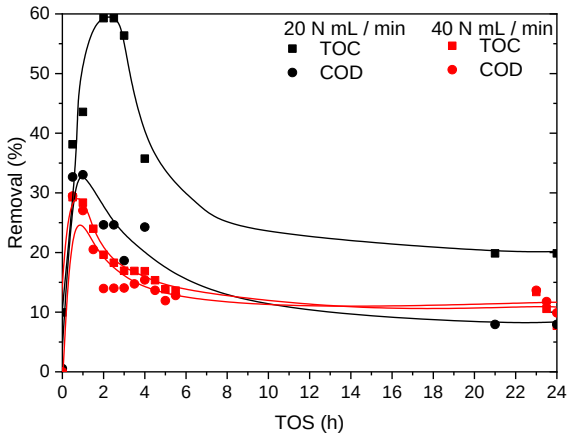

Figure VI-16. TOC and COD removal using different carrier gas flow vs TOS*

*Reaction conditions: 225 ºC, 28 bar, 1 g of PtRe(1:2)/MER catalyst, *WHSV* = 0.12 h^{-1}.

As in former experiments, *CC gas* showed a significant decline with TOS (Figure VI-17). The *CC gas* was slightly higher when a carrier gas flow of 40 N mL / min was used, indicating that a higher carrier gas flow helps to remove the gas products from the catalyst surface. In contrast, a lower TOC removal was obtained using a carrier gas flow of 40 N mL / min, this could indicate that at high carrier gas flow a lower contact between the substrate in

the liquid phase and the catalyst is achieved due to poorer wetting [115], although the substrate converted is transformed into gases in a higher extent. At low TOS, a maximum of 6.2 % of *CC gas* was obtained using 20 N mL / min of Ar, while the maximum value increased to 8.5 % when 40 N mL / min of Ar was used.

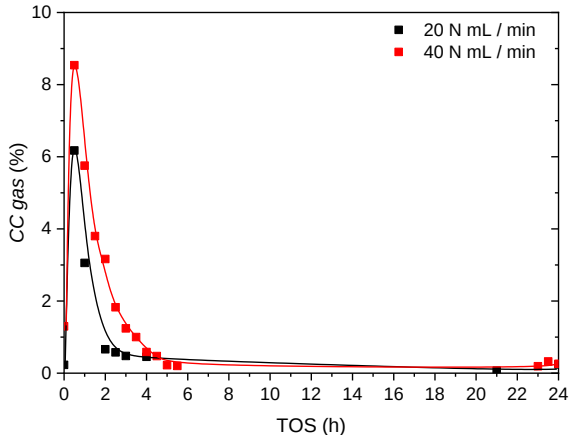

Figure VI-17. *CC gas* using different carrier gas flow vs TOS*

*Reaction conditions: 225 ºC, 28 bar, 1 g of PtRe(1:2)/MER catalyst, *WHSV* = 0.12 h^{-1}.

Figure VI-18 shows the evolution of the production of individual gas components with TOS using different carrier gas flow. It can be observed that the increase of the carrier gas flow was especially beneficial for H_2 production (Figure VI-18 (a)). At low TOS, the maximum of H_2 production increased from 5.6 μmol / min to 27.9 μmol / min, when the carrier gas flow increased from 20 to 40 N mL / min. This boost in H_2 production can be related to lower consumption in secondary reactions and in shifting in reactions leading to H_2 [61,69]. In this sense, Neira D'Angelo *et al.* [69] reported that the N_2 stripping in the APR of sorbitol decrease the partial pressure of H_2, enhance the reforming reaction rate at the expense of secondary reactions that consume H_2. The performance of microchannel and fixed bed reactors was analogous,

and H_2 selectivity and sorbitol conversion were improved by adding N_2 as a stripping agent.

After 6 h TOS the H_2 production decreased by more than 92 % at both carrier gas flows, although the residual H_2 production was higher for a carrier gas flow of 40 N mL / min. However, this last observation cannot be only explained in terms of consumption in secondary reactions, as the production of alkanes is similar for both carrier gas flows. In fact, residual production of alkanes is slightly lower for a carrier gas flow of 40 N mL / min, but only slightly. However, at low TOS, before deactivation of the catalysts, the generation of alkanes was lower for a carrier gas flow of 20 N mL / min (4.4 μmol / min) than for 40 N mL / min (6.4 μmol / min). Interestingly, the maximum of CO_2 production was similar (7.4 – 8.0 μmol / min) for both carrier gas flow studied.

The results indicate that there could be an alternative route for H_2 production, independent of catalyst activity under these reaction conditions, since for the long TOS tested the catalyst can be assumed to be almost completely deactivated. This route could be related to HTC of the organic matter present in the wastewater. The temperature gradient across the liquid boundary layer on the internal wall of the reactor can contribute to this route, as in the reactor used temperature is controlled using a thermocouple inserted in the catalytic bed.

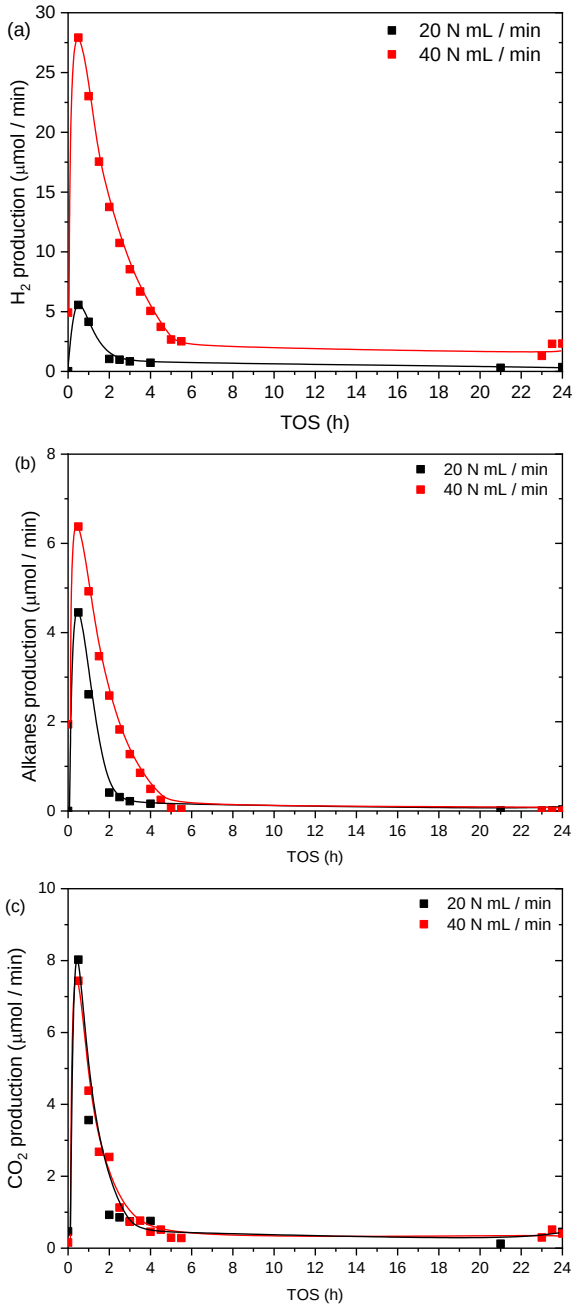

Figure VI-18. (a) H_2, (b) total alkanes and (c) CO_2 production using different carrier gas flow vs TOS*

*Reaction conditions: 225 ºC, 28 bar, 1 g of PtRe(1:2)/MER catalyst, *WHSV* = 0.12 h^{-1}.

3.4. Conclusions

PtRe/C and Pt/C were tested in the continuous APR of brewery wastewater at 225 ºC and 28 bar for H_2 production. PtRe(1:2)/MER was found to be more active than Pt/MER and the maximum of H_2 production increased of 0.6 μmol / min to 5.6 μmol / min with addition of Re to Pt phase. The effect of different W*HSV* and carrier gas flow on the catalytic performance was evaluated using the PtRe(1:2)/MER catalyst. At the lowest *WHSV* (0.03 h^{-1}) the maximum of H_2 production was 17.6 μmol / min and these value decreased to 1.8 μmol / min when the *WHSV* increased to 0.48 h^{-1}, due to shorter contact times. The alkanes production and *CC gas* also was higher at lower values of *WHSV*. When the carrier gas flow increased from 20 to 40 N mL / min, the maximum of H_2 production increased from 5.6 to 27.9 μmol / min. The alkanes production also increased at higher carrier gas flow. In all experiments, a relevant catalyst deactivation was observed after the first hours of reaction, which could be related to solid phase formation under the reaction conditions, since a large unbalance was observed between the organic matter removed from the liquid phase and the gas phase produced. A residual H_2 production was maintained even for long TOS, suggesting a generation route not dependent on the catalysts, and most probably related to HTC.

4. Catalytic performance and deactivation of Pt/C and PtRe/C catalysts in continuous aqueous phase reforming of brewery wastewater

This chapter was adapted from: Oliveira, A.S., Cordero-Lanzac, T., Baeza, J.A., Calvo, L., Rodriguez, J.J., Gilarranz, M.A., **Catalytic performance and deactivation of Pt/C and PtRe/C catalysts in continuous aqueous phase reforming of brewery wastewater**, (submitted).

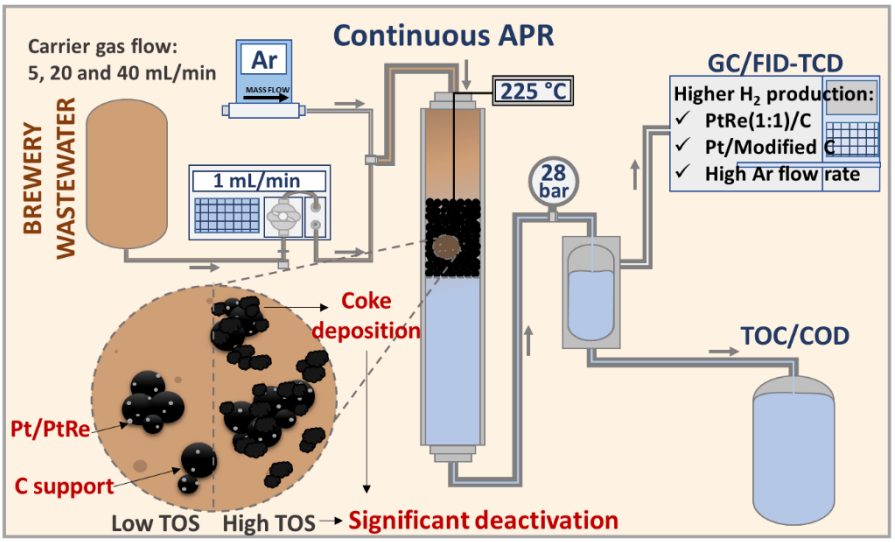

4.1. Introduction

The deactivation of carbon supported catalysts under severe APR hydrothermal conditions is a common characteristic for all systems investigated, especially when complex feedstocks are used. However, there are very few studies on this matter and mainly using alumina and simple model compounds. Loss of the surface area, due to the collapse of the support structure [39], sintering [31,44] and leaching of metal phase [67] were reported as the main causes of deactivation. In addition, some studies also reported coke deposition on the catalyst surface [67,68]. However, none of studies involves a thorough investigation of the deactivation of carbon supported catalysts using more complex feedstocks. Therefore, more research is required to understand the factors that affect catalyst stability and it can be improved.

Relevant deactivation has been described in the previous chapter on the continuous APR of brewery wastewater. This chapter analyses in more depth the catalytic performance and the deactivation of carbon supported Pt and PtRe catalysts in the APR of brewery wastewater. Likewise, the influence of the textural properties of the carbons support is evaluated by using carbon with different porosity obtained by impregnation of resol resin in a commercial carbon and further calcination.

4.2. Experimental

Pt/C (3 wt. % Pt) and PtRe/C (3 wt. %, metal ratio 1:1, 1:2 and 2:1) were prepared and characterized according to the procedure reported in Chapter III. Pt/C was prepared using MER and MERxRES as supports, while PtRe/C was prepared using only MER.

SBW feedstock (described in Chapter III) was prepared without addition of NaH_2PO_4 and Na_2HPO_4. Moreover, KOH was added to the SBW to adjust pH value to 10. SBW was characterized by TOC and COD measurements, and values of 1968 ± 111 mg / L and 6229 ± 341 mg / L of were obtained, respectively.

APR experiments were carried out in a continuous reactor (described in Chapter III, first setup) at 225 ºC and 28 bar during 24 h TOS using 1 g of catalyst. SBW was fed into was fed into the reactor with a HPLC pump providing a 1 mL / min flow, which corresponds to 0.12 h^{-1} *WHSV* based on C content in brewery wastewater (i.e. g of C per h and per g of catalyst). Ar was used to purge the reaction system and as carrier gas throughout the reaction using different flow rates (5, 20 and 40 mL / min) in order to evaluate the effect of gas products removal in catalytic performance and deactivation.

4.3. Results and discussion

4.3.1. Effect of carrier gas flow

Figure VI-19 shows the effect of carrier gas flow on TOC removal in APR of SBW at constant liquid flow rate for Pt/MER catalyst. As can be observed, TOC removal was initially higher for low Ar flow rate values (5 and 20 N mL / min), but a gradual decline suggesting deactivation was observed. When a 40 N mL / min Ar flow rate was used the stabilization of the catalyst was slower and lower initial TOC removal was achieved. Former works have shown that the use of a carrier gas can increase activity by increasing fluid dynamic conditions for mass transfer, although excessive gas flow can be detrimental due to poorer wetting and channelling [115]. In spite of lower TOC removal at 40 N mL / min, a higher stability was observed and lower loss of activity in TOC removal occurred after 24 h on stream.

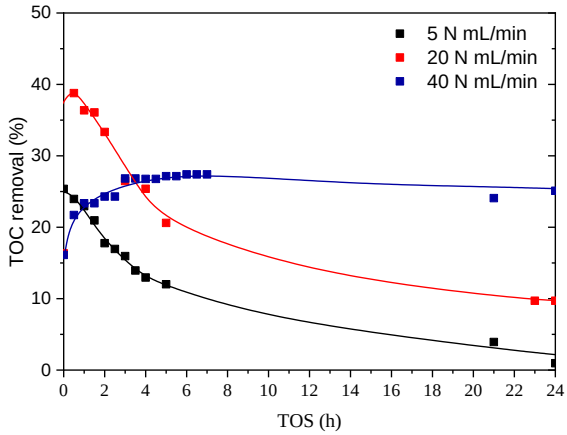

Figure VI-19. TOC removal using different carrier gas flows vs TOS*

*Reaction conditions: 225 ºC, 28 bar, 1 g of Pt/MER catalyst, *WHSV* = 0.12 h^{-1}.

The *CC gas* was low for all experiments (< 2 %) and a similar trend to the TOC removal was observed (Figure VI-20). The *CC gas* was initially higher for low Ar flow rate values, but when a 40 N mL / min Ar flow rate was used, a higher stability was observed.

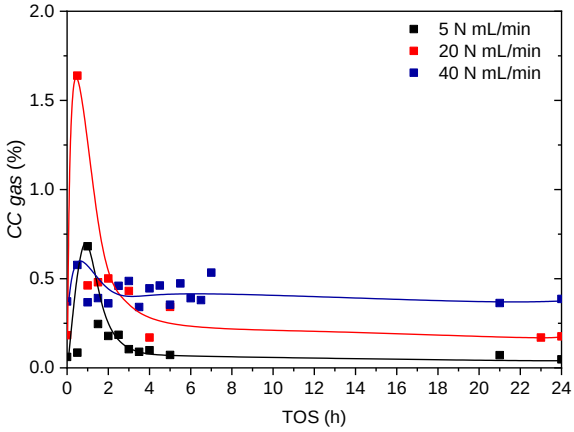

Figure VI-20. *CC gas* using different carrier gas flows vs TOS*

*Reaction conditions: 225 ºC, 28 bar, 1 g of Pt/MER catalyst, *WHSV* = 0.12 h^{-1}.

The gas production in APR of SBW at constant liquid flow rate for Pt/MER catalyst is shown in Figure VI-21. The increase of carrier gas flow was beneficial for H_2 production (Figure VI-21 (a)), whereas a decrease was observed for total alkanes production (Figure VI-21 (b)). H_2 production was similar for 5 and 20 N mL / min Ar flow rates, showing stabilization of the catalyst during the first hour on time-on-stream and then a maximum H_2 production around 0.6 μmol / min. When Ar flow rate was increased to 40 N mL / min, H_2 production stabilization was also found after ca. 1 h on stream, but production was much higher, with a maximum of 2 μmol / min. Some authors [61] also reported an increase of sorbitol conversion and H_2 selectivity by use of N_2 carrier gas for APR in a wash-coated microchannel reactor. The improvement of conversion was attributed to lower mass transfer constrains and increasing reaction rates due to lower H_2 concentration on the catalyst surface, which also led to higher H_2 selectivity and lower extent of side reactions involving H_2. In the current chapter, a decrease in alkane production can be observed as Ar flow rate increased, coherent with lower H_2 availability for secondary reactions. In the case of alkanes, a decline in production is observed with TOS. In accordance with *CC gas*, CO_2 production was higher using low Ar flow rate values in the first hours of reaction and it was more stable using 40 N mL / min Ar flow rate (Figure VI-21 (c)). It is also important to note that CO_2 production is affected by the addition of KOH to wastewater, which abstracts CO_2 through formation of carbonates in the liquid phase.

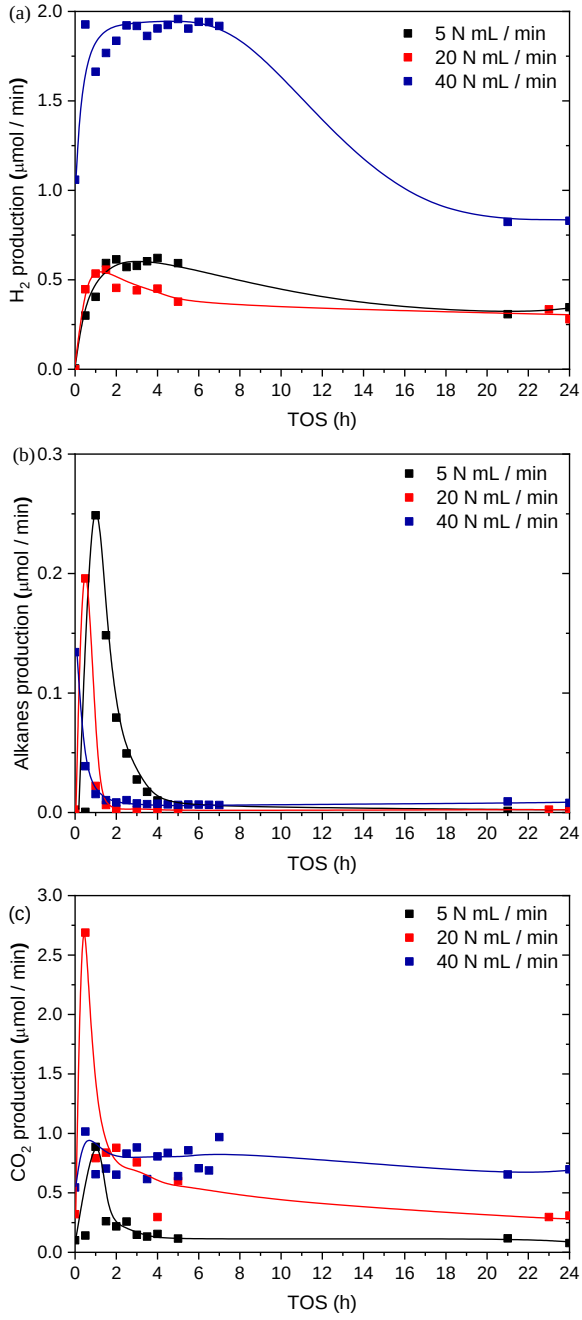

Figure VI-21. (a) H_2, (b) alkanes and (c) CO_2 production using different carrier gas flows vs TOS*

*Reaction conditions: 225 ºC, 28 bar, 1 g of Pt/MER catalyst, *WHSV* = 0.12 h^{-1}.

4.3.2. Effect of textural properties

The effect of textural properties of the catalysts in the APR of brewery wastewater was evaluated using the catalysts with modified supports (MERxRES), whose microporosity was gradually decreased by impregnation and carbonization of resol resin. All the experiments were performed using 40 N mL / min Ar flow rate, as it enhances the H_2 production and stability of the catalyst. Figure VI-22 shows the evolution of TOC removal with TOS for Pt/MER and the different Pt/MERxRES catalysts tested. All Pt/MERxRES catalysts showed a higher initial TOC removal, with maximum values at 1-2 h TOS and a significant decrease in the first 8 h TOS. After this period, TOC removal values remained relatively constant with the increase of TOS, showing that deactivation occurred mainly during the first hours on stream. For Pt/MER catalyst, TOC removal increased during the first 4 h TOS and remained relatively constant. A clear trend regarding pore texture of the catalyst cannot be observed, however during the first hours on stream TOC removal was higher for Pt/MERxRES catalysts. After stabilization, the TOC removal obtained for Pt/MER and Pt/MER10RES was similar. A direct correlation of the maximum TOC removal in Figure VI-22 and the mean NPs size (Figure IV-2) was observed, suggesting that the Pt NPs size and dispersion could indirectly affect the catalysts performance.

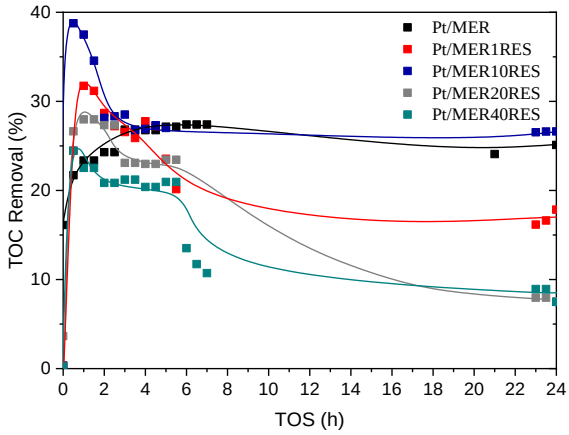

Figure VI-22. TOC removal for the Pt/MER and Pt/MERxRES catalysts vs TOS*

*Reaction conditions: 225 ºC, 28 bar, 1 g of catalyst, *WHSV* = 0.12 h^{-1}, 40 N mL / min Ar.

The CC values were low in all cases (< 6 %) and significantly decreased with TOS for all catalysts (Figure VI-23). It can be observed that *CC gas* was higher for Pt/MERxRES catalysts than for Pt/MER catalyst, especially at lower TOS values, which is in accordance with trends in TOC removal. However, for high TOS values small differences were observed among the different catalysts. Catalyst Pt/MER1RES, the one prepared with the lowest amount of resol, showed the highest *CC gas*. The *CC gas* values decreased with the increase of the amount of resol in the support.

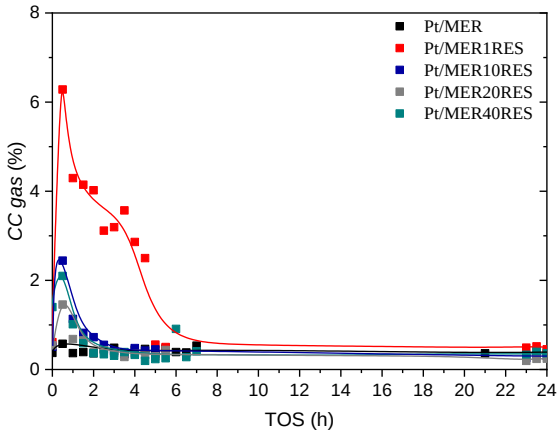

Figure VI-23. *CC gas* for the Pt/MER and Pt/MERxRES catalysts vs TOS*

*Reaction conditions: 225 ºC, 28 bar, 1 g of catalyst, *WHSV* = 0.12 h^{-1}, 40 N mL / min Ar.

Figure VI-24 shows H_2, CO_2 and total alkanes production for Pt/MER and different Pt/MERxRES catalysts with TOS. The catalytic activity significantly decreased with TOS for all catalysts, also following similar patterns and indicating similar deactivation mechanism. At low TOS values Pt/MERxRES catalysts showed higher H_2 production than Pt/MER, indicating that a lower microporosity of the catalysts facilitates the transport of reactants to catalytic active sites and removal of gas products. During the first hour on stream Pt/MER40RES catalyst showed a maximum in H_2 production of 12 μmol / min, while for Pt/MER a significantly lower production of 2 μmol / min was observed. Although the microporosity decreased with the increase of the percentage of resol added to the support, at lower TOS values the order of H_2 production among these catalysts was Pt/MER40RES > Pt/MER10RES > Pt/MER20RES > Pt/MER1RES > Pt/MER. Pt/MER10RES achieved a higher H_2 production (10 μmol / min) than Pt/MER20RES (8 μmol / min) at lower TOS values, in spite of having a higher micropore volume. This behaviour could be attributed to the different

size of Pt NPs in these catalysts, clearly enhanced with Pt/MER10RES catalyst. Chen *et al.* [27] reported that the gas volume produced and the H_2 selectivity increased when the Pt NPs size decreased from 5.7 nm to 1.6 nm in the APR of low-boiling fraction of bio-oil. They suggested that smaller NPs size could provide more stable Pt-C bond than Pt-O bond and facilitate the C-C bond cleavage for H_2 production. On the other hand, Ciftci *et al.* [28] investigated the influence of Pt NPs size in the range from 1.2 nm to 4.2 nm in the APR of glycerol and found that the catalyst with an intermediate NPs size of 2 nm exhibits optimum C-C bond cleavage rates as well as optimum activity towards H_2 production. Therefore, the higher H_2 production of Pt/MER10RES catalyst could be attributed to its NPs mean size closer to 2 nm.

The alkanes production presented a behaviour similar to that of H_2 production at low TOS values. However for long TOS, the alkanes production decreased to very low values for all the catalysts, showing that it is much more affected by deactivation than H_2 production. Pt/MER40RES catalyst showed a maximum of alkanes production of around 2 μmol / min (87 % of CH_4) at 0.5 h TOS, while at this TOS alkanes production for Pt/MER was lower than 0.05 μmol / min. CO_2 production was in accordance with *CC gas*, the Pt/MER1RES catalyst showed the highest CO_2 production and, consequently, the *CC gas* for this catalyst was higher.

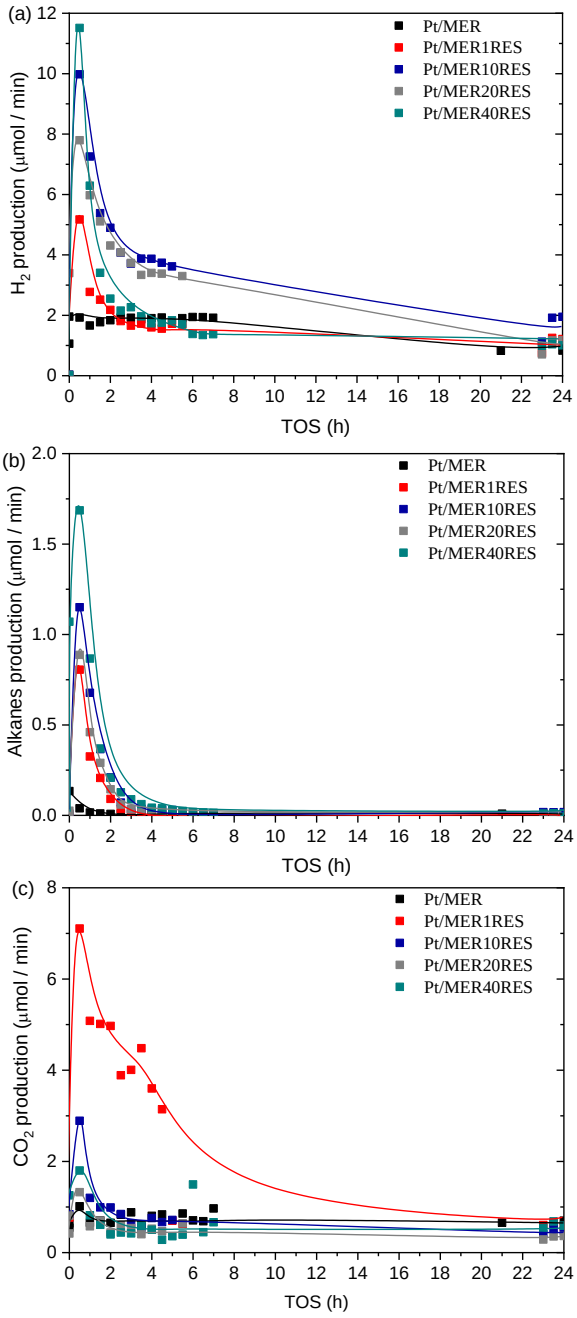

Figure VI-24. (a) H_2, (b) total alkanes and (c) CO_2 production for Pt/MER and Pt/MERxRES catalysts vs TOS*

*Reaction conditions: 225 ºC, 28 bar, 1 g of catalyst, *WHSV* = 0.12 h^{-1}, 40 N mL / min Ar.

4.3.3. Effect of active metal

Pt/MER and PtRe/MER catalysts were tested to evaluate the effect of active metal in the catalytic performance and deactivation of carbon-supported catalysts. An Ar flow rate of 40 N mL / min was used in the experiments in order to improve TOC removal and H_2 production. Figure VI-25 shows TOC removal as a function of TOS. PtRe(1:1)/MER catalyst showed the highest TOC removal at lower TOS values, however, the TOC removal significantly decreased between 1 and 6 h TOS, indicating that a significant deactivation occurs during the first hours on stream for this catalyst. A similar trend was observed for PtRe(1:2)/MER, but this catalyst achieved lower TOC removal in all the TOS range tested. The PtRe(2:1)/MER catalyst, which had a lower loading of Re compared to the other bimetallics catalysts, showed a similar behaviour to that of Pt/MER. Both of them showed a gradual increase of TOC removal at low TOS values and then approximately constant TOC removal at higher TOS values, indicating a lower deactivation of these catalysts. Therefore, the Re addition seems to favour the deactivation, which could be attributed to a higher contribution of dehydration reactions. Dehydration of carbohydrates, such as glucose and fructose, leads to formation of furan compounds, such as HMF and furfural. These compounds can react by aldol condensation to form larger organic molecules with unsaturated bonds [116] that can easily condense towards to coke structures [117] and therefore lead to catalyst deactivation.

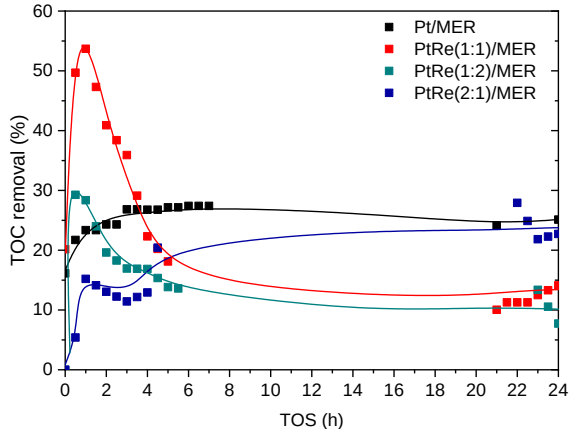

Figure VI-25. TOC removal for Pt/MER and PtRe/MER catalysts vs TOS*

*Reaction conditions: 225 ºC, 28 bar, 1 g of catalyst, *WHSV* = 0.12 h^{-1}, 40 N mL / min Ar.

Figure VI-26 shows the *CC gas* for Pt/MER and PtRe/MER catalysts with TOS. All bimetallic catalysts showed a higher *CC gas* than monometallic ones at low TOS values. The highest *CC gas* was achieved with PtRe(1:1)/MER (34 %) at 0.5 h TOS. After 4 h TOS only this catalyst showed *CC gas* values higher than 1 %.

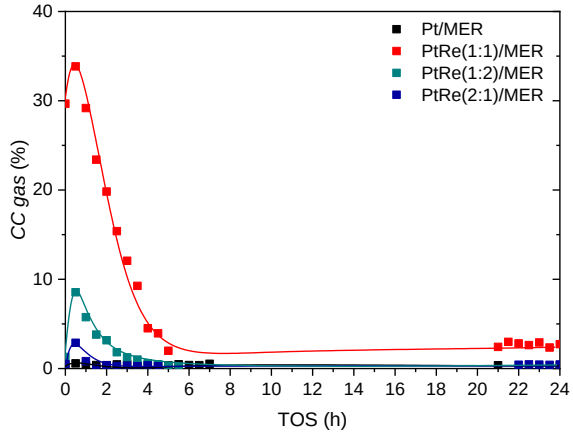

Figure VI-26. *CC gas* for Pt/MER and PtRe/MER catalysts vs TOS*

*Reaction conditions: 225 ºC, 28 bar, 1 g of catalyst, *WHSV* = 0.12 h^{-1}, 40 N mL / min Ar.

Figure VI-27 shows H_2, CO_2 and total alkanes production for Pt/MER and PtRe/MER catalysts with TOS. All bimetallic catalysts showed a higher activity than Pt/MER. Several authors [23,54,112] have reported a higher catalytic activity for PtRe/C catalysts than for Pt/C ones. They attributed this higher activity to improvement of the WGS reaction with PtRe alloys, because the Re in the bimetallic catalysts facilitates water activation, an important step to WGS reaction, since the most significant reaction pathway involves the formation of carboxyl (COOH) intermediate by the reaction of CO with OH [118]. Consequently, the H_2 production increased in the presence of PtRe/C catalysts (Figure VI-27 (a)), although some authors [54,112] have also reported that H_2 selectivity decreased due to a higher rate of dehydration reactions facilitated by the acidity generated in the PtRe alloy. In the current study, PtRe(1:1)/MER showed the highest gas production of all catalysts and a maximum of H_2 production of 117 μmol / min and alkane production of 25 μmol / min (96 % of CH_4), which were observed during the first hour on stream (Figure VI-27 (a) and (b)). CO_2 production was in accordance with *CC gas* and it was also affected by the presence of KOH, forming carbonates in the liquid phase (Figure VI-27 (c)). Finally, the catalysts activity significantly decreased with TOS for all catalysts, showing similar patterns that suggest equivalent deactivation mechanism, despite the differences in the metal phase.

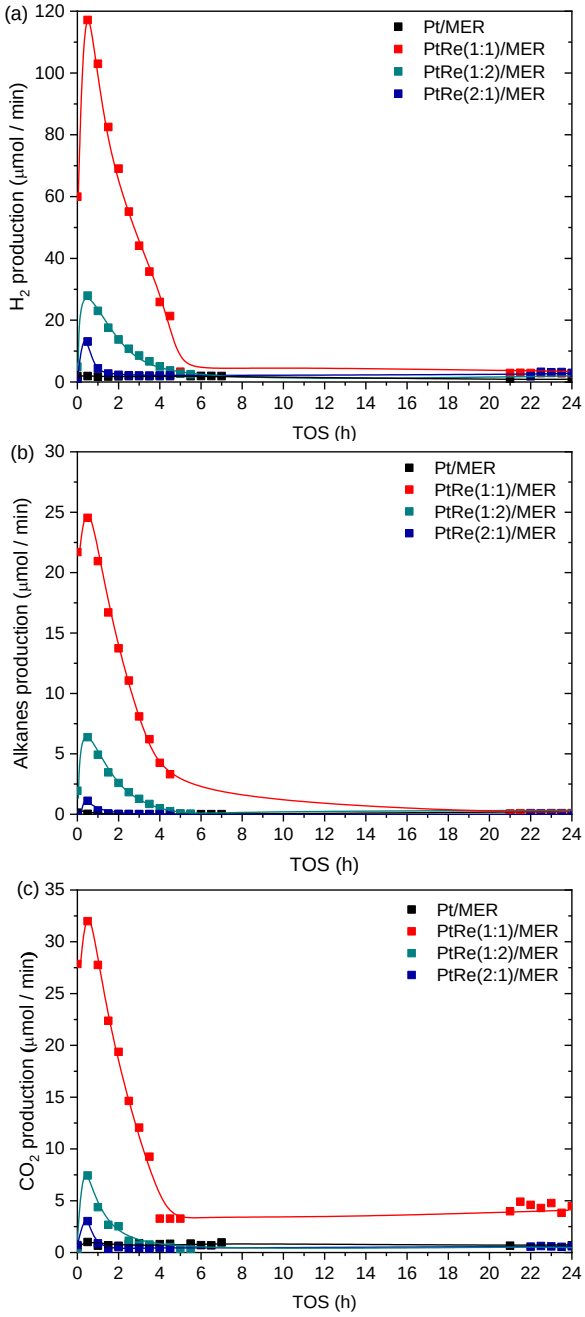

Figure VI-27. (a) H_2, (b) total alkanes and (c) CO_2 production for Pt/MER and PtRe/MER catalysts vs TOS *

*Reaction conditions: 225 ºC, 28 bar, 1 g of catalyst, *WHSV* = 0.12 h^{-1}, 40 N mL / min Ar.

Regarding alkanes production, Zhang *et al.* [81] and Ciftci *et al.* [23] have reported that the addition of Re to Pt/C catalyst in the APR of glycerol significantly changed the products distribution, mainly increasing the selectivity toward C_2^+ alkanes (C_2H_6 and C_3H_8), alcohols and carboxylic acids, at the expense of H_2, CH_4 and CO_2 selectivity. In the current chapter, the percentage of CH_4 in the total of alkanes was high in all the experiments. At low TOS values (up to 5 h TOS), when the catalysts still had significant activity, these percentages ranged between 68 and 98 % and for the bimetallic catalysts these percentages were higher than for Pt/MER, ranging between 92 and 98 % (Figure VI-28). This lower contribution of C_2^+ alkanes could be due to the presence of KOH in reaction medium, since some authors have reported that the pathway to C_2^+ formation become disfavoured in the presence of KOH, probably reducing the dehydration-hydrogenation of alcohols [54]. This could be most notably seen in bimetallic catalysts because the base addition could neutralize the acidity provided by the PtRe alloy, reducing the importance of dehydration pathways [54,81].

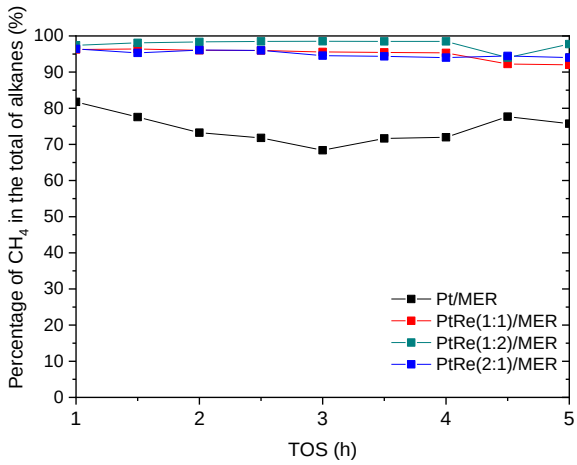

Figure VI-28. Percentage of CH_4 in the total of alkanes up to 5 h TOS*

*Reaction conditions: 225 ºC, 28 bar, 1 g of catalyst, *WHSV* = 0.12 h^{-1}, 40 N mL / min Ar.

4.3.4. Deactivation of catalysts

In order to evaluate the possible factors that affect the catalytic performance and deactivation, the used catalysts in the experiments described above were characterized. N_2 adsorption/desorption isotherms of the used catalysts show that all of them lost almost all their S_{BET} and A_{EXT} after 24 h TOS. Table VI-15 shows the textural parameters for PtRe(1:1)/MER catalyst, presenting only 30 m^2 / g of S_{BET}, without significant micropore and low mesopore volume (ca. 0.05 cm^3 / g). PtRe(1:1)/MER catalyst was also characterized after 1 h TOS, showing a 26 % loss of its S_{BET}, with both micro and mesoporosity decreasing. The results indicate that all catalysts lost BET surface area rapidly, probably due to adsorption of organic species and/or carbon-rich species (coke) deposition on the catalysts surface, which led to deactivation. The important loss during the first hour on stream would be consistent with the early deactivation observed.

Table VI-15. Pore texture of fresh and used PtRe(1:1)/MER catalyst

Samples	S_{BET} (m^2 / g)	A_{EXT} (m^2 / g)	Micropore volume (cm^3 / g)	Mesopore volume (cm^3 / g)
PtRe(1:1)/MER fresh	820	120	0.34	0.15
PtRe(1:1)/MER 1 h TOS	610	100	0.26	0.12
PtRe(1:1)/MER 24 h TOS	30	30	< 0.001	0.05

Table VI-16 summarizes data from elemental analysis of fresh and used catalysts. The results showed that the percentage of H, N, S and O increased after 24 h TOS, while the percentage of C decreased. This trend is consistent with the adsorption of organic matter and/or deposition of coke or hydrothermal carbon formed on the surface of the catalysts. The aliphatic character of the deposited carbon matter seems clear according to the elemental analysis results. Then, the increases in the H and N content to the

detriment of C suggest that the deposited matter corresponds to lower developed carbon structures than that of the support (with ca. 86 % C).

Table VI-16. Elemental analysis of fresh and used Pt/MER catalysts

Catalyst	% C	% H	% N	% S	% O**
Pt/MER fresh	86.1 ± 0.1	0.4 ± 0.1	0.5 ± 0.1	0.7 ± 0.1	12.3 ± 0.1
Pt/MER 20 N mL / min Ar*	81.4 ± 0.6	2.1 ± 0.1	2.8 ± 0.1	0.6 ± 0.1	13.1 ± 0.5
Pt/MER 40 N mL / min Ar*	79.5 ± 0.5	2.1 ± 0.1	2.6 ± 0.1	1.1 ± 0.1	14.7 ± 0.4

*24 h TOS
**Calculated by difference

The STEM analysis of used catalysts were performed to investigate the stability of the metal phase. Table VI-17 shows the mean NPs size of the fresh catalysts and after 24 h TOS. The mean NPs size of Pt/MER catalyst increased slightly after 24 h TOS, from 4.6 to 5.6 – 6.2 nm, due to the sintering. No significant differences can be observed for catalysts tested using different carrier gas flow. Used Pt/MERxRES also showed a higher mean NPs, except for Pt/MER40RES catalyst, which had a similar mean NPs size to the fresh catalyst. Nevertheless, it is important to mention that these catalysts showed in some STEM images agglomeration of NPs that were not considered for histograms. In the case of PtRe(1:1)/MER catalyst, no significant changes in mean NPs size with TOS were observed after 1 h or 24 h TOS, whereas the used PtRe(1:2)/MER catalyst showed a smaller NPs size than the fresh catalyst. The smaller particle sizes of the Pt−Re bimetallic catalysts indicates a stabilization of Pt against sintering at elevated temperatures by the presence of Re [82]. Although some catalysts showed sintering of NPs, others kept the mean NPs size of the fresh catalysts. Therefore, changes in the mean NPs size are unlikely to be the main cause of the pronounced deactivation observed.

Table VI-17. Mean NPs size of the fresh and used catalysts

Samples	Mean NPs size (nm)	
	Fresh	Used (24 h TOS)
Pt/MER	4.6 ± 2.2	6.2 ± 3.1 (20 N mL / min Ar) 5.6 ± 5.2 (40 N mL / min Ar)
Pt/MER10RES	1.8 ± 0.7	4.3 ± 1.8
Pt/MER20RES	3.1 ± 1.5	4.1 ± 3.3
Pt/MER40RES	3.5 ± 1.6	3.3 ± 2.0
PtRe(1:1)/MER	1.2 ± 0.3	1.5 ± 0.4* 1.4 ± 0.3
PtRe(1:2)MER	3.6 ± 1.4	1.7 ± 0.6

*1 h TOS

The used catalysts also were characterized by TG-TPD/TPO. Figure VI-29 shows the weight loss TG-TPD profiles and the corresponding differential profile (DTG) for fresh and used Pt/MER, Pt/MER40RES and PtRe(1:1)/MER catalysts. Likewise, Figure VI-30 shows the weight loss TG-TPO profiles and the corresponding DTG profile for these catalysts. The quantitative weight loss for all the catalysts analysed is summarized in Table VI-18.

The initial peak in the Figure VI-29 at around 100 ºC can be ascribed to the loss of water adsorbed on the catalysts. After that, fresh catalysts do not show weight loss indicating a good thermal stability conferred by the support and the preparation conditions used (TPD temperature is lower than preparation temperature). On the contrary, the used catalysts have a significant peak extending from 140 to 430 ºC that can be attributed to the loss of coke precursor species or to reactants/products physically adsorbed on the catalyst surface. The increase of Ar flow rate during the operation of the reactor displaces the main peak towards higher temperatures, from 380 to 430 ºC, which could be attributed to higher development of structures or to a stronger physisorption (Figure VI-29 (a)). This would be consistent with a lower availability of H_2 for the hydrogenation of precursors. Indeed, a

comparison of the quantitative weight losses of these catalysts reveals that the weight loss was lower as the Ar flow rate increased (Table VI-18). The percentage of weight loss using 5 N mL / min of Ar flow rate was 9.4 %, being reduced to 8.6 when an Ar flow rate of 40 N mL / min was used. According to the TG-TPO profiles in Figure VI-30 (a), the peak observed for the fresh catalyst is associated with the carbon support burnt off. A shift of the maximum towards lower temperatures and an early initiation of weight loss was observed upon increasing the Ar flow rate. The aging of the species that leads to the displacement of the DTG-TPD profiles is in accordance with the more homogeneous TG-TPO profile (including the support burnt off) with the highest Ar flow rate. Nevertheless, the presence of burnt species below 450 ºC suggests the presence of coke on the catalyst surface. Despite its lower content as significant peaks are not observed in Figure VI-30 (a), this coke leads to the total loss of the catalysts porous texture.

In the case of Pt/MER40RES catalyst, in the DTG-TPD profile of the used catalyst (24 h TOS), the main peak is located around 400 ºC as the one observed for the used Pt/MER catalyst. Nevertheless, the relative intensity of the peak at 150 ºC is higher, indicating a lower degree of structure development (Figure VI-29 (b)). The percentages of weight loss in the TG-TPD increases from 1.9 to 8.6 %, comparing the fresh and used Pt/MER catalyst, respectively, while for the Pt/MER40RES catalyst, the percentage increases from 1.4 to only 4.1 % (Table VI-18). Therefore, it seems that the reduction of the porosity of the support, respect to MER, decreases the amount of adsorbed species and prevented their development, but it is not enough to reduce catalyst deactivation. Regarding the TG-TPO profile of Pt/MER40RES (Figure VI-30 (b)), a sudden decrease in the sample weight was observed when resol was added into the catalyst. This could be associated with its lower combustion temperature that induces a faster combustion of the catalyst. Again, big differences are not observed compared to fresh catalyst.

However, the shift of the curve to lower combustion temperatures suggests light species deposited on the catalyst surface.

Analysing the differential TG-TPD/TPO profiles of the PtRe(1:1)/MER catalyst at 1 and 24 h TOS (Figure VI-29 (c) and Figure VI-30 (c)), a clear aging effect of the deposited species can be observed as the time on stream is increased. A clear increase in the TPD species, which the maximum located at 400 ºC is observed over TOS. The percentages of weight loss in the TG-TPD increased from 1.6 %, for the fresh catalyst, to 5.8 % at 1 h TOS and 7.1 % at 24 h TOS (Table VI-18). The incorporation of Re also accelerates the combustion of the support, observing a similar sharp peak in the DTG-TPO profile of Figure VI-30 (c). The displacement of the peak towards higher combustion temperatures over TOS is clear, then corroborating the aging effect of the deposits with time.

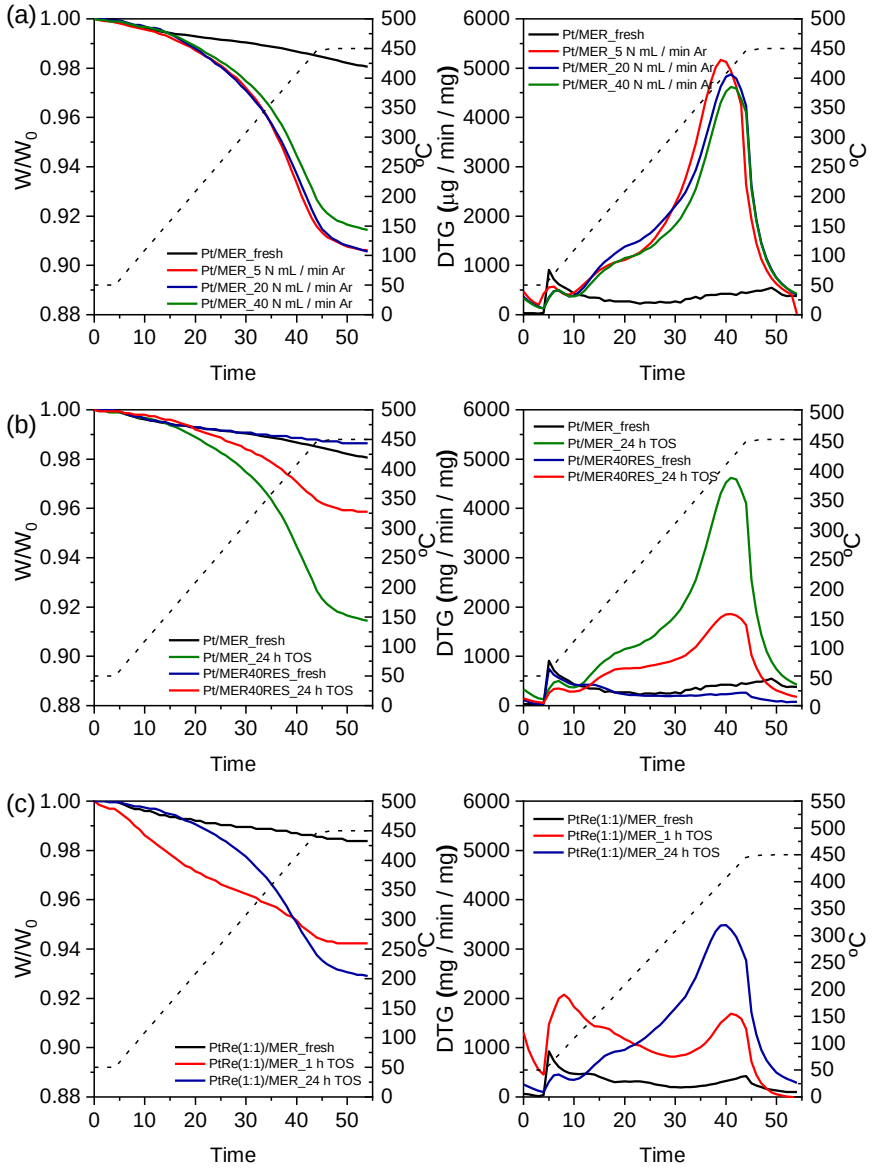

Figure VI-29. TG-TPD profiles and the corresponding derivative of the (a) fresh and used Pt/MER catalyst at different Ar flow rate at 24 h TOS, (b) fresh and used Pt/MER40RES catalyst at 24 h TOS and (c) fresh and used PtRe(1:1)/MER catalysts at 1 and 24 h TOS

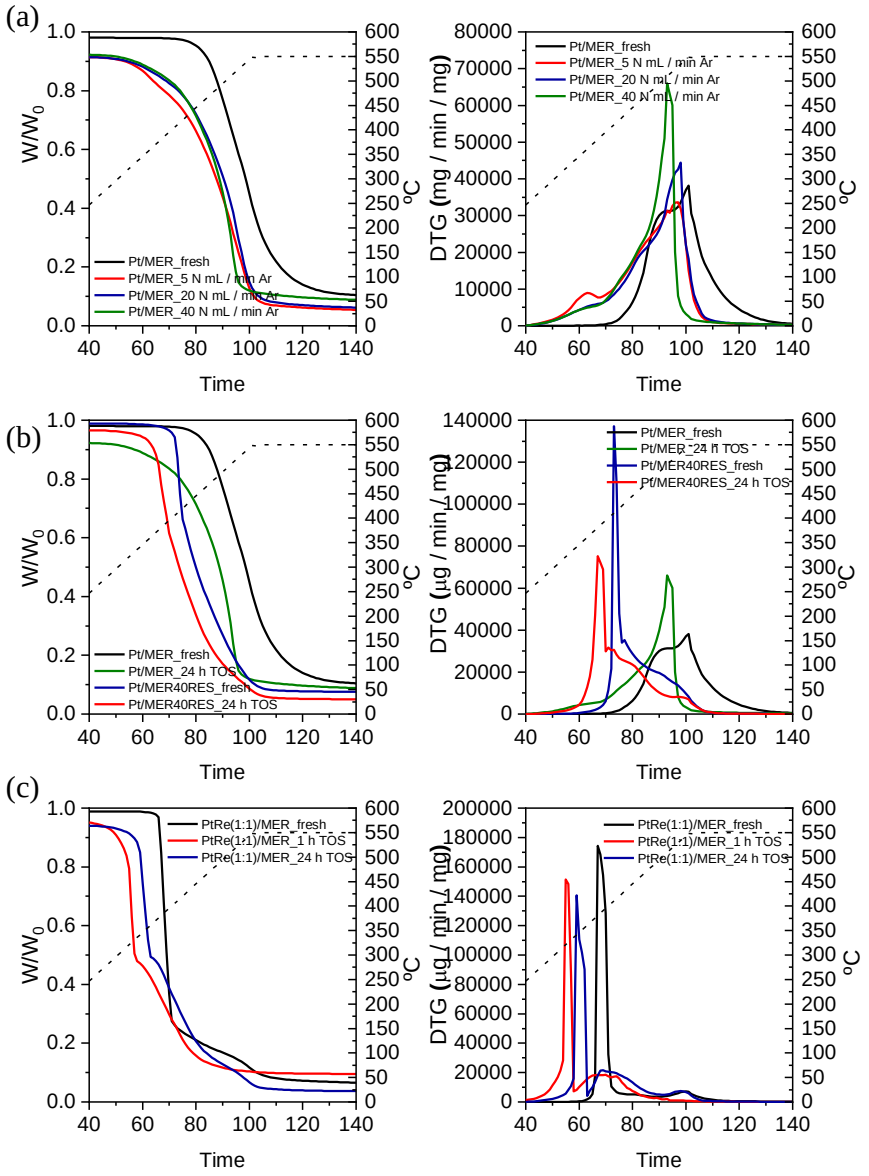

Figure VI-30. TG-TPO profiles and the corresponding derivative of the (a) fresh and used Pt/MER catalyst at different Ar flow rate at 24 h TOS, (b) fresh and used Pt/MER40RES catalyst at 24 h TOS and (c) fresh and used PtRe(1:1)/MER catalysts at 1 and 24 h TOS

Table VI-18. Quantitative weight losses of fresh catalysts and after 24 h TOS

Catalyst	TG-TPD (%)	TG-TPO (%)
Fresh		
Pt/MER	1.9	88.3
PtRe(1:1)/MER	1.6	92.2
Pt/MER40RES	1.4	91.2
Used (24 h TOS)		
Pt/MER 5 N mL / min Ar	9.4	90.6
Pt/MER 20 N mL / min Ar	9.4	84.7
Pt/MER 40 N mL / min Ar	8.6	83.0
PtRe(1:1)/MER*	5.8	84.8
PtRe(1:1)/MER	7.1	89.3
Pt/MER40RES	4.1	90.9

*1 h TOS

4.4. Conclusions

The catalytic performance and the deactivation of carbon supported Pt and PtRe catalysts in the APR of brewery wastewater was evaluated. A significant loss of catalysts activity with TOS was observed for all catalysts systems analysed.

Using Pt/MER catalyst the TOC removal was more stable and H_2 production increased at higher Ar flow rate (40 N mL / min), coherent with lower H_2 availability for secondary reactions. The influence of the textural properties of the carbons support was evaluated by using modified carbon supports (MERxRES) with different porosity obtained by impregnation and carbonization of resol resin. A clear trend regarding TOC removal and pore texture of the catalyst could not be observed, however a direct correlation of the maximum TOC removal in and the mean NPs size suggest that the Pt NPs size and dispersion could indirectly have affected the catalysts performance. At low TOS values Pt/MERxRES catalysts showed higher H_2 production than Pt/MER, indicating that a lower microporosity of the catalysts facilitates the

transport of reactants to catalytic active sites and removal of gas products. At low TOS values, Pt/MER10RES achieved a higher H_2 production (10 μmol / min) than Pt/MER20RES (8 μmol / min), in spite of having a higher micropore volume. This behaviour could be attributed to the optimum mean NPs size of Pt/MER10RES (closer to 2 nm).

The Re addition to Pt/MER catalyst seems to favour the catalyst deactivation, since TOC removal was more stable for Pt/MER and PtRe(2:1)/MER than PtRe(1:1)/MER and PtRe(1:2)/MER. This was attributed to the formation of larger organic molecules with unsaturated bonds that can easily condense towards to coke structures. In spite of this, all bimetallic catalysts showed a higher activity than Pt/MER and PtRe(1:1)/MER showed the highest gas production of all catalysts (a maximum of H_2 production of 117 μmol / min).

The characterization of used catalysts showed an important loss of S_{BET} during the first hour on stream consistent with the early deactivation observed. This loss of S_{BET}, and the elemental and TG-TPD/TPO analysis were consistent with the adsorption of organic species and/or carbon-rich species (coke) deposition on the catalysts surface. On the other hand, although some catalysts showed sintering of NPs, these changes are probably not the main cause of the pronounced deactivation observed. TG-TPD/TPO analysis also revealed that the weight loss was lower as the Ar flow rate increase. In the case of Pt/MER40RES catalyst, the reduction of the porosity of the support (MER40RES), respect to MER, could decrease the amount of adsorbed species and prevented their development, but this was not enough to reduce catalyst deactivation. Analysing the PtRe(1:1)/MER catalyst profiles at 1 and 24 h TOS, a clear aging effect of the deposited species can be observed as the time on stream is increased.

5. Enhanced H_2 production in the continuous aqueous phase reforming of maltose by feedstock pre-hydrogenation

This chapter was adapted from: Oliveira, A.S., Aho, A., Baeza, J.A., Calvo, L., Rodriguez, J.J., Gilarranz, M.A., Murzin, D., **H_2 production via aqueous phase reforming of maltose**, (not published).

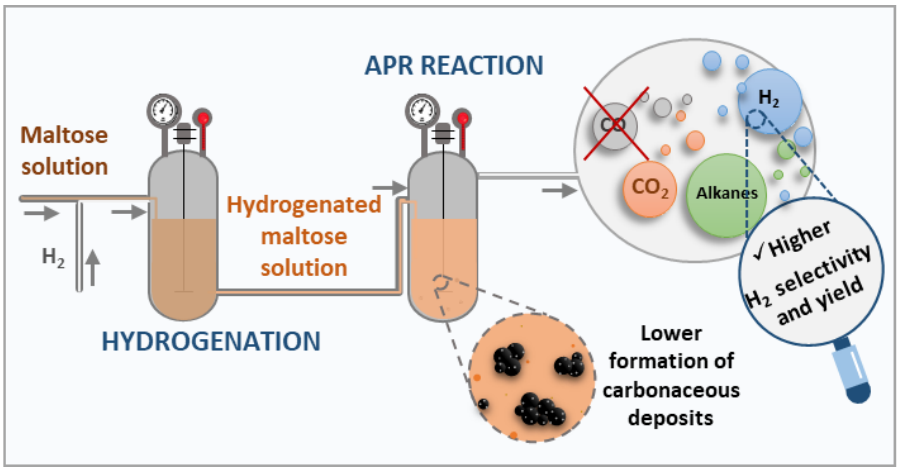

5.1. Introduction

In the previous chapters, APR was proposed as a potential route for valorisation and treatment of brewery wastewater, and although good results in terms of removal of organic matter and production of valuable gases were obtained, a relevant catalyst deactivation was observed for all systems analysed, which would affect the real application of the process. The main cause identified for catalyst deactivation was coke deposition on the catalyst surface.

The treatment by APR of sugars, especially using concentrated solutions, leads to an increase in the rate of homogeneous side reactions to form organic acids, aldehydes and carbonaceous deposits [9,47]. In addition to this, H_2 yield and selectivity is higher in the APR of reduced molecules [47,71], while most naturally occurring sugars contain aldehyde and ketone groups [119]. These functional groups are also involved in side reactions leading to catalyst deactivation during APR, mostly by coking [9]. On the other hand, the APR of very dilute solutions has not been recognized as economically attractive due to the energy inputs to the system imposed by the reaction temperatures between 200 and 250 ºC required, which decreases the ratio between valuable gases output and process input. Nevertheless, higher inputs may be affordable in the context of applying APR as part of waste management.

The use of reduced compounds as APR feedstock can be an alternative to reduce these undesirable reactions observed with sugars [8] and improve H_2 production [47]. Even if some H_2 is consumed in the hydrogenation of the feedstocks, it can be compensated by a higher net H_2 production, the possibility to use solutions with a higher concentration, and the lower deactivation of the catalysts.

Sugars are main constituents of waste streams in food and beverage industries, including brewing and fruit juice production [74,93]. Maltose is the main compound present in brewery wastewater. It is a disaccharide built from two glucose units preserving the reducing abilities. The hydrogenation of maltose is characterized by the formation of a main product, maltitol, together with the formation of several secondary products that include glucose and sorbitol [120]. Accordingly, hydrogenation of maltose could be performed as a pre-treatment of APR with the objective of converting maltose into more reduced compounds, thus reducing the extent of undesirable side reactions and increasing the H_2 selectivity and yield [47,71].

In this chapter, hydrogenation of maltose was evaluated as an approach to increase suitability of brewery wastewater as a feedstock for valorisation by APR and H_2 production. Likewise, the APR of brewery wastewater was performed to compare the results with the APR of maltose and hydrogenated maltose feedstock.

5.2. Experimental

PtPd/C (2.5 wt. % Pt and 1.25 wt. % Pd) catalyst was prepared according to the procedure reported in Chapter III using SIB as support. This catalyst was characterized by CO chemisorption and a NPs dispersion value of 42.3 % was obtained

Maltose solutions (1 and 2.5 wt. %) were used in the APR experiments. For the purposes of the current chapter a more concentrated SBW feedstock than in previous chapter was used, in order to obtain a carbon content equivalent to that of a 1 wt. % maltose solution. In addition, SBW feedstock (described in Chapter III) was prepared without addition of NaH_2PO_4, Na_2HPO_4 and $(NH_4)_2SO_4$. SBW wastewater was characterized by

TOC and COD measurements, which rendered values of 4124 ± 222 mg / L and 11204 ± 1486 mg / L, respectively.

APR experiments were carried out in a continuous reactor (described in Chapter III, second setup) at 175, 200 and 225 ºC and 30 bar during at least 56 h TOS using 0.5 g of catalyst. The APR experiments were started at a temperature of 175 ºC, which was raised to 200 ºC after 24 h TOS and to 225 ºC after 48 h TOS. N_2 containing 1 % He was used to purge the reaction system, to maintain the pressure inside the reactor and as carrier gas throughout the reaction, using a constant flow rate 34 N mL / min. Maltose solutions and SBW were fed into the reactor with a HPLC pump using 0.1 mL / min of liquid flow rate. The *WHSV* calculated as mass of substrate per mass of catalyst per hour were 0.12 h^{-1} and 0.3 h^{-1}.

The hydrogenation of aqueous maltose solution (2.5 wt. %) was performed as described in Chapter III (coupled hydrogenation and APR). At the beginning of reaction, liquid samples (2.5 mL) were taken at least every 15 min and then every 30 min until the reaction was stopped after 2 h. After each sample, the pressure of reaction was restarted at 20 bar by addition of H_2 into the system. After hydrogenation, a solution was prepared with the main compounds obtained in the hydrogenation of maltose and it was subjected to APR as indicated above.

In order to compare the results at different feedstock concentrations, the APR experiments with the main compound resulting from hydrogenation were conducted using 1 and 2.5 wt. %, which are the same concentrations as for APR of maltose. Comparison at similar conversion level was performed at 200 ºC using a 2.5 wt. % of solution and a *WHSV* of 0.105 h^{-1}.

5.3. Results and discussion

5.3.1. Hydrogenation of maltose

The maltose hydrogenation scheme is represented in Figure VI-31. It is characterized by the formation of maltitol as main product and other side products such as glucose and sorbitol [120].

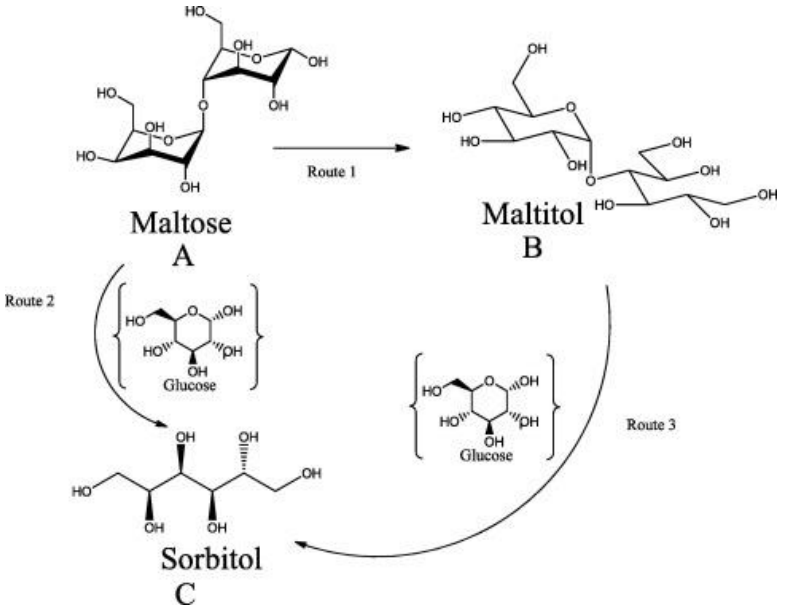

Figure VI-31. Scheme of hydrogenation of maltose [79]

The evolution of maltose and maltitol concentration with time during the hydrogenation experiments is showed in Figure VI-32. After 2 h of reaction, a maltose conversion of 99.6 % was obtained, with a maltitol yield of 94.1 wt. %. Sorbitol was also identified in the liquid phase resulting in a yield of 1.2 wt. % after 2 h of reaction, while glucose was not detected in the final effluent under the reaction conditions used. Traces of acids, such as acetic, formic and lactic, were also identified in the liquid phase. These acids

can be formed through intermediate HMF, which can be formed by glucose dehydration [121]. Finally, the carbon mass balance closure was 95.7 wt. %.

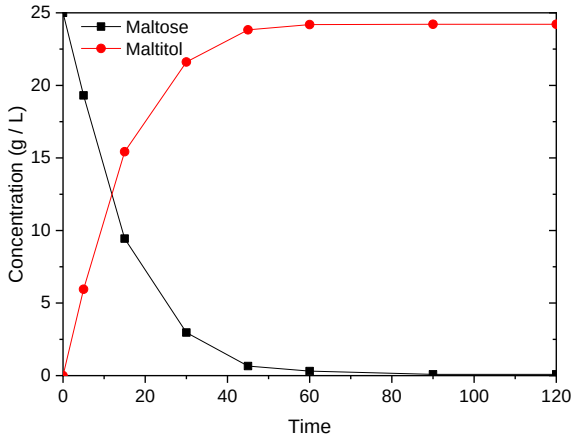

Figure VI-32. Evolution of maltose and maltitol concentration with time during the hydrogenation experiment*

*Reaction conditions: 120 ºC, 20 bar of H_2, 2 h of reaction, 100 mL of 2.5 wt % of maltose, 0.2 g of 4.6 wt. % Ru/C catalyst, 1000 rpm.

5.3.2. APR experiments

5.3.2.1. APR of maltose and hydrogenated maltose

Maltitol was the main compound obtained in the hydrogenation of maltose and it was obtained with very high yield, therefore APR experiments were conducted using maltitol solutions with concentration ranging between 1 and 2.5 wt. %. The APR of maltose was also tested at the same conditions for comparison purposes. As indicated above, the experiments were started at 175 ºC, and then temperature was raised to 200 ºC and 225 ºC. At each temperature, a stabilization period of 1 – 6 h TOS was needed until the conversion and gas production remained stable. Experiments were performed

for up to 72 h TOS without significant deactivation or increase of pressure in the reactor, both for a maltitol concentration of 1 and 2.5 % (Figure VI-33).

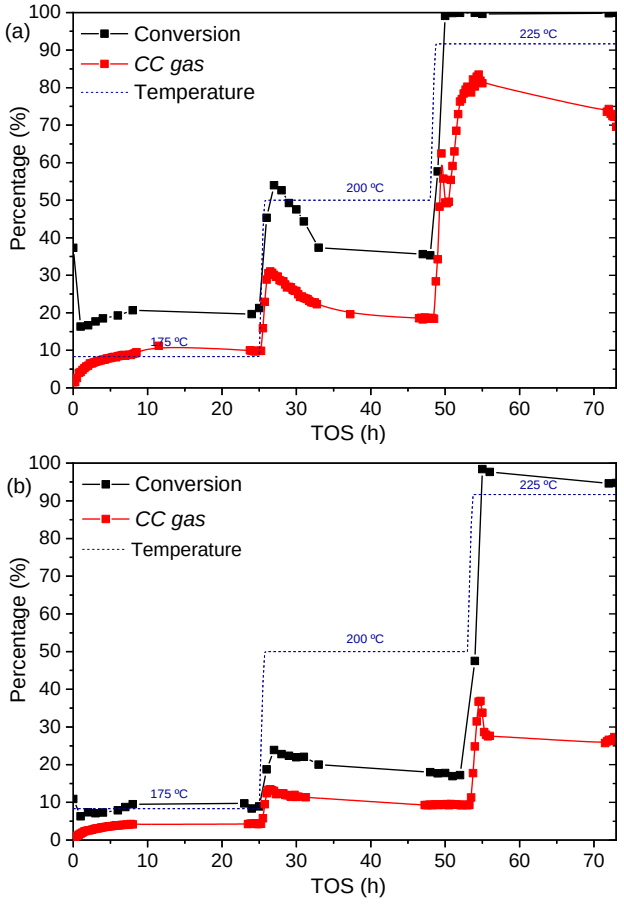

Figure VI-33. Conversion and *CC gas* for APR of (a) 1 and (b) 2.5 wt. % of maltitol[*]

[*]Reaction conditions: 30 bar, 0.5 g of PtPd/SIB catalyst, *WHSV* = 0.12 and 0.3 h^{-1}.

In the case of the experiments with maltose solutions, the catalyst showed a significant deactivation after 48 h TOS, in a more evident way when the temperature was raised to 225 ºC, even for a maltose concentration of 1 wt. % (Figure VI-34). Likewise, an important increase in reactor pressure was

observed after 56 h TOS in the case of experiments with 2.5 wt. % of maltose, and 60 h TOS in the case of experiments with 1 wt. % maltose, leading to flow collapse. The rise in pressure may be ascribed to the formation of carbonaceous deposits inside the reactor. The carbon mass balance closure in the maltitol APR experiments was higher (87.2 to 100 %) than in maltose experiments (70.2 and 98.1 %), with a higher lack of closure for the reaction at higher temperature.

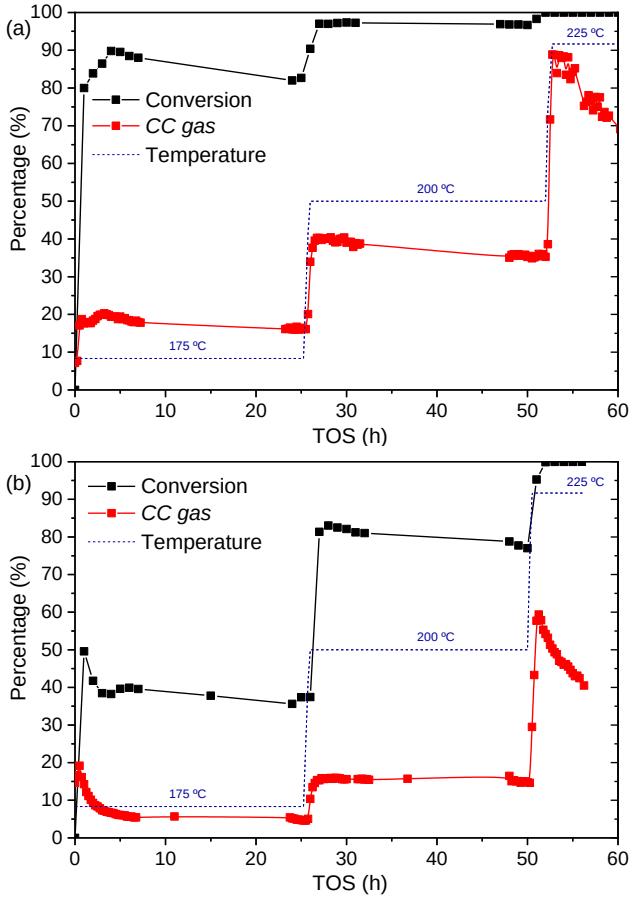

Figure VI-34. Conversion and *CC gas* for APR of (a) 1 and (b) 2.5 wt. % of maltose*

*Reaction conditions: 30 bar, 0.5 g of PtPd/SIB catalyst, *WHSV* = 0.12 and 0.3 h^{-1}.

The results above proved that in the APR of maltose undesirable side reactions leading to carbonaceous deposits affect catalytic activity and reactor performance [47]. The side reactions are less favoured in the APR of maltitol, due to the more reduced nature of this molecule. In addition, the side reactions are favoured at higher temperatures and for more concentrated feedstock solutions, since the experiment with 2.5 wt. % of maltose at 225 ºC could only be carried out during 8 h TOS, while with 1 wt. % of maltose at the same temperature could be carried out up to 12 h TOS. In the literature [122], a higher solid phase production with the increase in the initial concentration of the feedstock was also reported for APR of glucose and xylose, and the authors have attributed this phenomenon to the formation of high molecular weight compounds by condensation reactions.

The results of APR of maltose and maltitol after catalyst stabilization (average of the stable period) are showed below. For APR of maltose at 225 ºC, the results presented are an average of the first hours of reaction. Conversion of initial feedstock at the different temperatures tested is showed in Figure VI-35. As can be seen, APR of maltose led to higher conversion values than APR of maltitol, especially at lower temperatures. In addition, the conversion values increased with increasing temperature and decreased with increasing concentration of initial feedstock solution. Thus, at 175 ºC and using 1 wt. % of maltitol the conversion was 18.4 % and this value decreased to 8.3 % using 2.5 wt. % of maltitol. At the same temperature, the conversion of maltose was 86.4 and 38.2 % using an initial concentration of 1 and 2.5 wt. %, respectively. When the temperature increased to 225 ºC, both compounds showed very high conversion values, well above 94.5 %.

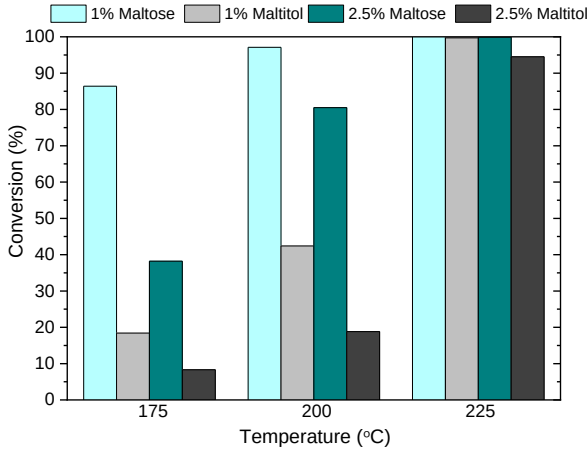

Figure VI-35: Conversion of maltose and maltitol after APR at different temperatures and initial concentration*

*Reaction conditions: 30 bar, 0.5 g of PtPd/SIB catalyst, *WHSV* = 0.12 and 0.3 h^{-1}.

Figure VI-36 shows the *CC gas* at different temperatures. The least concentrated solutions and the highest reaction temperatures led to a higher *CC gas* values. Moreover, APR of maltose showed higher *CC gas* values than APR of maltitol, due to the higher conversion values of the former. At 175 ºC, the *CC gas* of APR of 1 wt. % of maltose and maltitol was 18.1 and 9.1 %, respectively, and these values decreased to 5.8 and 4.0 % when the initial concentration increased to 2.5 wt. %. The highest *CC gas*, 79. 1 and 71.8 %, were obtained in the APR at 225 ºC of 1 wt. % of maltose and maltitol, respectively, whereas under these same conditions and using 2.5 wt. % of initial concentration *CC gas* decreased to 47.8 and 27.4 %, respectively.

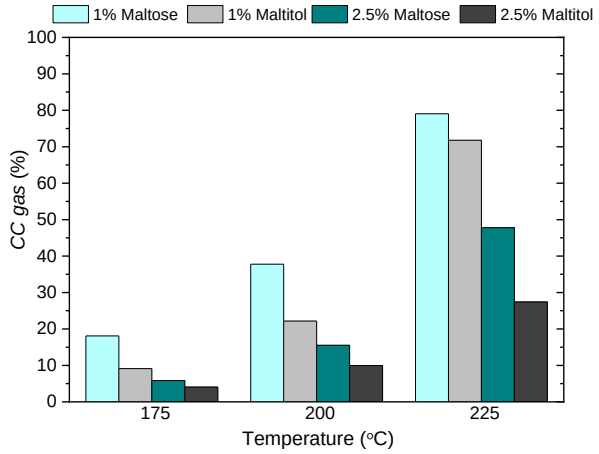

Figure VI-36. *CC gas* in the APR of maltose and maltitol at different temperatures and initial concentration*

*Reaction conditions: 30 bar, 0.5 g of PtPd/SIB catalyst, *WHSV* = 0.12 and 0.3 h^{-1}.

Regarding the composition of gas produced, Figure VI-37 shows the selectivity to H_2, CO_2 and alkanes at different temperatures. The selectivity to alkanes was calculated as a lump considering all hydrocarbons identified, i.e. CH_4, C_2H_6, C_3H_8, n-C_4H_{10}, iso-C_4H_{10}, n-C_5H_{12}, iso-C_5H_{12}, neo-C_5H_{12}, n-C_6H_{14}, iso-C_6H_{14}, C_6H_{12} and n-C_7H_{16}. APR of maltose was more selective to alkanes production than APR of maltitol. The alkanes selectivity in the reactions with maltose varied from 23.5 to 37.7 %, while in the reactions with maltitol only reached between 14.9 and 23.2 %. In contrast, the selectivity to H_2 was higher in the APR of maltitol (68.7 – 84. 2 %) than in the APR of maltose (30.3 – 64.0 %). Davda and Dumesic [47] also reported that H_2 selectivity increased from 13.4 to 62.4 % and alkanes selectivity decreased from 47.5 to 21.3 % by combining hydrogenation and APR of glucose, where the main hydrogenation product was sorbitol. Pipitone *et al.* [122] also observed that APR of sorbitol and xylitol was more selective for H_2 production than APR of glucose and xylose. Irmak *et al.* [71] also reported that in the APR of glucose and biomass hydrolysate, the more reduced

feedstocks produced significantly higher H_2 selectivity and yield than non-reduced forms.

In the APR of both maltose and maltitol compounds, the H_2 selectivity decreased when the solution concentration increased from 1 to 2.5 wt. %, although this effect was more pronounced in the case of maltose, probably due to a higher contribution of undesired side reactions to form acids, aldehydes and carbonaceous deposits [47]. In the case of APR of maltitol, the H_2 selectivity gradually decreased from 84. 2 to 74.9 % using 1 wt. % of initial concentration (Figure VI-37 (b)) and from 82.8 to 68.7 % using 2.5 wt. % (Figure VI-37 (d)) when the temperature increased from 175 to 225 ºC. This decrease in H_2 selectivity was followed by an increase in alkanes selectivity, which was more pronounced at the highest temperature. Similar trends were observed for the APR of maltose, although the selectivity to alkanes was higher at the expense of H_2 selectivity.

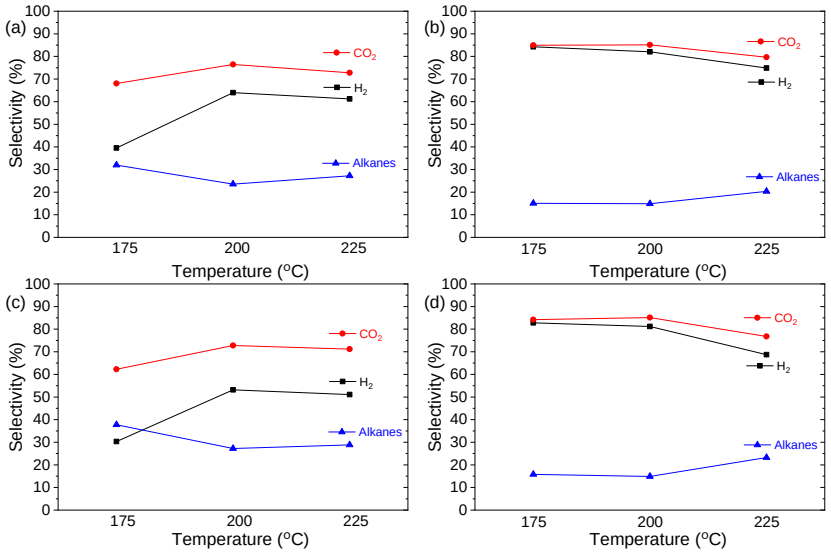

Figure VI-37. H_2, CO_2 and alkanes selectivities for APR of (a) 1 wt. % of maltose, (b) 1 wt. % of maltitol, (c) 2.5 wt. % of maltose and (d) 2.5 wt. % of maltitol at different temperatures*

*Reaction conditions: 30 bar, 0.5 g of PtPd/SIB catalyst, *WHSV* = 0.12 and 0.3 h^{-1}.

A more detailed speciation of alkanes selectivity is provided in Figure VI-38, where the identified hydrocarbons were grouped according to the chain length, from C1 to C7. Similar alkanes distribution was observed in the APR of xylitol using PtRe/C catalyst, although the selectivity to a particular alkane showed large differences for different active metals [19]. On the other hand, in the APR of sorbitol, a higher alkanes selectivity was achieved using Pd than Pt catalysts, and both metal showed high selectivity to C4 - C6 alkanes formation [53]. APR of maltose at 175 ºC was mainly selective to C5, achieving up to 24.3 % of selectivity of this compound when a 2.5 wt. % initial concentration was used (Figure VI-38 (c)). The C5 selectivity significantly decreased with increasing temperature and at 225 ºC the selectivity to C5 reached a maximum of 1.3 % (Figure VI-38 (a) and (c)). The APR of maltitol also showed a maximum of C5 selectivity at 175 ºC,

although the values were significantly lower than for the APR of maltose (Figure VI-38 (b) and (d)).

The increase in temperature and initial feedstock conversion favoured selectivity to short chain alkanes for both maltose and maltitol, and at 225 ºC the APR of maltose was more selective to C2 while the APR of maltitol was more selective to C1. In addition, at all temperatures evaluated, initial feedstock concentration and conversion, the APR of maltitol was more selective to C1 than to other alkanes. These results indicate that the increase of the temperature and the use of more reduced compounds changed the reaction pathways, favouring the fragmentation of the initial feedstock trough C-C and C-O bond cleavages [57], producing short chain alkanes.

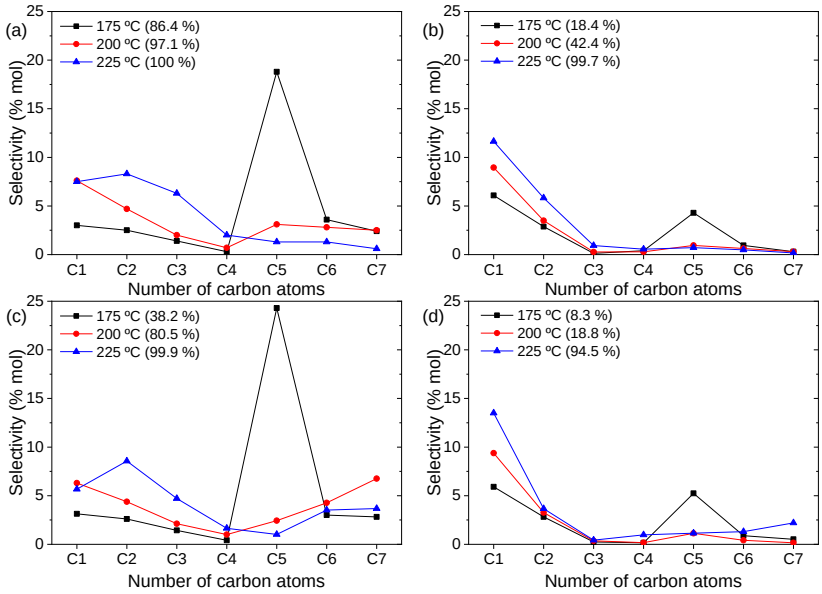

Figure VI-38. Selectivity towards C1 to C7 alkanes at different temperatures for APR of (a) 1 wt. % of maltose, (b) 1 wt. % of maltitol, (c) 2.5 wt. % of maltose and (d) 2.5 wt. % of maltitol. Numbers in brackets indicate conversion in the experiments at different temperatures[*]

[*]Reaction conditions: 30 bar, 0.5 g of PtPd/SIB catalyst, *WHSV* = 0.12 and 0.3 h^{-1}.

Figure VI-39 (a) shows the yield to H_2 and Figure VI-39 (b) shows the turnover frequency for H_2 production (TOF H_2) at different temperatures. Both H_2 yield and TOF H_2 increased with reaction temperature and when less concentrated solutions were treated. Under all the operating conditions tested, the APR of maltitol always led to a higher H_2 yield and TOF H_2 than the APR of maltose. In a former study on the APR of glucose [47], the net production of H_2 per mol of glucose was improved a 290 % by addition of a hydrogenation stage before reforming leading to sorbitol. In the current chapter, the H_2 production was maximized for a reaction temperature of 225 ºC and using 1 wt. % of initial feedstock concentration, resulting in a H_2 yield and TOF H_2 for maltose of 26.4 % and 0.35 min^{-1}, respectively, while in the APR of maltitol these values increased to 36.6 % and 0.51 min^{-1}. Therefore, the addition of a hydrogenation stage before reforming showed an improvement of 39 % of H_2 yield and 46 % of TOF H_2.

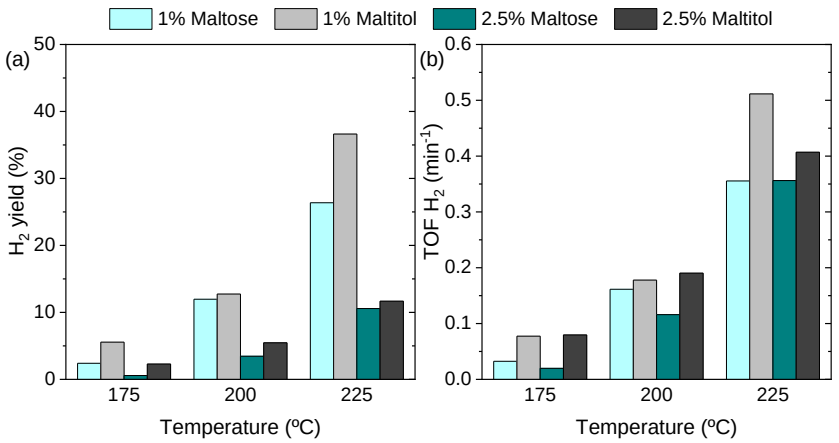

Figure VI-39. (a) H_2 yield and (b) TOF H_2 in the APR of maltose and maltitol at different temperatures and initial feedstock concentration*

*Reaction conditions: 30 bar, 0.5 g of PtPd/SIB catalyst, *WHSV* = 0.12 and 0.3 h^{-1}.

Regarding the efficiency of overall process coupling hydrogenation and APR, it has to be considered that 1 mol of H_2 is utilized to obtain 1 mol of maltitol from 1 mol of maltose (Equation 18). On the other hand, considering the theoretical mechanism of APR, it is possible to produce 24 mol of H_2 from 1 mol of maltose (Equation 19) and 25 mol of H_2 from 1 mol of maltitol (Equation 20). Therefore, the coupled process could be considered as efficient if more than 1 mol of H_2 is produced in the APR of maltitol than in the APR of maltose.

$$C_{12}H_{22}O_{11} + H_2 \rightarrow C_{12}H_{24}O_{11} \quad (18)$$

$$C_{12}H_{22}O_{11} + 13\,H_2O \rightleftarrows 12\,CO_2 + 24\,H_2 \quad (19)$$

$$C_{12}H_{24}O_{11} + 13\,H_2O \rightleftarrows 12\,CO_2 + 25\,H_2 \quad (20)$$

The APR of 1 wt. % of maltose at 225 ºC produced about 6 mol of H_2 per mol maltose (around 26 % of yield), while the APR of maltitol under same conditions produced about 9 mol of H_2 per mol maltitol (around 36 % of yield). Thus, the addition of a hydrogenation stage before reforming generated 3 mol of H_2 more than the direct reforming of the compound. Therefore, the overall process could be considered efficient under these conditions, since the amount of H_2 produced compensated the need for hydrogenation and generated 2 mol of H_2 more per mol of compound. On the other hand, using a more concentrated solution (2.5 wt. %) the H_2 yields obtained were low and although the H_2 production was higher in the APR of maltitol than in the APR of maltose, the amount of H_2 produced does not cover the needs for hydrogenation. A possible solution to improve the efficiency of the overall process with more concentrated solutions could be the hydrogenation of maltose to compounds more reduced than maltitol, such as sorbitol [123,124], which in the literature has presented higher values of H_2 yield [14,47]. Anyhow, as it was indicated above the hydrogenation to

maltitol has a clear impact in the durability of the catalyst, which also contributes to the efficiency of the overall process.

The liquid phase resulting from APR at different temperatures was analysed by HPLC to identify the main reaction products, resulting in chromatograms that showed a different pattern for maltose and maltitol. Figure VI-40 shows the HPLC chromatograms for reactions at 175 ºC (24 h TOS), 200 ºC (48 h TOS) and 225 ºC (56 h TOS for maltose, 72 h TOS for maltitol). Zoomed inserts in the Figure VI-40 (b), (c) and (d) shows the ratio between major and minor peaks.

In the APR of maltose at 175 – 200 ºC the main identified compounds, besides maltose (1), were glucose (3) and fructose (5), while at 225 ºC only a few compounds were detected due to the high conversion achieved. Glucose can be obtained through hydrolysis of maltose by slightly acidic medium or acidic sites of the catalyst [125], while glucose can follow an isomerization reaction to produce fructose, which is promoted by the presence of Pt catalyst and H_2 [126]. In the APR of maltitol, besides this compound (2), sorbitol (7) was the main compound identified, while glucose and fructose were not detected at any of the temperatures studied. Sorbitol could be produced by the hydrogenation of maltitol or maltose [79], although hydrogenation of maltose does not appear to be favoured under these conditions since this compound was not observed in the APR of maltose.

Xylose (4) and mannitol (6) also were detected in the APR of maltitol, but the poor separation of these compounds and the low concentration level lead to uncertainty in the calculation of individual concentrations. Mannitol could be produced by isomerisation of sorbitol or hydrogenation of fructose [127]. On the other hand, sorbitol could be also produced by hydrogenation of glucose or fructose [127]. Therefore, although glucose and fructose were not detected in the APR of maltitol, these

compounds could have been produced in the reaction, but they may have reacted to form more reduced molecules, such as sorbitol and mannitol. Erythritol (10) was only detected in the APR of maltose at lowest temperatures, while hydroxyacetone (20) was identified in the APR of both compounds. Erythritol could be obtained by hydrogenation of glucose [71] and it was also observed in the APR of sorbitol [128], while hydroxyacetone was one of the main product obtained in the APR of glycerol [105,129], propanol and 1,2 propanediol [105].

A number of aldehydes including glyceraldehyde (8), formaldehyde (14) and acetaldehyde (21) were identified in the APR of both maltose and maltitol, while pyruvaldehyde (10) was only detected in the APR of maltose and glycolaldehyde (11) was only detected at very low concentrations in the APR of maltitol. Regarding alcohols, ethylene glycol (17), 1-2 butanediol (23), isopropanol (26) and mainly ethanol (24) were also identified in all reactions, while propylene glycol (19) and methanol (22) were only detected at low concentrations in the APR of maltitol. Some organic acids were also identified in all experiments, being the most relevant glycolic (12), lactic (13), acetic (16) and butyric (25) acids, whereas in the APR of maltose, formic (15) and levulinic (18) acids were also observed. Finally, HMF (not shown, 35.5 min) was also detected in the APR of maltose at 200 ºC. Glyceraldehyde, pyruvaldehyde, glycolaldehyde, HMF and organic acids such as formic, acetic, lactic and levulinic have been reported as degradation products of glucose and fructose at high temperatures [130–132]. In addition, most of the compounds identified in this study were also obtained in the liquid phase of APR of other feedstocks, such sorbitol, galactitol, glycerol or xylitol [14,57,105,133].

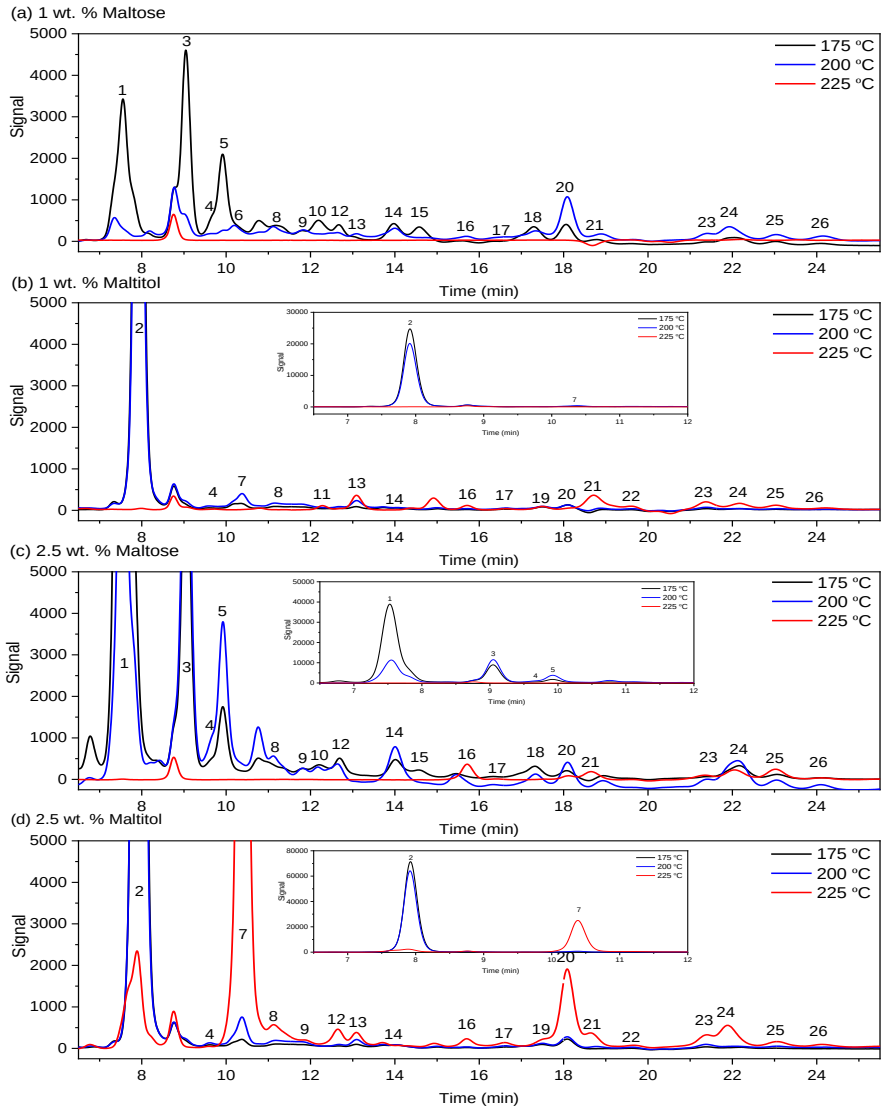

Figure VI-40. HPLC chromatograms of liquid samples during APR of maltose and maltitol at different temperatures and initial feedstock concentrations*

*Identified compounds: (1) maltose, (2) maltitol, (3) glucose, (4) xylose, (5) fructose, (6) mannitol, (7) sorbitol, (8) glyceraldehyde, (9) erythritol, (10) pyruvaldehyde, (11) glycolaldehyde, (12) glycolic acid, (13) lactic acid, (14) formaldehyde, (15) formic acid, (16) acetic acid, (17) ethylene glycol, (18) levulinic acid, (19) propylene glycol, (20) hydroxyacetone, (21) acetaldehyde, (22) methanol, (23) 1-2 butanediol, (24) ethanol, (25) butyric acid and (26) isopropanol. Reaction conditions: 30 bar, 0.5 g of PtPd/SIB catalyst, *WHSV* = 0.12 and 0.3 h^{-1}.

Table VI-19 compares yield to individual liquid-phase products and mass balance for APR of maltose and maltitol at 200 ºC using 2.5 wt. % initial feedstock. *WHSV* for APR of maltose was 0.3 h^{-1} while *WHSV* for maltitol adjusted to 0.105 h^{-1} in order to achieve similar conversion. Significant differences were observed in the composition of the liquid phase resulting from the experiments with maltose and maltitol. Higher yields to sugars, sugar alcohols, alcohols, acids, aldehydes and ketones were obtained in the APR of maltose, and HMF was only detected in the APR of this compound, in line with the relative height of the peaks shown in Figure VI-40. On the other hand, in the APR of maltitol the carbon conversion to gas phase was higher.

Table VI-19. Yields of liquid phase obtained during APR of maltose and maltitol*

	Maltose	Maltitol
Conversion (%)	75.9	74.3
Yield to product (%)		
sugar/sugar alcohol		
glucose	10.17	-
xylose	0.23	0.35
fructose	4.67	-
sorbitol	-	0.58
erythritol	1.00	-
alcohols		
ethylene glycol	0.55	0.20
propylene glycol	-	0.02
methanol	-	0.58
1-2 butanediol	0.96	1.05
ethanol	3.92	2.48
isopropanol	1.20	0.08
acids		
glycolic acid	2.14	0.19
lactic acid	-	0.69
acetic acid	0.20	0.20
levulinic acid	2.20	-
butyric acid	1.58	0.23
aldehydes/ketones		
glyceraldehyde	2.86	2.34
pyruvaldehyde	0.63	-
formaldehyde	1.14	0.05
hydroxyacetone	3.87	0.81
acetaldehyde	-	2.35
furans		
HMF	0.41	-
Total yield to identified products	37.71	12.19
Total carbon in liquid phase (%)**	63.4	41.5
Total carbon in the gas phase (%)**	14.8	24.5

*Reaction conditions: 200 ºC, 30 bar, 0.5 g of PtPd/SIB catalyst, 2.5 wt. % initial concentration solution, WHSV = 0.3 h^{-1} maltose and 0.015 h^{-1} maltitol.
**Calculated from identified products, carbon in initial feedstock basis.

Arrhenius representations for the reaction rate for APR of 2.5 wt. % of maltose and maltitol, expressed as TOF H_2, are shown in Figure VI-41. The apparent activation energies calculated were 108 kJ / mol for H_2 production by APR of maltose and 61 kJ / mol for APR of maltitol. These values are within the range of values found in the literature for the APR of other compounds (20 – 67 kJ / mol for APR of glycerol, 140 kJ / mol for APR of methanol and 100 kJ / mol for ethylene glycol) [34,134].

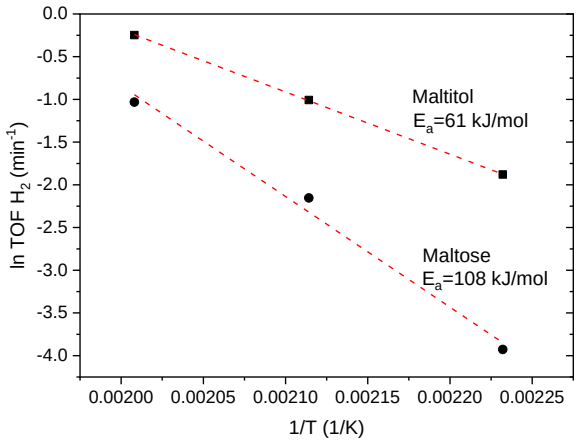

Figure VI-41. Arrhenius plot for APR of maltose and maltitol*

*Reaction conditions: 30 bar, 0.5 g of PtPd/SIB catalyst, 2.5 wt. % initial concentration solution, *WHSV* = 0.3 h^{-1}.

5.3.2.2. APR of brewery wastewater

APR of maltose and SBW were compared in order to assess the role of maltose and the rest of SBW components during reaction experiments, as maltose is the main component in brewery wastewater. Important catalyst deactivation was observed even at low APR temperature, therefore the experiments were carried out for 24 h TOS only at 175 ºC. Maltose conversion values in the APR of pure maltose and SBW with TOS are shown in the Figure VI-42. At low TOS values the maltose conversion was similar,

however, in the APR of SBW a more pronounced decline in the maltose conversion was observed with TOS due to catalyst deactivation. These results indicate the disproportionate contribution of minor compounds in SWB to catalyst deactivation, with proteins from malt extract and yeast probably having a major role. Ethanol in SBW is not considered to have a negative influence since an improvement in the H_2 yield was observed by the adding ethanol to sorbitol APR medium [43]. Regarding the composition of the liquid effluents, APR of SBW resulted in a distribution of reaction products similar to that observed in the APR of maltose. In the APR of SBW, in addition to maltose, also glucose, fructose and mainly ethanol were identified in the liquid phase. Formaldehyde, hydroxyacetone, and organics acids such as formic, acetic, levulinic and glycolic acid were also detected in low concentration.

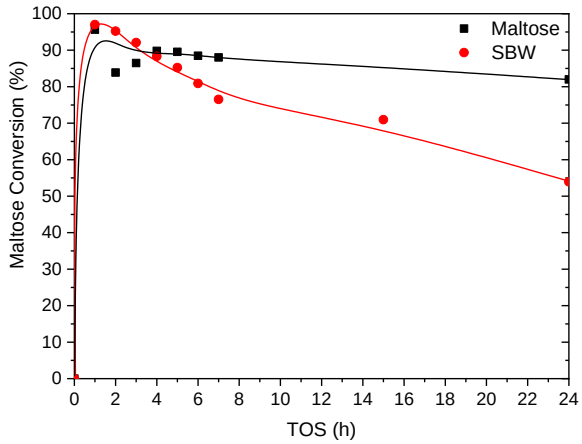

Figure VI-42. Maltose conversion values in the APR of pure maltose and SBW with TOS*

*Reaction conditions: 175 ºC, 30 bar, 0.5 g of PtPd/SIB catalyst, *WHSV* = 0.12 h^{-1}.

Figure VI-43 shows the *CC gas* for the APR of pure maltose and SBW at 175 ºC. APR of pure maltose led to *CC gas* values three times higher

(aprox.) than the APR of SBW during the whole experiment, even though maltose conversion values were quite similar during the first TOS hours. This indicates that conversion of maltose during APR of SBW takes place in a higher extent through routes leading to liquid phase products or carbon deposits in the reactor and the catalysts. For both feedstocks, a maximum of *CC gas* was observed at low TOS values between 2 and 4 h, likewise a similar pattern was observed for the decline.

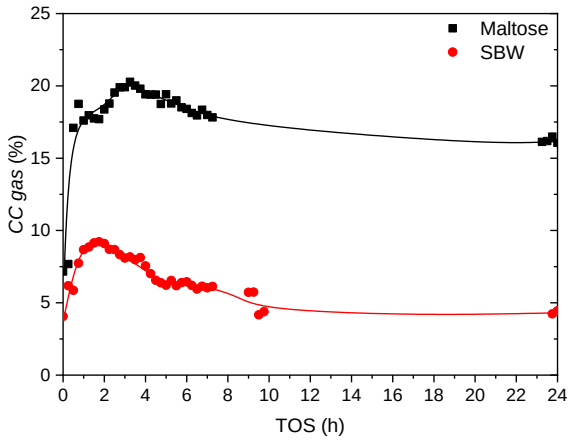

Figure VI-43. Evolution of *CC gas* for the APR of pure maltose and SBW with TOS*

*Reaction conditions: 175 ºC, 30 bar, 0.5 g of PtPd/SIB catalyst, *WHSV* = 0.12 h^{-1}.

More details on the gas production are shown in Figure VI-44. The gas obtained at low TOS is mainly composed of CO_2 and the maximum *CC gas* values are related to a maximum of CO_2 production. This trend can also be observed in H_2 production, although the amount produced is lower. As expected from *CC gas*, H_2 and CO_2 production in the APR of maltose (Figure VI-44 (a)) was higher than in the APR of SBW (Figure VI-44 (b)), while alkanes production was quite similar for both feedstocks. In addition, the gas production in the APR of SBW showed a significant decrease with TOS,

maintaining only a residual gas production of H_2 and alkanes after 10 h TOS, while in the experiment with maltose, the gas production was more stable. Interestingly, the ratio between H_2 and CO_2 production is significantly different for the two feedstocks, with values around 0.4 for the APR of maltose and 0.8 for APR of SBW. This may be related to alternative route of degradation and H_2 generation by HTC, as indicated in previous chapters.

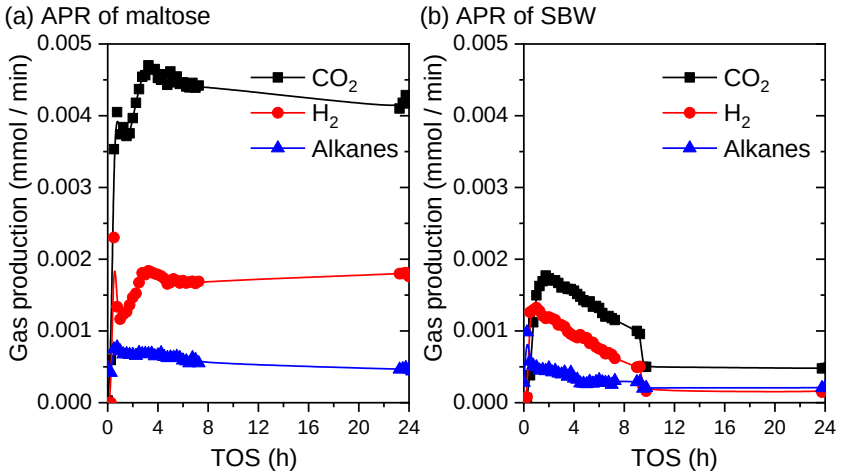

Figure VI-44. Evolution of H_2, CO_2 and alkanes production in the APR of (a) maltose and (b) SBW with TOS*

*Reaction conditions: 175 ºC, 30 bar, 0.5 g of PtPd/SIB catalyst, *WHSV* = 0.12 h^{-1}.

As indicated above, the production of alkanes was quite similar for both substrates and although a significant catalyst deactivation was observed in the APR of SBW, the speciation of alkanes also showed a similar trend to that of APR of maltose. This can be observed in Figure VI-45, where the average production for 24 h TOS is shown. APR of maltose and SBW at 175 ºC were mainly selective to C5, achieving 36.4 % and 21.9 % of selectivity of this compound when SBW and maltose were used as feedstocks, respectively. In addition, the selectivity to C2, C6 and C7 was similar for both

feedstocks, while the selectivity to C1, C3 and C4 was slightly higher in the APR of SBW.

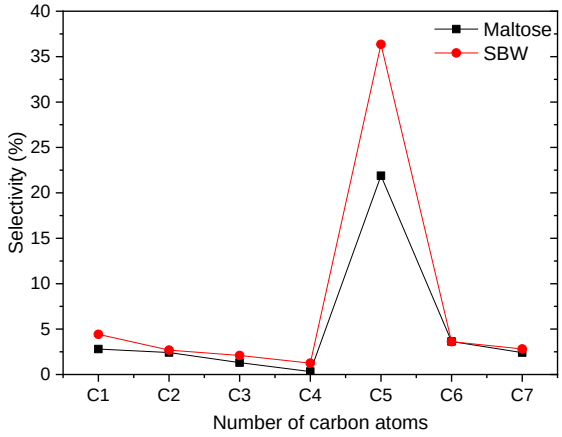

Figure VI-45. Selectivity towards C1 to C7 alkanes for APR of maltose and SBW*

*Reaction conditions: 175 ºC, 30 bar, 0.5 g of PtPd/SIB catalyst, *WHSV* = 0.12 h^{-1}.

The evolution of H_2 selectivity and TOF H_2 with TOS is shown in Figure VI-46. The H_2 selectivity was similar at low TOS values (average 37 %), however after 8 h TOS in the case of APR of SBW it dramatically decreased maintaining only around 10 % of selectivity between 10 and 24 TOS, while in the APR of maltose the H_2 selectivity slightly increased after 8 h TOS. On the other hand, TOF H_2 in the APR of maltose showed a maximum at low TOS values, with a longer acclimation time followed by a slightly decline and then approximately constant values between 5 and 24 h TOS (around 0.03 min^{-1}). In the APR of SBW the TOF H_2 was lower and gradually decreased with TOS producing a TOF H_2 of less than 0.01 min^{-1} after 8 h TOS. In this case, most probably catalyst deactivation started even before finalizing the acclimation time.

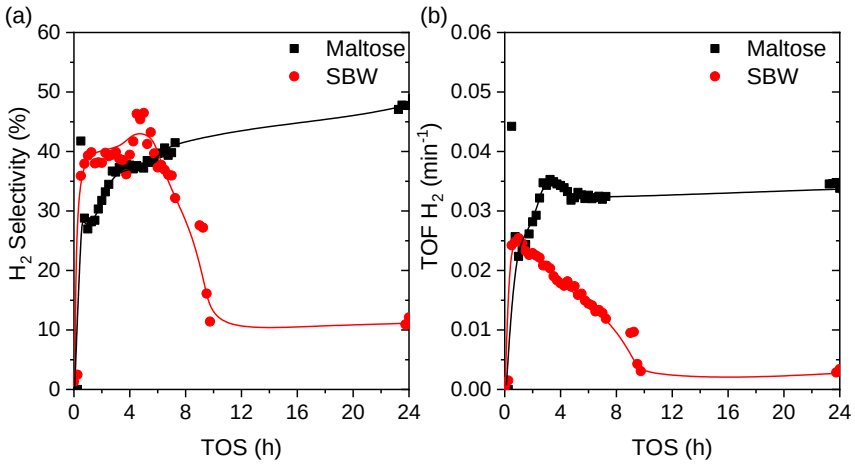

Figure VI-46. Evolution of (a) H_2 selectivity and (b) TOF H_2 for APR of maltose and SBW with TOS*

*Reaction conditions: 175 ºC, 30 bar, 0.5 g of PtPd/SIB catalyst, *WHSV* = 0.12 h^{-1}.

The comparison of the results of APR of maltose and SBW indicate that a relevant catalyst deactivation occurs in the case of the experiments with SBW. This deactivation occurred despite the fact that the main component of the wastewater is maltose, since the APR of maltose was more stable under the same reaction conditions. Hydrogenation of maltose could contribute to lower deactivation and higher H_2 production, but deactivation seems to occur with an important contribution of minority components in the SBW, most probably the protein fraction from malt or yeast, which should be removed in a pretreatment to increase processability.

5.4. Conclusions

The hydrogenation of maltose was performed as a pre-stage of APR to increase overall H_2 production and reduce the formation of carbonaceous deposits. Maltose was selected as model compound because it is the main compound present in the composition of brewery wastewater. Under the

reaction conditions used for hydrogenation of maltose, maltitol was the main compound obtained. In the APR of maltose after 48 h TOS, when the temperature was raised to 225 ºC, a significant catalyst deactivation and increase of the pressure of the reactor was observed, probably due to formation of carbonaceous deposits inside the reactor. In contrast, in the coupled hydrogenation and APR lower deactivation was observed, indicating that undesirable reactions that take place in the liquid phase to form carbonaceous deposits are less favoured when the feedstock is hydrogenated.

The conversion of initial feedstock and *CC gas* were higher in the APR of maltose, however higher H_2 selectivity was achieved in the coupled hydrogenation and APR. The overall process can be considered as efficient since H_2 production increased and compensated for the need for hydrogenation and the durability of the catalyst was increased, probably due to lower formation of carbonaceous deposits.

APR of maltose was more selective to alkanes than APR of maltitol and both compounds showed high selectivity to C5 at 175 ºC. On the other hand, at 225 ºC the APR of maltose was more selective to C2 while the APR of maltitol was more selective to C1. At same temperature (200 ºC) and similar conversion level, in the liquid phase, higher yields of sugar, sugar alcohols, alcohols, acids, aldehydes and ketones were obtained in the APR of maltose, while the *CC gas* was higher in the APR of maltitol. Both H_2 yield and TOF H_2 were higher increased the temperature of reaction and using solutions less concentrated. In addition, the APR of maltitol always led to a higher H_2 yield and TOF H_2 than the APR of maltose, and the value of apparent activation energy calculated was lower for APR of maltitol.

Finally, the comparison of brewery wastewater and maltose APR showed a much higher catalyst deactivation for brewery wastewater.

Therefore, deactivation seems to be caused by minority components in the SBW, most probably the protein fraction from malt or yeast.

Chapter VII. Treatment and valorisation of fruit juice wastewater

1. Aqueous phase reforming of fruit juice wastewater: effect of pH, organic load and salinity

This chapter was adapted from: Saenz de Miera, B., Oliveira, A.S., Baeza, J.A., Calvo, L., Rodriguez, J.J., Gilarranz, M.A., **Treatment and valorisation of fruit juice wastewater by aqueous phase reforming: Effect of pH, organic load and salinity**, J. Clean. Prod. 252 (2020) 119849. doi:10.1016/J.JCLEPRO.2019.119849.

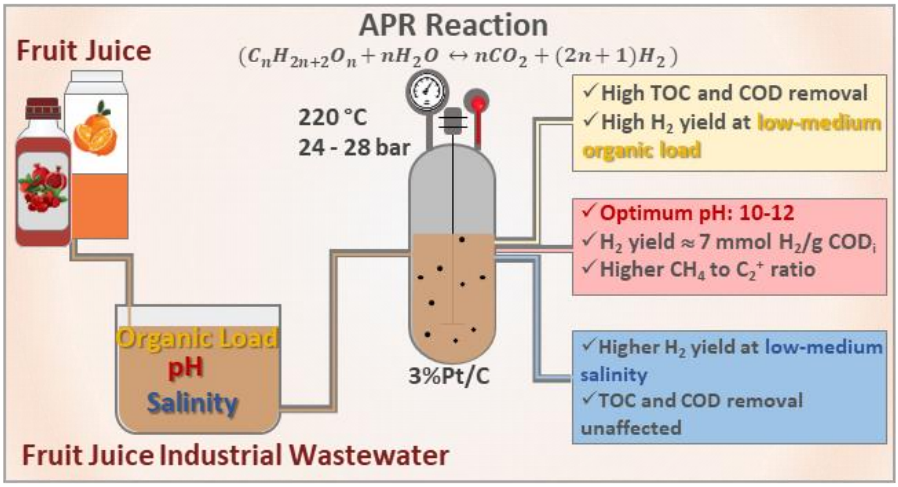

1.1. Introduction

In the previous chapters, the application of APR for the treatment and valorisation of biomass-derived wastewaters, such as those from fish-canning industry or breweries was evaluated. So far, interesting results were obtained with brewery wastewater, where the main component is maltose. In this context, wastewaters from juice industry could be also a suitable feedstock for APR, since they contain relatively high organic load, consisting mainly of monosaccharides, such as glucose and fructose [75,76], and organic acids, such as citric, ascorbic and galacturonic (from pectin) acids [74], which could be appropriate substrates for that process. Moreover, fruit juice industry produces large amounts of wastewater (10 L wastewater / L juice) [135] with high organic load, which requires treatment before disposal. Traditionally, biological processes have been proposed for treating and/or valorising of this type of wastewater [73,136]. However, large fluctuations in organic load, salinity, pH and suspended solids, can be a drawback for biological treatment, because the microbial biomass involved usually requires large acclimation periods, as well as stable salinity and pH values in order to maintain a good performance. Large fluctuations of parameters such as pH, salinity and organic load are common in the FJW due to seasonal production and the various operations involved [137]. Likewise, CIP processes are widely extended in food industry, which can lead to wastewater with high alkalinity. These parameters could also affect the catalytic performance during treatment and valorisation by APR, as observed in the previous chapters and, therefore, its effect should be evaluated.

On the basis of above considerations, the current chapter analyses the behaviour of different feedstocks varying from single compounds to mixtures usually found in FJW in order to assess the potential application of APR for

the treatment and valorisation of these effluents. Likewise, the influence of pH, organic load and salinity was addressed.

1.2. Experimental

Pt/C (3 wt. % Pt) catalyst was prepared and characterized according to the procedure reported in Chapter III using a carbon black (E250) as support.

Single compounds typically present in a real FJW (glucose (GLU), fructose (FRU), citric acid (CIT), ascorbic acid (ASC) and galacturonic acid (GAL)) and a synthetic FJW were tested as feedstock for APR experiments. In the case of single compounds, 1 wt. % aqueous solutions were used. FJW was prepared and characterized according to the procedure reported in Chapter III.

In order to analyse the effect of initial pH, feedstocks pH was adjusted to 2, 7, 10 and 12, using HCl or KOH. In order to evaluate the influence of organic load, wastewater samples with different COD values, within the usual range for this type of wastewater [73] and keeping the same proportion of individual components, were prepared, diluting or concentrating the standard FJW described in Chapter III.

Salinity effect was evaluated by adding to feedstock the most representative inorganic compounds reported in FJW literature [73,137,138], where a high variability is reported. The feedstock with high salt concentration, denoted as FJW-HSC, contained 300 mg / L $(NH_4)_2SO_4$, 27 mg / L KH_2PO_4 and 640 mg / L NaCl and the feedstock with low salt concentration, denoted as FJW-LSC, contained 150 mg / L $(NH_4)_2SO_4$, 13 mg / L KH_2PO_4 and 320 mg / L NaCl.

APR experiments were carried out in a batch reactor (described in Chapter III) during 4 h, using 0.3 g of catalyst in 15 mL of reaction volume under Ar atmosphere. The experiments were performed at 220 ºC and the total reaction pressure was 24 – 28 bar.

1.3. Results and discussion

1.3.1. Characterization of feedstocks

TOC of the single model feedstocks varied between 3500 and 4200 mg / L and COD between 8300 and 12800 mg / L, while TOC of FJW was 2317 mg / L and COD value was 5925 mg / L. Table VII-1 shows the TOC and COD values of the standard FJW, as well as the values for all of wastewaters concentrations studied in this chapter.

Table VII-1. TOC and COD of the FJW tested with different organic load

TOC (mg / L)	COD (mg / L)
930 ± 19	2873 ± 84
2317 ± 64*	5925 ± 263*
4018 ± 97	11592 ± 435

*Standard FJW feedstock.

1.3.2. Effect of initial feedstock pH on the catalytic performance

1.3.2.1. APR of single compounds

TOC and COD removal in APR experiments carried out with single compounds at different feedstock pH values is shown in Figure VII-1. A significant influence of pH can be observed, with different trends for the single compounds tested. Low TOC and COD removal values were achieved for GLU and FRU at acidic pH (pH 2), these values increasing with pH and

peaking between pH 7 and 10. APR of GLU achieved higher removal values, compared to the FRU, with 94.1 % of TOC removal at pH 7 and 81.3 % of COD removal at pH 10. In the literature, some authors [139] reported a similar TOC removal (starting solution 4400 mg / L) at neutral feedstock pH in the APR of glucose at 250 ºC using a Pt (5 wt. %) catalyst supported on activated carbon.

TOC and COD removal values with organic acid substrates (CIT, ASC and GAL) at acidic pH were higher than for GLU and FRU, decreasing gradually at increasing pH. The highest TOC and COD removal values (94.9 and 79.7 %, respectively) were obtained with CIT at pH 2. King *et al.* [54] also observed a higher selectivity towards liquid phase products in the APR of glycerol a pH 12 with a 3 % Pt/C catalyst when KOH was added to the feedstock, although glycerol conversion was higher at this pH. They suggested that the C-O bond cleavage was more favoured than C-C in the presence of KOH, possibly through base-catalysed dehydration reactions of aldehydic intermediates followed by hydrogenation reactions, which could justify the lower removal values at very high pH (pH 12). In the case of GLU and FRU, the addition of HCl in the reactions a pH 2 also could favours C-O bond cleavage through dehydration reactions catalysed by protons in the liquid phase [8], which could justify a lower TOC and COD removal at this pH.

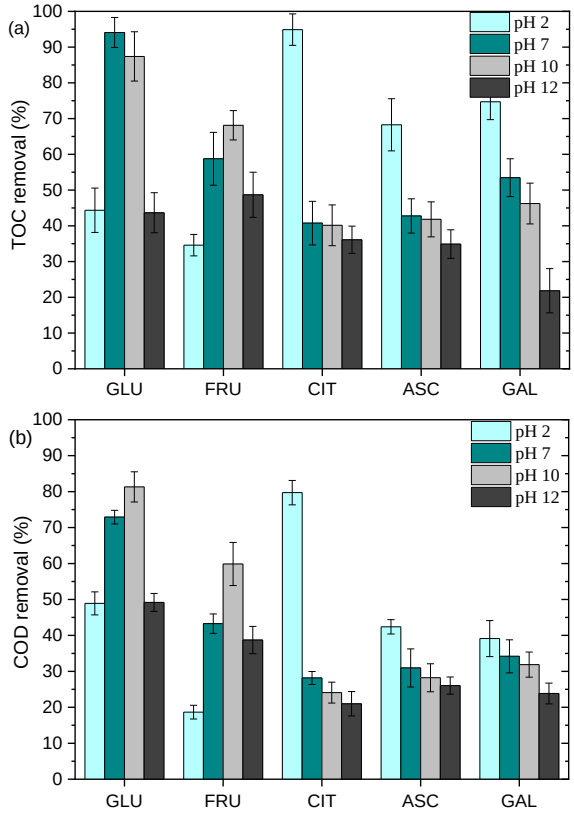

Figure VII-1. (a) TOC and (b) COD removal upon APR of single compounds at different initial pH*

*Reaction conditions: 220 ºC, total reaction pressure: 24 – 28 bar, 15 mL of feedstock (1 wt. %), 0.3 g of Pt/E250 catalyst, 500 rpm, 4 h.

During APR, in addition to the reforming reaction, several other reactions take place, such as WGS, cracking, Fischer-Tropsch, dehydration, dehydrogenation/hydrogenation, deoxygenation, thermal decomposition, hydrogenolysis, as well as condensation and cyclization reactions [8,140]. Gas and liquid products or carbon deposits can result from these reactions, involving not only the starting compounds but also liquid phase intermediates. In the current work, in addition to gas products (H_2, CO_2, CO,

CH_4, C_2H_6 and C_3H_8), some acids, such as acetic, formic and oxalic, were also identified in the liquid phase (not shown). However, the analysis of the liquid phase could not be used to reveal the reaction mechanism at different pH values, since the identified compounds represented less than 30 % of the C remaining in the liquid. On the other hand, although an APR mechanism has been proposed for GRU [47] and FRU [141], other reactions that compete with the reforming may be favoured with the change of pH [142]. Likewise, Kirilin *et al.* [57] reported the identification of over 260 compounds involved in the APR of sorbitol, showing the complexity of the mechanisms involved.

Regarding the gas products, Table VII-2 shows the gas production and composition from APR of single compounds, while Table VII-3 shows the *CC liq*, *CC gas*, *CC sol*, C_2^+, Y_{H2}, S_{H2} and S_{CH4} values from APR of single compounds. As a general trend the gas volume produced increased when pH increased within the range tested (2 – 12), except in the case of CIT, where the opposite trend was observed (Table VII-2), possibly, because the reforming may not be the main decomposition mechanism for this compound. Similar trends were observed for *CC gas* accordingly, although this parameter was also affected by CO_2 abstraction of the gas fraction by the addition of the KOH (Table VII-3).

For all the single compounds, at pH 2, the gas fraction was composed majorly of CO_2 (Table VII-2), and its percentage decreased significantly at increasing pH, due to formation of carbonate in the liquid phase [52,107]. This reduction of CO_2 percentage was quite significant even at neutral pH, confirming that the addition of base is responsible for the removal of CO_2 from the gas fraction. CO was only detected in the experiments at acidic and neutral pH, which indicates that CO_2 abstraction at high pH favours WGS reaction, displacing reaction towards H_2 formation. Liu *et al.* [52] suggested that KOH addition could influence WGS reaction, through the direct provision of hydroxyl anions and/or inducing water polarization and

dissociation. Moreover, these authors showed that CO_x-free H_2 could be produced by combination of APR of ethylene glycol with KOH-carbonation, where addition of KOH could favour APR process by hindering methanation, promotion of WGS reaction and abstraction of CO_2.

In general, S_{H2} and Y_{H2} increased at increasing pH (Table VII-3). As mentioned above, the addition of a base to APR feedstock could favour WGS reaction thus improving H_2 yield [52,107]. However, King *et al.* [54] and Karim *et al.* [55] reported a decrease in both H_2 and CO_2 selectivity upon KOH addition (pH 12) in APR of glycerol with 3 % Pt/C catalyst, while a higher production of liquid phase products was observed. In the current work, the base addition also led to higher production of liquid phase products, possibly via dehydration reactions catalysed by the base, especially at pH 12, where all compounds showed a higher *CC liq* than at pH 10 (Table VII-3). Although it is important to highlight that, the *CC liq* showed also includes the unreacted components.

Under APR conditions, processes such as HTC can also take place, leading to the formation of solids that contribute to lack of carbon balance closure. For this reason, *CC sol* was estimated from *CC liq* and *CC gas* (Table VII-3). All compounds showed higher *CC sol* at pH values closer to original pH of the feedstock, pH 2 in the case of acids and pH 7 in the case of monosaccharides. When HCl or KOH were added to achieve extreme pH values a decrease in *CC sol* and an increase in *CC liq* was observed. Former works also reported lower solid yields with the addition of acidic and basic solutions (H_2SO_4 and NaOH) to feedstock in the HTC of sucrose, which was attributed to reaction shift towards the formation of liquid products [143].

CIT was the single compound leading to the highest S_{CH4} (59.6 %) at pH 12, while low S_{H2} and Y_{H2} were obtained at all pH values tested. The presence of a higher percentage of C_3H_8 in the gas fraction at pH 2, compared

to the other single compounds, could indicate consecutive decarboxylations leading to the formation of C_3H_8, as reported by Verduyckt and De Vos [144]. On the other hand, the difficulty to reform CIT could be associated to the presence of C not activated by hydroxyl groups and/or by direct fragmentation of CIT in recalcitrant compounds such as acetic acid. The proposed reforming mechanisms [8] may change for compounds with a C:O ratio different than 1:1 [13] and some authors also suggest that C activated by O-binding would weaken the C-C bonds favouring the production of H_2 and CO [43]. In addition, Verduyckt and De Vos [144] also reported that under similar reaction conditions (Pt/C catalysts, 225 ºC) the formation of CIT degradation products (acetic and pyruvic acids and acetone) could be promoted by addition of a base. This could justify the higher S_{CH4} here observed in comparison to other single compounds, especially when KOH was added, since the APR of acetic acid [145] or compounds with recalcitrant groups, such as ketone or carboxyl, mainly lead to production of CH_4 and CO_2 [56].

ASC yielded the highest selectivity to H_2 (58.8 %) at pH 12, however, the highest Y_{H2} was obtained with GLU (12.4 %) at the same pH (Table VII-3). Cortright *et al.* [8] studied H_2 production by APR of glucose under similar reaction conditions (1 wt. % glucose, 225 ºC and 29 bar) and observed *CC gas* and S_{H2} values around 50 %. These differences could be due to the type of catalyst (3 % Pt/Al_2O_3), which exhibits high *CC gas* and S_{H2} and low alkanes production [34], and reactor (continuous fixed bed) and consequently the residence times used in that work. On the other hand, Kaya *et al.* [21] reported a lower percentage of H_2 in the gas fraction (20 %) in the APR of a glucose feedstock of similar initial concentration with a 10 % Pt/C catalyst at 250 ºC using a batch reactor. This observation could be due to a lower dispersion of Pt nanoparticles because of the high Pt load used, which can

result in lower catalytic activity and H_2 production [102], and/or the differences in residence time during the reaction experiments (2 versus 4 h).

In all the experiments, the ratio between C_2^+ ($C_2H_6 + C_3H_8$) and total alkanes ($CH_4 + C_2H_6 + C_3H_8$) was higher at acidic pH than at neutral and basic (Table VII-3). With organic acid feedstocks, less C_2^+ were produced when pH increased to 7, especially in the case of CIT, when that ratio decreased from 90.2 to 5.0 %. For ASC and GAL the ratio decreased from 74.9 to 18.3 % and 88.5 % to 25.2 %, respectively, when the pH increased from 2 to 7. For the monosaccharides, the highest decrease in C_2^+ occurred at pH values between 10 and 12, with GLU yielding the highest amount of C_2^+. Therefore, the addition of a base provokes a clear reduction of relative amount of C_2^+ in the gas fraction. Similar conclusions were reported by King *et al.* [54] in the APR of glycerol, suggesting that the pathway to C_2^+ formation was hindered at high pH, possibly due to a lower contribution of dehydration-hydrogenation of alcohols. Some authors have also reported that the selectivity to heavier alkanes increases by increasing acidity of the feedstock [9].

Table VII-2. Gas composition and volume obtained from APR of single compound feedstocks*

Compound	Initial pH	Gas composition (% mol)						Gas volume (mL)
		H_2	CO_2	CO	CH_4	C_2H_6	C_3H_8	
GLU	pH 2	0.7 ± 0.1	92.6 ± 0.7	2.3 ± 0.7	1.5 ± 0.1	2.0 ± 0.1	1.0 ± 0.1	15.5 ± 0.6
	pH 7	28.5 ± 0.6	61.3 ± 0.5	0.0 ± 0.0	3.6 ± 0.1	3.5 ± 0.1	3.2 ± 0.1	54.5 ± 1.4
	pH 10	23.7 ± 2.7	58.4 ± 2.3	0.0 ± 0.0	7.1 ± 0.4	8.6 ± 5.8	2.3 ± 0.3	55.2 ± 1.3
	pH 12	45.6 ± 1.6	45.7 ± 0.1	0.0 ± 0.0	6.6 ± 1.2	1.5 ± 0.3	0.6 ± 0.1	64.9 ± 11.1
FRU	pH 2	2.4 ± 0.1	92.7 ± 0.2	0.4 ± 0.1	2.4 ± 0.1	0.7 ± 0.1	1.4 ± 0.1	14.0 ± 0.1
	pH 7	3.6 ± 3.5	87.6 ± 6.1	3.3 ± 0.1	3.0 ± 2.0	1.1 ± 0.2	1.4 ± 0.6	20.7 ± 9.5
	pH 10	22.8 ± 0.4	62.2 ± 0.3	0.0 ± 0.0	10.3 ± 0.1	3.5 ± 0.1	1.2 ± 0.1	42.5 ± 0.4
	pH 12	42.1 ± 0.4	47.3 ± 0.6	0.0 ± 0.0	8.9 ± 0.1	1.2 ± 0.1	0.5 ± 0.1	53.1 ± 0.8
CIT	pH 2	1.9 ± 0.1	75.2 ± 7.4	0.0 ± 0.0	2.2 ± 0.2	9.0 ± 0.1	11.7 ± 1.2	55.4 ± 2.9
	pH 7	1.5 ± 0.1	45.0 ± 0.2	0.0 ± 0.0	50.8 ± 0.2	1.7 ± 0.1	0.9 ± 0.1	20.9 ± 0.1
	pH 10	0.2 ± 0.1	40.3 ± 0.5	0.0 ± 0.0	57.6 ± 0.6	1.4 ± 0.1	0.5 ± 0.1	19.9 ± 0.2
	pH 12	1.7 ± 1.4	38.1 ± 7.6	0.0 ± 0.0	58.3 ± 9.3	1.3 ± 0.2	0.6 ± 0.1	18.9 ± 5.6
ASC	pH 2	0.2 ± 0.1	91.7 ± 0.1	0.2 ± 0.1	2.0 ± 0.1	3.2 ± 0.1	2.7 ± 0.1	38.3 ± 0.3
	pH 7	30.7 ± 0.2	61.3 ± 0.3	0.0 ± 0.0	6.5 ± 0.1	1.0 ± 0.1	0.4 ± 0.1	45.8 ± 0.5
	pH 10	32.4 ± 0.2	57.0 ± 0.3	0.0 ± 0.0	9.1 ± 0.1	1.1 ± 0.1	0.4 ± 0.1	55.8 ± 0.5
	pH 12	50.2 ± 0.6	41.6 ± 0.7	0.0 ± 0.0	7.0 ± 0.1	0.9 ± 0.1	0.3 ± 0.1	41.4 ± 0.6
GAL	pH 2	5.8 ± 5.7	86.6 ± 12.1	0.8 ± 0.8	0.8 ± 0.5	4.4 ± 0.3	1.6 ± 1.6	22.6 ± 12.9
	pH 7	27.2 ± 0.6	62.3 ± 0.9	0.0 ± 0.0	7.9 ± 0.3	2.2 ± 0.1	0.4 ± 0.1	39.4 ± 1.4
	pH 10	32.1 ± 0.9	58.3 ± 0.4	0.0 ± 0.0	7.2 ± 0.6	1.9 ± 0.1	0.5 ± 0.2	43.5 ± 1.3
	pH 12	23.0 ± 8.3	69.1 ± 9.1	0.0 ± 0.0	5.6 ± 3.0	1.3 ± 0.6	1.0 ± 0.4	18.4 ± 6.1

*Reaction conditions: 220 ºC, total reaction pressure: 24 – 28 bar, 15 mL of feedstock (1 wt. %), 0.3 g of Pt/E250 catalyst, 500 rpm, 4 h.

Table VII-3. Results obtained from APR of single compound feedstocks*

Compound	Initial pH	*CC liq* (%)	*CC gas* (%)	*CC sol* (%)	C_2^+ (% mol)	Y_{H2} (%)	S_{H2} (%)	S_{CH4} (%)
GLU	pH 2	55.6 ± 6.2	15.3 ± 0.7	29.1 ± 5.5	65.7 ± 0.7	< 0.1	0.3 ± 0.1	1.5 ± 0.1
	pH 7	5.9 ± 4.2	42.7 ± 0.8	51.4 ± 3.4	66.7 ± 0.5	6.5 ± 0.3	17.5 ± 0.5	4.4 ± 0.1
	pH 10	12.6 ± 6.9	47.5 ± 5.3	39.9 ± 1.6	58.4 ± 13.9	5.4 ± 0.5	13.2 ± 2.7	7.9 ± 1.1
	pH 12	56.3 ± 5.6	35.4 ± 4.9	8.0 ± 0.7	23.7 ± 0.5	12.4 ± 2.5	40.1 ± 2.8	11.6 ± 1.7
FRU	pH 2	65.4 ± 3.0	10.7 ± 0.1	23.9 ± 2.9	46.5 ± 1.2	0.1 ± 0.1	1.2 ± 0.1	2.4 ± 0.1
	pH 7	41.2 ± 7.4	17.7 ± 9.4	41.1 ± 16.8	48.1 ± 10.1	0.4 ± 0.4	1.8 ± 1.8	3.0 ± 2.0
	pH 10	31.9 ± 4.1	27.3 ± 0.2	40.8 ± 3.9	31.1 ± 0.1	4.0 ± 0.1	13.8 ± 0.3	12.5 ± 0.1
	pH 12	51.3 ± 6.3	28.7 ± 0.6	20.0 ± 5.7	16.0 ± 0.1	9.3 ± 0.1	35.0 ± 0.6	14.8 ± 0.3
CIT	pH 2	5.1 ± 4.4	64.5 ± 4.6	30.4 ± 9.0	90.2 ± 0.5	0.6 ± 0.1	0.9 ± 0.1	1.7 ± 0.2
	pH 7	59.2 ± 6.1	20.1 ± 0.1	20.7 ± 6.0	5.0 ± 0.1	0.2 ± 0.1	1.0 ± 0.1	49.8 ± 0.2
	pH 10	59.9 ± 5.7	18.1 ± 0.2	22.0 ± 5.5	3.3 ± 0.1	< 0.1	0.1 ± 0.1	56.3 ± 0.5
	pH 12	63.9 ± 3.8	17.2 ± 5.6	18.9 ± 9.4	2.5 ± 0.9	0.3 ± 0.3	2.0 ± 1.0	59.6 ± 8.8
ASC	pH 2	31.7 ± 7.3	34.4 ± 0.2	33.9 ± 7.1	74.9 ± 0.1	< 0.1	0.1 ± 0.1	1.8 ± 0.1
	pH 7	57.2 ± 4.8	27.0 ± 0.3	15.8 ± 4.5	18.3 ± 0.1	6.9 ± 0.1	25.9 ± 0.2	9.1 ± 0.1
	pH 10	58.2 ± 4.9	32.1 ± 0.4	9.7 ± 4.5	14.0 ± 0.1	8.8 ± 0.1	28.0 ± 0.2	13.1 ± 0.1
	pH 12	65.1 ± 4.0	17.5 ± 0.4	17.4 ± 3.6	14.4 ± 0.1	10.1 ± 0.1	58.8 ± 1.3	13.6 ± 0.3
GAL	pH 2	25.3 ± 5.0	22.3 ± 11.5	52.4 ± 16.5	88.5 ± 16.5	0.7 ± 0.6	3.4 ± 3.3	0.8 ± 0.5
	pH 7	46.5 ± 5.3	29.7 ± 1.2	23.8 ± 4.1	25.2 ± 0.1	5.8 ± 0.1	21.5 ± 0.6	10.4 ± 0.4
	pH 10	53.8 ± 5.7	31.5 ± 0.1	14.7 ± 5.6	25.4 ± 2.5	7.5 ± 0.1	27.1 ± 1.0	10.1 ± 0.8
	pH 12	78.2 ± 6.2	14.6 ± 5.5	7.2 ± 0.7	28.6 ± 8.2	2.3 ± 1.3	17.2 ± 8.3	7.0 ± 3.8

*Reaction conditions: 220 ºC, total reaction pressure: 24 – 28 bar, 15 mL of feedstock (1 wt. %), 0.3 g of Pt/E250 catalyst, 500 rpm, 4 h.

1.3.2.2. APR of fruit juice wastewater

FJW was subjected to APR under different initial pH values to compare the behaviour of single compounds and complex matrices. TOC and COD removal is shown in Figure VII-2. Although FJW was composed mainly of GLU and FRU (80 wt. %), TOC and COD removal showed a trend closer to the one observed for organic acids in the single compounds experiments. Thus, when pH increased TOC and COD removal decreased significantly. At pH 2, removal values of up 91.7 % were achieved and these values were reduced to a minimum of 48.9 % at pH 12.

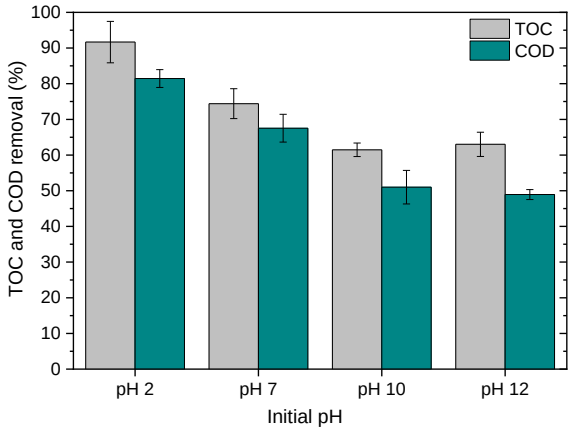

Figure VII-2. TOC and COD removal upon APR of FJW at different initial pH*

*Reaction conditions: 220 ºC, total reaction pressure: 24 – 28 bar, 15 mL of FJW (2317 mg / L TOC_i, 5925 mg / L COD_i), 0.3 g of Pt/E250 catalyst, 500 rpm, 4 h.

As can be seen in Table VII-4, the gas volume produced remained almost constant in the pH range tested, except at pH 12, where a decline was observed, although CO_2 abstraction at high pH contributes to lower gas production. The *CC gas* decreased monotonically at increasing pH, while the *CC liq* increased and the *CC sol* decreased with the addition of KOH to the

mixture (Table VII-5), as observed in the APR of the simple compounds. The Y_{H2} increased until pH 10, which can be attributed to enhanced WGS reaction, as it was observed for single compounds. A maximum Y_{H2} of 7.8 mmol H_2 / g COD_i was obtained at pH 10, then decreasing to 6.6 mmol H_2 / g COD_i at pH 12. This can be due to a higher contribution of base-catalysed dehydration reactions at pH 12, which are followed by hydrogenation [54,55] decreasing H_2 production. Y_{CH4} was relatively low in comparison to Y_{H2}, with values between 0.8 and 2.3 mmol CH_4 / g COD_i. As observed in the APR of single compounds, addition of base provokes a decrease of C_2^+ alkanes, especially when the pH increased from 2 to 7. The H_2 yield (7.8 mmol H_2 / g COD_i at pH 10) is similar to that reported for acidogenic fermentation of FJW [76]. It is worthy to mention that relatively low changes in Y_{H2} where observed in APR of FJW at different pH, therefore this treatment can be a good alternative to overcome the drawbacks of acidogenic fermentation derived from the variability of pH, such as the need of longer retention times or acclimatization [137].

Table VII-4. Gas composition and volume from APR of FJW at different initial pH*

Initial pH	Gas composition (% mol)						Gas volume (mL)
	H_2	CO_2	CO	CH_4	C_2H_6	C_3H_8	
pH 2	27.8 ± 3.6	60.1 ± 3.0	0.3 ± 0.1	4.0 ± 0.3	3.6 ± 0.5	4.3 ± 0.4	40.4 ± 2.5
pH 7	34.9 ± 1.4	49.3 ± 1.4	0.2 ± 0.2	11.9 ± 0.1	2.9 ± 0.2	0.9 ± 0.1	41.5 ± 3.6
pH 10	40.8 ± 1.7	45.1 ± 0.1	0.0 ± 0.0	11.3 ± 1.4	2.0 ± 0.4	0.8 ± 0.1	40.6 ± 2.3
pH 12	40.0 ± 0.4	48.2 ± 0.1	0.0 ± 0.0	9.5 ± 0.6	1.7 ± 0.1	0.6 ± 0.3	35.3 ± 0.4

*Reaction conditions: 220 ºC, total reaction pressure: 24 – 28 bar, 15 mL of FJW (2317 mg / L TOC_i, 5925 mg / L COD_i), 0.3 g of Pt/E250 catalyst, 500 rpm, 4 h.

Table VII-5. Results obtained from APR of FJW at different initial pH*

Initial pH	*CC liq* (%)	*CC gas* (%)	*CC sol* (%)	C_2^+ (% mol)	Y_{H2} (mmol H_2 / g COD_i)	Y_{CH4} (mmol CH_4 / g COD_i)
pH 2	8.3 ± 5.8	48.8 ± 0.2	42.9 ± 5.6	66.0 ± 4.3	5.3 ± 1.0	0.8 ± 0.1
pH 7	25.6 ± 4.2	41.6 ± 3.0	32.8 ± 1.2	24.2 ± 1.3	6.8 ± 0.9	2.3 ± 0.2
pH 10	38.5 ± 1.9	36.7 ± 3.2	24.8 ± 5.1	20.0 ± 0.1	7.8 ± 0.1	2.2 ± 0.4
pH 12	37.0 ± 3.4	31.9 ± 0.4	31.1 ± 3.0	19.8 ± 2.5	6.6 ± 0.1	1.6 ± 0.1

*Reaction conditions: 220 ºC, total reaction pressure: 24 – 28 bar, 15 mL of FJW (2317 mg / L TOC_i, 5925 mg / L COD_i), 0.3 g of Pt/E250 catalyst, 500 rpm, 4 h.

1.3.3. Effect of organic load on the APR of fruit juice wastewater

The effect of organic load was investigated at pH 10, since the highest Y_{H2} was obtained at this pH. Moreover, basic pH values are common in the wastewater from industries such as processing food, beverages or brewing due to the CIP operations performed, where basic cleaning solution are used. TOC and COD removal values at different initial organic load are shown in Figure VII-3. The percentage of COD removal remained almost unchanged, while a small variation was observed for TOC removal. This is a relevant finding with regard to the potential application of APR to these wastewater since with other type of effluents (e.g. brewery wastewater) a substantial decline in TOC and COD removal was observed when increasing the initial organic load within a similar range of COD_i (Chapter VI, Section 1).

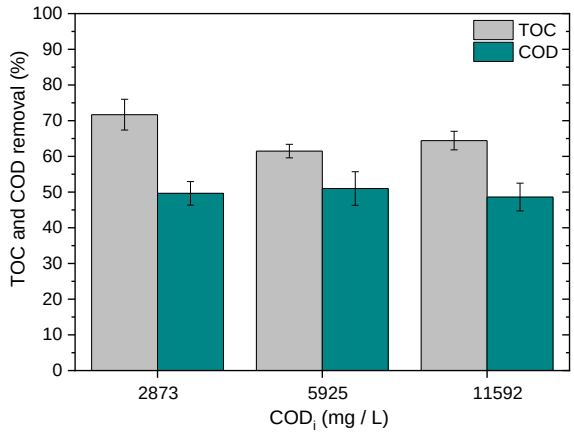

Figure VII-3. TOC and COD removal upon APR of FJW with different organic load*

*Reaction conditions: 220 ºC, total reaction pressure: 24 – 28 bar, 15 mL of FJW, 0.3 g of Pt/E250 catalyst, 500 rpm, 4 h.

Table VII-6 shows the gas volume and composition from APR of JFW with different organic load and Table VII-7 summarizes the results obtained from the APR at different organic loads. The increase of the organic load of FJW affected the composition of the resulting gas, as showed in Table VII-6. At the lowest COD_i tested the gas fraction showed the highest percentage of alkanes (22.1 %) and the lowest of H_2 (25.2 %). This last increased significantly with the organic load of the feedstock, showing the highest value at intermediated COD_i and then decreasing at the highest organic load tested, where the higher contribution of HTC increases the generation of CO_2.

The volume of gas generated increased with organic load (Table VII-6), but *CC gas* was twice higher for the less concentrated FJW (70.6 versus 35.7 %), while the *CC sol* increased from 1.1 % to 28.7 % with organic load, as shown in Table VII-7. This may indicate that at higher organic load there is a higher contribution of HTC. In previous works in the literature,

Kirilin *et al.* [57] also reported that reforming more concentrated feedstock resulted in lower transformation of organic matter to gaseous products. Likewise, Pipitone *et al.* [122] reported that APR of glucose and xylose concentrated solutions led to a higher solid phase production due to the formation of high molecular weight compounds by condensation reactions.

Table VII-6. Gas composition and volume from the APR of FJW with different organic load*

COD_i (mg / L)	Gas composition (% mol)						Gas volume (mL)
	H_2	CO_2	CO	CH_4	C_2H_6	C_3H_8	
2873	25.2 ± 0.7	52.7 ± 1.7	0.0 ± 0.0	15.8 ± 0.7	4.9 ± 0.2	1.4 ± 0.1	16.1 ± 0.8
5925	40.8 ± 1.7	45.1 ± 0.1	0.0 ± 0.0	11.3 ± 1.4	2.0 ± 0.4	0.8 ± 0.1	40.6 ± 2.3
11592	33.4 ± 0.3	51.8 ± 0.6	0.0 ± 0.0	11.7 ± 0.2	2.5 ± 0.1	0.7 ± 0.1	61.3 ± 0.9

*Reaction conditions: 220 ºC, total reaction pressure: 24 – 28 bar, 15 mL of FJW, 0.3 g of Pt/E250 catalyst, 500 rpm, 4 h.

Table VII-7. Results obtained from the APR of FJW with different organic load*

COD_i (mg / L)	*CC liq* (%)	*CC gas* (%)	*CC sol* (%)	C_2^+ (% mol)	Y_{H2} (mmol H_2 / g COD_i)	Y_{CH4} (mmol CH_4 / g COD_i)
2873	28.3 ± 4.3	70.6 ± 3.6	1.1 ± 0.7	28.7 ± 0.1	3.9 ± 0.1	2.5 ± 0.1
5925	38.5 ± 1.9	36.7 ± 3.2	24.8 ± 5.1	20.0 ± 0.1	7.8 ± 0.1	2.2 ± 0.4
11592	35.6 ± 2.6	35.7 ± 0.7	28.7 ± 1.9	21.2 ± 0.1	4.9 ± 0.1	1.7 ± 0.1

*Reaction conditions: 220 ºC, total reaction pressure: 24 – 28 bar, 15 mL of FJW, 0.3 g of Pt/E250 catalyst, 500 rpm, 4 h.

1.3.4. Effect of salinity on the APR of fruit juice wastewater

The juice industry produces wastewater with variable salt concentration depending on season and batches. Different salt concentrations have been tested to learn on the effect of this variable in APR. As in the previous section, all the experiments were performed at pH 10. Within the salinity range tested (see Section 2.3 of General experimental (Chapter III)), salinity did not significantly affect the TOC and COD removal, as can be seen in the Figure VII-4.

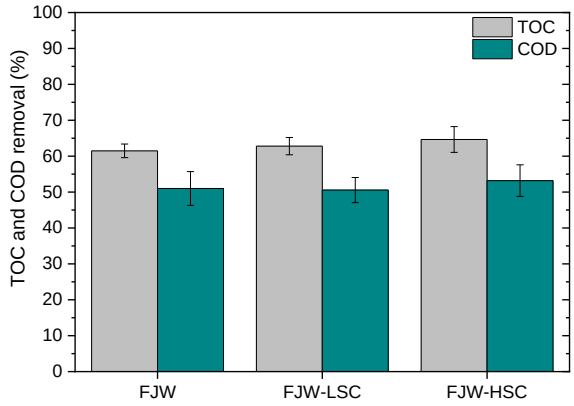

Figure VII-4. TOC and COD removal upon APR of FJW with different salinity*

*Reaction conditions: 220 ºC, total reaction pressure: 24 – 28 bar, 15 mL of FJW (2317 mg / L TOC_i, 5925 mg / L COD_i), 0.3 g of Pt/E250 catalyst, 500 rpm, 4 h.

Table VII-8 shows the gas production and composition from APR of JFW with different salinity, while Table VII-9 summarizes the results obtained regarding gas production, as well as the *CC liq* and *CC sol*. There were no significant variations in the gas volume and *CC gas* within the low salinity range (FJW and FJW-LSC), while at the highest salinity (FJW-HSC) substantially lower values were obtained. Similarly, Y_{H2} and the percentage of H_2 in the gas were also significantly lower at the highest salinity. On the

other hand, *CC sol* increased from 24.8 %, in the experiment without salts, to 35.2 % at the highest salinity. Boga *et al.* [48] reported deactivation of APR catalysts by NaCl, giving rise to decreased glycerol conversion and H_2 selectivity. Lehnert and Claus [26] also reported that the presence of NaCl was responsible of catalyst deactivation and lower H_2 production. In the previous chapter (Chapter V) a negative effect of salts on the APR of a fish-canning wastewater was observed, leading to low gas production with a high proportion of CO_2. Remón *et al.* [146] also reported that the presence of salt in cheese whey negatively affected to the catalyst performance in APR, because the presence of salts promotes the dehydration, condensation and polymerisation reactions increasing the proportion of char and coke precursors favouring catalyst deactivation, which leads to lower gas production and higher solids production. In addition, it was reported that Na salts showed a catalytic effect to accelerate HTC of biomass [147] and the presence of $(NH_4)_2SO_4$ considerably increased the yields of hydrochar from sucrose in acidic and basic conditions [143]. However, for the purpose of the current work it is noteworthy that there is a wide salinity range where no relevant affection is observed in the APR of FJW.

Table VII-8. Gas composition and volume from the APR of FJW with different salinity*

Wastewater	Gas composition (% mol)						Gas volume (mL)
	H_2	CO_2	CO	CH_4	C_2H_6	C_3H_8	
FJW	40.8 ± 1.7	45.1 ± 0.1	0.0 ± 0.0	11.3 ± 1.4	2.0 ± 0.4	0.8 ± 0.1	40.6 ± 2.3
FJW-LSC	38.1 ± 0.9	46.4 ± 1.4	0.0 ± 0.0	12.3 ± 0.4	2.7 ± 0.1	0.5 ± 0.1	42.9 ± 1.4
FJW-HSC	35.1 ± 1.4	48.6 ± 1.6	0.0 ± 0.0	13.3 ± 0.1	2.3 ± 0.1	0.7 ± 0.1	29.9 ± 3.7

*Reaction conditions: 220 ºC, total reaction pressure: 24 – 28 bar, 15 mL of FJW (2317 mg / L TOC_i, 5925 mg / L COD_i), 0.3 g of Pt/E250 catalyst, 500 rpm, 4 h.

Table VII-9. Results obtained from the APR of FJW with different salinity*

Wastewater	*CC liq* (%)	*CC gas* (%)	*CC sol* (%)	C_2^+ (% mol)	Y_{H2} (mmol H_2 / g COD_i)	Y_{CH4} (mmol CH_4 / g COD_i)
FJW	38.5 ± 1.9	36.7 ± 3.2	24.8 ± 5.1	20.0 ± 0.1	7.8 ± 0.1	2.2 ± 0.4
FJW-LSC	37.2 ± 2.4	40.6 ± 1.8	22.2 ± 0.6	21.0 ± 0.1	6.5 ± 0.1	2.1 ± 0.1
FJW-HSC	35.4 ± 3.6	29.4 ± 3.1	35.2 ± 0.5	18.4 ± 0.3	4.2 ± 0.7	1.6 ± 0.2

*Reaction conditions: 220 ºC, total reaction pressure: 24 – 28 bar, 15 mL of FJW (2317 mg / L TOC_i, 5925 mg / L COD_i), 0.3 g of Pt/E250 catalyst, 500 rpm, 4 h.

1.4. Conclusions

APR of wastewater from fruit juice production has been investigated and the effect of pH, organic load and salinity have been addressed. Previous experiments with single components showed that TOC and COD removal was higher for glucose and fructose feedstocks in the 7 - 10 pH range, whereas with ascorbic, galacturonic and citric acids, the acidic pH led to higher removal. FJW behaved closer to organic acids feedstocks, even though the main components of those wastewaters are monosaccharides.

In general, H_2 yield and selectivity increased at increasing pH, accompanied by a decrease in percentage of CO_2 in the gas, due to CO_2 abstraction as carbonate. CH_4 selectivity also increased with pH, mostly due to CO_2 abstraction and a lower formation of C_2^+ alkanes, possibly through lower contribution of dehydration-hydrogenation of alcohols. H_2 yield averaged around 6.6 mmol H_2 / g COD_i in the APR of FJW with little influence of initial pH. The highest H_2 yield values were observed with low-medium organic load of FJW. Salinity did not affect the TOC and COD

removal within the range tested, while a negative effect was found on the H_2 yield at high salinity, most probably due to the catalyst deactivation giving rise to a higher contribution of HTC.

Chapter VIII. Treatment and valorisation of wastewater with phenolic compounds

1. Catalytic wet air oxidation coupled to aqueous phase reforming for the removal and valorisation of phenolic compounds

This chapter was adapted from: Oliveira, A.S., Baeza, J.A., Saenz de Miera, B., Calvo, L., Rodriguez, J.J., Gilarranz, M.A., **Catalytic wet air oxidation coupled to aqueous phase reforming for the removal and valorisation of phenolic compounds**, (submitted).

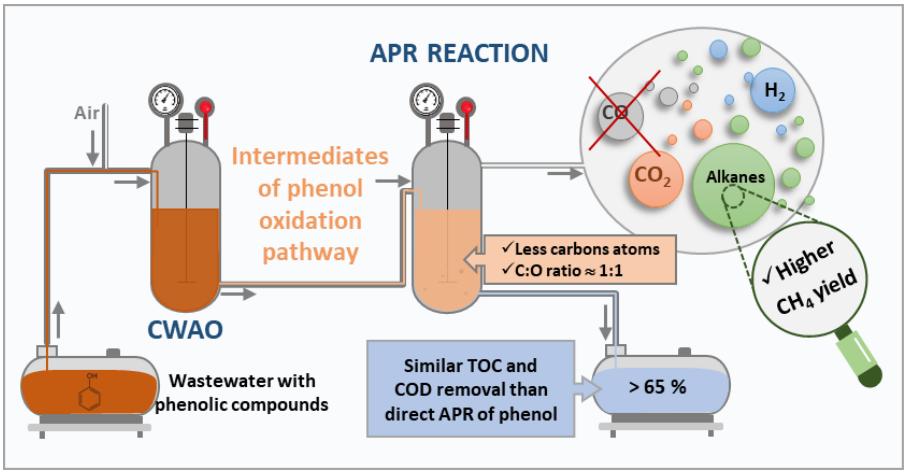

1.1. Introduction

Phenolic compounds are widely used in chemical, oil, gas, coal, and pesticides industries, among others. They have been considered as priority concern pollutants by several national agencies and institutions, such as the Environmental Protection Agency (USA) or the European Union, because of their proved toxic effects on environment and human health [148]. Phenol is usually found in the wastewater discharged from the coal tar, petroleum refinery, steel, plastic, disinfectant, pharmaceutical, and rubber plants [149]. Phenols-bearing wastewaters are usually treated by physico-chemical and biological systems, although special acclimatization is required since phenols inhibit biological processes. In addition, the conventional treatment used allows removing the hazardous effects but not the valorisation of the pollutants. Therefore, APR could be an alternative to treat and valorise wastewater with this type of compounds.

In the application of the APR to substrates with abundant high-weight molecules and aromatics, condensation and HTC are competing reactions resulting in major drawbacks [150,151]. For example, in the case of lignin HTC, the resulting hydrochar is mainly composed by polyaromatic and phenolic compounds [152]. On the other hand, CWAO could be used to degrade phenolic compounds into intermediates in the oxidation pathway that could be more easily converted by APR process. The catalysts used in APR and CWAO are compatible and inexpensive air is used for the oxidation process. The intermediates generated by oxidation have less carbon atoms and a C:O ratio closer or equal to 1:1 [77,78] that may be more selective to H_2 production. Therefore, a partial oxidation of phenolic compounds would generate species that can be converted into valuable gases by APR, avoiding some drawbacks of direct APR of phenolic compounds.

Accordingly, in this chapter, coupling of CWAO and APR is studied as an approach for phenol-bearing wastewater treatment and valorisation. Wastewater was subjected in a first stage to CWAO and in a subsequent stage to APR. APR of feedstocks consisting in mixtures of representative species from phenol oxidation pathway was studied to learn on the contribution of the corresponding individual compounds.

1.2. Experimental

Pt/C (3 wt. % Pt) catalyst was prepared and characterized according to the procedure described in Chapter III using a carbon black (E250) as support.

Different feedstocks were used in the APR experiments. Table VIII-1 shows theoretical composition of these feedstocks prepared as mixtures of selected representative compounds identified in the phenol oxidation routes proposed by Zazo *et al*. [77] and Joglekar *et al.* [78]. Initial theoretical TOC was 76.5 mg / L for all feedstocks. FPhOH feedstock consisted exclusively of phenol, while FAromatic feedstock simulates a first partial oxidation stage in phenol oxidative route leading to compounds where aromatic ring is still preserved. FLargeAcid and FShortAcid feedstocks simulate last oxidation states, where the feedstock is composed entirely of long (C2 – C4) and short (C1 – C2) chain organic acids, respectively. The composition of the mixtures prepared from those feedstocks are summarized in Table VIII-2. Mixture M-1 simulates oxidation conditions where phenol is partially oxidized to aromatic intermediates, whereas in M-2, it is considered that phenol is partially oxidized to organics acids. M-3 is considered a mixture of all compounds that may be present in phenol partial oxidation route.

Table VIII-1. Composition of feedstocks

Feedstock	Compound	Concentration	
		(mg / L)	(mg C / L)*
FPhOH	Phenol	100	76.5(100)
FAromatic	Hydroquinone	58	38.3(50)
	Catechol	58	38.3(50)
FLargeAcid	Oxalic acid	115	30.6 (40)
	Malonic acid	22	7.7 (10)
	Maleic acid	74	30.6 (40)
	Fumaric acid	19	7.7 (10)
FShortAcid	Oxalic acid	86	23.0 (30)
	Formic acid	59	15.3 (20)
	Acetic acid	96	38.3 (50)

*in brackets percentage of total organic carbon.

Table VIII-2. Mixtures of feedstocks

Mixture	Feedstock	(%)	Compounds	Concentration	
				(mg / L)	(mg C / L)*
M-1	FPhOH	50	Phenol	50	38.3(50)
	FAromatic	50	Hydroquinone	29	19.1(25)
			Catechol	29	19.1(25)
M-2	FPhOH	34	Phenol	34	26.0(34)
	FLargeAcid	33	Oxalic acid	66	17.7(23)
	FShortAcid	33	Malonic acid	7	2.5(3)
			Maleic acid	24	10.1(13)
			Fumaric acid	6	2.5(3)
			Formic acid	19	5.0(7)
			Acetic acid	32	12.6(17)
M-3	FPhOH	25	Phenol	25	19.1(25)
	FAromatic	25	Hydroquinone	15	9.6(12)
	FLargeAcid	25	Catechol	15	9.6(12)
	FShortAcid	25	Oxalic acid	50	13.4(18)
			Malonic acid	6	1.9(3)
			Maleic acid	19	7.7(10)
			Fumaric acid	5	1.9(3)
			Formic acid	15	3.8(5)
			Acetic acid	24	9.6(12)

*in brackets percentage of total organic carbon.

APR experiments were carried out in a batch reactor (described in Chapter III) during 4 h, using 0.6 g of catalyst in 30 mL of reaction volume under Ar atmosphere. The experiments were performed at 220 ºC and the total reaction pressure was 24 – 28 bar.

The results obtained with feedstocks of the Table VIII-1 were quantified with the equations described in Chapter III. The results obtained with mixtures of feedstocks were compared with theoretical results calculated from the behaviour of individual feedstocks, considering the mixture compositions given in Table VIII-2. For example, theoretical result for TOC removal was calculated according to Equation (21) for mixture M-1, while Equations (22) and (23) where applied to mixtures M-2 and M-3, respectively.

$$TOC\ Removal\ (\%) = 0.5 * TOC\ Removal_{\ FPhOH}\ (\%) + 0.5 * TOC\ Removal_{FAromatic}\ (\%) \quad (21)$$

$$TOC\ Removal\ (\%) = 0.34 * TOC\ Removal_{FPhOH}\ (\%) + 0.33 * TOC\ Removal_{FLargeAcid}\ (\%) + 0.33 * TOC\ Removal_{FShortAcid}\ (\%) \quad (22)$$

$$TOC\ Removal\ (\%) = 0.25 * TOC\ Removal_{FPhOH}\ (\%) + 0.25 * TOC\ Removal_{FAromatic}\ (\%) + 0.25 * TOC\ Removal_{FLargeAcid}\ (\%) + 0.25 * TOC\ Removal_{FShortAcid}\ (\%)) \quad (23)$$

Finally, adsorption tests were carried out to learn on the adsorption contribution to TOC removal. These tests were carried out during 24 h at room temperature and ambient pressure using the same feedstock to support mass ratio as in APR experiments.

1.3. Results and discussion

1.3.1. Adsorption on support

TOC removal from adsorption tests can be seen in Figure VIII-1. Higher removal of TOC was observed in the case of FPhOH and FAromatic (57 and 67 % respectively). These feedstocks contain phenol, hydroquinone and catechol, which can interact more strongly with the surface of the E250 support, due to the aromatic ring of their structures. In adsorption experiments with FLargeAcid and FShortAcid, containing organic acids mixtures, lower TOC removal values of 31 and 14 %, respectively, were observed. These results provide useful information about adsorption behaviour of feedstocks onto the support, even though adsorption conditions tested differ from APR conditions.

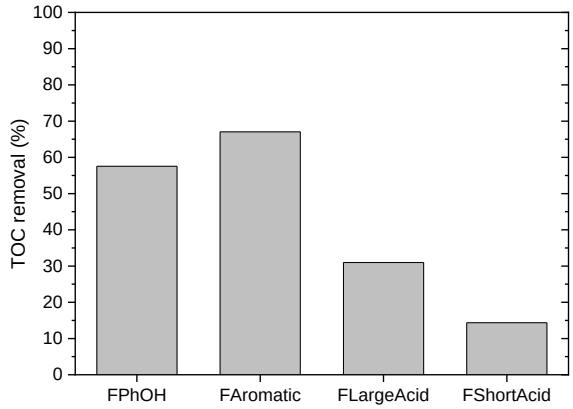

Figure VIII-1. TOC removal in adsorption test*

*Reaction conditions: room temperature and ambient pressure, 30 mL of feedstock, 0.6 g of E250 support, 500 rpm, 24 h.

1.3.2. APR of feedstocks

Figure VIII-2 shows TOC and COD removal from the APR experiments. The runs performed without catalysts (blank) showed a wide range of TOC and COD removal, varying between 5 and 62 %. HTC must be the main way of TOC and COD removal in the blank experiments. After blank experiments a black solid was separated by filtration and the aqueous phase contained short chain acids such as oxalic, acetic or formic, which are common by-products of HTC [153]. In the blank experiments, FPhOH feedstock yielded the lowest removal values (5 %), while the highest were obtained from FLargeAcid (62 %). Removal was higher for TOC than for COD, probably due to degradation of initial compounds to lower molecular weight species with higher oxygen content.

In addition to blanks experiments, some runs were conducted in the presence of metal-free support. TOC and COD removal increased up to 48 – 81 %, which can be ascribed to HTC and adsorption onto the support. Some contribution of the support to HTC may also occur. Krishnan *et al.* [154] showed that graphene oxide accelerated carbonization in HTC of glucose. Higher TOC removal was observed from FLargeAcid feedstock, although with a value more similar to that of blank run. FPhOH and FAromatic feedstocks led to low removal values in the blank experiments, but removal increased substantially in experiments with the support. Interestingly, adsorption onto the support was also found to be high for FPhOH and FAromatic feedstocks.

APR experiments performed with catalyst yielded the highest values of TOC and COD removal (in the range of 74 – 90 %) with most of the feedstocks tested. The FLargeAcid feedstock gave the highest TOC removal, with around 90 %. Significant differences can found respect to FShortAcid, which may be related to lower both adsorption and conversion of short

organic acids under the APR operating conditions [122]. However, the contribution of the HTC is also much higher in the case of FLargeAcid feedstock as can be seen comparing the results of blank experiments.

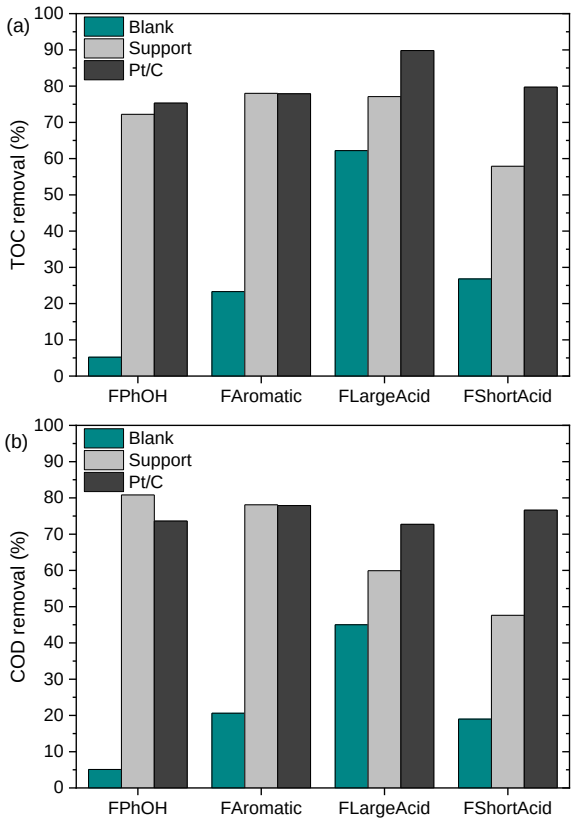

Figure VIII-2. (a) TOC and (b) COD removal in APR experiments with different feedstocks*

*Reaction conditions: 220 ºC, total reaction pressure: 24 – 28 bar, 30 mL of feedstock, 0.6 g of Pt/E250 catalyst, 500 rpm, 4 h.

Table VIII-3 shows the concentration of individual components identified in the feedstock and after the APR experiments. In catalysed runs performed with FPhOH feedstock significant amounts of hydroquinone and catechol were found. These compounds were not observed in blanks and in

the experiments with the bare support, due to different mechanisms for APR and HTC. This can also be observed in the case of the runs performed with FAromatic, where lower amounts of intermediate species were detected in the degradation pathway of catalysed APR. Interestingly, some phenol was detected in the catalysed runs, which can be due to dehydration of hydroquinone or catechol [155,156]. In the catalytic experiments, 84 % of the starting phenol from FPhOH disappeared, and removal of hydroquinone and catechol from FAromatic was as high as 99 % and 94 %, respectively. In general, acetic and formic acids were found as end products of the degradation pathway, even though the mechanism for APR and HTC in the presence of support are different for FPhOH and FAromatic feedstocks.

Runs carried out with feedstocks constituted by organic acids showed high conversion in catalysed experiments. In the case of FLargeAcid, conversion of oxalic, maleic, malonic and fumaric acids was close to 99 %. In the case of FShortAcid feedstock, the values of conversion of oxalic, acetic and formic acids were close to 100, 96 and 88 %, respectively.

Removal of carbon from the liquid phase calculated from the individual compounds in Table VIII-3 is higher than that measured by TOC and displayed in Figure VIII-2. This is due to the complexity of HTC and APR mechanism, leading to a large number of minor species [57,97,133]. The set of compounds selected and shown in Table VIII-3 describe between 50 and 100 % of C in the liquid phase.

Table VIII-3. Composition of the aqueous phase in blank and catalysed APR experiments with different feedstocks

Feedstock	Run	Compounds (mg / L)								
		Phenol	Hydroquinone	Catechol	Oxalic	Maleic	Malonic	Fumaric	Acetic	Formic
FPhOH	Initial	102.0	-	-	-	-	-	-	-	-
	Blank	81.5	-	-	0.4	-	-	-	4.8	0.7
	Support	26.0	-	-	0.1	-	4.5	-	1.4	-
	Pt/C	16.0	3.3	0.8	0.3	-	-	-	2.5	0.5
FAromatic	Initial	-	57.5	58.0	-	-	-	-	-	-
	Blank	-	19.8	26.3	0.4	1.3	-	-	6.9	5.3
	Support	-	2.2	5.6	0.5	0.4	4.4	-	12.8	3.7
	Pt/C	10.9	0.3	3.3	0.1	-	-	-	0.9	0.6
FLargeAcid	Initial	-	-	-	112.5	68.5	20.4	13.4	-	-
	Blank	-	-	-	0.3	0.7	9.5	1.0	23.4	6.5
	Support	-	-	-	0.4	-	9.6	-	13.5	2.3
	Pt/C	-	-	-	0.2	-	-	-	2.1	0.8
FShortAcid	Initial	-	-	-	75.7	-	-	-	97.2	54.3
	Blank	-	-	-	0.3	-	-	-	97.0	11.3
	Support	-	-	-	1.5	-	-	-	75.3	0.6
	Pt/C	-	-	-	0.2	-	-	-	4.4	6.3

*Reaction conditions: 220 ºC, total reaction pressure: 24 – 28 bar, 30 mL of feedstock, 0.6 g of Pt/E250 catalyst, 500 rpm, 4 h.

Figure VIII-3 shows the values obtained for *CC gas* in APR runs with the different feedstocks tested. The blank runs and those with the bare support did not show important differences, giving rise to *CC gas* in the 6 – 40 % range, the highest values corresponding to the FLargeAcid feedstock. The runs performed with catalyst yielded higher *CC gas*, but also within a wide range (21 – 74 %). The FShortAcid feedstock gave significantly higher *CC gas*. Phenol, as well as hydroquinone and catechol, gave always significantly poorer values than carboxylic acids in terms of gas yield. The differences are higher than the observed for the removal of TOC and individual compounds from the feedstocks.

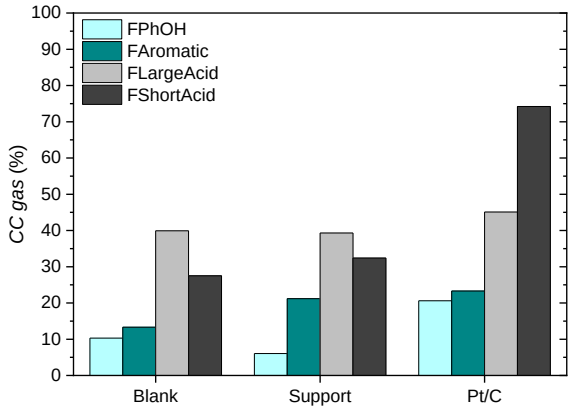

Figure VIII-3. *CC gas* obtained in APR runs with different feedstocks*

*Reaction conditions: 220 ºC, total reaction pressure: 24 – 28 bar, 30 mL of feedstock, 0.6 g of Pt/E250 catalyst, 500 rpm, 4 h.

Table VIII-4 shows gas production, gas composition and Y_{CH4} from the APR experiments with the feedstocks tested. Consequently with previous *CC gas* results, the use of catalyst increased the gas volume produced. The percentage of H_2 in the gas fraction was low in all the experiments (0 to 1.7 %). When compared to results obtained from APR of other substances such as glycerol [23,157] or brewery wastewater (Chapter VI), the H_2 production

was certainly poor. CO_2 was the major component of the gas even in the catalytic APR experiments. Using carboxylic acids feedstocks, the percentage of CO_2 in the gas decreased significantly in favour of alkanes in the catalytic runs, being CH_4 the main alkane component, so that the Y_{CH4} increased substantially upon catalytic APR with those feedstocks. On the opposite, phenol, catechol and hydroquinone yielded essentially CO_2, indicating that with those phenolics HTC is by far the prevailing route, being very low the contribution of reforming. Condensation reactions of phenolic compounds on the surface of the carbon support would mean an additional competing pathway in phenol degradation [158].

Table VIII-4. Gas production and composition from APR runs of different feedstocks*

Runs	Feedstock	Gas Volume (mL)	Gas composition (% mol)			Y_{CH4} (mmol CH_4 / g TOC_i)
			H_2	CO_2	Alkanes	
Blank	FPhOH	0.4	0.1	91.3	8.6	0.6
Blank	FAromatic	0.6	1.1	98.4	0.6	0.1
Blank	FLargeAcid	1.8	0.2	98.9	0.9	0.2
Blank	FShortAcid	1.2	0.6	99.1	0.2	< 0.1
Support	FPhOH	0.3	0.4	96.4	3.2	0.1
Support	FAromatic	0.9	0.3	98.9	0.8	0.1
Support	FLargeAcid	1.8	0.9	96.0	3.1	1.0
Support	FShortAcid	1.5	0.2	99.4	0.4	0.1
Pt/C	FPhOH	0.9	1.7	96.4	2.0	0.3
Pt/C	FAromatic	1.0	0.5	96.7	2.7	0.5
Pt/C	FLargeAcid	2.0	0.4	72.9	26.7	8.4
Pt/C	FShortAcid	3.4	< 0.1	71.0	28.9	17.8

*Reaction conditions: 220 ºC, total reaction pressure: 24 – 28 bar, 30 mL of feedstock, 0.6 g of Pt/E250 catalyst, 500 rpm, 4 h.

1.3.3. APR of mixed feedstocks

Figure VIII-4 shows the experimental results of TOC and COD removal upon APR of mixed feedstocks (see Table VIII-2). For the sake of

comparison, the corresponding values calculated from the previous results obtained with the individual feedstocks are also included in the Figure VIII-4. As can be seen, in general, the experimental values were better than the expected, particularly in the cases of M-1 and M-3 mixtures, suggesting some synergistic effect of hydroquinone and catechol. This could be ascribed to the formation of semiquinone free radicals produced by the thermal decomposition of hydroquinone and/or catechol [159].

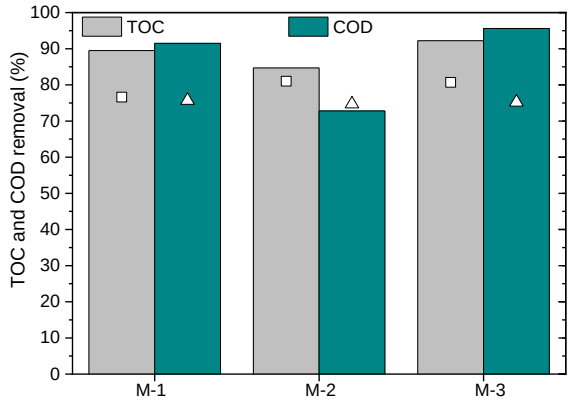

Figure VIII-4. TOC and COD removal upon APR runs of mixed feedstocks with Pt/C catalyst. Symbols correspond to the calculated values from the results with individual compounds (Figure VIII-2)*

*Reaction conditions: 220 ºC, total reaction pressure: 24 – 28 bar, 30 mL of mixed feedstock, 0.6 g of Pt/E250 catalyst, 500 rpm, 4 h.

Table VIII-5 shows the initial and final concentration of compounds in the liquid phase for the experiments of Figure VIII-4. All compounds showed high conversion values (between 87 and 100 %), except malonic acid. In the runs performed with mixtures containing malonic acid (M-2 and M-3), a low conversion of this compound was observed (7 – 22 %), opposite to what can be observed with the FLargeAcid feedstock, where the final concentration of the species was negligible, despite its higher initial concentration. The identified compounds represent 48 and 35 % of C

remaining in the liquid phase for mixtures M-1 and M-2, respectively, while for mixture M-3, they represent 85 %.

Table VIII-5. Initial and final composition of the aqueous phase in APR of feedstock mixtures with Pt/C catalyst*

Mixture	Run	Compounds (mg / L)								
		Phenol	Hydroquinone	Catechol	Oxalic	Maleic	Malonic	Fumaric	Acetic	Formic
M-1	Initial	53.4	32.5	32.1	-	-	-	-	-	-
	Pt/C	1.9	0.2	0.5	0.2	3.9	-	-	2.5	0.2
M-2	Initial	33.4	-	-	62.8	21.3	6.8	4.3	35.0	18.2
	Pt/C	0.6	0.2	0.4	0.8	-	6.3	-	1.5	0.3
M-3	Initial	25.4	19.0	16.0	48.3	15.8	4.9	3.3	25.4	13.3
	Pt/C	3.3	1.0	0.3	0.2	-	3.8	0.2	-	-

*Reaction conditions: 220 ºC, total reaction pressure: 24 – 28 bar, 30 mL of mixed feedstock, 0.6 g of Pt/E250 catalyst, 500 rpm, 4 h.

Table VIII-6 shows the comparison between gas production, gas fraction composition, *CC gas* and Y_{CH4} obtained upon APR of mixed feedstocks with Pt/C catalyst. *CC gas* values were in a range from 32 to 66 %, being the highest values those obtained with M-2 and M-3 mixtures. Small differences were found between gas composition and the corresponding results calculated from the behaviour of the individual feedstocks. The highest Y_{CH4} was achieved for M-2 mixture (11.0 mmol CH_4 / g TOC_i), which contained the highest concentration of organic acids, while Y_{H2} was very low in all cases (< 0.2 mmol H_2 / g TOC_i).

Table VIII-6. Gas production and composition from APR of mixed feedstocks with Pt/C catalyst*

Run	Mixture	Gas Volume (mL)	Gas composition (% mol)			*CC gas* (%)	Y_{CH4} (mmol CH_4 / g TOC_i)
			H_2	CO_2	Alkanes		
Pt/C	M-1 Exp.	1.4	0.4	96.2	3.4	32.2	0.9
Pt/C	M-1 Calc.	1.0	1.1	96.5	2.4	21.9	0.4
Pt/C	M-2 Exp.	2.9	0.3	76.4	23.3	65.7	11.0
Pt/C	M-2 Calc.	2.1	0.7	80.1	19.2	46.6	8.9
Pt/C	M-3 Exp.	2.2	0.2	85.6	14.2	51.1	5.0
Pt/C	M-3 Calc.	1.8	0.7	84.2	15.1	40.8	6.8

*Reaction conditions: 220 ºC, total reaction pressure: 24 – 28 bar, 30 mL of mixed feedstock, 0.6 g of Pt/E250 catalyst, 500 rpm, 4 h.

1.3.4. Coupling of APR and CWAO

Looking at the poor results of APR of aromatic compounds, giving rise to gases containing CO_2 as the major component versus the significantly better ones from carboxylic acids feedstocks, a new approach was tested. This consists in submitting the phenolic feedstock to CWAO before the catalytic APR step. The previous CWAO allows oxidation of phenol into carboxylic acids and can be carried out to a limited extension, so that phenol and the aromatic intermediates are reduced to low concentrations but maintaining

high TOC for subsequent reforming where the carboxylic acids can be converted into H_2 and CH_4.

Figure VIII-5 shows TOC and COD removal upon coupled CWAO-APR of FPhOH feedstock with Pt/C catalyst. TOC and COD removal decreased from around 74 % in direct APR of FPhOH to 53 and 31 %, respectively, for APR of CWAO feedstock. However, considering the total removal of the process, CWAO-APR, the removal was similar (average of 72 %).

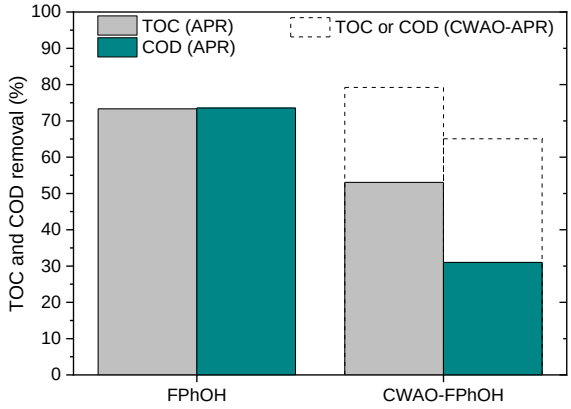

Figure VIII-5. TOC and COD removal in APR and CWAO-APR of FPhOH with Pt/C catalyst*

*Reaction conditions: CWAO: 220 ºC, 20 bar, 30 mL of feedstock, 0.05 g of Pt/Al2O3, 500 rpm, 4 h. APR: 220 ºC, total reaction pressure: 24 – 28 bar, 30 mL of feedstock, 0.6 g of Pt/E250 catalyst, 500 rpm, 4 h.

Table VIII-7 shows the concentration of main components in the liquid phase resulting from CWAO and from CWAO-APR of FPhOH. About 100 % of the carbon remaining in the liquid phase after CWAO was identified and the conversion of phenol amounted 39 %. In addition to phenol, oxalic, maleic and formic acids were identified in a very low concentration (< 0.2 mg / L), while the concentration of malonic and acetic acids were

significantly higher. After the subsequent stage (APR), the individual compounds identified were removed by more than 95 %, except malonic acid, whose concentration increased. Catechol, which was not identified in the initial feedstock, was detected after the APR stage. The concentration of the main compounds analysed after the APR stage corresponded only to 27 % of the organic carbon present in the liquid phase, showing that the effluent generated by CWAO-APR of FPhOH is more complex than the resulting from direct APR of FPhOH, where 90 % of organic carbon was identified.

Table VIII-7. Composition of the liquid phase after CWAO and CWAO-APR of FPhOH feedstock with Pt/C catalyst*

Run	Compounds (mg / L)								
	Phenol	Hydroquinone	Catechol	Oxalic	Maleic	Malonic	Fumaric	Acetic	Formic
CWAO	62.5	-	-	0.2	0.1	5.2	-	14.6	0.2
CWAO-APR		-	1.7	-	-	12.8	-	0.8	-

*Reaction conditions: CWAO: 220 ºC, 20 bar, 30 mL of feedstock, 0.05 g of Pt/Al2O3, 500 rpm, 4 h. APR: 220 ºC, total reaction pressure: 24 – 28 bar, 30 mL of feedstock, 0.6 g of Pt/E250 catalyst, 500 rpm, 4 h.

Table VIII-8 shows the comparison between gas production, composition of the gas fraction, *CC gas* and yield to CH_4 obtained by CWAO-APR and direct APR of FPhOH. *CC gas* for CWAO-APR was 100 % higher than for direct APR. Y_{CH4} was also significantly higher, but the percentage of H_2 in the gas fraction and Y_{H2} were not improved.

These results indicate that partial oxidation of feedstocks containing aromatic compounds can be used to improve the performance of the APR process. However, that improvement is only effective to increase the CH_4 yield, since the species generated and the acid medium favour the production of this compound. *CC gas*, gas composition and Y_{CH4} obtained from CWAO-APR of FPhOH were similar to those from the M-2 mixture, consistently with the similitude in composition of the effluent from CWAO of the phenolic feedstock and the M-2 mixture.

Table VIII-8. Gas production and composition from direct APR and CWAO-APR of FPhOH with Pt/C catalysts*

Runs	Gas Volume (mL)	Gas composition (% mol)			*CC gas* (%)	Y_{CH4} (mmol CH_4 / g TOC_i)
		H_2	CO_2	Alkanes		
APR	0.9	1.7	96.4	2.0	20.6	0.3
CWAO-APR	1.6	< 0.1	77.6	22.4	48.3	8.2

*Reaction conditions: CWAO: 220 ºC, 20 bar, 30 mL of feedstock, 0.05 g of Pt/Al2O3, 500 rpm, 4 h. APR: 220 ºC, total reaction pressure: 24 – 28 bar, 30 mL of feedstock, 0.6 g of Pt/E250 catalyst, 500 rpm, 4 h.

1.4. Conclusions

Coupled CWAO-APR was performed as approach to removal and valorisation of phenolics compounds to valuable gases. APR experiments were carried out with different representative compounds of phenol oxidation pathway. APR experiments showed that the high TOC and COD removal could be achieved from FPhOH and FAromatic feedstocks. However, the

production of gases was low evidencing hindered pathways, probably due to competing of HTC. On the contrary, relevant TOC removal and *CC gas* was observed for organic acid feedstocks. CH_4 was the main component in the gas produced and yield to H_2 was very low in all cases. In the experiments with mixtures of feedstocks the TOC and COD removal and *CC gas* were significantly higher than for individual feedstocks, indicating that mixtures favoured APR.

Coupled CWAO-APR of FPhOH feedstock led to a similar TOC and COD removal to direct APR (more than 65 %). In addition, much higher conversion to gases and yield to CH_4 (8.2 mmol CH_4 / g TOC_i) was achieved, although H_2 production remained low. The results show that coupled CWAO-APR process can be a promising approach to remove and valorise phenolics by overcoming low both conversion to gas and production of valuable gases observed in APR of phenol.

Chapter IX. General conclusions

This thesis deals with the treatment and valorisation of wastewater by APR process. In order to verify the flexibility of the process, wastewaters from different types of industries were used, with the focus mainly in H_2 production. In addition, the effect of some process parameters on the catalytic performance were also investigated. The main conclusions of this work are summarized below.

Treatment and valorisation of fish-canning wastewater

- Pt catalysts supported on different carbon materials were proved in the APR of TCW at 200 ºC. TOC and COD removal ranged within 45 – 60 %, which was ascribed to a combination of adsorption on the supports, HTC and APR. The total of gas produced was low in all experiments, probably due to the presence of impurities that lead to catalyst deactivation. The percentage of valuable gases (H_2 and alkanes) reached up 18 % of the gas fraction showing the potential of APR for the valorisation and treatment of wastewater. The use of a catalyst with a basic support significantly increased the production of gases and the H_2 percentage in the gas fraction. Gas production was higher in semi-continuous compared to batch operation, probably because the withdrawn gas displaces the reaction towards the products. The percentage of alkanes in the gas phase decreased upon successive catalyst reuse cycles at the expense of H_2, which was attributed to the decreasing of low-coordinated Pt sites (responsible for methanation) as the size of Pt NPs increased.

Treatment and valorisation of brewery wastewater

- Pt catalysts supported on different carbon materials were tested in the APR of SBW at different temperatures (200 and 225 ºC). The effect of organic load of the wastewater was also evaluated. HTC was observed as main contribution in the experiments without catalyst. The best catalytic performance was observed at higher temperature for catalyst supported on

highly mesoporous carbon blacks with virtually no microporosity and high pH slurry (≈ 50 % of H_2 and 12.2 mmol H_2 / g COD_i). The removal of organic matter decreased at increasing organic load of the wastewater. At the lowest wastewater organic load (1531 mg / L COD_i), TOC and COD removal up 99 % was achieved and the *CC gas* was 93 %, with valuable gases representing more than 70 % of the gas fraction. Some catalyst deactivation was observed after successive reuse cycles, which was attributed to partial blockage of the active Pt sites by carbonaceous deposits.

- RBW and SBW were treated by APR with different Pt/C catalysts. The effect of basicity was evaluated at 220 ºC. The addition of KOH or NaOH to SBW resulted in a slightly lower TOC and COD removal, however higher H_2 yields and percentage of valuable gases were obtained in those cases where KOH was added. Catalyst with basic support and low contribution of micropores showed the best performance in the APR of SBW+KOH (≈ 50 % of H_2 and 8.9 mmol H_2 / g COD_i). Increasing the KOH concentration led to CO_2-free H_2 without significant changes in H_2 yield. The result obtained with RBW were relatively similar to those from SBW, although also suggested that the wastewater composition should be considered for the sake of optimization.

- H_2 production through continuous APR of SBW was studied for its optimisation. The effect of reaction conditions such as *WHSV* and carrier gas flow, and active metal was evaluated, while the temperature and pressure of reactions remained constant (225 ºC and 28 bar). PtRe/C catalyst exhibited higher catalytic activity and H_2 production than Pt/C attributed to an increase in the WGS activity. At lowest *WHSV* (0.03 h^{-1}) the H_2 production was higher due to a longer contact time between the catalyst and the organic matter present in the wastewater. A higher H_2 production was achieved with the increase of the carrier gas flow due to the removal of H_2 from the catalyst surface, which prevents its consumption in side reactions. Despite the

different reaction conditions, the catalysts showed an important deactivation with TOS.

- The catalytic performance and the deactivation of carbon supported Pt and PtRe catalyst in the continuous APR of SBW was evaluated at 225 ºC and 28 bar. A significantly catalyst deactivation was observed in the first hours of reaction for all catalyst systems analysed. H_2 production was improved by the increase of carrier gas flow, coherent with lower H_2 availability for side reactions. At low TOS values Pt catalysts supported on different modified carbons, prepared by impregnation and carbonization of resol resin, showed higher H_2 production than the reference Pt catalyst, indicating that a lower microporosity of the catalysts facilitates the transport of reactants to catalytic active sites and removal of gas products. On the other hand, the results suggested an indirectly effect of the Pt NPs size and the catalyst with mean NPs size closer to 2 nm showed a higher H_2 production. All bimettalic PtRe catalyst showed higher catalytic activity than Pt catalyst although Re addition could favours catalyst deactivation. The characterization of used catalyst revealed that the main cause of the pronounced catalyst deactivation in the first hours of reaction was the coke deposition on the catalyst surface.

- H_2 production by coupling the hydrogenation and continuous APR of maltose (main compound of brewery wastewater) was studied. The APR experiments of maltose and maltitol (main compound obtained in the hydrogenation of maltose) were performed at different temperatures (175, 200 and 225 ºC) and initial feedstock concentrations (1 and 2.5 wt. %) keeping the pressure constant (30 bar). The conversion of initial feedstock and, consequently, the *CC gas*, as well as the selectivity to alkanes were higher in the APR of maltose, however higher H_2 selectivity and yield were achieved in the APR of maltitol. In the liquid phase, at same temperature and similar conversion level, higher yields of liquids products were obtained in

the APR of maltose. The overall process was considered efficient since H_2 production compensated for the need for hydrogenation and the durability of the catalyst increased, due to the reducing of the formation of carbonaceous deposits. Finally, a relevant catalyst deactivation occurred when SBW was used in APR experiments, indicating that minority compound, such as protein fraction from malt or yeast, should contribute in a higher extent to catalyst deactivation.

Treatment and valorisation of fruit juice wastewater

- The treatment and valorisation of FJW by APR was analysed using model compounds and FJW as feedstocks with Pt/C catalyst at 220 ºC. The variables considered were pH, organic load and salinity. Organic carbon removal was higher in the reforming of glucose and fructose within 7 – 10 pH range, while for organic acids and FJW a higher removal was obtained at pH 2. H_2 yield and selectivity increased at increasing pH, due to better conditions for WGS reaction and abstraction of CO_2. H_2 production by APR of FJW was little affected by pH, yielding around 6.6 mmol H_2 / g COD_i, in the pH range tested. A wide operation window was observed regarding organic load of FJW, although organic carbon removal declined slightly at the highest loads tested. A decreased of H_2 yield from 7.8 to 4.2 mmol H_2 / g COD_i was observed at high salinity, due to catalyst deactivation. Despite this, APR was considered a flexible method for the treatment and valorisation of FJW within a wide operation window regarding pH, organic load and salinity.

Treatment and valorisation of wastewater with phenolic compounds

- CWAO coupled to APR was investigated as an approach to remove phenolic compounds, converting them into valuable gases. Partial oxidation was achieved in the CWAO stage trying to minimize mineralization so to allow a high yield to gases in the subsequent APR stage. APR runs were

carried out with individual compounds representative of phenol oxidation pathway, and mixtures of them, to learn on the corresponding contribution of those individual compounds. A range of TOC and COD removal (74 – 90 %) was observed for the individual compounds, with higher values for long chain acids. H_2 production was low in all cases, due to competing direct conversion of long and short chain acids into CH_4. The highest yield to CH_4 (11.0 mmol CH_4 / g TOC_i) was achieved for APR of mixtures rich in acids. CWAO-APR resulted in a similar TOC and COD removal and higher *CC gas* and CH_4 yield than direct APR, indicating that coupled CWAO-APR can overcome the low conversion and gas production observed in direct APR of phenol.

Chapter IX. Conclusiones generales

Esta tesis trata sobre el tratamiento y valorización de aguas residuales mediante el proceso de APR. Con el objetivo de verificar la flexibilidad del proceso, se utilizaron aguas residuales de diferentes tipos de industrias, centrándose principalmente en la producción de H_2. Además, también se investigó el efecto de algunos parámetros de proceso sobre el rendimiento catalítico. Las principales conclusiones generadas en este trabajo se resumen a continuación.

Tratamiento y valorización de aguas residuales de conservas de pescado

- Se utilizaron catalizadores de Pt soportados en diferentes materiales de carbono en el APR de TCW a 200 ºC. La eliminación de TOC y COD varió entre 45 – 60 %, lo que se atribuyó a la combinación de la adsorción en los soportes, HTC y APR. El total de gases producidos fue bajo en todos los experimentos, probablemente debido a la presencia de impurezas que llevan a la desactivación del catalizador, como por ejemplo cloruros. El porcentaje de gases valiosos (H_2 y alcanos) alcanzó el 18 % de la fracción gaseosa mostrando el potencial del APR para la valorización y tratamiento de aguas residuales. El uso de un catalizador con un soporte de carácter básico aumentó significativamente la producción de gases y el porcentaje de H_2 en la fracción gaseosa. La producción de gases fue mayor en modo semi-continuo en comparación con el modo discontinuo, probablemente porque el gas retirado desplaza la reacción hacia los productos. El porcentaje de alcanos en la fase gaseosa disminuyó en ciclos sucesivos de reutilización del catalizador a expensas del H_2, lo que se atribuyó a la disminución de los centros activos Pt de baja coordinación (responsables de la metanación) a medida que aumentaba el tamaño de las NPs de Pt.

Tratamiento y valorización de aguas residuales de cerveceras

- Los catalizadores de Pt soportados en diferentes materiales de carbono fueron probados en el APR de SBW a diferentes temperaturas (200 y 225 ºC). También se evaluó el efecto de la carga orgánica de las aguas residuales. Se observó como la HTC tienen una contribución principal en los experimentos sin catalizador. El mejor rendimiento catalítico se observó a una temperatura más alta para el catalizador soportado en negro de humo altamente mesoporoso, prácticamente sin microporosidad y pH slurry alto (≈ 50 % de H_2 y 12,2 mmol H_2 / g COD_i). La eliminación de materia orgánica disminuyó al aumentar la carga orgánica de las aguas residuales. Con la carga orgánica más baja, se logró una eliminación de TOC y COD de hasta el 99 % y la *CC gas* fue del 93 %, con gases valiosos que representan más del 70 % de la fracción de gas. Se observó cierta desactivación del catalizador después de ciclos sucesivos de reutilización, lo que se atribuyó al bloqueo parcial de los sitios activos de Pt por depósitos carbonosos.

- Se trataron RBW y SBW por APR con diferentes catalizadores de Pt/C. El efecto de basicidad se evaluó a 220 ºC. La adición de KOH o NaOH a SBW resultó en una eliminación de TOC y DQO ligeramente menor, sin embargo, se obtuvieron mayores rendimientos de H_2 y porcentaje de gases valiosos en los casos en que se agregó KOH. El catalizador con soporte básico y baja contribución de microporos mostró el mejor rendimiento en la APR de SBW + KOH (≈ 50% de H_2 y 8,9 mmol H_2 / g COD_i). El aumento de la concentración de KOH condujo a una producción de H_2 sin CO_2 y sin cambios significativos en el rendimiento de H_2. Los resultados obtenidos con RBW fueron relativamente similares a los de SBW, aunque también sugirieron que la composición de las aguas residuales se debe considerar en aras de la optimización.

- Se estudió la producción de H_2 mediante el APR continuo de SBW para su optimización. Se evaluó el efecto de las condiciones de reacción tales como *WHSV* y el caudal de gas portador, y el metal activo, mientras que

la temperatura y la presión de las reacciones se mantuvieron constantes (225 ºC y 28 bar). El catalizador PtRe/C mostró mayor actividad catalítica y producción de H_2 que el Pt/C, atribuido a un aumento en la actividad de la reacción de WGS. Con el *WHSV* más bajo (0,03 h^{-1}) la producción de H_2 fue mayor debido a un mayor tiempo de contacto entre el catalizador y la materia orgánica presente en las aguas residuales. También se logró una mayor producción de H_2 con el aumento del flujo de gas portador debido a la eliminación de H_2 de la superficie del catalizador, lo que evita su consumo en reacciones secundarias. A pesar de las diferentes condiciones de reacción, los catalizadores mostraron una desactivación importante con el TOS.

- El rendimiento catalítico y la desactivación de los catalizadores Pt y PtRe soportados en carbono en el APR continuo de SBW se evaluó a 225 ºC y 28 bar. Se observó una desactivación significativa del catalizador en las primeras horas de reacción para todos los sistemas catalizadores analizados. La producción de H_2 fue mejorada por el aumento del flujo de gas portador, coherente con una menor disponibilidad de H_2 para reacciones secundarias. A valores bajos de TOS, los catalizadores de Pt soportados en diferentes carbonos modificados, preparados por impregnación y carbonización de resina resol, mostraron una mayor producción de H_2 que el catalizador de Pt de referencia, lo que indica que una menor microporosidad de los catalizadores facilita el transporte de reactivos a los sitios activos catalíticos y la eliminación de los gases producidos. Por otro lado, los resultados sugirieron un efecto indirecto del tamaño de las NPs de Pt; así el catalizador con un tamaño medio de NPs más cercano a 2 nm mostró una mayor producción de H_2. Todos los catalizadores bimetálicos (PtRe) mostraron una mayor actividad catalítica que el catalizador Pt, aunque la adición de Re parece favorecer la desactivación del catalizador. La caracterización del catalizador usado reveló que la causa principal de la desactivación pronunciada del catalizador en las primeras horas de reacción fue la deposición de coque en su superficie.

- Se estudió la producción de H_2 mediante el acoplamiento de la hidrogenación y el APR continuo de maltosa (principal compuesto de las aguas residuales de cerveceras). Los experimentos de APR de maltosa y maltitol (principal compuesto obtenido en la hidrogenación de maltosa) se realizaron a diferentes temperaturas (175, 200 y 225 ºC) y concentraciones iniciales de materia prima (1 y 2,5% en peso) manteniendo la presión constante (30 bar). La conversión de la materia prima inicial y, en consecuencia, la *CC gas*, así como la selectividad a alcanos fueron mayores en la APR de maltosa, sin embargo, se logró una mayor selectividad y rendimiento de H_2 en el APR de maltitol. En la fase líquida, a la misma temperatura y un nivel de conversión similar, se obtuvieron mayores rendimientos de productos líquidos en el APR de maltosa. El proceso general se consideró eficiente ya que la producción de H_2 compensó la necesidad de hidrogenación y aumentó la durabilidad del catalizador, debido a la reducción de la formación de depósitos carbonosos. Finalmente, se produjo una desactivación del catalizador relevante cuando se usó SBW en los experimentos de APR, lo que indica que compuestos minoritarios, como la fracción de proteína de malta o levadura, parecen contribuir en mayor medida a la desactivación del catalizador.

Tratamiento y valorización de aguas residuales de zumos de frutas

- El tratamiento y la valorización de FJW por APR se analizaron utilizando compuestos modelo y FJW como materias primas con un catalizador de Pt/C a 220 ºC. Las variables consideradas fueron pH, carga orgánica y salinidad. La eliminación de carbono orgánico fue mayor en el reformado de glucosa y fructosa dentro del intervalo de pH 7 – 10, mientras que para los ácidos orgánicos y FJW se obtuvo una mayor eliminación a pH 2. El rendimiento y la selectividad de H_2 aumentaron al aumentar el pH, debido a mejores condiciones para la reacción de WGS y abstracción de CO_2.

La producción de H_2 por APR de FJW se vio poco afectada por el pH, produciendo alrededor de 6,6 mmol de H_2 / g COD_i, en el intervalo de pH estudiado. Se observó una amplia ventana de operación con respecto a la carga orgánica de FJW, aunque la eliminación de carbono orgánico disminuyó ligeramente en las cargas más altas probadas. Se observó una disminución del rendimiento de H_2 de 7,8 a 4,2 mmol de H_2 / g de COD_i a alta salinidad, debido a la desactivación del catalizador. A pesar de esto, el APR se consideró un método flexible para el tratamiento y la valorización de FJW dentro de una amplia ventana de operación con respecto al pH, la carga orgánica y la salinidad.

Tratamiento y valorización de aguas residuales con compuestos fenólicos.

- Se estudió la CWAO acoplada al APR como un enfoque innovador para eliminar compuestos fenólicos convirtiéndolos en gases valiosos. La oxidación parcial se logró en la etapa CWAO tratando de minimizar la mineralización para permitir un alto rendimiento a gases en la etapa de APR posterior. Los experimentos de APR se llevaron a cabo con compuestos individuales representativos de la ruta de oxidación de fenol, y con mezclas de ellos, para conocer la contribución correspondiente de esos compuestos individuales. Se observó una alta eliminación de TOC y COD (74 – 90 %) para los compuestos individuales, con valores más altos para los ácidos de cadena larga. La producción de H_2 fue baja en todos los casos, debido a la conversión directa competitiva a CH_4 de los ácidos cadena larga y corta. El mayor rendimiento de CH_4 (11,0 mmol de CH_4 / g TOC_i) se logró para el APR de mezclas ricas en ácidos. El acoplamiento CWAO-APR resultó en una eliminación similar de TOC y COD y mayores *CC gas* y rendimiento de CH_4 que la APR directa, lo que indica que dicho acoplamiento puede superar la baja conversión y producción de gas observada en el APR directa de fenol.

References

[1] Kirchherr, J., Reike, D., Hekkert, M., **Conceptualizing the circular economy: An analysis of 114 definitions**, Resour. Conserv. Recycl. 127 (2017) 221–232. doi:10.1016/J.RESCONREC.2017.09.005.

[2] Momirlan, M., Veziroglu, T.N., **The properties of hydrogen as fuel tomorrow in sustainable energy system for a cleaner planet**, Int. J. Hydrogen Energy. 30 (2005) 795–802. doi:10.1016/J.IJHYDENE.2004.10.011.

[3] Marchenko, O.V., Solomin, S.V., **The future energy: Hydrogen versus electricity**, Int. J. Hydrogen Energy. 40 (2015) 3801–3805. doi:10.1016/J.IJHYDENE.2015.01.132.

[4] Balat, H., Kırtay, E., **Hydrogen from biomass – Present scenario and future prospects**, Int. J. Hydrogen Energy. 35 (2010) 7416–7426. doi:10.1016/J.IJHYDENE.2010.04.137.

[5] Nicoletti, G., Arcuri, N., Nicoletti, G., Bruno, R., **A technical and environmental comparison between hydrogen and some fossil fuels**, Energy Convers. Manag. 89 (2015) 205–213. doi:10.1016/J.ENCONMAN.2014.09.057.

[6] Logan, B.E., **Biologically extracting energy from wastewater: Biohydrogen production and microbial fuel cells**, Environ. Sci. Technol. 38 (2004) 160A-167A.

[7] Kothari, R., Buddhi, D., Sawhney, R.L., **Comparison of environmental and economic aspects of various hydrogen production methods**, Renew. Sustain. Energy Rev. 12 (2008) 553–563. doi:10.1016/J.RSER.2006.07.012.

[8] Cortright, R.D., Davda, R.R., Dumesic, J.A., **Hydrogen from catalytic reforming of biomass-derived hydrocarbons in liquid water**, Nature. 418 (2002) 964–967. doi:10.1038/nature01009.

[9] Davda, R.R., Shabaker, J.W., Huber, G.W., Cortright, R.D., Dumesic, J.A., **A review of catalytic issues and process conditions for renewable hydrogen and alkanes by aqueous-phase reforming of oxygenated hydrocarbons over supported metal catalysts**, Appl. Catal. B Environ. 56 (2005) 171–186. doi:10.1016/j.apcatb.2004.04.027.

[10] Martín, M., Grossmann, I.E., **Optimal simultaneous production of hydrogen and liquid fuels from glycerol: Integrating the use of biodiesel byproducts**, Ind. Eng. Chem. Res. 53 (2014) 7730–7745. doi:10.1021/ie500067d.

[11] Davda, R.R., Shabaker, J.W., Huber, G.W., Cortright, R.D., Dumesic, J.A., **Aqueous-phase reforming of ethylene glycol on silica-supported metal catalysts**, Appl. Catal. B Environ. 43 (2003) 13–26. doi:10.1016/S0926-

3373(02)00277-1.

[12] Wen, G., Xu, Y., Ma, H., Xu, Z., Tian, Z., **Production of hydrogen by aqueous-phase reforming of glycerol**, Int. J. Hydrogen Energy. 33 (2008) 6657–6666. doi:10.1016/j.ijhydene.2008.07.072.

[13] Wei, Y., Lei, H., Liu, Y., Wang, L., Zhu, L., Zhang, X., Yadavalli, G., Ahring, B., Chen, S., **Renewable hydrogen produced from different renewable feedstock by aqueous-phase reforming process**, J. Sustain. Bioenergy Syst. 4 (2014) 113–127. doi:10.4236/jsbs.2014.42011.

[14] Kirilin, A. V., Tokarev, A. V., Kustov, L.M., Salmi, T., Mikkola, J.-P., Murzin, D.Y., **Aqueous phase reforming of xylitol and sorbitol: Comparison and influence of substrate structure**, Appl. Catal. A Gen. 435–436 (2012) 172–180. doi:10.1016/j.apcata.2012.05.050.

[15] Sladkovskiy, D.A., Godina, L.I., Semikina, K. V., Sladkovskaya, E. V., Smirnova, D.A., Murzin, D.Y., **Process design and techno-economical analysis of hydrogen production by aqueous phase reforming of sorbitol**, Chem. Eng. Res. Des. 134 (2018) 104–116. doi:10.1016/j.cherd.2018.03.041.

[16] Iriondo, A., Cambra, J.F., Barrio, V.L., Guemez, M.B., Arias, P.L., Sanchez-Sanchez, M.C., Navarro, R.M., Fierro, J.L.G., **Glycerol liquid phase conversion over monometallic and bimetallic catalysts: Effect of metal, support type and reaction temperatures**, Appl. Catal. B Environ. 106 (2011) 83–93. doi:10.1016/j.apcatb.2011.05.009.

[17] Coronado, I., Stekrova, M., Reinikainen, M., Simell, P., Lefferts, L., Lehtonen, J., **A review of catalytic aqueous-phase reforming of oxygenated hydrocarbons derived from biorefinery water fractions**, Int. J. Hydrogen Energy. 41 (2016) 11003–11032. doi:10.1016/j.ijhydene.2016.05.032.

[18] El Doukkali, M., Iriondo, A., Cambra, J.F.F., Jalowiecki-Duhamel, L., Mamede, A.S.S., Dumeignil, F., Arias, P.L.L., **Pt monometallic and bimetallic catalysts prepared by acid sol-gel method for liquid phase reforming of bioglycerol**, J. Mol. Catal. A Chem. 368–369 (2013) 125–136. doi:10.1016/j.molcata.2012.12.006.

[19] Godina, L.I., Kirilin, A. V., Tokarev, A. V., Simakova, I.L., Murzin, D.Y., **Sibunit-supported mono- and bimetallic catalysts used in aqueous-phase reforming of xylitol**, Ind. Eng. Chem. Res. 57 (2018) 2050–2067. doi:10.1021/acs.iecr.7b04937.

[20] Huber, G.W., Shabaker, J.W., Evans, S.T., Dumesic, J.A., **Aqueous-phase reforming of ethylene glycol over supported Pt and Pd bimetallic catalysts**, Appl. Catal. B Environ. 62 (2006) 226–235. doi:10.1016/j.apcatb.2005.07.010.

[21] Kaya, B., Irmak, S., Hasanoglu, A., Erbatur, O., **Developing Pt based bimetallic and trimetallic carbon supported catalysts for aqueous-phase**

reforming of biomass-derived compounds, Int. J. Hydrogen Energy. 40 (2015) 3849–3858. doi:10.1016/j.ijhydene.2015.01.131.

[22] He, C., Zheng, J., Wang, K., Lin, H., Wang, J.-Y., Yang, Y., **Sorption enhanced aqueous phase reforming of glycerol for hydrogen production over Pt-Ni supported on multi-walled carbon nanotubes**, Appl. Catal. B Environ. 162 (2015) 401–411. doi:10.1016/j.apcatb.2014.07.012.

[23] Ciftci, A., Ligthart, D.A.J.M., Hensen, E.J.M., **Aqueous phase reforming of glycerol over Re-promoted Pt and Rh catalysts**, Green Chem. 16 (2014) 853–863. doi:10.1039/C3GC42046A.

[24] Kim, T.-W., Kim, H.-D., Jeong, K.-E., Chae, H.-J., Jeong, S.-Y., Lee, C.-H., Kim, C.-U., **Catalytic production of hydrogen through aqueous-phase reforming over platinum/ordered mesoporous carbon catalysts**, Green Chem. 13 (2011) 1718–1728. doi:10.1039/c1gc15235a.

[25] Jeong, K.E., Kim, H.D., Kim, T.W., Kim, J.W., Chae, H.J., Jeong, S.Y., Kim, C.U., **Hydrogen production by aqueous phase reforming of polyols over nano- and micro-sized mesoporous carbon supported platinum catalysts**, Catal. Today. 232 (2014) 151–157. doi:10.1016/j.cattod.2014.02.005.

[26] Lehnert, K., Claus, P., **Influence of Pt particle size and support type on the aqueous-phase reforming of glycerol**, Catal. Commun. 9 (2008) 2543–2546. doi:10.1016/j.catcom.2008.07.002.

[27] Chen, A., Chen, P., Cao, D., Lou, H., **Aqueous-phase reforming of the low-boiling fraction of bio-oil for hydrogen production: The size effect of Pt/Al_2O_3**, Int. J. Hydrogen Energy. 40 (2015) 14798–14805. doi:10.1016/j.ijhydene.2015.09.030.

[28] Ciftci, A., Michel, D.A.J., Hensen, E.J.M., **Influence of Pt particle size and Re addition by catalytic reduction on aqueous phase reforming of glycerol for carbon-supported Pt(Re) catalysts**, Appl. Catal. B Environ. 174–175 (2015) 126–135. doi:10.1016/j.apcatb.2015.02.027.

[29] Callison, J., Subramanian, N.D., Rogers, S.M., Chutia, A., Gianolio, D., Catlow, C.R.A., Wells, P.P., Dimitratos, N., **Directed aqueous-phase reforming of glycerol through tailored platinum nanoparticles**, Appl. Catal. B Environ. 238 (2018) 618–628. doi:10.1016/J.APCATB.2018.07.008.

[30] Duarte, H.A., Sad, M.E., Apesteguía, C.R., **Bio-hydrogen production by APR of C2 -C6 polyols on Pt/Al_2O_3: Dependence of H_2 productivity on metal content**, Catal. Today. 296 (2017) 59–65. doi:10.1016/j.cattod.2017.04.067.

[31] Stekrova, M., Rinta-Paavola, A., Karinen, R., **Hydrogen production via aqueous-phase reforming of methanol over nickel modified Ce, Zr and La oxide supports**, Catal. Today. 304 (2018) 143–152. doi:10.1016/J.CATTOD.2017.08.030.

[32] Guo, Y., Azmat, M.U., Liu, X., Wang, Y., Lu, G., **Effect of support's basic properties on hydrogen production in aqueous-phase reforming of glycerol and correlation between WGS and APR**, Appl. Energy. 92 (2012) 218–223. doi:10.1016/j.apenergy.2011.10.020.

[33] Wang, X., Li, N., Zhang, Z., Wang, C., Pfefferle, L.D., Haller, G.L., **High-yield hydrogen production from aqueous phase reforming over single-walled carbon nanotube supported catalysts**, ACS Catal. 2 (2012) 1480–1486. doi:10.1021/cs300274m.

[34] Shabaker, J.W., Davda, R.R., Huber, G.W., Cortright, R.D., Dumesic, J.A., **Aqueous-phase reforming of methanol and ethylene glycol over alumina-supported platinum catalysts**, J. Catal. 215 (2003) 344–352. doi:10.1016/S0021-9517(03)00032-0.

[35] Luo, N., Fu, X., Cao, F., Xiao, T., Edwards, P.P., **Glycerol aqueous phase reforming for hydrogen generation over Pt catalyst – Effect of catalyst composition and reaction conditions**, Fuel. 87 (2008) 3483–3489. doi:10.1016/j.fuel.2008.06.021.

[36] Koichumanova, K., Vikla, A.K.K., de Vlieger, D.J.M., Seshan, K., Mojet, B.L., Lefferts, L., **Towards stable catalysts for aqueous phase conversion of ethylene glycol for renewable hydrogen**, ChemSusChem. 6 (2013) 1717–1723. doi:10.1002/cssc.201300445.

[37] M. Ravenelle, R., R. Copeland, J., Kim, W.-G.G., C. Crittenden, J., Sievers, C., Ravenelle, R.M., Copeland, J.R., Kim, W.-G.G., Crittenden, J.C., Sievers, C., **Structural changes of γ-Al_2O_3-supported catalysts in hot liquid water**, ACS Catal. 1 (2011) 552–561. doi:10.1021/cs1001515.

[38] El Doukkali, M., Iriondo, A., Cambra, J.F., Gandarias, I., Jalowiecki-Duhamel, L., Dumeignil, F., Arias, P.L., **Deactivation study of the Pt and/or Ni-based γ-Al_2O_3 catalysts used in the aqueous phase reforming of glycerol for H_2 production**, Appl. Catal. A Gen. 472 (2014) 80–91. doi:10.1016/j.apcata.2013.12.015.

[39] Liu, F., Okolie, C., Ravenelle, R.M., Crittenden, J.C., Sievers, C., Bruijnincx, P.C.A., Weckhuysen, B.M., **Silica deposition as an approach for improving the hydrothermal stability of an alumina support during glycerol aqueous phase reforming**, Appl. Catal. A Gen. 551 (2018) 13–22. doi:10.1016/J.APCATA.2017.11.025.

[40] Kim, M.C., Kim, T.W., Kim, H.J., Kim, C.U., Bae, J.W., **Aqueous phase reforming of polyols for hydrogen production using supported Pt-Fe bimetallic catalysts**, Renew. Energy. 95 (2016) 396–403. doi:10.1016/j.renene.2016.04.020.

[41] de Vlieger, D.J.M., Lefferts, L., Seshan, K., **Ru decorated carbon nanotubes – a promising catalyst for reforming bio-based acetic acid in the aqueous phase**, Green Chem. 16 (2014) 864–874. doi:10.1039/c3gc41922c.

[42] Chheda, J.N., Huber, G.W., Dumesic, J.A., **Liquid-phase catalytic processing of biomass-derived oxygenated hydrocarbons to fuels and chemicals**, Angew. Chemie - Int. Ed. 46 (2007) 7164–7183. doi:10.1002/anie.200604274.

[43] Tokarev, A. V., Kirilin, A. V., Murzina, E. V., Eränen, K., Kustov, L.M., Murzin, D.Y., Mikkola, J.P., **The role of bio-ethanol in aqueous phase reforming to sustainable hydrogen**, Int. J. Hydrogen Energy. 35 (2010) 12642–12649. doi:10.1016/j.ijhydene.2010.07.118.

[44] Shabaker, J.. W., Huber, G.. W., Dumesic, J.. A., **Aqueous-phase reforming of oxygenated hydrocarbons over Sn-modified Ni catalysts**, J. Catal. 222 (2004) 180–191. doi:10.1016/j.jcat.2003.10.022.

[45] Seretis, A., Tsiakaras, P., **Aqueous phase reforming (APR) of glycerol over platinum supported on Al_2O_3 catalyst**, Renew. Energy. 85 (2016) 1116–1126. doi:10.1016/j.renene.2015.07.068.

[46] Manfro, R.L., da Costa, A.F., Ribeiro, N.F.P., Souza, M.M.V.M., **Hydrogen production by aqueous-phase reforming of glycerol over nickel catalysts supported on CeO_2**, Fuel Process. Technol. 92 (2011) 330–335. doi:10.1016/J.FUPROC.2010.09.024.

[47] Davda, R.R., Dumesic, J.A., **Renewable hydrogen by aqueous-phase reforming of glucose**, Chem. Commun. 10 (2004) 36–37. doi:10.1002/anie.200353050.

[48] Boga, D.A., Liu, F., Bruijnincx, P.C.A., Weckhuysen, B.M., **Aqueous-phase reforming of crude glycerol: effect of impurities on hydrogen production**, Catal. Sci. Technol. 6 (2016) 134–143. doi:10.1039/C4CY01711K.

[49] Remón, J., Ruiz, J., Oliva, M., García, L., Arauzo, J., **Effect of biodiesel-derived impurities (acetic acid, methanol and potassium hydroxide) on the aqueous phase reforming of glycerol**, Chem. Eng. J. 299 (2016) 431–448. doi:10.1016/j.cej.2016.05.018.

[50] Remón, J., Jarauta-Córdoba, C., García, L., Arauzo, J., **Effect of acid (CH_3COOH, H_2SO_4 and H_3PO_4) and basic (KOH and NaOH) impurities on glycerol valorisation by aqueous phase reforming**, Appl. Catal. B Environ. 219 (2017) 362–371. doi:10.1016/j.apcatb.2017.07.068.

[51] Seretis, A., Tsiakaras, P., **Crude bio-glycerol aqueous phase reforming and hydrogenolysis over commercial SiO_2-Al_2O_3 nickel catalyst**, Renew. Energy. 97 (2016) 373–379. doi:10.1016/j.renene.2016.05.085.

[52] Liu, J., Chu, X., Zhu, L., Hu, J., Dai, R., Xie, S., Pei, Y., Yan, S., Qiao, M., Fan, K., **Simultaneous aqueous-phase reforming and KOH carbonation to produce CO_x-free hydrogen in a single reactor**, ChemSusChem. 3 (2010) 803–806. doi:10.1002/cssc.201000093.

[53] Huber, G.W., Cortright, R.D., Dumesic, J.A., **Renewable alkanes by**

aqueous-phase reforming of biomass-derived oxygenates, Angew. Chemie - Int. Ed. 43 (2004) 1549–1551. doi:10.1002/anie.200353050.

[54] King, D.L., Zhang, L., Xia, G., Karim, A.M., Heldebrant, D.J., Wang, X., Peterson, T., Wang, Y., **Aqueous phase reforming of glycerol for hydrogen production over Pt-Re supported on carbon**, Appl. Catal. B Environ. 99 (2010) 206–213. doi:10.1016/j.apcatb.2010.06.021.

[55] Karim, A.M., Howard, C., Roberts, B., Kovarik, L., Zhang, L., King, D.L., Wang, Y., **In situ X-ray absorption fine structure studies on the effect of pH on Pt electronic density during aqueous phase reforming of glycerol**, ACS Catal. 2 (2012) 2387–2394. doi:10.1021/cs3005049.

[56] Pipitone, G., Zoppi, G., Ansaloni, S., Bocchini, S., Deorsola, F.A., Pirone, R., Bensaid, S., **Towards the sustainable hydrogen production by catalytic conversion of C-laden biorefinery aqueous streams**, Chem. Eng. J. 377 (2019) 120677. doi:10.1016/j.cej.2018.12.137.

[57] Kirilin, A. V., Tokarev, A. V., Murzina, E. V., Kustov, L.M., Mikkola, J.P., Murzin, D.Y., **Reaction products and transformations of intermediates in the aqueous-phase reforming of sorbitol**, ChemSusChem. 3 (2010) 708–718. doi:10.1002/cssc.200900254.

[58] Roy, B., Sullivan, H., Leclerc, C.A., **Effect of variable conditions on steam reforming and aqueous phase reforming of n-butanol over Ni/CeO_2 and Ni/Al_2O_3 catalysts**, J. Power Sources. 267 (2014) 280–287. doi:10.1016/j.jpowsour.2014.05.090.

[59] Özgür, D.Ö., Uysal, B.Z., **Hydrogen production by aqueous phase catalytic reforming of glycerine**, Biomass and Bioenergy. 35 (2011) 822–826. doi:10.1016/J.BIOMBIOE.2010.11.012.

[60] Remón, J., Giménez, J.R., Valiente, A., García, L., Arauzo, J., **Production of gaseous and liquid chemicals by aqueous phase reforming of crude glycerol: Influence of operating conditions on the process**, Energy Convers. Manag. 110 (2016) 90–112. doi:10.1016/j.enconman.2015.11.070.

[61] Neira D'Angelo, M.F., Ordomsky, V., Van Der Schaaf, J., Schouten, J.C., Nijhuis, T.A., **Continuous hydrogen stripping during aqueous phase reforming of sorbitol in a washcoated microchannel reactor with a Pt-Ru bimetallic catalyst**, Int. J. Hydrogen Energy. 39 (2014) 18069–18076. doi:10.1016/j.ijhydene.2014.02.167.

[62] Duarte, H.A., Sad, M.E., Apesteguía, C.R., **Production of bio-hydrogen by liquid processing of xylitol on Pt/Al_2O_3 catalysts: Effect of the metal loading**, Int. J. Hydrogen Energy. 42 (2017) 4051–4060. doi:10.1016/J.IJHYDENE.2016.11.119.

[63] Pan, C., Chen, A., Liu, Z., Chen, P., Lou, H., Zheng, X., **Aqueous-phase reforming of the low-boiling fraction of rice husk pyrolyzed bio-oil in the presence of platinum catalyst for hydrogen production**, Bioresour. Technol. 125 (2012) 335–339. doi:10.1016/j.biortech.2012.09.014.

[64] Wen, G., Xu, Y., Xu, Z., Tian, Z., **Direct conversion of cellulose into hydrogen by aqueous-phase reforming process**, Catal. Commun. 11 (2010) 522–526. doi:10.1016/j.catcom.2009.12.008.

[65] Soták, T., Hronec, M., Vávra, I., Dobročka, E., **Sputtering processed tungsten catalysts for aqueous phase reforming of cellulose**, Int. J. Hydrogen Energy. 41 (2016) 21936–21944. doi:10.1016/j.ijhydene.2016.08.183.

[66] Meryemoglu, B., Kaya, B., Irmak, S., Hesenov, A., Erbatur, O., **Comparison of batch aqueous-phase reforming of glycerol and lignocellulosic biomass hydrolysate**, Fuel. 97 (2012) 241–244. doi:10.1016/j.fuel.2012.02.011.

[67] Van Haasterecht, T., Ludding, C.C.I., De Jong, K.P., Bitter, J.H., **Stability and activity of carbon nanofiber-supported catalysts in the aqueous phase reforming of ethylene glycol**, J. Energy Chem. 22 (2013) 257–269. doi:10.1016/S2095-4956(13)60032-7.

[68] Reynoso, A.J., Ayastuy, J.L., Iriarte-Velasco, U., Gutiérrez-Ortiz, M.A., **Cobalt aluminate spinel-derived catalysts for glycerol aqueous phase reforming**, Appl. Catal. B Environ. 239 (2018) 86–101. doi:10.1016/J.APCATB.2018.08.001.

[69] Neira D'Angelo, M.F., Ordomsky, V., van der Schaaf, J., Schouten, J.C., Nijhuis, T.A., **Aqueous phase reforming in a microchannel reactor: the effect of mass transfer on hydrogen selectivity**, Catal. Sci. Technol. 3 (2013) 2834–2842. doi:10.1039/c3cy00577a.

[70] D'Angelo, M.F.N., Ordomsky, V., Schouten, J.C., Van Der Schaaf, J., Nijhuis, T.A., **Carbon-coated ceramic membrane reactor for the production of hydrogen by aqueous-phase reforming of sorbitol**, ChemSusChem. 7 (2014) 2007–2015. doi:10.1002/cssc.201301324.

[71] Irmak, S., Meryemoglu, B., Hasanoglu, A., Erbatur, O., **Does reduced or non-reduced biomass feed produce more gas in aqueous-phase reforming process?**, Fuel. 139 (2015) 160–163. doi:10.1016/J.FUEL.2014.08.028.

[72] Habte Lemji, H., Eckstädt, H., **A pilot scale trickling filter with pebble gravel as media and its performance to remove chemical oxygen demand from synthetic brewery wastewater**, J Zhejiang Univ-Sci B (Biomed & Biotechnol). 14 (2013) 924–933. doi:10.1631/jzus.B1300057.

[73] El-Kamah, H., Tawfik, A., Mahmoud, M., Abdel-Halim, H., **Treatment of high strength wastewater from fruit juice industry using integrated anaerobic/aerobic system**, Desalination. 253 (2010) 158–163. doi:10.1016/J.DESAL.2009.11.013.

[74] Viuda-Martos, M., Fernandez-Lopez, J., Sayas-Barbera, E., Sendra, E., Perez-Alvarez, J.A., **Physicochemical characterization of the orange juice waste water of a citrus by-product**, J. Food Process. Preserv. 35 (2011)

264–271. doi:10.1111/j.1745-4549.2009.00450.x.

[75] González del Campo, A., Cañizares, P., Rodrigo, M.A., Fernández, F.J., Lobato, J., **Microbial fuel cell with an algae-assisted cathode: A preliminary assessment**, J. Power Sources. 242 (2013) 638–645. doi:10.1016/J.JPOWSOUR.2013.05.110.

[76] González del Campo, A., Fernández, F.J., Cañizares, P., Rodrigo, M.A., Pinar, F.J., Lobato, J., **Energy recovery of biogas from juice wastewater through a short high temperature PEMFC stack**, Int. J. Hydrogen Energy. 39 (2014) 6937–6943. doi:10.1016/J.IJHYDENE.2014.02.119.

[77] Zazo, J.A., Casas, J.A., Mohedano, A.F., Gilarranz, M.A., Rodríguez, J.J., **Chemical pathway and kinetics of phenol oxidation by Fenton's reagent**, Environ. Sci. Technol. 39 (2005) 9295–9302. doi:10.1021/es050452h.

[78] Joglekar, H.S., Samant, S.D., Joshi, J.B., **Kinetics of wet air oxidation of phenol and substituted phenols**, Water Res. 25 (1991) 135–145. doi:10.1016/0043-1354(91)90022-I.

[79] Sulman, E.M.M., Grigorev, M.E.E., Doluda, V.Y.Y., Wärnå, J., Matveeva, V.G.G., Salmi, T., Murzin, D.Y.Y., **Maltose hydrogenation over ruthenium nanoparticles impregnated in hypercrosslinked polystyrene**, Chem. Eng. J. 282 (2015) 37–44. https://www.sciencedirect.com/science/article/pii/S1385894715004775 (accessed November 18, 2019).

[80] Lee, D.-K., Kim, D.-S., Kim, T.-H., Lee, Y.-K., Jeong, S.-E., Le, N.T., Cho, M.-J., Henam, S.D., **Deactivation of Pt catalysts during wet oxidation of phenol**, Catal. Today. 154 (2010) 244–249. doi:10.1016/J.CATTOD.2010.03.052.

[81] Zhang, L., Karim, A.M., Engelhard, M.H., Wei, Z., King, D.L., Wang, Y., **Correlation of Pt-Re surface properties with reaction pathways for the aqueous-phase reforming of glycerol**, J. Catal. 287 (2012) 37–43. doi:10.1016/j.jcat.2011.11.015.

[82] Falcone, D.D., Hack, J.H., Klyushin, A.Y., Knop-gericke, A., Schlo, R., Davis, R.J., **Evidence for the bifunctional nature of Pt − Re catalysts for selective glycerol hydrogenolysis**, ACS Catal. 5 (2015) 5679–5695. doi:10.1021/acscatal.5b01371.

[83] Zufía, J., Aurrekoetxea, G., **Integrated Processing of Fish Canning Industry Wastewater**, J. Aquat. Food Prod. Technol. 11 (2002) 303–315. doi:10.1300/J030v11n03_22.

[84] Muthukumaran, S., Baskaran, K., **Organic and nutrient reduction in a fish processing facility – A case study**, Int. Biodeterior. Biodegradation. 85 (2013) 563–570. doi:10.1016/J.IBIOD.2013.03.023.

[85] Lemus, J., Palomar, J., A. Gilarranz, M., J. Rodriguez, J., **On the kinetics of ionic liquid adsorption onto activated carbons from aqueous solution**,

Ind. & Eng. Chem. Res. 52 (2013) 2969–2976. doi:10.1021/ie3028729.

[86] Fang, J., Zhan, L., Ok, Y.S., Gao, B., **Minireview of potential applications of hydrochar derived from hydrothermal carbonization of biomass**, J. Ind. Eng. Chem. 57 (2018) 15–21. doi:10.1016/J.JIEC.2017.08.026.

[87] de Vlieger, D.J.M., Thakur, D.B., Lefferts, L., Seshan, K., **Carbon nanotubes: A promising catalyst support material for supercritical water gasification of biomass waste**, ChemCatChem. 4 (2012) 2068–2074. doi:10.1002/cctc.201200318.

[88] Lu, X., Flora, J.R.V., Berge, N.D., **Influence of process water quality on hydrothermal carbonization of cellulose**, Bioresour. Technol. 154 (2014) 229–239. doi:10.1016/j.biortech.2013.11.069.

[89] He, R., Davda, R.R., Dumesic, J.A., **In situ ATR-IR spectroscopic and reaction kinetics studies of water-gas shift and methanol reforming on Pt/Al_2O_3 catalysts in vapor and liquid phases**, J. Phys. Chem. B. 109 (2005) 2810–2820. doi:10.1021/jp045470k.

[90] Andersson, M.P., Abild-Pedersen, F., Remediakis, I.N., Bligaard, T., Jones, G., Engbæk, J., Lytken, O., Horch, S., Nielsen, J.H., Sehested, J., Rostrup-Nielsen, J.R., Nørskov, J.K., Chorkendorff, I., **Structure sensitivity of the methanation reaction: H_2-induced CO dissociation on nickel surfaces**, J. Catal. 255 (2008) 6–19. doi:10.1016/J.JCAT.2007.12.016.

[91] Mostany, J., Martínez, P., Climent, V., Herrero, E., Feliu, J.M., **Thermodynamic studies of phosphate adsorption on Pt(1 1 1) electrode surfaces in perchloric acid solutions**, Electrochim. Acta. 54 (2009) 5836–5843. doi:10.1016/J.ELECTACTA.2009.05.040.

[92] Heikkinen, O., Pinto, H., Sinha, G., K. Hämäläinen, S., Sainio, J., Öberg, S., R. Briddon, P., S. Foster, A., Lahtinen, J., **Characterization of a hexagonal phosphorus adlayer on Platinum (111)**, J. Phys. Chem. C. 119 (2015) 12291–12297. doi:10.1021/jp5126816.

[93] Simate, G.S., Cluett, J., Iyuke, S.E., Musapatika, E.T., Ndlovu, S., Walubita, L.F., Alvarez, A.E., **The treatment of brewery wastewater for reuse: State of the art**, Desalination. 273 (2011) 235–247. doi:10.1016/j.desal.2011.02.035.

[94] Dennis E. Briggs, Malts and Malting, Thomson Science, London, UK, 1998.

[95] Simsir, H., Eltugral, N., Karagoz, S., **Hydrothermal carbonization for the preparation of hydrochars from glucose, cellulose, chitin, chitosan and wood chips via low-temperature and their characterization**, Bioresour. Technol. 246 (2017) 82–87. doi:10.1016/j.biortech.2017.07.018.

[96] Knežević, D., van Swaaij, W.P.M., Kersten, S.R.A., **Hydrothermal Conversion of Biomass: I, Glucose Conversion in Hot Compressed Water**, Ind. Eng. Chem. Res. 48 (2009) 4731–4743. doi:10.1021/ie801387v.

[97] Funke, A., Ziegler, F., **Hydrothermal carbonization of biomass: A summary and discussion of chemical mechanisms for process engineering**, Biofuels, Bioprod. Biorefining. 4 (2010) 160–177. doi:10.1002/bbb.198.

[98] Quitain, A.T., Faisal, M., Kang, K., Daimon, H., Fujie, K., **Low-molecular-weight carboxylic acids produced from hydrothermal treatment of organic wastes**, J. Hazard. Mater. 93 (2002) 209–220. doi:10.1016/S0304-3894(02)00024-9.

[99] Shabaker, J.W., Dumesic, J.A., **Kinetics of Aqueous-Phase Reforming of Oxygenated Hydrocarbons: Pt/Al_2O_3 and Sn-Modified Ni Catalysts**, Ind. Eng. Chem. Res. 43 (2004) 3105–3112. doi:10.1021/ie049852o.

[100] Joo, S.H., Kwon, K., You, D.J., Pak, C., Chang, H., Kim, J.M., **Preparation of high loading Pt nanoparticles on ordered mesoporous carbon with a controlled Pt size and its effects on oxygen reduction and methanol oxidation reactions**, Electrochim. Acta. 54 (2009) 5746–5753. doi:10.1016/j.electacta.2009.05.022.

[101] Wang, Y.G., Cheng, L., Li, F., Xiong, H.M., Xia, Y.Y., **High electrocatalytic performance of Mn_3O_4/mesoporous carbon composite for oxygen reduction in alkaline solutions**, Chem. Mater. 19 (2007) 2095–2101. doi:10.1021/cm062685t.

[102] Kim, T.W., Park, H.J., Yang, Y.C., Jeong, S.Y., Kim, C.U., **Hydrogen production via the aqueous phase reforming of polyols over three dimensionally mesoporous carbon supported catalysts**, Int. J. Hydrogen Energy. 39 (2014) 11509–11516. doi:10.1016/j.ijhydene.2014.05.106.

[103] Arantes, M.K., Alves, H.J., Sequinel, R., da Silva, E.A., **Treatment of brewery wastewater and its use for biological production of methane and hydrogen**, Int. J. Hydrogen Energy. 42 (2017) 26243–26256. doi:10.1016/j.ijhydene.2017.08.206.

[104] Shi, X.Y., Jin, D.W., Sun, Q.Y., Li, W.W., **Optimization of conditions for hydrogen production from brewery wastewater by anaerobic sludge using desirability function approach**, Renew. Energy. 35 (2010) 1493–1498. doi:10.1016/j.renene.2010.01.003.

[105] Godina, L.I., Tokarev, A. V., Simakova, I.L., Mäki-Arvela, P., Kortesmäki, E., Gläsel, J., Kronberg, L., Etzold, B., Murzin, D.Y., **Aqueous-phase reforming of alcohols with three carbon atoms on carbon-supported Pt**, Catal. Today. 301 (2018) 78–89. doi:10.1016/j.cattod.2017.03.042.

[106] De Vlieger, D.J.M., Mojet, B.L., Lefferts, L., Seshan, K., **Aqueous Phase Reforming of ethylene glycol - Role of intermediates in catalyst performance**, J. Catal. 292 (2012) 239–245. doi:10.1016/j.jcat.2012.05.019.

[107] Xu, Y., Tian, Z., Wen, G., Xu, Z., Qu, W., Lin, L., **Production of CO_x-free hydrogen by alkali enhanced hydrothermal catalytic reforming of biomass-derived alcohols**, Chem. Lett. 35 (2006) 216–217.

doi:10.1246/cl.2006.216.

[108] Poerschmann, J., Weiner, B., Koehler, R., Kopinke, F.D., **Hydrothermal carbonization of glucose, fructose, and xylose - Identification of organic products with medium molecular masses**, ACS Sustain. Chem. Eng. 5 (2017) 6420–6428. doi:10.1021/acssuschemeng.7b00276.

[109] Wang, T., Zhai, Y., Zhu, Y., Li, C., Zeng, G., **A review of the hydrothermal carbonization of biomass waste for hydrochar formation: Process conditions, fundamentals, and physicochemical properties**, Renew. Sustain. Energy Rev. 90 (2018) 223–247. doi:10.1016/J.RSER.2018.03.071.

[110] Pendem, C., Sarkar, B., Siddiqui, N., Konathala, L.N.S., Baskar, C., Bal, R., **K-Promoted Pt-hydrotalcite catalyst for production of H_2 by aqueous phase reforming of glycerol**, ACS Sustain. Chem. Eng. 6 (2018) 2122–2131. doi:10.1021/acssuschemeng.7b03512.

[111] Biller, P., Ross, A.B., **Production of biofuels via hydrothermal conversion**, Handb. Biofuels Prod. (2016) 509–547. doi:10.1016/B978-0-08-100455-5.00017-5.

[112] Ciftci, A., Ligthart, D.A.J.M., Sen, A.O., Van Hoof, A.J.F., Friedrich, H., Hensen, E.J.M., **Pt-Re synergy in aqueous-phase reforming of glycerol and the water-gas shift reaction**, J. Catal. 311 (2014) 88–101. doi:10.1016/j.jcat.2013.11.011.

[113] Kirilin, A. V., Tokarev, A. V., Manyar, H., Hardacre, C., Salmi, T., Mikkola, J.-P., Murzin, D.Y., **Aqueous phase reforming of xylitol over Pt-Re bimetallic catalyst: Effect of the Re addition**, Catal. Today. 223 (2014) 97–107. doi:10.1016/j.cattod.2013.09.020.

[114] Kim, H.D., Park, H.J., Kim, T.W., Jeong, K.E., Chae, H.J., Jeong, S.Y., Lee, C.H., Kim, C.U., **The effect of support and reaction conditions on aqueous phase reforming of polyol over supported Pt-Re bimetallic catalysts**, Catal. Today. 185 (2012) 73–80. doi:10.1016/j.cattod.2011.08.012.

[115] D'Angelo, M.F.N., Ordomsky, V., Paunovic, V., Van Der Schaaf, J., Schouten, J.C., Nijhuis, T.A., **Hydrogen production through aqueous-phase reforming of ethylene glycol in a washcoated microchannel**, ChemSusChem. 6 (2013) 1708–1716. doi:10.1002/cssc.201200974.

[116] Chheda, J.N., Dumesic, J.A., **An overview of dehydration, aldol-condensation and hydrogenation processes for production of liquid alkanes from biomass-derived carbohydrates**, Catal. Today. 123 (2007) 59–70. doi:10.1016/j.cattod.2006.12.006.

[117] Koichumanova, K., Vikla, A.K.K., Cortese, R., Ferrante, F., Seshan, K., Duca, D., Lefferts, L., **In situ ATR-IR studies in aqueous phase reforming of hydroxyacetone on Pt/ZrO_2 and Pt/AlO(OH) catalysts: The role of aldol condensation**, Appl. Catal. B Environ. 232 (2018) 454–463. doi:10.1016/J.APCATB.2018.03.090.

[118] Grabow, L.C., Gokhale, A.A., Evans, S.T., Dumesic, J.A., Mavrikakis, M., **Mechanism of the water gas shift reaction on Pt: First principles, experiments, and microkinetic modeling**, J. Phys. Chem. C. 112 (2008) 4608–4617. doi:10.1021/jp7099702.

[119] Stick, R. V., Williams, S.J., **Carbohydrates: The Essential Molecules of Life**, 2nd Editio, Elsevier (2009). doi:10.1016/B978-0-240-52118-3.X0001-4.

[120] Toufeili, I., Dziedzic, S., **Synthesis and taste properties of maltose and maltitol analogues**, Food Chem. 47 (1993) 17–22. doi:10.1016/0308-8146(93)90296-R.

[121] Song, J., Fan, H., Ma, J., Han, B., **Conversion of glucose and cellulose into value-added products in water and ionic liquids**, Green Chem. 15 (2013) 2619–2635. doi:10.1039/c3gc41141a.

[122] Pipitone, G., Zoppi, G., Frattini, A., Bocchini, S., Pirone, R., Bensaid, S., **Aqueous phase reforming of sugar-based biorefinery streams: from the simplicity of model compounds to the complexity of real feeds**, Catal. Today. (2019). doi:10.1016/J.CATTOD.2019.09.031.

[123] Zhang, J., Li, J., Wu, S., Liu, Y., **Efficient Conversion of Maltose into Sorbitol over Magnetic Catalyst in Extremely Low Acid**, BioResources. 8 (2013) 4676–4686. doi:10.15376/biores.8.3.4676-4686.

[124] Negahdar, L., Hausoul, P.J.C., Palkovits, S., Palkovits, R., **Direct cleavage of sorbitol from oligosaccharides via a sequential hydrogenation-hydrolysis pathway**, Appl. Catal. B Environ. 166–167 (2015) 460–464. doi:10.1016/J.APCATB.2014.11.049.

[125] Abbadi, A., Gotlieb, K.F., van Bekkum, H., **Study on solid acid catalyzed hydrolysis of maltose and related polysaccharides**, Starch - Stärke. 50 (1998) 23–28. doi:10.1002/(sici)1521-379x(199801)50:1<23::aid-star23>3.3.co;2-k.

[126] Kanie, Y., Akiyama, K., Iwamoto, M., **Reaction pathways of glucose and fructose on Pt nanoparticles in subcritical water under a hydrogen atmosphere**, Catal. Today. 178 (2011) 58–63. doi:10.1016/J.CATTOD.2011.07.031.

[127] Ahmed, M.J., Hameed, B.H., **Hydrogenation of glucose and fructose into hexitols over heterogeneous catalysts: A review**, J. Taiwan Inst. Chem. Eng. 96 (2019) 341–352. doi:10.1016/J.JTICE.2018.11.028.

[128] Godina, L.I., Heeres, H., Garcia, S., Bennett, S., Poulston, S., Murzin, D.Y., **Hydrogen production from sucrose via aqueous-phase reforming**, Int. J. Hydrogen Energy. 44 (2019) 14605–14623. doi:10.1016/j.ijhydene.2019.04.123.

[129] Wei, Z., Karim, A., Li, Y., Wang, Y., **Elucidation of the roles of Re in aqueous-phase reforming of glycerol over Pt–Re/C catalysts**, ACS Catal.

5 (2015) 7312–7320. doi:10.1021/acscatal.5b01770.

[130] Kabyemela, B.M., Adschiri, T., Malaluan, R.M., Arai, K., **Glucose and Fructose Decomposition in Subcritical and Supercritical Water: Detailed Reaction Pathway, Mechanisms, and Kinetics**, Ind. Eng. Chem. Res. 38 (1999) 2888–2895. doi:10.1021/ie9806390.

[131] Bicker, M., Endres, S., Ott, L., Vogel, H., **Catalytical conversion of carbohydrates in subcritical water: A new chemical process for lactic acid production**, J. Mol. Catal. A Chem. 239 (2005) 151–157. doi:10.1016/J.MOLCATA.2005.06.017.

[132] Sınağ, A., Gülbay, S., Uskan, B., Canel, M., **Biomass decomposition in near critical water**, Energy Convers. Manag. 51 (2010) 612–620. doi:10.1016/J.ENCONMAN.2009.11.009.

[133] Godina, L.I., Kirilin, A. V., Tokarev, A. V., Murzin, D.Y., **Aqueous phase reforming of industrially relevant sugar alcohols with different chiralities**, ACS Catal. 5 (2015) 2989–3005. doi:10.1021/cs501894e.

[134] Gutiérrez Ortiz, F.J., Campanario, F.J., Ollero, P., **Turnover rates for the supercritical water reforming of glycerol on supported Ni and Ru catalysts**, Fuel. 180 (2016) 417–423. doi:10.1016/J.FUEL.2016.04.065.

[135] Akbay, H.E.G., Akarsu, C., Kumbur, H., **Treatment of fruit juice concentrate wastewater by electrocoagulation: Optimization of COD removal**, Int. Adv. Res. Eng. J. 2 (2018) 53–57. https://dergipark.org.tr/iarej/issue/34178/400881 (accessed May 14, 2019).

[136] Tawfik, A., El-Kamah, H., **Treatment of fruit-juice industry wastewater in a two-stage anaerobic hybrid (AH) reactor system followed by a sequencing batch reactor (SBR)**, Environ. Technol. 33 (2012) 429–436. doi:10.1080/09593330.2011.579178.

[137] Gonzalez del Campo, A., Cañizares, P., Lobato, J., Rodrigo, M.A., Fernandez, F.J., **Electricity production by integration of acidogenic fermentation of fruit juice wastewater and fuel cells**, Int. J. Hydrogen Energy. 37 (2012) 9028–9037. doi:10.1016/J.IJHYDENE.2012.03.007.

[138] Can, O.T., **COD removal from fruit-juice production wastewater by electrooxidation electrocoagulation and electro-Fenton processes**, Desalin. Water Treat. 52 (2014) 65–73. doi:10.1080/19443994.2013.781545.

[139] Irmak, S., Öztürk, L., **Hydrogen rich gas production by thermocatalytic decomposition of kenaf biomass**, Int. J. Hydrogen Energy. 35 (2010) 5312–5317. doi:10.1016/j.ijhydene.2010.03.081.

[140] Huber, G.W., Dumesic, J.A., **An overview of aqueous-phase catalytic processes for production of hydrogen and alkanes in a biorefinery**, Catal. Today. 111 (2006) 119–132. doi:10.1016/j.cattod.2005.10.010.

[141] Tanksale, A., Beltramini, J.N., Lu, G.Q., **Reaction mechanisms for**

renewable hydrogen from liquid phase reforming of sugar compounds, Dev. Chem. Eng. Miner. Process. 14 (2006) 9–18. doi:10.1002/apj.5500140102.

[142] Yang, B.Y., Montgomery, R., Yun Yang, B., Montgomery, R., **Alkaline degradation of glucose: Effect of initial concentration of reactants**, Carbohydr. Res. 280 (1996) 27–45. doi:10.1016/0008-6215(95)00294-4.

[143] Latham, K.G., Jambu, G., Joseph, S.D., Donne, S.W., **Nitrogen Doping of Hydrochars Produced Hydrothermal Treatment of Sucrose in H_2O, H_2SO_4, and NaOH**, ACS Sustain. Chem. Eng. 2 (2014) 755–764. doi:10.1021/sc4004339.

[144] Verduyckt, J., De Vos, D.E., **Higly selective on-step dehydration, decarboxylation and hydrogenation of citric acid to methylsuccinic acid**, Chem. Sci. 8 (2017) 2616–2620. doi:10.1039/c6sc04541c.

[145] Gutiérrez Ortiz, F.J., Campanario, F.J., Ollero, P., **Supercritical water reforming of model compounds of bio-oil aqueous phase: Acetic acid, acetol, butanol and glucose**, Chem. Eng. J. 298 (2016) 243–258. doi:10.1016/j.cej.2016.04.002.

[146] Remón, J., García, L., Arauzo, J., **Cheese whey management by catalytic steam reforming and aqueous phase reforming**, Fuel Process. Technol. 154 (2016) 66–81. doi:10.1016/j.fuproc.2016.08.012.

[147] Ming, J., Wu, Y., Liang, G., Park, J.B., Zhao, F., Sun, Y.K., **Sodium salt effect on hydrothermal carbonization of biomass: A catalyst for carbon-based nanostructured materials for lithium-ion battery applications**, Green Chem. 15 (2013) 2722–2726. doi:10.1039/c3gc40480c.

[148] Mahugo-Santana, C., Sosa-Ferrera, Z., Torres-Padrón, M.E., Santana-Rodríguez, J.J., **Analytical methodologies for the determination of nitroimidazole residues in biological and environmental liquid samples: A review**, Anal. Chim. Acta. 665 (2010) 113–122. doi:10.1016/J.ACA.2010.03.022.

[149] Dargahi, A., Mohammadi, M., Amirian, F., Karami, A., Almasi, A., **Phenol removal from oil refinery wastewater using anaerobic stabilization pond modeling and process optimization using response surface methodology (RSM)**, Desalin. Water Treat. 87 (2017) 199–208. doi:10.5004/dwt.2017.21064.

[150] Kang, S., Li, X., Fan, J., Chang, J., **Characterization of hydrochars produced by hydrothermal carbonization of lignin, cellulose, d-xylose, and wood meal**, Ind. Eng. Chem. Res. 51 (2012) 9023–9031. doi:10.1021/ie300565d.

[151] Chen, X., Li, H., Sun, S., Cao, X., Sun, R., **Effect of hydrothermal pretreatment on the structural changes of alkaline ethanol lignin from wheat straw**, Sci. Rep. 6 (2016) 1–9. doi:10.1038/srep39354.

[152] Zhang, S., Zhu, X., Zhou, S., Shang, H., Luo, J., **Hydrothermal carbonization for hydrochar production and its application**, Biochar from Biomass Waste. (2019) 275–294. doi:10.1016/B978-0-12-811729-3.00015-7.

[153] Li, X., Li, M.F., Bian, J., Wang, B., Xu, J.K., Sun, R.C., **Hydrothermal carbonization of bamboo in an oxalic acid solution: Effects of acid concentration and retention time on the characteristics of products**, RSC Adv. 5 (2015) 77147–77153. doi:10.1039/c5ra15063a.

[154] Krishnan, D., Raidongia, K., Shao, J., Huang, J., **Graphene oxide assisted hydrothermal carbonization of carbon hydrates**, ACS Nano. 8 (2014) 449–457. doi:10.1021/nn404805p.

[155] Bai, G., Li, F., Fan, X., Wang, Y., Qiu, M., Ma, Z., Niu, L., **Continuous hydrogenation of hydroquinone to 1,4-cyclohexanediol over alkaline earth metal modified nickel-based catalysts**, Catal. Commun. 17 (2012) 126–130. doi:10.1016/J.CATCOM.2011.10.026.

[156] Li, H., Ji, D., Li, Y., Liang, Y., Li, G.X., **Effect of alkaline earth metals on the liquid-phase hydrogenation of hydroquinone over Ru-based catalysts**, Solid State Sci. 50 (2015) 85–90. doi:10.1016/j.solidstatesciences.2015.10.014.

[157] Menezes, A.O., Rodrigues, M.T., Zimmaro, A., Borges, L.E.P., Fraga, M.A., **Production of renewable hydrogen from aqueous-phase reforming of glycerol over Pt catalysts supported on different oxides**, Renew. Energy. 36 (2011) 595–599. doi:10.1016/j.renene.2010.08.004.

[158] Zazo, J.A., Casas, J.A., Mohedano, A.F., Rodríguez, J.J., **Catalytic wet peroxide oxidation of phenol with a Fe/active carbon catalyst**, Appl. Catal. B Environ. 65 (2006) 261–268. doi:10.1016/j.apcatb.2006.02.008.

[159] Dellinger, B., Lomnicki, S., Khachatryan, L., Maskos, Z., Hall, R.W., Adounkpe, J., McFerrin, C., Truong, H., **Formation and stabilization of persistent free radicals**, Proc. Combust. Inst. 31 (2007) 521–528. doi:10.1016/j.proci.2006.07.172.

FACULTAD DE
CIENCIAS
UNIVERSIDAD AUTÓNOMA DE MADRID